



Mechanisms for exceptional preservation in the Fezouata Lagerstätte (Early Ordovician, Morocco)

Farid Saleh

► To cite this version:

Farid Saleh. Mechanisms for exceptional preservation in the Fezouata Lagerstätte (Early Ordovician, Morocco). Earth Sciences. Université de Lyon, 2020. English. NNT : 2020LYSE1126 . tel-03328479

HAL Id: tel-03328479

<https://theses.hal.science/tel-03328479>

Submitted on 30 Aug 2021

HAL is a multi-disciplinary open access archive for the deposit and dissemination of scientific research documents, whether they are published or not. The documents may come from teaching and research institutions in France or abroad, or from public or private research centers.

L'archive ouverte pluridisciplinaire **HAL**, est destinée au dépôt et à la diffusion de documents scientifiques de niveau recherche, publiés ou non, émanant des établissements d'enseignement et de recherche français ou étrangers, des laboratoires publics ou privés.

N°d'ordre NNT : 2020LYSE1126



THESE de DOCTORAT DE L'UNIVERSITE DE LYON

opérée au sein de

l'Université Claude Bernard Lyon 1

Ecole Doctorale N° ED 341

(Évolution, Écosystèmes, Microbiologie, Modélisation)

Spécialité de doctorat : Sciences de la Terre/Earth Sciences

Discipline : Taphonomie/Taphonomy

Soutenue publiquement le 16/07/2020, par :

Farid SALEH

Mechanisms for exceptional preservation in the Fezouata *Lagerstätte* (Early Ordovician, Morocco)

Devant le jury composé de :

Daniel, Isabelle	Pr	Univ. Lyon 1	Présidente
Mangano, Gabriela	Pr	Univ. Saskatchewan	Rapporteure
Ma, Xiaoya	Pr	Yunnan Univ.	Rapporteure
Daley, Allison	Pr	Univ. Lausanne	Examinatrice
Harper, David	Pr	Durham Univ.	Examineur
Lefebvre, Bertrand	CR	CNRS	Directeur de thèse
Pittet, Bernard	MCF	Univ. Lyon 1	Co-directeur
Perrillat, Jean-Philippe	MCF	Univ. Lyon 1	Co-directeur

TABLE OF CONTENT

ACKNOWLEDGMENTS

ABSTRACT

RÉSUMÉ

- 1. INTRODUCTION**
- 2. GENERAL BACKGROUND**
- 3. MATERIAL AND METHODS**
- 4. BURIAL BY STORM DEPOSITS**
- 5. DECAY AND MINERALIZATION**
- 6. FOSSIL MATURATION AND WEATHERING**
- 8. TAPHONOMIC BIAS IN THE FEZOUATA SHALE**
- 9. CONCLUSION AND OUTLOOK**

REFERENCES

ACKNOWLEDGMENTS

A lot can happen in a few years. Back in 2012, I was studying aiming to be a physician. Here, I am now writing the acknowledgments of my Ph.D. in Earth Sciences. I would take this opportunity not only to thank the people that supported me during the last 30 months but also to thank those who were by my side in each and every step during this long bumpy, yet exciting journey.

I cannot express enough gratitude to Bertrand Lefebvre, and Bernard Pittet, my supervisors since my Master's internship. They both helped me gain the knowledge I currently have. I couldn't do any of the work without their presence. They were all the time here, by my side, encouraging me when I had one of those crazy ideas you'll be reading in the upcoming chapters. But also, bringing me down to Earth when I went in my interpretation too far or too fast. You both taught me how a researcher should be. I will be remembering your remarks each and every single time I write a paper in the future, for the rest of my academic career.

Many thanks to Jean Philippe Perrillat, my co-director, whose curiosity brought us to work together. His rigorous comments helped me concretize two (3 in total) of what I think are the most exciting projects of my Ph.D.

Allison Daley is the superwoman of my Ph.D. She was here, whenever I needed to talk with someone either on a scientific topic or just on my daily life problems. The Ph.D. would have been a tougher journey without her presence.

This thesis also benefited from the positive environment provided by the LGLTPE, and the extreme kindness and support of Emanuela Mattioli, in addition to numerous collaborations with talented researcher: Jonathan Antcliffe, Muriel Vidal, Martina Nohejlová, Francesc Perez Peris, Lukas Laibl, Lorenzo Lustri, Pierre Gueriau, David Harper, Yves Candela, Aaron Hunter, Pierre Sansjofre, Stefan Lalonde, Khadija El Hariri, Marika Polechová, and Khaoula Kouraiss. In addition to fruitful discussions with colleagues: Isabelle Daniel, Gilles Escarguel, Vincent Perrier, Claude Colombié, Guillaume Suan, Frédéric Quillévéré, Vincent Grossi, Ingrid Antheaume, and passionate amateurs: Eric Monceret, and Daniel Vizcaíno.

I would also like to thank Gabriella Mángano, and Xiaoya Ma for agreeing to evaluate my work and write their reports. I am sure that many collaborations will emerge with you in the future.

To the friends that I met in France: Nevena, Genia, Bea, Raimon, Auguste, Pauline, Lorenza, Ophélie, and Claire, I really appreciate you guys for supporting me during the day at the university and during the night at the "LookBar". To my Lebanese friends Antonia, Sylia, Moukbel, Joe, Leba, Wael, and Yorgo, thank you for being able to deal with all my "philosophical" thinking over the last twenty years. Noura and Rawan M., you wrote most of my memories in the streets of Hamra. You are a main part of the happy moments during the last two years. Doph you are a cornerstone in my life. Thank you for being here in all my ups and downs.

Many thanks to all my family members especially my uncles: Bassam and Houssam for all the socio-political challenging and motivating conversations we had when I was taking a break from research. And lots of appreciations go to my cousin and my academic mentor Dane. Without your help, I wouldn't be in France now. Many hugs to my little cousins: Lynn, Céline, and George. You give me loads of inspiration and emotional support with every smile you put on your faces.

Last but not least, I would like to express my gratitude towards my parents Leila, and Nassim. Thank you for loving me, believing in me, and doing everything for me to succeed. I know you are my biggest fans and please know that I am yours too. I love you so much.

ABSTRACT

The Fezouata Shale is the most diverse Lower Ordovician unit with exceptional fossil preservation. Fossils from this formation altered our understanding of early metazoan communities at the transition between the Cambrian Explosion and the Ordovician Radiation. The paleontology and the general sedimentological context of the Fezouata Shale are well established. However, little was done to understand the interaction between both, and studies regarding fossil preservation remain scarce. In this thesis, we investigate the general conditions and mechanisms responsible for soft-tissue preservation in the Fezouata Shale. Comparing brachiopod, bivalve, and trilobite size fluctuations between sites allowed us to constrain burial rates in this formation. This permitted the discovery of a relative post-mortem burial tardiness in sites where exceptional fossil preservation occurred. Moreover, mineralogical investigations showed a correlation between particular chlorite phases (i.e. chamosite/berthierine) and preserved soft parts. This mineralogy may have slowed down oxic decay and its deposition was most probably due to periods with high seasonality. Furthermore, we hypothesized for the first time, a possible implication of biomolecules (i.e. ferritin) in the preservation of soft parts. This, if confirmed, would resolve the observed discrepancies between the fossil record preserving nervous systems to the exclusion to everything else, and decay experiments showing that nervous tissues are among the first structures to decay and disappear in laboratory conditions. Additionally, we show that metamorphism was not operational in the Fezouata Shale. However, modern weathering leached organic material from surface sediments and transformed pyrite into iron oxides. This finding infers that the original mode of preservation of the Fezouata Shale comprises both carbonaceous compressions and accessory authigenic pyritization. The direct implication of this work was shown through a comparison of enigmatic patterns preserved in three groups of echinoderms. It appears that some of these patterns in eocrinoids and somasteroids do not reflect original anatomies and are preservation artifacts. However, it is certain that the structures preserved in stylophorans are real, closing a long-standing debate on the affinity of this animal group. Finally, a general comparison between the Fezouata Shale and Cambrian *Lagerstätten* allowed us to decipher the implication of the suggested taphonomic pathway on fossil preservation. It appears that the Fezouata Shale mechanism for preservation failed to preserve completely cellular organisms (e.g. chordates, ctenophores, medusoids) implying a possible underestimation of the original Fezouata Biota and confirming that the Cambrian Explosion and the Ordovician Radiation are one single episode of anatomical innovation. Thus, all these results have implications on understanding ecosystems, and evolution at the dawn of animal life and may contribute in the future to the development of a predictive approach for the discovery of exceptionally preserved biotas.

RÉSUMÉ

La Formation des Fezouata a livré les assemblages à préservation exceptionnelle les plus diversifiés de l'Ordovicien inférieur. Les fossiles de cette unité ont bouleversé notre compréhension des premières communautés animales à la transition entre l'explosion cambrienne et la diversification ordovicienne. La paléontologie et le contexte sédimentologique général de la Formation des Fezouata sont bien établis. Cependant, l'interaction entre les deux demeurait peu connue, et les études concernant la préservation des fossiles étaient rares. Dans cette thèse, nous étudions les conditions et les mécanismes qui ont abouti de la préservation des tissus mous dans la Formation des Fezouata. La comparaison des fluctuations de taille des brachiopodes, des bivalves et des trilobites entre les différents sites nous a permis de contraindre le taux d'enfouissement dans cette formation. Cela nous a permis de mettre en évidence un enfouissement post-mortem relativement tardif dans les sites à préservation exceptionnelle de cette formation. De plus, les recherches minéralogiques ont montré une corrélation entre certains minéraux de chlorite (chamosite / berthierine) et les parties molles. Cette minéralogie peut avoir inhibé la dégradation oxydante des tissus durant les périodes à forte saisonnalité. De plus, nous avons émis l'hypothèse d'une possible implication des biomolécules (ferritine) dans la préservation des parties molles. Ce scénario permettrait d'expliquer les écarts observés entre le registre fossile préservant les systèmes nerveux à l'exclusion de tout le reste, et les expériences de dégradation montrant que les tissus nerveux sont parmi les premières structures à disparaître au laboratoire. De plus, nous montrons que l'influence du métamorphisme est négligeable dans la Formation des Fezouata. Cependant, l'altération récente a lessivé la matière organique des sédiments de surface et transformé la pyrite en oxydes de fer. Cette découverte implique que le mode original de préservation des fossiles de la Formation des Fezouata comprend à la fois les compressions carbonées et la pyritisation authigénique. Une conséquence directe de ce résultat a consisté en la comparaison de motifs énigmatiques préservés dans trois groupes d'échinodermes. Il apparaît ainsi que deux de ces motifs, observés chez les éocrinoïdes et les somastéroïdes, ne reflètent pas les anatomies originales et ne sont que des artefacts de préservation. Cependant, il est démontré que les structures préservées chez les stylophores sont bien réelles, mettant fin au débat sur l'affinité de ce groupe. Enfin, une comparaison générale entre la Formation des Fezouata et les *Lagerstätten* cambriens nous a permis de déterminer quelle a été l'influence de la voie taphonomique empruntée sur la préservation des fossiles. Il semblerait que le mécanisme de préservation dans la Formation des Fezouata n'ait pas permis la conservation des organismes complètement cellulaires (par exemple, les chordés, les cténophores, les médusoïdes), ce qui impliquerait une sous-estimation de la biodiversité originelle dans les Fezouata et confirmerait que l'explosion cambrienne et la radiation ordovicienne ne représentent qu'un seul et même épisode d'innovation anatomique. Ainsi, tous ces résultats ont des implications sur la compréhension des écosystèmes et de l'évolution à l'aube de la vie animale et pourraient contribuer ultérieurement au développement d'une approche prédictive permettant la découverte de nouveaux sites à préservation exceptionnelle.

1. INTRODUCTION

Studying the fossil record is crucial for our understanding of past life on Earth. Much of our knowledge on biodiversification and extinction events comes from mineralized parts such as bones and shells, because these are relatively abundant and are commonly found around the globe¹. However, organisms having mineralized parts constituting at least part of their bodies are not the sole players in modern ecosystems. A large number of animals are completely soft having cuticularized bodies (i.e. formed of polysaccharides), such as annelids and priapulids, or even entirely cellular bodies, such as jellyfishes and sponges. Thus, studies based on mineralized parts in the fossil record give incomplete snapshots of past animal life on Earth. For this reason, incorporating information from localities with exceptional fossil preservation yielding labile anatomies is crucial to properly reconstruct ancient ecosystems with high fidelity². Although generally rare over the geological time scale, exceptionally preserved biotas discovered in deposits called “*Lagerstätten*” are common in the Cambrian³. The most famous Cambrian site with exceptional preservation is the Burgess Shale (Cambrian, Canada)³. The discovery of soft animal taxa in this locality transformed our knowledge on the earliest eumetazoan dominated communities: the Cambrian Explosion^{2,4–7}. Since numerous Burgess Shale-type (BST) assemblages have been discovered. Fossils from the Chengjiang Biota (Cambrian, China) preserved tissues that decay fast in laboratory conditions, and shed light on the evolution of numerous animals⁸. For instance, nervous tissues were discovered in different arthropod groups ending long-standing debates on the systematic affinities of these taxa^{9–12}. The Chengjiang Biota holds as well the record of the best-preserved cardiovascular system ever discovered¹³. All these animals from Cambrian BST assemblages were preserved under similar environmental conditions and share the same mode of preservation^{14,15}. They were transported from their living environment, alive or shortly after their death by obrution events, to another setting for their preservation³. The rapid transport and burial of these animals provided a short time for oxic decay to take place, and increased the chances of tissues to survive oxygen in the water column in their original environment³. In deeper facies under which they were deposited, anoxia was permissive at least at the sea bottom, and carbonate cements precipitated on top of event deposits blocking exchange between the water column and sediments and inhibiting oxidants from attaining decaying carcasses¹⁵. It was also recently suggested that specific clay minerals may have helped BST preservation by slowing down bacterial decay¹⁶. Thus, carcasses were isolated in a fine lithology allowing their preservation in minute details as carbonaceous compressions¹⁴. In some cases, authigenic mineralization (i.e. pyritization, phosphatization) may occur but this remains secondary to the primary carbonaceous mode of preservation¹⁴. Then, the compressed organic matter was kerogenized and matured under metamorphic conditions at temperatures between 300 and 400 degrees¹⁷. Even though the general conditions for exceptional fossil preservation are relatively well-known for Cambrian *Lagerstätten*, the mechanism at play for soft-tissue preservation in younger deposits remain largely unexplored.

In the early 2000s, a new site with exceptional fossil preservation was discovered. The Fezouata Shale Formation (Early Ordovician, Morocco) which was deposited in a storm dominated environment^{18–20} is the only unit to yield an Ordovician highly diverse exceptionally preserved biota^{18,21}. With over than 185 taxa of marine invertebrates recovered from specific intervals in the Zagora area, this formation offers new insights into the diversification of metazoans, at a key interval between the Cambrian Explosion and the Ordovician Radiation^{21–23}. The majority of these taxa are shelly organisms typical of the Great Ordovician Biodiversification Event including asterozoans, bivalves, rhynchonelliformean brachiopods, cephalopods, crinoids, gastropods, graptolites, ostracods, and trilobites²². The Fezouata Biota also comprises a high number of soft-bodied to lightly sclerotized taxa. Some of these exceptionally preserved

organisms (e.g. cirriped crustaceans, eurypterid and xiphosuran chelicerates) represent the oldest occurrences of particular marine invertebrates, previously recorded from younger Paleozoic *Lagerstätten*²². However, the Fezouata Biota also includes numerous representatives of soft-bodied to lightly sclerotized groups typical of Cambrian, BST *Lagerstätten* (e.g. anomalocaridids, protomonaxonids, armored lobopodians, marrellomorphs, naraoids)^{21,24–26}. In terms of preservation, two modes have been documented in the Fezouata Shale. The first one occurs in concretions and results from a vigorous sulfate reduction around large carcasses (e.g. *Aegirocassis*), leading to the establishment of prominent chemical gradients and to the early precipitation and mineral overgrowth around non-biomineralized tissues²⁷. The other type of preservation is associated with shales in a generally shallower environment in comparison to the classical Burgess Shale^{18,20}. Most BST fossils collected in shales are preserved as molds or imprints on the sediments¹⁸. However, it is unclear whether these organisms were originally preserved as carbonaceous compressions. Other non-biomineralized tissues, such as trilobite digestive tracts and echinoderm water-vascular systems, are preserved in 3D red to orange iron oxides²¹.

Considering that numerous mechanisms may favor or alter the preservation of original anatomies, deciphering the taphonomic processes is essential for palaeontological interpretations, especially for taxa without extant representatives. Consequently, the aim of this study is to provide insights into soft tissue taphonomy in the Fezouata Shale based on a multidisciplinary approach combining paleontology, sedimentology, geochemistry and mineralogy. This in-depth reconstruction starts at the life of an organism in its environment and ends at its discovery in surface sediments passing through diagenesis, metamorphism, and modern weathering (Fig. 1)^{28–30} while trying to answer the following questions:

- Was burial fast enough in the Fezouata Shale?
- What was the impact of burial on living communities?
- Did fossil transport occur in the Fezouata Shale?
- What was the impact of decay and mineralization on the current patterns of soft tissue preservation?
- What are the conditions that controlled decay and mineralization?
- Were the fossils subject to extreme maturation?
- What is the impact of modern weathering on these deposits?

Once these questions are answered, the direct impact of this work on fossil interpretation is shown, and a comparison between the Fezouata Shale and both the Burgess Shale and Chengjiang Biota is established. This comparison is essential to constrain preservational biases within exceptionally preserved biotas and thus reconstruct more complete pictures of early animal life. This work has implications in understanding the earliest radiations of complex metazoans on Earth from a fresh perspective independently from individual preservational biases that might be operational at each site. If all the previous questions are answered, they constitute as well a first step in developing a predictive approach for the discovery of exceptionally preserved faunas. These discoveries will definitely help finding new fossils; thus, completing the lack of information in the tree of life.

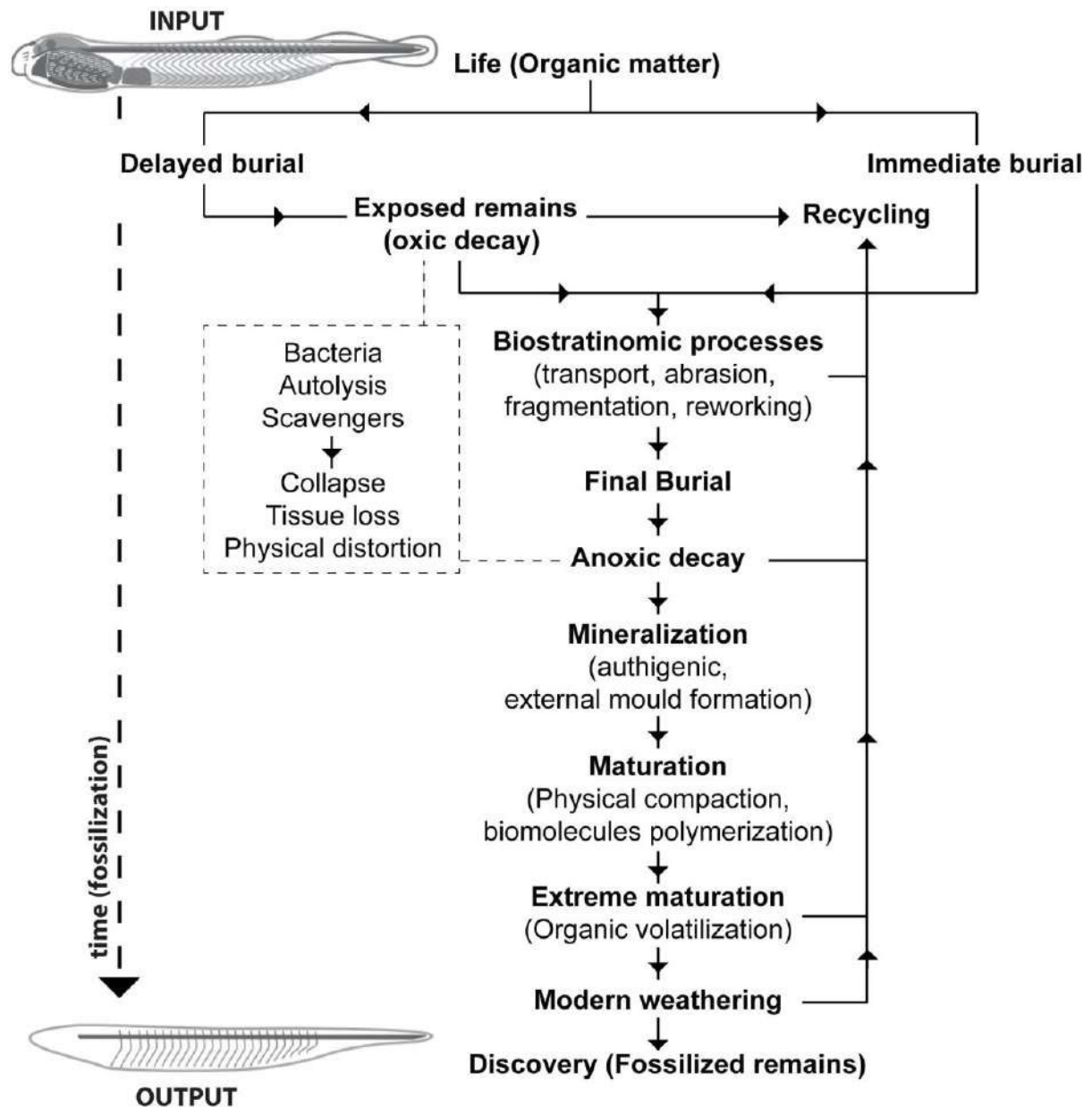


Figure 1. The processes and pathways involved as organic matter passes from the biosphere into the lithosphere (i.e. fossilization). These processes determine what characters from the original morphology are lost or retained^{30,31}.

2. GENERAL BACKGROUND

The Fezouata Shale is one of the rare if not the only diverse Early Ordovician *Lagerstätte* documenting the early stages of the Ordovician Radiation^{18,21,22}. This formation was deposited in the Anti-Atlas of Morocco. During the Early Ordovician, the Central Anti-Atlas was located at high latitudes close to the paleo-South pole^{32,33}. The Ordovician Anti-Atlas deposits (maximum ~2500m to the West) were originally divided into four lithostratigraphic groups which are in chronological order: the Outer Feijas Shale, the First Bani Sandstone, the Ktaoua Clay and Sandstone, and the Second Bani Sandstone (Fig. 2)^{34,35}. Following the stratigraphic work lead by Jacques Destombes in the second half of the 20th century, these stratigraphic groups were subdivided into several formations (Fig. 2)^{36,37}. The Fezouata Shale is comprised within the Outer Feijas Group along with the Zini Sandstone, and the Tachilla Shale formations (Fig. 2). The Fezouata Shale (Tremadocian-Floian) is deposited over the sandstones of the underlying middle Cambrian Tabanite Group and is conformably overlined by the Zini Formation (late Floian) that is itself deposited under the Tachilla Shale Formation (Middle Ordovician)^{36,37}. The Fezouata Shale is entirely constituted by silts outcropping in the Zagora region with a thickness between 900 and 1000m^{18,38}. These silts were deposited in a storm-wave dominated, cold-water, shallow environment modulated by tides^{18–20}. Although mineralized fossils were discovered since the early excavations in the second half of the 20th century, exceptional fossil preservation in the Fezouata Shale was not documented until the early years of the 21st century²¹. In the Fezouata Shale, the distribution of exceptionally preserved fossils (EPF) is not random but associated with a narrow window of favorable environmental conditions around the storm weather wave base located at two distinct stratigraphic intervals³⁹. Based on acritarchs, conodonts, and graptolites^{39–42} a late Tremadocian age (Tr3) was proposed for the lower, about 70-m thick interval (*A. murrayi* graptolite biozone). The upper EPF-bearing interval is narrower (~50 m thick), and it occurs about 240 m higher in the succession³⁹. Graptolites suggest a mid-Floian age (Fl2) for this upper interval^{39,40}. This thesis focuses on the lower interval with EPF, because it is stratigraphically well constrained and comprises most sites with exceptional fossil preservation from the Lower Ordovician of Morocco^{18,21,39}.

	Cambrian	Ordovician						Silurian
Series/ Stages	Middle Cambrian	Lower		Middle	Upper			Lower Silurian
		Tremadocian	Floian	Darriwilian	Sandbian	Katian	Hirnantian	
Groups	Tabanite sandstones	Outer Feijas shales		First Bani sandstones	Ktaoua shales and sandstones		Second Bani sandstones	Taskala shales
Formations	Tilemsoun	Fezouata	Zini	Tachilla Ouinelnirne Guezzart Bou Zeroual Taadrist	Izeguirène Lower Ktaoua	Rouid Aïssa Upper Ktaoua	2 nd Lower Bani 2 nd Upper Bani	Deliouine

Figure 2. Ordovician lithostratigraphic sequencing of the Zagora Region (modified from Marante, 2008)³⁴.

3. MATERIAL AND METHODS

3.1. Paleontology

More than 300 specimens of brachiopods, bivalves, and trilobites from the Fezouata Shale were measured for their body size. The localities bearing these fossils were positioned along a proximal-distal axis according to their sedimentological characteristics. Size distribution of trilobites was investigated between localities by measuring the full length of individuals from the anterior margin of the cephalon to the posterior margin of the pygidium or based on the sagittal length of the pygidium including articulation half ring. The width W , the length L , and the height H of bivalves and brachiopods were measured using a Zeiss SteREO Discovery V8 stereomicroscope linked to a Zeiss AxioCam MRc5 digital camera with a precision of 0.01 mm. The body size $G = (L+W)/2$ was calculated for brachiopods according, and for bivalves: $G = (H+L)/2$.

3.2. Sedimentology

Two successive field campaigns were carried out in the Zagora region in 2018 and 2019 and three cores were obtained. The first two cores (total of 13.2m) were drilled in the intermediate settings of Bou Izargane. The third core (~2.5m) was made in Ouled Slimane, crossing the interval in which large trilobites were discovered. Cores were described for their lithology, grain size, depositional sedimentary structures and bioturbation intensity and size at the University of Lyon, France, and the University of Lausanne, Switzerland, and are currently deposited at the University of Brest.

3.3. Geochemistry and Mineralogy

The cores were cut and scanned, using a core XRF-scanner, for major elements (Si, Al, K) expressed as oxides (wt% SiO_2 , Al_2O_3 and K_2O) at the University of Brest, France. Twelve thin sections were made from the cores. Transect analyses, on nine samples, combined into elemental maps from fresh and weathered core sediments were made using a Bruker M4 Tornado micro-XRF instrument operating at 50kV, 600 μ A. This mapping of the major elements was done to better visualize discrete lithological changes in the facies and to determine the composition of silty to very fine sand grains. In addition, around 100 Raman spectra were collected from nine core specimens using a Labram HR800 - Jobin Yvon Horiba spectrometer equipped with semi-confocal optics at the University of Lyon, France. A microscope with a x100 objective was used to focus the excitation laser beam, 532 nm exciting line, on a 1-3 μ m size spot and to collect the Raman signal in the backscattered direction. Acquisitions were performed using two accumulations of 30s and a laser power of about 5 mW on the sample surface. The position of Raman bands were determined by fitting Lorentzian functions using PeakFit, and were assigned to a phase based on a comparison with ENS Lyon database (<http://www.geologie-lyon.fr/Raman/>) RUFF database (<https://rruff.info/>) and literature data. Mineral assemblages of levels yielding exceptional preservation were compared to those in levels bearing only sclerotized remains. Matrix samples from each level were prepared as randomly oriented powdered aggregates (<10 μ m), without any specific treatments, on thermoplastic polymer [poly(methyl methacrylate), PMMA] substrates. X-ray diffraction (XRD) was performed using a Bruker D8 Advance diffractometer, employing a $\text{CuK}\alpha$ source and Bruker LynxeyeX detector. Peak positions were adjusted, using the positions of quartz peaks as internal standards, to avoid the preparation height displacement error. Mineral phases were then retrieved, based on indexation of their diffraction lines, between 0° and 75° 2θ values, from the International Centre for Diffraction Data PDF-4+ 2016 reference database (<http://www.icdd.com/index.php/pdf-4/>). Illite is generally characterized by its basal (001) peak at ~10 Å. Quartz is characterized by its intense (011) reflection at 3.34 Å. The differentiation

between chlorite minerals is verified based on the lateral variations of their characteristic (001) and (002) peaks, respectively at 14 and 7 Å, as iron enrichment causes an increase in d-spacing that shifts peaks positions toward higher 2θ values. Phase proportions were estimated from the relative intensity of diffraction lines of each mineral species. In addition to sediment analyses, twenty fossil specimens collected from late Tremadocian localities in the Zagora area, Morocco were included in this study. Some of these fossils were analyzed using a FEI Quanta 250 scanning electron microscope (SEM) equipped with backscattered and secondary electron detectors in addition to an energy-dispersive X-ray analyzer (EDX) operating at accelerating voltages ranging from 5 to 15 kV. At low energies, light elements such as C can be detected, while at higher energies, detection of heavier elements is optimized. Some samples were analyzed using a synchrotron beam X-ray fluorescence at the DIFABBS beamline at the Soleil synchrotron, Paris, France, in order to determine the minor-to-trace elemental composition of the fossils, as well as of the surrounding matrix.

3.4. Statistics

3.4.1. Correlation of core sediments with outcrop levels bearing exceptional preservation

Cores give precise information in terms of sedimentary facies and their evolution, but only minimal information on the vertical occurrences of exceptionally preserved fossils. Conversely, field and hand sample observations made at outcrop provide important information on the occurrence of exceptional preservation, but with unprecise information on the facies in which exceptional preservation occurred, due to surface weathering. Thus, the stratigraphic sequence from the 13.2m core was compared to the field-based sequence logged along the same section. A statistical approach was developed to link these two distinct, though complementary, sets of data gathered from outcrops (i.e. occurrences of exceptional preservation) and from drill cores (i.e. detailed sedimentary facies). The obtained 13.2 m-thick core succession was divided into 22 intervals of 60 cm in thickness. Then, the proportion of each identified sedimentary facies was calculated in these intervals. A Principal Component Analysis (PCA) was performed to identify the facies accounting for the largest variance between the 22 intervals. Facies that are homogeneously distributed are less likely to explain discrepancies in occurrences of exceptionally preserved fossils and therefore were removed from further statistical analysis. The facies exhibiting the highest dissimilarity (i.e. with the largest variance) were selected for a Classical Cluster Analysis (CCA). CCA allows investigating the heterogeneities in terms of sedimentary facies between the 22 intervals by separating them into several groups defined as clusters. Vertical alternation of intervals between the groups was plotted against the pattern of soft tissue preservation in the field to check any direct link between the sedimentary facies and exceptional fossil preservation. Then, a similarity percentage test was made to identify which facies caused the highest dissimilarity between these clusters and thus, to decipher the correlation of different facies with the absence/presence of exceptional preservation. Finally, a student t-test was applied to investigate whether the difference in the proportions of facies causing the dissimilarity between clusters was significant.

3.4.2. Comparing the preservation potential of the Fezouata Shale with the Burgess Shale and the Chengjiang Biota

In order to compare the preservation potential of the mechanism responsible for soft tissue preservation in the Fezouata Shale with the processes at play for this type of preservation in the Chengjiang Biota and the Burgess Shale we developed a new statistical method. This method is based on biological “tissue”-type preservation because all animals are formed of the same type of structures: A (biomineralized), B (sclerotized), C (unsclerotized, cuticularized), D (cellular body walls), and E (internal tissues). The occurrences of these structures were

investigated at a generic level. The data matrix for the generic composition and biological tissue occurrences were constructed based on the public collections of the University of Lyon, and the University of Lausanne, in addition to the published material held at the Royal Ontario Museum, and the Yale Peabody Museum, and Yunnan Key Laboratory for Palaeobiology. The number of times each of the different possible tissue type combinations occurred was identified. Tissue types can occur alone A, B, C, D, E in a certain genus; or in one of ten possible pairs: AB, AC, AD, AE, BC, BD, BE, CD, CE, and DE. There are also 10 different possible three-set intersections ABC, ABD, ABE, ACD, ACE, ADE, BCD, BCE, BDE, and CDE. Finally, there are five different possible associations of four-set intersections ABCD, ABCE, ABDE, ACDE, BCDE, and one five-set combination ABCDE. As two of these characters are biologically mutually exclusive (C and D; an organism cannot be cuticularized and non-cuticularized) this simplifies the problem as CD and all its subsets are empty. Consequently, the five-way intersection ABCDE is impossible. Furthermore, the only combination of four possible tissue types that can occur are ABCE and ABDE. So rather than having to deal with a five-variable problem (with $2^5 - 1 = 31$ intersections) a solution is required for only $2^4 - 1 = 15$ intersections. Searching for the character combinations was performed using an “if” function e.g. to find all the occurrences of types A and B in the same genus:

IF(value in column X + value in column Y = 2 then report 1 in column Z, otherwise 0)

This produces a column of binary data that shows whether the character combination has been identified in a given taxon. This column was summed to reveal the number of taxa that contain an AB combination. This strategy was then applied to all the different possible character combinations. However, each count of a higher order intersection will also lead to multiple counts of lower order intersections. For example, finding an ABC combination using an IF function also causes a count of the pairs AB, AC, and BC, and consequently, the taxon is counted 4 times. This has to be removed from the data in order to find unique character combinations. This problem is best visualized as a five-set Venn diagram. As this problem contains the non-intersection of two of the variables (C and D see above), it can be treated as two intersecting four-set problems because the highest order intersections that could take a value are $A \cap B \cap C \cap E$ and $A \cap B \cap D \cap E$ which can be found directly from the data matrix as there are no values in a higher-order subset. These values can then be used to calculate the number of taxa that preserve three tissue types because of the identity:

$$X \cap Y = X \cap Y \cap Z' + X \cap Y \cap Z \text{ (with } Z' \text{ meaning “not } Z\text{”)}$$

Which can be rearranged to:

$$X \cap Y \cap Z' = X \cap Y - X \cap Y \cap Z$$

Thus knowing a value for $A \cap B \cap C \cap E$ and for instance $A \cap B \cap C$, the desired value of $A \cap B \cap C \cap E'$ can be calculated.

$$A \cap B \cap C = A \cap B \cap C \cap E + A \cap B \cap C \cap E'$$

Which can be simply rearranged to:

$$A \cap B \cap C \cap E' = A \cap B \cap C - A \cap B \cap C \cap E$$

In this equation, an unknown exclusive three tissue type association ($A \cap B \cap C \cap E'$) can be calculated from two known quantities which were recovered during the “IF search” chart. It is then trivial to extend this to all other possible three variable intersections. A corollary of this approach is that some intersections require the subtraction of two four-variable intersections. This is because some three-set intersections contain subsets of both of the four variable intersections. For instance:

$$A \cap B \cap E \cap C' \cap D' = A \cap B \cap E - (A \cap B \cap C \cap E + A \cap B \cap D \cap E)$$

Once the unique associations of three variables are known they can be used, following similar logic, to calculate all the unique two-variable intersections (e.g. $A \cap B \cap C' \cap D' \cap E'$). Finally, the one variable intersections (e.g. $A \cap B' \cap C' \cap D' \cap E'$) can be found.

The association of soft internal organs (E) with other structures, in all three localities was also investigated. For this, the probabilities of discovering two classes of structures together having already found one of them were calculated. For example, $p(E|A)$ is the probability of E occurring if A has occurred. The reverse conditional approach was also made and the probability of finding A given that E has been found $p(A|E)$ was also calculated. Then, the likelihood of producing the distribution of combinations of structures found in the Burgess Shale and the Chengjiang Biota assuming that the Fezouata Shale has the “true” preservation regime was investigated using the following parametrized binomial $P(x \geq n)|Bi(n, p)$:

$$P(x) = \binom{n}{x} p^x q^{n-x} = \frac{n!}{(n-x)! x!} p^x q^{n-x}$$

In this equation, $p=p(E|A)$ for the Fezouata Shale, $q=1-p$, n is the number of genera preserving an A in the Burgess Shale or the Chengjinag Biota, and x is the number of desired success which is, in this case, at least the actual number n of genera preserving both A and E in the Burgess Shale/Chengjiang Biota. All calculated probabilities are added up and the probability $P(x \geq n)|Bi(n, p)$, of producing the actual Burgess Shale/Chengjinag Biota AE category, considering that the Fezouata Shale regime is “true”, is then obtained. This was then performed for other tissues combinations (i.e. BE, CE, and DE). This approach was then extended to the assumption that the Burgess Shale preservation distribution is “true” and finally assuming that the Chengjiang Biota preservation distribution is the “true” preservation model. Finally, the probability of finding organisms with only soft cellular tissues (both internal and external to the exclusion of everything else $p(A' \cap B' \cap C' \cap D \cap E|E)$ for all three *Lagerstätten* was calculated.

4. BURIAL BY STORM DEPOSITS

This chapter consists of two papers:

- **Paper 1:** Saleh, F., Candela, Y., Harper, D.A., Polechová, M., Lefebvre, B. and Pittet, B., 2018. Storm-induced community dynamics in the Fezouata Biota (Lower Ordovician, Morocco). **Palaios**, 33(12), 535-541.
- **Paper 2:** Saleh, F., Vidal, M., Laibl, L., Sansjofre, P., Gueriau, P., Perez Peris, F., Lustri, L., Lucas, V., Lefebvre, B., Pittet, B., El Hariri, K., Daley, A.C., 2020. Large trilobites in a stress-free Early Ordovician environment. **Geological Magazine**.

Summary

A striking feature reported from several horizons yielding exceptionally preserved animals from the Fezouata Biota is body size variations between sites and localities. This phenomenon has been previously described in eocrinoid and stylophoran echinoderms, gastropods, and trilobites^{23,35}. Previous studies have explained differences in body sizes in marine settings, either by post-mortem processes (e.g., fossil sorting and preservation)^{43,44} or by the pre-mortem chemical conditions of the water column and sediments⁴⁵. These conditions reflect mainly oxygen fluctuations and nutrient availability⁴⁵⁻⁴⁹. In this chapter, we investigate body size fluctuations of brachiopods, bivalves, and trilobites because they constitute key elements of benthic communities in the Fezouata Biota, and their diversification was a major component of the Great Ordovician Biodiversification Event²². The size distributions of four benthic taxa (i.e. the bivalve *Babinka*, the two brachiopods *Celdobolus* and *Wosekella*, in addition to the trilobite *Platypeltoides*) are analyzed, because they are relatively abundant, well preserved, easily identifiable and all occur at various sites spanning a wide range of environmental conditions. Both *Celdobolus* and *Babinka* (that are epifaunal and shallow infaunal respectively)⁵⁰ show normal distributions at all sites with an increase in size from proximal to distal localities⁵⁰. The difference in body size between sites is significant⁵⁰. While the deep infaunal *Wosekella* has a normal distribution at all localities with no evident trends from shallow to deep environments⁵⁰. The increase in size from proximal to distal sites for epifaunal and shallow infaunal sessile taxa cannot result from fossil sorting and transport because these fossils are preserved in situ at bed junctions and not within storm deposits^{18-20,50}. Most importantly, preserved valves do not show any preferred orientation and are complete with little evidence of abrasion and even minute details of the shells, such as setae in siphonotretoid brachiopods, are often perfectly preserved⁵⁰. Chemical stress from nutrient and oxygen deficiencies could not explain as well size reduction in proximal sites because any chemical stress should affect the whole benthos and not selectively choose a couple of taxa in a certain site⁴⁵. Furthermore, the benthic community in proximal sites of the Fezouata Shale is diversified⁵⁰. The discrepancy in sizes of epifaunal and shallow infaunal taxa between proximal and distal localities can be explained by differences in burial rates between localities. Proximal sites are very frequently affected by storms. Storm deposits can bury, kill, and preserve epibenthic and shallow infaunal sessile taxa. However, deep infaunal taxa are little affected by a few centimeters of sediments added on top of previously existing sediments⁵⁰. Infaunal taxa can continue to grow and attain larger sizes and this can explain why they do not show any significant difference in sizes between proximal and distal sites⁵⁰. The pattern observed for epifaunal and shallow infaunal sessile taxa is also observed for vagile trilobites in the Fezouata Shale⁵¹. The size of the genus *Platypeltoides* increased by four times between proximal and distal sites⁵¹. This cannot be due to ontogeny in which younger -and therefore smaller- developmental stages favored shallower environments, and older and larger ones preferred deeper settings, because the material measured here consistently excluded juvenile stages (defined by the number of thoracic segments)⁵¹. Even if future work shows a correlation between changes in habitats and developmental stages of some

trilobites, this fails to explain why older and bigger individuals preferred deeper environments. Therefore, there must have been external biotic and abiotic conditions that selected for larger bodies in deeper settings and smaller bodies in more proximal environments. It is likely that trilobites, similarly to modern vagile arthropods, were able to adapt against physical instabilities and were little affected by storm turbulences in proximal sites⁵¹. However, they may have preferred a distal setting because it is calm. Some of them even showed collective behavior by migrating during storm seasons⁵². The distal settings of the Fezouata Shale were also rich in oxygen and nutrients as suggested by the extreme bioturbation of the sediments⁵¹. The stress-free environment in the distal settings (little storms, with oxygen and nutrients) explains why trilobites attained large sizes, died, and are disarticulating on the seafloor⁵¹. Even though the general conditions in the bottom of the water column along the proximal-distal axis are oxic for the Fezouata Shale, some levels in intermediate settings of this formation are characterized by low diversity assemblages characterized by an abundance of juveniles^{35,38}. This possibly reflects that oxygenation was not stable and periods with lower oxygen concentration existed in these settings possibly pointing to the presence of a temporary oxygen minimum zone OMZ (Fig. 3). This hypothesis needs further testing using a geochemical approach. However, at this stage and independently from oxygen availability in the water column, rapid burial occurred mainly in the most proximal settings of the Fezouata Shale and impacted size distribution of taxa there. Burial tardiness exists mainly in distal settings and to some extent in intermediate environments, possibly exposing carcasses to the chemical gradient of the water column.

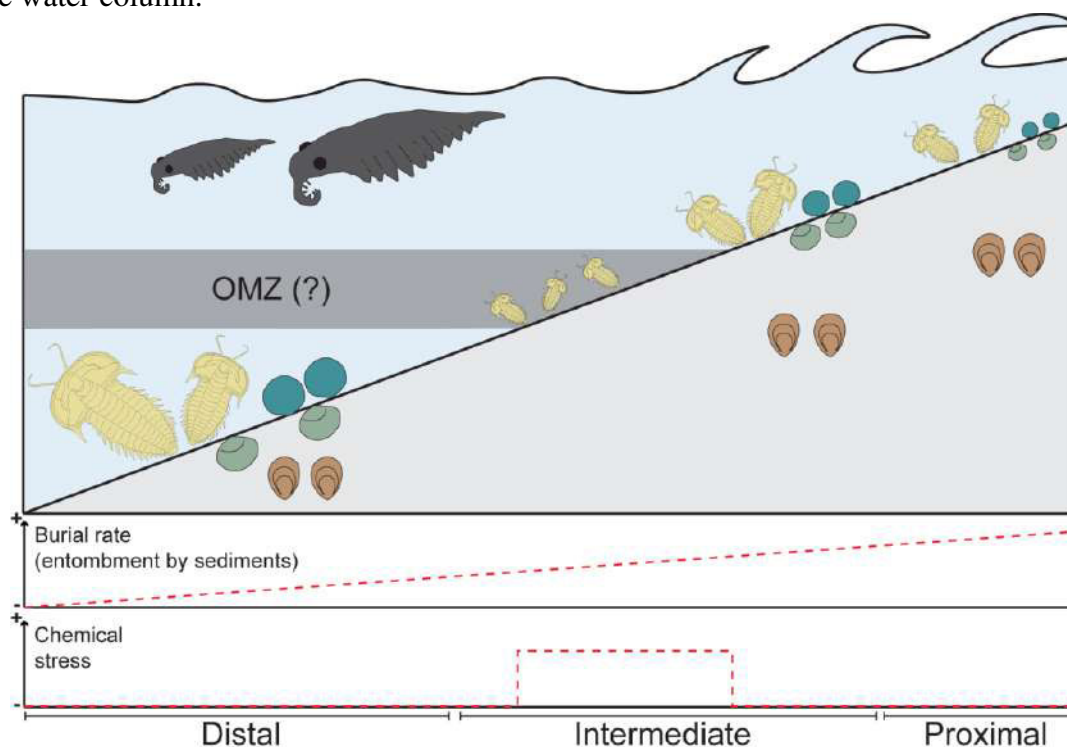


Figure 3. Body size variations of epifaunal, shallow infaunal, and deep infaunal taxa along the proximal-distal axis of the Fezouata Shale accordingly with differences in burial rates and oxygenation (OMZ= Oxygen Minimum Zone).

STORM-INDUCED COMMUNITY DYNAMICS IN THE FEZOUATA BIOTA (LOWER ORDOVICIAN, MOROCCO)

FARID SALEH,¹ YVES CANDELA,² DAVID A. T. HARPER,³ MARIKA POLECHOVÁ,⁴ BERTRAND LEFEBVRE,¹ AND BERNARD PITTET¹

¹Université Lyon, Université Claude Bernard Lyon 1, ENS Lyon, CNRS, UMR 5276 Laboratoire de Géologie de Lyon: Terre, Planètes, Environnement, F-69622 Villeurbanne, France

²Department of Natural Sciences, National Museums Scotland, Edinburgh EH1 1JF, UK

³Palaeoecosystems Group, Department of Earth Sciences, Durham University, Durham DH1 3LE, UK

⁴Czech Geological Survey, Klárov 3, Prague 1, 118 21, Czech Republic
email: farid.saleh@univ-lyon1.fr

ABSTRACT: In the Central Anti-Atlas (Morocco), the lower part of the Fezouata Shale has yielded locally abundant remains of soft-bodied to lightly sclerotized taxa, occurring in low diversity assemblages characterized by strong spatial and taxonomic heterogeneities, and frequently, by the occurrence of small-sized individuals. Size frequency analyses of *Celdobolus* sp., *Wosekella* sp. (both linguliformean brachiopods) and *Babinka prima* (babinkid bivalve) collected in deposits of the Fezouata Shale and associated with distinct paleoenvironmental conditions show that short-lived communities of epifaunal and shallow infaunal taxa were regularly smothered and killed by distal storm deposits. Small-sized individuals more likely represent juveniles, rather than ‘dwarfed’ adults (Lilliput Effect). Consequently, unstable environmental conditions (regular storms, and possibly low oxygenation of the water column) probably explain the unusual community dynamics of late Tremadocian assemblages of the Fezouata Biota (high density of individuals, low α -diversity, and high γ -diversity), interpreted as short-lived, opportunistic populations. This process has wider implications for the understanding of occurrences of small individuals elsewhere in the fossil record.

INTRODUCTION

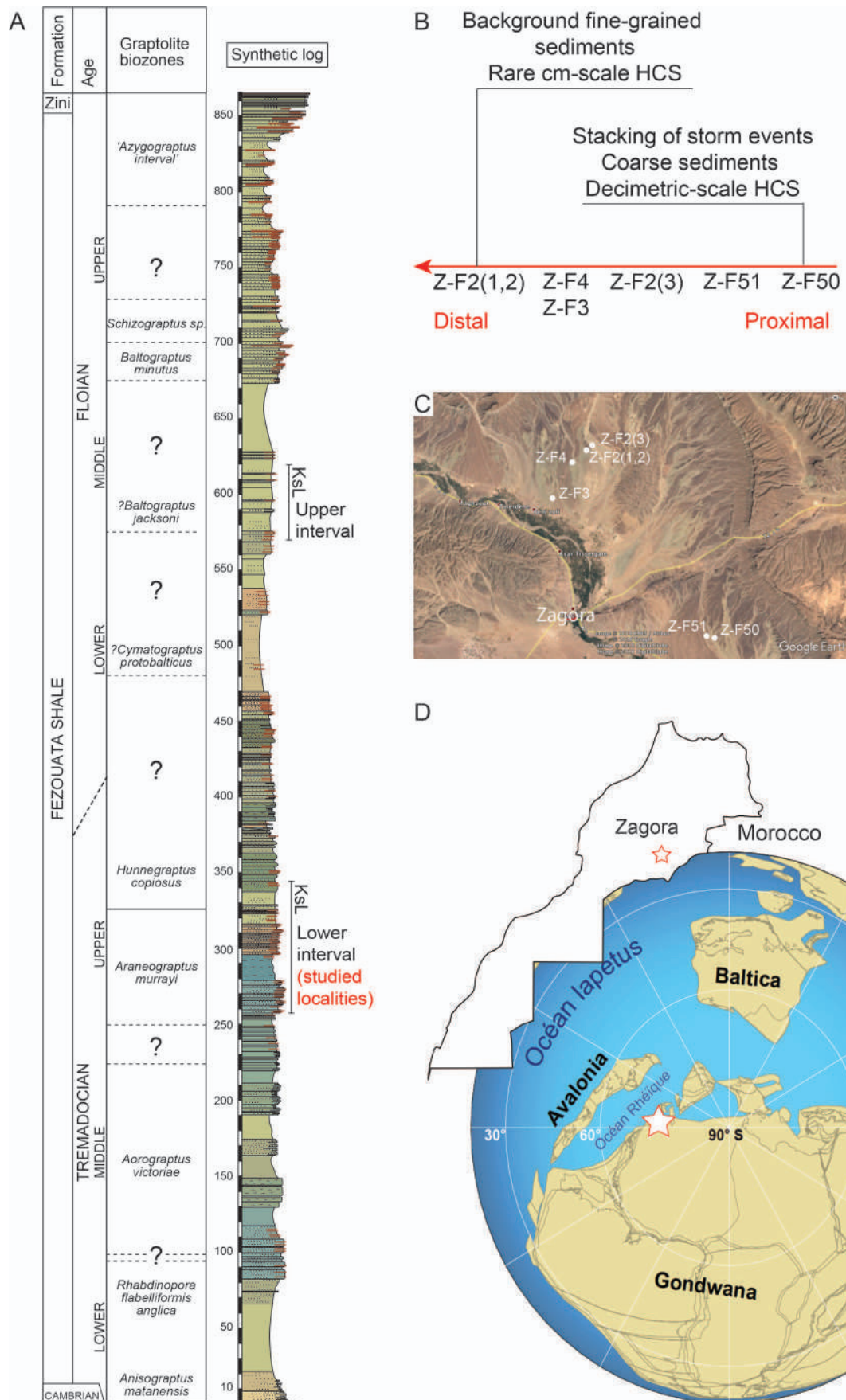
Discovered in the early 2000s in the Central Anti-Atlas of Morocco, the Early Ordovician Fezouata Lagerstätte has dramatically altered evolutionary scenarios on the initial diversification of metazoans during the early Paleozoic (Van Roy et al. 2010, 2015a; Lefebvre et al. 2016b; Martin et al. 2016a). In the Zagora area, the ~ 900 meter sediments of the Fezouata Shale (Fig. 1A) have yielded over 200 taxa of marine invertebrates, the majority of which are shelly organisms typical of the Great Ordovician Biodiversification Event including asterozoans, bivalves, rhynchonelliformean brachiopods, cephalopods, crinoids, gastropods, graptolites, ostracods, and trilobites (Havlicek 1971; Destombes et al. 1985; Ebbestad 2016; Gutiérrez-Marco and Martin 2016; Lefebvre et al. 2016a; Martin et al. 2016b; Polechová 2016). The Fezouata Biota also comprises a high number of soft-bodied to lightly sclerotized taxa, generally preserved as colorful iron oxides, resulting from the weathering of pyrite (Van Roy 2006; Van Roy et al. 2010, 2015a; Lefebvre et al. 2016b; Martin et al. 2016a). Some of these exceptionally preserved organisms (e.g., cirripede crustaceans, eurypterid, and xiphosuran chelicerates) represent the oldest occurrences of particular marine invertebrates, previously recorded from younger Paleozoic Lagerstätten (Van Roy et al. 2010, 2015a). However, the Fezouata Biota also includes numerous representatives of soft-bodied to lightly sclerotized groups typical of early-middle Cambrian, Burgess Shale-type Lagerstätten (e.g., anomalocaridids, protomonaxonids, armored lobopodians, marrellomorphs, naraoiids; Botting 2007, 2016; Van Roy et al. 2010, 2015b; Van Roy and Briggs 2011; Legg 2016).

During the Early Ordovician, the Central Anti-Atlas was located at high latitudes close to the paleo-South pole (Fig. 1D; see Torsvik and Cocks 2011, 2013). In the Zagora area, the Fezouata Shale deposition occurred in a storm-wave dominated, cold-water, shallow environment modulated by

tides (Martin et al. 2016a; Vaucher et al. 2016, 2017). The corresponding paleoenvironment ranges from the shoreface (*sensu* Reading 1996) to the offshore, i.e., right below the storm wave base as described in Vaucher et al. (2017). In the Fezouata Shale, the distribution of exceptionally preserved fossils (EPF) is not random, but associated with a narrow window of favorable environmental conditions, around the storm-wave base (Martin et al. 2016a; Vaucher et al. 2016, 2017). EPF-bearing levels typically occur as lenses, located immediately below thin (mm to cm) levels of coarse siltstones to sandstones (Martin et al. 2015; Vaucher et al. 2016). The Fezouata Biota was thus interpreted as *in situ* assemblages, smothered by distal storm deposits (Lefebvre et al. 2016b; Martin et al. 2016a; Vaucher et al. 2016, 2017).

In the Lower Ordovician succession of the Zagora area, favorable environmental conditions for exceptional preservation are located at two distinct stratigraphic intervals (Fig. 1A; Lefebvre et al. 2016b, 2018; Martin et al. 2016a). Based on acritarchs, conodonts, and graptolites (Gutiérrez-Marco and Martin 2016; Lefebvre et al. 2016b, 2018; Lehnert et al. 2016; Martin et al. 2016a; Nowak et al. 2016) a late Tremadocian age (Tr3) was proposed for the lower, about 70-m thick interval. The upper EPF-bearing interval is narrower (~ 50 m thick), and it occurs about 240 m higher in the succession (Lefebvre et al. 2016b, 2018). Graptolites suggest a mid-Floian age (Fl2) for this upper interval (Gutiérrez-Marco and Martin 2016; Lefebvre et al. 2016b, 2018).

Community structures are markedly different in the two EPF-bearing intervals (Lefebvre et al. 2018). In the Zagora area, all fossiliferous horizons sampled in the upper interval have yielded comparable, particularly abundant and diverse fossil assemblages (~ 50 taxa), dominated by bivalves, rhynchonelliformean brachiopods, cephalopods, gastropods, and trilobites (Destombes et al. 1985; Vidal 1998; Kröger and Lefebvre 2012; Ebbestad 2016; Polechová 2016). Exceptionally preserved



taxa are rare and constitute a minor component of the fauna (Van Roy 2006; Van Roy and Tetlie 2006; Botting 2016; Lefebvre et al. 2016b, 2018; Ortega-Hernández et al. 2016). In contrast, EPF are particularly abundant and diverse in the lower interval. Both EPF and shelly fossils occur abundantly in thin, discontinuous levels, yielding low diversity assemblages generally dominated by one or two taxa, e.g., anomalocaridids, linguliformean brachiopods, conulariids, cornute stylophorans, eocrinoids, graptolites, hyolithids, marrellomorphs, sponges, trilobites, and/or xyphosurans (Botting 2007, 2016; Van Roy et al. 2010, 2015a, 2015b; Van Roy and Briggs 2011; Martin et al. 2015; Gutiérrez-Marco and Martín 2016; Lefebvre et al. 2016a; Van Iten et al. 2016; Allaire et al. 2017). In this interval, each individual horizon yields a unique assemblage, in terms of faunal content and/or relative proportions of occurring taxa. Thus, one of the most striking features of fossil assemblages recovered from the lower EPF-bearing interval is the extreme taxonomic and spatial heterogeneity of each horizon (Van Roy et al. 2015a; Botting 2016; Lefebvre et al. 2016a). The high cumulative diversity (γ -diversity) recorded in this interval (~ 150 taxa) suggests that the low diversity observed for each individual assemblage (α -diversity) could represent a kind of random sampling of a larger pool of taxa.

Another intriguing feature reported from several upper Tremadocian horizons yielding EPF in the Zagora area is the repeated occurrence of taxa represented exclusively by small-sized individuals: this phenomenon has been described in eocrinoid and stylophoran echinoderms (Lefebvre and Botting 2007; Lefebvre et al. 2016a), gastropods (Ebbestad 2016), and trilobites (Martin 2016). In both echinoderms and gastropods it is difficult to identify whether such assemblages of small-sized individuals are comprised of only juveniles, or if they correspond to populations of 'dwarfed' adults (Lefebvre and Botting 2007; Ebbestad 2016; Lefebvre et al. 2016a). On the other hand, the assemblage of small-sized trilobites (*Anacheirus adserai* and *Bavarilla zemmourensis*) reported by Martin (2016) is apparently composed of meraspid (adult) individuals, about half their 'standard' size documented in other levels and/or geographic areas.

The study of body size is important to understand the biological and ecological adaptations of an individual to its environment (Jablonski 1996; Vermeij 2016). Previous studies have explained spatial differences in body sizes in marine settings, either by post-mortem processes (e.g., fossil sorting and preservation; Brenchley and Harper 1998) or by the pre-mortem chemical conditions of the water column and sediments. These conditions reflect mainly oxygen fluctuations (Savrdá and Bottjer 1986; Payne and Clapham 2012; He et al. 2017) and nutrient availability (Twitchett 2007; He et al. 2010). Consequently, the aim of this paper is to identify the physical mechanisms (e.g., storm influence) possibly involved in body-size changes in late Tremadocian fossil assemblages of the Fezouata Shale. This study is focused on brachiopods and bivalves, which constitute a key element of benthic communities in the Fezouata Biota (Havlíček 1971; Mergl 1981; Babin and Destombes 1990; Destombes et al. 1985; Van Roy et al. 2010, 2015a; Polechová 2016), and the diversification of which was a major component of the Great Ordovician Biodiversification Event (Harper 2006; Servais and Harper 2018). The size distribution of three benthic taxa (the bivalve *Babinka* and the two brachiopods *Celdobolus* and *Wosekella*) is analyzed, because they are relatively abundant, well preserved, easily identifiable and all occur at various horizons spanning a wide range of environmental conditions in the late Tremadocian EPF-bearing interval of the Zagora area.

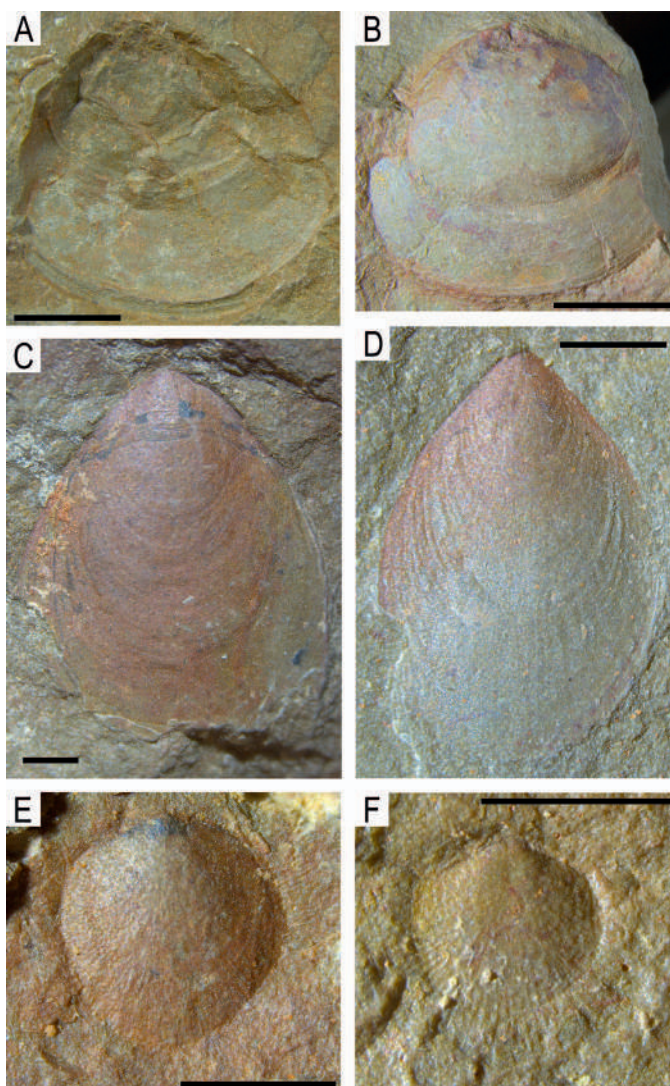


FIG. 2.—Late Tremadocian babinkid bivalves and linguliformean brachiopods from the Fezouata Shale, hill east of Tamegroute, Zagora area, Central Anti-Atlas (Morocco). **A, B** *Babinka prima* Barrande, 1881: AA-TGR1c-OI-178 and AA-TGR1c-OI-14, respectively. Scale bars = 2 mm. **C, D** *Wosekella* sp.: AA-TGR1c-OI-102 and AATGR1c-OI-155, respectively. Scale bars = 2 mm. **E, F** *Celdobolus* sp.: AA-TGR1c-OI-78 and AA-TGR1c-OI-62, respectively. Scale bars = 2 mm.

MATERIAL AND METHODS

Over 300 specimens of bivalves and brachiopods were collected from seven different localities in the lower interval yielding EPF (*Araneograptus murrayi* graptolite Zone, late Tremadocian) in the Fezouata Shale. The position of these localities along a proximal-distal axis and in the Zagora area is shown (Fig. 1B, 1C, respectively). For this study, only specimens belonging to the three genera *Celdobolus*, *Wosekella*, and *Babinka* were included (Fig. 2), because these three taxa are suitably abundant at all sites. This choice was further motivated by the putative modes of life of these

FIG. 1.—Geologic context of the studied material. **A**) Synthetic stratigraphic column of the Lower Ordovician succession in the Zagora area, Morocco showing the position of the two intervals yielding exceptionally preserved faunas (KsL); modified from Gutiérrez-Marco and Martín (2016) and Lefebvre et al. (2018). Colors on the log correspond to those of the rocks exposed. **B**) The position of studied levels along a proximal-distal axis. **C**) The position of studied localities in the Zagora region. **D**) The Early Ordovician and current position of the Zagora area.

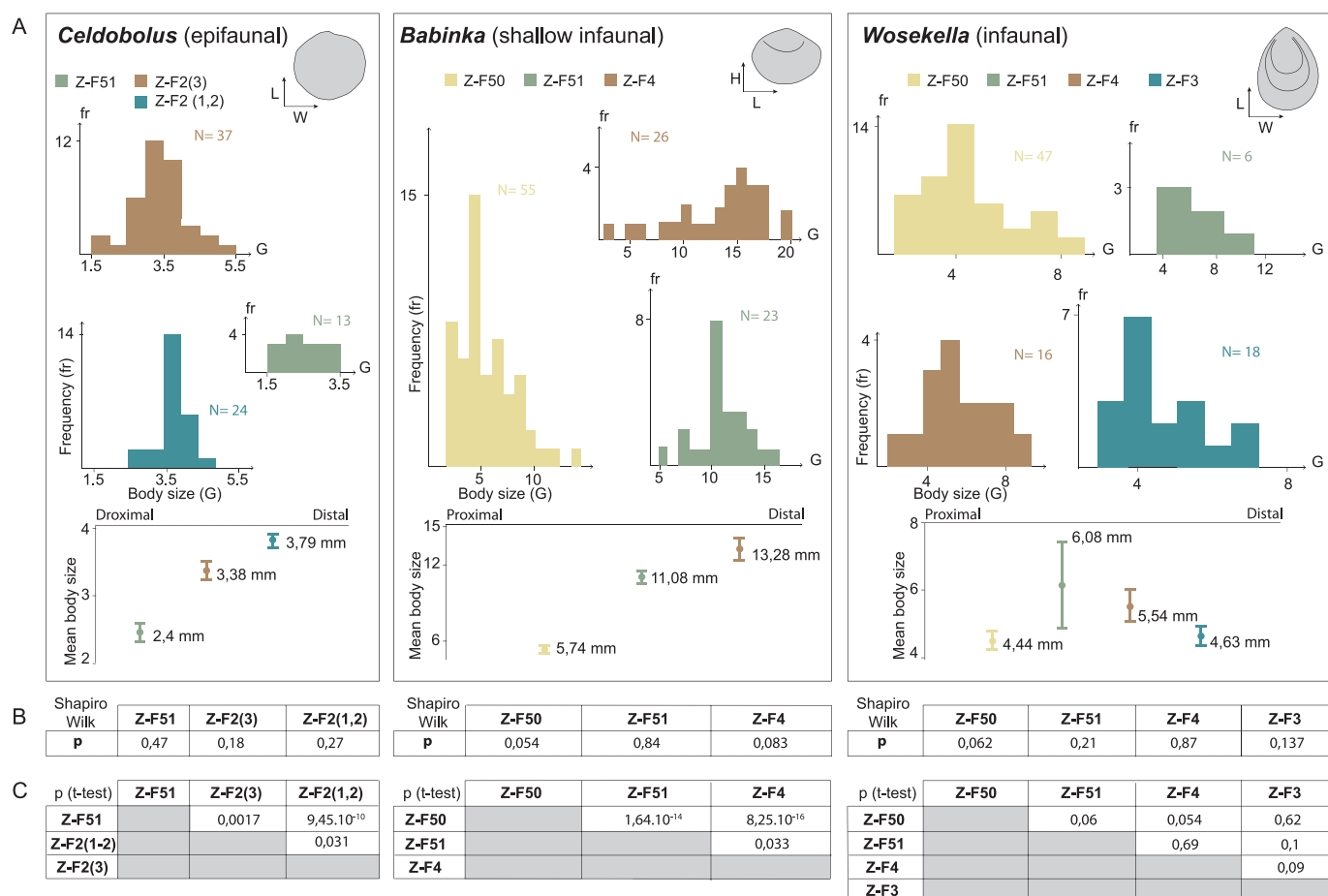


FIG. 3.—Statistical analysis on brachiopods and bivalves in the Fezouata Shale, Zagora area (Morocco). **A**) Size distribution for *Celdobolus* sp., *Babinka prima* Barrande, 1881 and *Wosekella* sp. at all sites. **B**) Shapiro-Wilk p-values for normality. **C**) T-test p-values for significant differences in size between sites.

three taxa. *Celdobolus* has been interpreted as a typical epifaunal genus, possibly epizooic on sponges (Mergl 2002). Cambrian species of *Wosekella* have been interpreted in some occurrences as semi-infaunal low suspension feeders (Mergl and Kordule 2008) or epifaunal (attached with the pedicle to the substrate; see Pettersson Stolk et al. 2010). However, Ordovician *Wosekella* is generally interpreted as endobenthic (Mergl 2002). *Babinka*, a primitive bivalve, is regarded as a shallow-water infaunal taxon (Guild G5 suspensivorous—free endofaunal of Sánchez 2008; see also McAlester 1965; Polechová 2016), based on the subcircular outline and globose profile of the shell. For measurements and analyses, only complete shells were retained.

The width W, the length L, and the height H of different shells were measured using a Zeiss SteREO Discovery V8 stereomicroscope linked to a Zeiss AxioCam MRc5 digital camera with a precision of 0.01 mm. The body size $G = (L+W)/2$ (Fig. 3) was calculated for brachiopods according to Jablonski (1996), and for bivalves: $G = (H+L)/2$ (Fig. 3) according to Carter et al. (2012). Afterward, the mean size for each genus was determined. Data were plotted as size-frequency histograms in PAST; the Shapiro-Wilk test for normality was then made and for normal distributions, a Student t-test was applied to check if there is a significant difference in size between sites (Hammer et al. 2001).

All studied material is registered in the collections of the Cadi Ayyad University, Marrakesh (Morocco). Precise GPS coordinates of the studied localities are reported on specimen labels, and are available upon request.

RESULTS

The studied specimens consist of disarticulated valves that do not show any preferential orientation (simply disarticulated by wave orbitals, with no or limited transport before burial; Vaucher et al. 2016, 2017). The majority of sampled valves were complete without any evidence of damage or abrasion. They were preserved at the base of storm events (covered by very fine to fine-grained sandstones or coarse siltstones showing normal grading or oscillatory structures; Vaucher et al. 2016, 2017).

Both *Celdobolus* and *Babinka* show normal distributions at all sites (Fig. 3A, 3B) with an increase in size from proximal to distal localities (Fig. 3A). The difference in body size between sites is significant (Fig. 3C). *Wosekella* has a normal distribution at all localities (Fig. 3A, 3B). However, no trend is evident from shallow to deeper environments (Fig. 3A) and the size differences between sites is not significant (Fig. 3C).

DISCUSSION

The mean size values observed for *Wosekella* at all sites are comparable to those reported for this genus in Lower Ordovician deposits from other regions (e.g., Bohemia; Mergl 2002). Similarly, the mean size values obtained for both *Babinka* and *Celdobolus* in the distal-most site are similar to those described for this genus in other areas (e.g., Bohemia; McAlester 1965; Mergl 2002; Polechová 2013). In marked contrast, specimens of both *Babinka* and *Celdobolus* from Z-F50 are about half the

size of those occurring in both Z-F4 and other Lower Ordovician assemblages (McAlester 1965; Mergl 2002; Polechová 2013). This significant difference in the mean size of *Babinka* and *Celdobolus* from the Fezouata Shale can be explained either by post-mortem or pre-mortem processes.

Post-mortem taphonomic processes include fossil sorting and preservation (Kidwell 1991; Brenchley and Harper 1998). At all sites, brachiopods and bivalves are apparently preserved *in situ* with little to no evidence of significant lateral transport (disarticulated but complete valves with no preferential orientation) (Vaucher et al. 2016, 2017), and even minute details of the shells, such as setae in siphonotretoid brachiopods, are often perfectly preserved. The preservation of such extremely delicate and brittle structures rather suggests the *in situ* burial of autochthonous benthic populations by distal storm deposits. Thus, the abundance of small-sized assemblages of bivalves and *Celdobolus* in proximal sites cannot simply be interpreted as resulting from sorting and preservation.

During pre-mortem processes, chemical parameters (e.g., low oxygen concentrations, oligotrophic waters) have been frequently invoked to explain severe reductions in the mean size of adults in populations of marine invertebrates (Tasch 1953; Urlichs 2012; Botting et al. 2013). This phenomenon ('Lilliput Effect') has been advocated for marine faunas, particularly those associated with the survival and recovery phases following extinction events (e.g., Huang et al. 2010; Twitchett 2007). The Lilliput Effect generally affects most elements of the biota, across a wide range of taxonomic levels. In the Fezouata Shale, the possible occurrence of a Lilliput Effect was questioned for several low-diversity assemblages from the lower EPF-bearing interval, yielding small-sized trilobites (Martin 2016), echinoderms (Lefebvre et al. 2016a), and gastropods (Ebbestad 2016). At proximal sites, however, there is no evidence supporting the existence of a putative Lilliput Effect: with the exception of *Babinka*, *Celdobolus* and possibly some other co-occurring epibenthic brachiopod genera (*Elliptoglossa*, *Monobolina*, and *Orbithela*), all other components of the associated benthic fauna (including trilobites and some brachiopods, such as *Wosekella*; Fig. 2A) do not show any reduction in size. Unfavorable chemical conditions should have affected the whole benthos. In these sites, small-sized specimens of *Babinka* thus more likely correspond to juveniles, rather than to 'dwarfed' adults.

Physical parameters of the water column (e.g., storm intensity, currents) are other pre-mortem processes possibly involved in the observed pattern of size distribution. When entombed by sediment, deep infaunal organisms have a greater chance of physically being able to react than epifaunal or shallow infaunal ones (Freeman et al. 2013). Taxa like *Wosekella* with a reduced dorsal pseudointerarea and smooth, elongate suboval valves (Emig 1997; Bassett et al. 1999) have the capability to re-orient upward and the possibility of burrowing upwards. Hammond (1983) described that in experimental conditions, 100% of *Lingula anatina* buried in 5 to 10 cm of sediment survived, and 70% of *L. anatina* with pedicles emerged from 20 cm of sediment. Moreover, Thayer and Steele-Petrovic (1975) demonstrated that, using modern genus *Glottidia*, after entombment, reorientation and re-burrowing were successful, even in the case of animals losing their pedicles. On the other hand, Hutchinson et al. (2016) showed a high mortality of sessile epibenthic bivalves after their burial by sediment. As it is the case during storms, even shallow infaunal taxa are subjected to the power of the wave orbitals, which snatch the animals from their life position in the burrow. The result is that the organisms may become disoriented and lie in a position that is far from their normal life position.

In the Fezouata Shale, the storm record varies between localities and between different levels at the same locality (Vaucher et al. 2017). During storm events, wave orbitals generated in the water column, in addition to the quantity of burial material, if any, clearly had an impact on benthic communities. Proximal, shallow-water settings were more affected by storms and wave orbitals, and larger amounts of sediment were deposited

than in more distal, deeper-water environments (Vaucher et al. 2016, 2017). In this context, the demographics observed for *Babinka*, *Celdobolus*, and *Wosekella* in the Fezouata Shale can be simply explained by both their presumed mode of life and physical ability to re-burrow and reorient to their normal life orientation, and external physical parameters (e.g., storm intensity) depending on their position along a proximal-distal gradient. In proximal settings (e.g., Z-F50), shallow infaunal taxa (e.g., *Babinka*) are exclusively represented by small-sized, probably juvenile individuals, whereas deeper infaunal genera that actively respond to physical stress exhibit a much wider range of sizes, including putative adult individuals. This suggests that, in shallow-water settings, *Babinka* individuals were regularly smothered and killed by thin distal storm deposits. In contrast, individuals of *Wosekella* were less affected and could reach larger sizes. In more distal environments (e.g., Z-F4), both epibenthic/shallow infaunal (e.g., *Babinka*, *Celdobolus*) and deep infaunal (e.g., *Wosekella*) communities were little affected by storms, so that individuals could reach larger sizes and form stable, ageing populations (Fig. 4). Consequently, in the lower EPF-bearing interval of the Fezouata Shale, reaching large sizes in an environment constantly affected by storms seems to be related to better success colonizing the sea floor, due to larval transport by fair weather currents. These currents allowed randomly the (re)colonization of either a high or a low-energy setting, thus permitting or preventing the growth of *Babinka*, *Celdobolus* and possibly other epibenthic or shallow infaunal taxa into full-sized adults.

In the late Tremadocian of the Zagora area, the persistence of unstable environmental conditions in shallow settings prevented the colonization of the sea bottom by stable, long-ranging communities of sessile or slow-moving epibenthic/shallow infaunal taxa. These stressful environmental conditions probably explain the high spatial and taxonomic heterogeneity observed in this interval of the Fezouata Shale, and support the interpretation of the low-diversity assemblages occurring in these levels as opportunistic populations buried *in situ* by distal storm sedimentation. This interpretation is in good agreement with previous reports of similar, low diversity, Early-Mid Ordovician benthic assemblages dominated by primitive bivalves (Cope 1999; Sánchez and Benedetto 2007) and/or by linguliformean brachiopods (Popov et al. 2013).

CONCLUSIONS

The low-diversity, dense assemblages occurring in most fossiliferous horizons of the late Tremadocian EPF-bearing interval of the Fezouata Shale are not generated by currents, but they correspond to autochthonous communities smothered by distal storm deposits (Martin et al. 2015, 2016a; Vaucher et al. 2016, 2017). Both the spatial heterogeneity and unusual demographics displayed by these assemblages can be explained by relatively unstable environmental conditions, both in terms of oxygenation (dysoxic to anoxic settings; see Botting 2016; Martin et al. 2016b) and storm activity (Vaucher et al. 2016). It is thus very likely that the particularly dense and patchy, low-diversity assemblages observed in this interval correspond to successive colonization of the sea floor by opportunistic taxa (Botting 2016; Lefebvre et al. 2016a). At several horizons, the small size of most individuals suggests that these epibenthic or shallow infaunal populations were short-lived and repeatedly buried by distal storm deposits.

This study also constitutes the first step to elaborate a proxy, at generic level, relating shell sizes to bathymetry, in a storm-wave dominated environment. Additionally, it shows that a new mechanism, related to physical processes, can explain size differences independently from the chemical conditions of the water column and their related dwarfism. Finally, this study highlights the utility of understanding life habit and more broadly paleoecology for fully understanding fossil assemblages.

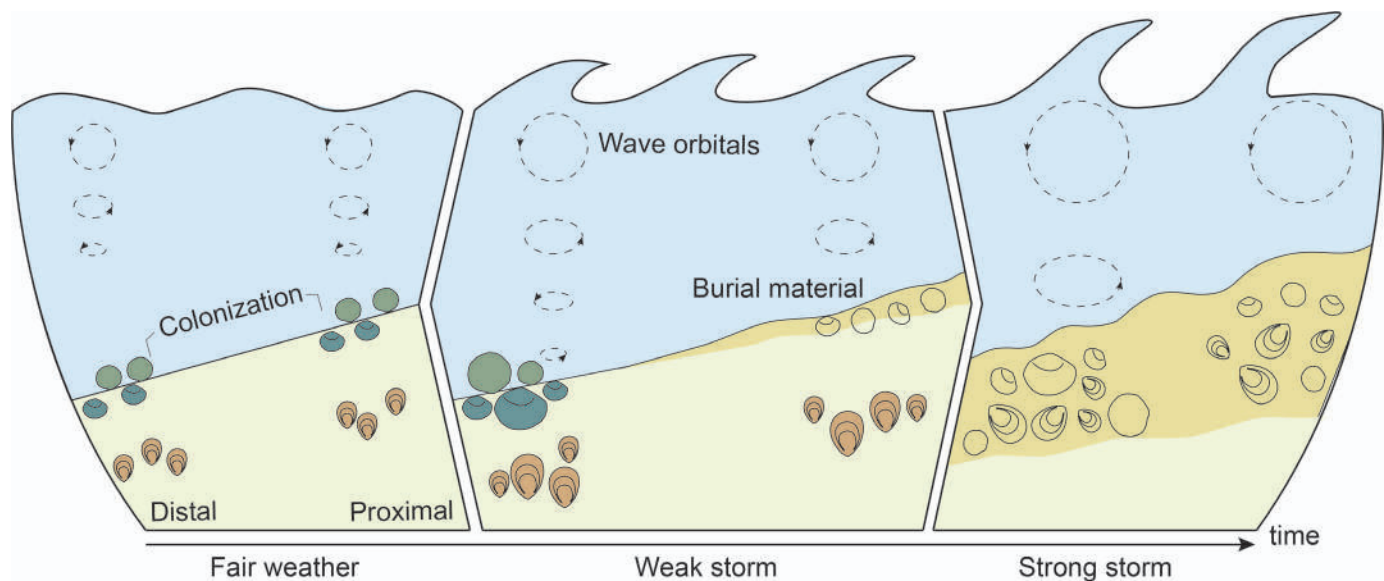


FIG. 4.—Model explaining the influence of storms on brachiopod and bivalve communities in the lower part of the Fezouata Shale (upper Tremadocian), Zagora area (Morocco).

ACKNOWLEDGMENTS

This paper is a contribution to the TelluS-SYSTER project 'Vers de nouvelles découvertes de gisements à préservation exceptionnelle dans l'Ordovicien du Maroc', funded by the INSU (Institut National des Sciences de l'Univers, France), CNRS. Harper is supported by the Leverhulme Trust (UK) and the Wenner-Gren Foundation (Sweden). This work was also funded by Grant Agency of the Czech Republic Project No.18-14575S and internal project of the Czech Geological Survey number 339900 to Polechová. The authors thank Pierre Sansjofre (Brest) for assistance during field work in Morocco, Muriel Vidal (Brest) and Daniel Vizcaíno (Carcassonne) for their help in the field and for the identification of trilobites, Juan Carlos Gutiérrez-Marco (Madrid) for the identification of the graptolites, Thomas Servais (Lille) for palynological analyses, as well as Vincent Perrier (Villeurbanne) and Peter Van Roy (Ghent) for their assistance in the identification of non-trilobite arthropods. Claude Colombié (Villeurbanne), Véronique Gardien (Villeurbanne), as well as Gabriela Mangano (Saskatoon), Andrew Bush (Storrs), Joe Botting and an anonymous reviewer are also thanked for their helpful and constructive remarks.

REFERENCES

- ALLAIRE, N., LEFEBVRE, B., NARDIN, E., MARTIN, E.L.O., VAUCHER, R., AND ESCARGUEL, G., 2017, Morphological disparity and systematic revision of the eocrinoid genus *Rhopalocystis* (Echinodermata, Blastozoa) from the Lower Ordovician of the central Anti-Atlas (Morocco): *Journal of Paleontology*, v. 91, p. 685–714.
- BABIN, C. AND DESTOMBES, J., 1990, Les mollusques bivalves et rostroconches ordoviciens de l'Anti-Atlas marocain: intérêt paléogéographique de leur inventaire. *Géologie Méditerranéenne*, v. 17, p. 243–261.
- BARRANDE, J., 1881, *Système Silurien du Centre de la Bohême*, Volume 6, Classe des Mollusques, Ordre des Acéphalées: Lemerier, Paris and Bellman, Prague, 342 p.
- BASSETT, M.G., POPOV, L.E., AND HOLMER, L.E., 1999, Organophosphatic brachiopods: patterns of biodiversification and extinction in the early Palaeozoic: *Geobios*, v. 32, p. 145–163.
- BOTTING, J.P., 2007, 'Cambrian' demosponges in the Ordovician of Morocco: insights into the early evolutionary history of sponges: *Geobios*, v. 40, p. 737–748.
- BOTTING, J.P., 2016, Diversity and ecology of sponges in the Early Ordovician Fezouata Biota, Morocco: *Palaeogeography, Palaeoclimatology, Palaeoecology*, v. 460, p. 75–86.
- BOTTING, J.P., MUIR, L.A., AND LEFEBVRE, B., 2013, Echinoderm diversity and environmental distribution in the Ordovician of the Builth Inlier, Wales: *PALAIOS*, v. 28, p. 293–304.
- BRENCHLEY, P.J. AND HARPER, D.A.T., 1998, *Palaeoecology: Ecosystems, Environments and Evolution*: Chapman and Hall, London, 407 p.
- CARTER, J.G., HARRIES, P.J., MALCHUS, N., SARTORI, A.F., ANDERSON, L.C., BIELER, R., BOGAN, A.E., COAN, E.V., COPE, J.C., CRAGG, S., AND GARCIA-MARCH, J., 2012, Illustrated glossary of the Bivalvia: *Treatise Online*, p. 1–209, doi: doi.org/10.17161/to.v0i0.4322.
- COPE, J.C.W., 1999, Middle Ordovician bivalves from Mid-Wales and the Welsh Borderland: *Palaeontology*, v. 42, p. 467–499.
- DESTOMBES, J., HOLLARD, H., AND WILLEFERT, S., 1985, Lower Palaeozoic rocks of Morocco, in C.H. Holland (ed.), *Lower Palaeozoic of North-Western and West Central Africa*: New York, Wiley, p. 91–336.
- EBBESTAD, J.O.R., 2016, Gastropoda, Tergomya and Paragastropoda (Mollusca) from the Lower Ordovician Fezouata Formation, Morocco: *Palaeogeography, Palaeoclimatology, Palaeoecology*, v. 460, p. 87–96.
- EMIG, C., 1997, Ecology of inarticulated brachiopods, in R.L. Kaesler (ed.), *Treatise on Invertebrate Paleontology, Part H, Brachiopoda 1 (Revised)*: Geological Society of America, Boulder, Colorado and The University of Kansas, Lawrence, Kansas, p. 473–495.
- FREEMAN, R.L., DATTILO, B.F., MORSE, A., BLAIR, M., FELTON, S., AND POJETA, J., JR., 2013, The "curse of *Rafinesquina*:" negative taphonomic feedback exerted by strophomenid shells on storm-buried lingulids in the Cincinnati Series (Katian, Ordovician) of Ohio: *PALAIOS*, v. 28, p. 359–372.
- GUTIERREZ-MARCO, J.C. AND MARTIN, E.L.O., 2016, Biostratigraphy and palaeoecology of Lower Ordovician graptolites from the Fezouata Shale: *Palaeogeography, Palaeoclimatology, Palaeoecology*, v. 460, p. 35–49.
- HAMMER, Ø., HARPER, D.A.T., AND RYAN, P.D., 2001, PAST—Paleontological Statistics software: package for education and data analysis: *Palaeontologia Electronica*, v. 4, p. 9.
- HAMMOND, L.S., 1983, Experimental studies of salinity tolerance, burrowing behavior and pedicle regeneration in *Lingula anatina* (Brachiopoda, Inarticulata): *Journal of Paleontology*, v. 57, p. 1311–1316.
- HARPER, D.A.T., 2006, The Ordovician biodiversification: setting an agenda for marine life: *Palaeogeography, Palaeoclimatology, Palaeoecology*, v. 232, p. 148–166.
- HAVLÍČEK, V., 1971, Brachiopodes de l'Ordovicien du Maroc: Notes et Mémoires du Service géologique du Maroc, v. 230, p. 1–135.
- HE, W., SHI, G.R., XIAO, Y., ZHANG, K., YANG, T., WU, H., ZHANG, Y., CHEN, B., YUE, M., SHEN, J., WANG, Y., YANG, H., AND WU, S., 2017, Body-size changes of latest Permian brachiopods in varied palaeogeographic settings in South China and implications for controls on animal miniaturization in a highly stressed marine ecosystem: *Palaeogeography, Palaeoclimatology, Palaeoecology*, v. 486, p. 33–45.
- HE, W.H., TWITCHETT, R.J., ZHANG, Y., SHI, G.R., FENG, Q.L., YU, J.X., WU, S.B., AND PENG, X.F., 2010, Controls on body size during the Late Permian mass extinction event: *Geobiology*, v. 8, p. 391–402.
- HUANG, B., HARPER, D.A.T., ZHAN, R., AND RONG, J., 2010, Can the Lilliput Effect be detected in the brachiopod faunas of South China following the terminal Ordovician mass extinction?: *Palaeogeography, Palaeoclimatology, Palaeoecology*, v. 285, p. 277–286.
- HUTCHINSON, Z.L., HENDRICK, V.J., BURROWS, M.T., WILSON, B., AND LAST, K.S., 2016, Buried alive: the behavioural response of the mussels *Modiolus modiolus* and *Mytilus edulis* to sudden burial by sediment: *PLoS ONE*, v. 11(3), doi: e0151471, doi:10.1371/journal.pone.0151471.

- JABLONSKI, D., 1996, Body size and macroevolution, in D. Jablonski, D.H. Erwin, and J.H. Lipps (eds.), *Evolutionary Paleobiology*: University of Chicago Press, Chicago, p. 256–289.
- KIDWELL, S., 1991, Taphonomy: releasing the data locked in the fossil record: *Topics in Geobiology*, v. 9, p. 211–290.
- KRÖGER, B. AND LEFEBVRE, B., 2012, Palaeogeography and palaeoecology of early Floian (Lower Ordovician) cephalopods from the Upper Fezouata Formation, Anti-Atlas, Morocco: *Fossil Record*, v. 15, p. 61–75.
- LEFEBVRE, B., ALLAIRE, N., GUENSBURG, T.E., HUNTER, A.W., KOURAÏSS, K., MARTIN, E.L.O., NARDIN, E., NOAILLES, F., PITTET, B., SUMRALL, C.D., AND ZAMORA, S., 2016a, Palaeoecological aspects of the diversification of echinoderms in the Lower Ordovician of central Anti-Atlas, Morocco: *Palaeogeography, Palaeoclimatology, Palaeoecology*, v. 460, p. 97–121.
- LEFEBVRE, B. AND BOTTING, J.P., 2007, First report of the mitrate *Peltocystis cornuta* Thoral (Echinodermata, Stylophora) in the Lower Ordovician of central Anti-Atlas (Morocco): *Annales de Paléontologie*, v. 93, p. 183–198.
- LEFEBVRE, B., EL HARIRI, K., LEROSSEY-AUBRIL, R., SERVAIS, T., AND VAN ROY, P., 2016b, The Fezouata Shale (Lower Ordovician, Anti-Atlas, Morocco): a historical review: *Palaeogeography, Palaeoclimatology, Palaeoecology*, v. 460, p. 7–23.
- LEFEBVRE, B., GUTIERREZ-MARCO, J.C., LEHNERT, O., MARTIN, E.L.O., NOWAK, H., AKODAD, M., EL HARIRI, K., AND SERVAIS, T., 2018, Age calibration of the Lower Ordovician Fezouata Lagerstätte, Morocco: *Lethaia*, v. 51, p. 296–311.
- LEGG, D.A., 2016, An acerostracan marrellomorph (Euarthropoda) from the Lower Ordovician of Morocco: *The Science of Nature*, v. 103, p. 1–7, doi: 10.1007/s00114-016-1352-5.
- LEHNERT, O., NOWAK, H., SARMIENTO, G.N., GUTIERREZ-MARCO, J.C., AKODAD, M., AND SERVAIS, T., 2016, Conodonts from the Lower Ordovician of Morocco—contributions to age and faunal diversity of the Fezouata Lagerstätte and peri-Gondwana biogeography: *Palaeogeography, Palaeoclimatology, Palaeoecology*, v. 460, p. 50–61.
- MARTIN, E.L.O., 2016, Communautés animales du début de l'Ordovicien (env. 480 Ma): études qualitatives et quantitatives à partir des sites à préservation exceptionnelle des Fezouata, Maroc: Unpublished Ph.D. Thesis, Lyon 1 University, France, 483 p.
- MARTIN, E.L.O., LEFEBVRE, B., AND VAUCHER, R., 2015, Taphonomy of a stylophoran-dominated assemblage in the Lower Ordovician of Zagora area (central Anti-Atlas, Morocco), in S. Zamora and I. Rabano (eds.), *Progress in Echinoderm Palaeobiology: Cuadernos del Museo Geominero*, v. 19, p. 95–100.
- MARTIN, E.L.O., PITTET, B., GUTIERREZ-MARCO, J.C., VANNIER, J., EL HARIRI, K., LEROSSEY-AUBRIL, R., MASROUR, M., NOWAK, H., SERVAIS, T., VANDENBROUCKE, T.R.A., VAN ROY, P., VAUCHER, R., AND LEFEBVRE, B., 2016a, The Lower Ordovician Fezouata Konservat-Lagerstätte: age, environment and evolutionary perspectives: *Gondwana Research*, v. 34, p. 274–283.
- MARTIN, E.L.O., VIDAL, M., VIZCAINO, D., VAUCHER, R., SANJOFRE, P., LEFEBVRE, B., AND DESTOMBES, J., 2016b, Biostratigraphic and palaeoenvironmental controls on the trilobite associations from the Lower Ordovician Fezouata Shale of the central Anti-Atlas, Morocco: *Palaeogeography, Palaeoclimatology, Palaeoecology*, v. 460, p. 142–154.
- MCALISTER, A.L., 1965, Systematics, affinities, and life habits of *Babinka*, a transitional Ordovician lucinoid bivalve: *Palaeontology*, v. 8, p. 231–246.
- MERGL, M., 1981, The genus *Orbithiele* (Brachiopoda, Inarticulata) from the Lower Ordovician of Bohemia and Morocco: *Věstník Ústředního ústavu geologického*, v. 56, p. 287–292.
- MERGL, M., 2002, Linguliformean and craniiformean brachiopods of the Ordovician (Těnice to Dobrotivá formations) of the Barrandian, Bohemia: *Sborník Národního muzea v Praze, B, Přírodní vědy*, v. 58, p. 1–82.
- MERGL, M. AND KORDULE, V., 2008, New middle Cambrian lingulate brachiopods from the Skryje-Týřovice area (Central Bohemia, Czech Republic): *Bulletin of Geosciences*, v. 83, p. 11–22.
- NOWAK, H., SERVAIS, T., PITTET, B., VAUCHER, R., AKODAD, M., GAINES, R.R., AND VANDENBROUCKE, T.R.A., 2016, Palynomorphs of the Fezouata Shale (Lower Ordovician, Morocco): age and environmental constraints of the Fezouata Biota: *Palaeogeography, Palaeoclimatology, Palaeoecology*, v. 460, p. 62–74.
- ORTEGA-HERNANDEZ, J., VAN ROY, P., AND LEROSSEY-AUBRIL, R., 2016, A new aglaspidid euarthropod with a six-segmented trunk from the Lower Ordovician Fezouata Konservat-Lagerstätte, Morocco: *Geological Magazine*, v. 153, p. 524–536.
- PAYNE, J.L. AND CLAPHAM, M.E., 2012, End-Permian Mass Extinction in the oceans: an ancient analog for the twenty-first century?: *Annual Review of Earth and Planetary Sciences*, v. 40, p. 89–111.
- PETTERSSON STOLK, S., HOLMER, L.E., AND CARON, J.-B., 2010, First record of the brachiopod *Lingulella waptaensis* with pedicle from the middle Cambrian Burgess Shale: *Acta Zoologica*, v. 91, p. 150–162.
- POLECHOVÁ, M., 2013, Bivalves from the Middle Ordovician Šarka Formation (Prague Basin, Czech Republic): *Bulletin of Geosciences*, v. 88, p. 427–461.
- POLECHOVÁ, M., 2016, The bivalve fauna from the Fezouata Formation (Lower Ordovician) of Morocco and its significance for palaeobiogeography, palaeoecology and early diversification of bivalves: *Palaeogeography, Palaeoclimatology, Palaeoecology*, v. 460, p. 155–169.
- POPOV, L.E., HOLMER, L.E., BASSETT, M.G., GHOBADI POUR, M., AND PERCIVAL, I.G., 2013, Biogeography of Ordovician linguliform and craniiform brachiopods, in D.A.T. Harper and T. Servais (eds), *Early Palaeozoic Biogeography and Palaeogeography: Geological Society of London, Memoir* 38, p. 117–126.
- READING, H.G., 1996, *Sedimentary Environments: Processes, Facies and Stratigraphy*, third edition: Blackwell Science, Oxford, 688 p.
- SÁNCHEZ, T.M., 2008, The early bivalve radiation in the Ordovician Gondwanan basins of Argentina: *Alcheringa*, v. 32, p. 223–246.
- SÁNCHEZ, T.M. AND BENEDETTO, J.L., 2007, The earliest known estuarine bivalve assemblage, Lower Ordovician of northwestern Argentina: *Geobios*, v. 40, p. 523–533.
- SAVRDA, C.E. AND BOTTIER, D.J., 1986, Trace-fossil model for reconstruction of paleo-oxygenation in bottom waters: *Geology*, v. 14, p. 3–6.
- SERVAIS, T. AND HARPER, D.A.T., 2018, The Great Ordovician Biodiversification Event (GOBE): definition, concept and duration: *Lethaia*, v. 51, p. 151–164.
- TASCH, P., 1953, Causes and paleontological significance of dwarfed fossil marine invertebrates: *Journal of Paleontology*, v. 27, p. 356–444.
- THAYER, C.W. AND STEELE-PETROVIC, H.M., 1975, Burrowing of the lingulid brachiopod *Glottidia pyramidata*: its ecologic and paleoecologic significance: *Lethaia*, v. 8, p. 209–221.
- TORVSIK, T.H. AND COCKS, L.R.M., 2011, The Palaeozoic palaeogeography of central Gondwana: *Geological Society of London, Special Publications*, v. 357, p. 137–166.
- TORVSIK, T.H. AND COCKS, L.R.M., 2013, Gondwana from top to base in space and time: *Gondwana Research*, v. 24, p. 999–1030.
- TWITCHETT, R.J., 2007, The Lilliput Effect in the aftermath of the end-Permian extinction event: *Palaeogeography, Palaeoclimatology, Palaeoecology*, v. 252, p. 132–144.
- URLICH, M., 2012, Stunting in some invertebrates from the Cassian Formation (Late Triassic, Carnian) of the Dolomites (Italy): *Neues Jahrbuch für Geologie und Paläontologie Abhandlungen*, v. 265, p. 1–25.
- VAN ITEN, H., MUIR, L., SIMOES, M.G., LEME, J.M., MARQUES, A.C., AND YODER, N., 2016, Palaeobiogeography, palaeoecology and evolution of Lower Ordovician conulariids and *Sphenothallus* (Meduzozoa, Cnidaria), with emphasis on the Fezouata Shale of southeastern Morocco: *Palaeogeography, Palaeoclimatology, Palaeoecology*, v. 460, p. 170–178.
- VAN ROY, P., 2006, Non-Trilobite Arthropods from the Ordovician of Morocco: Unpublished Ph.D. thesis, Ghent University, Belgium, 230 p.
- VAN ROY, P. AND BRIGGS, D.E.G., 2011, A giant Ordovician anomalocaridid: *Nature*, v. 473, p. 510–513.
- VAN ROY, P., BRIGGS, D.E.G., AND GAINES, R.R., 2015a, The Fezouata fossils of Morocco; an extraordinary record of marine life in the Early Ordovician: *Journal of the Geological Society*, v. 172, p. 541–549.
- VAN ROY, P., DALEY, A.C. AND BRIGGS, D.E.G., 2015b, Anomalocaridid trunk limb homology revealed by a giant filter-feeder with paired flaps: *Nature*, v. 522, p. 77–80.
- VAN ROY, P., ORR, P.J., BOTTING, J.P., MUIR, L.A., VINTHER, J., LEFEBVRE, B., EL HARIRI, K., AND BRIGGS, D.E.G., 2010, Ordovician faunas of Burgess Shale type: *Nature*, v. 465, p. 215–218.
- VAN ROY, P. AND TETLIE, O.E., 2006, A spinose appendage fragment of a problematic arthropod from the Early Ordovician of Morocco: *Acta Palaeontologica Polonica*, v. 51, p. 239–246.
- VAUCHER, R., MARTIN, E.L.O., HORMIERE, H., AND PITTET, B., 2016, A genetic link between Konservat- and Konservat-Lagerstätten in the Fezouata Shale (Lower Ordovician, Morocco): *Palaeogeography, Palaeoclimatology, Palaeoecology*, v. 460, p. 24–34.
- VAUCHER, R., PITTET, B., HORMIERE, H., MARTIN, E.L.O., AND LEFEBVRE, B., 2017, A wave-dominated, tide-modulated model for the Lower Ordovician of the Anti-Atlas, Morocco: *Sedimentology*, v. 64, p. 777–807.
- VERMEIL, G., 2016, Gigantism and its implications for the history of life: *PLoS ONE*, v. 11, e0146092, doi.org/10.1371/journal.pone.0146092.
- VIDAL, M., 1998, Trilobites (Asaphidae et Raphiophoridae) de l'Ordovicien inférieur de l'Anti-Atlas, Maroc: *Palaeontographica Abteilung A*, v. 251, p. 39–77.

Received 20 June 2018; accepted 13 November 2018.

Original Article

Cite this article: Saleh F, Vidal M, Laibl L, Sansjofre P, Gueriau P, Pérez-Peris F, Lustri L, Lucas V, Lefebvre B, Pittet B, El Hariri K, and Daley AC. Large trilobites in a stress-free Early Ordovician environment. *Geological Magazine* <https://doi.org/10.1017/S0016756820000448>

Received: 1 October 2019

Revised: 1 April 2020

Accepted: 17 April 2020




Keywords:

Arthropod; body size; Palaeozoic; Fezouata Shale

Author for Correspondence: Farid Saleh,

Email: farid.saleh@univ-lyon1.fr

Large trilobites in a stress-free Early Ordovician environment

Farid Saleh¹ , Muriel Vidal², Lukáš Laibl^{3,4,5}, Pierre Sansjofre⁶, Pierre Gueriau³ , Francisc Pérez-Peris³ , Lorenzo Lustri³, Victoire Lucas¹, Bertrand Lefebvre¹, Bernard Pittet¹, Khadija El Hariri⁷ and Allison C. Daley³

¹Université de Lyon, Université Claude Bernard Lyon1, École Normale Supérieure de Lyon, CNRS, UMR5276, LGL-TPE, Villeurbanne, France; ²Université de Brest, CNRS, IUEM Institut Universitaire Européen de la Mer, UMR 6538 Laboratoire Géosciences Océan, Place Nicolas Copernic, 29280 Plouzané, France; ³Institute of Earth Sciences, University of Lausanne, Géopolis, CH-1015 Lausanne, Switzerland; ⁴Czech Academy of Sciences, Institute of Geology, Rozvojová 269, 165 00 Prague 6, Czech Republic; ⁵Institute of Geology and Palaeontology, Faculty of Science, Charles University, Albertov 6, Prague, 12843, Czech Republic; ⁶MNHN, Sorbonne Université, CNRS UMR 7590, Institut de Minéralogie, de Physique des Matériaux et de Cosmochimie, Paris, France and ⁷Département des Sciences de la Terre, Faculté des Sciences et Techniques, Université Cadi-Ayyad, BP 549, 40000 Marrakesh, Morocco

Abstract

Understanding variations in body size is essential for deciphering the response of an organism to its surrounding environmental conditions and its ecological adaptations. In modern environments, large marine animals are mostly found in cold waters. However, numerous parameters can influence body-size variations other than temperatures, such as oxygenation, nutrient availability, predation or physical disturbances by storms. Here, we investigate trilobite size variations in the Lower Ordovician Fezouata Shale deposited in a cold-water environment. Trilobite assemblages dominated by small- to normal-sized specimens that are a few centimetres in length are found in proximal and intermediate settings, while those comprising larger taxa more than 20 cm in length are found in the most distal environment of the Fezouata Shale. Drill core material from distal settings shows that sedimentary rocks hosting large trilobites preserved *in situ* are extensively bioturbated with a high diversity of trace fossils, indicating that oxygen and nutrients were available in this environment. In intermediate and shallow settings, bioturbation is less extensive and shallower in depth. The rarity of storm events (minimal physical disturbance) and the lack of predators in deep environments in comparison to shallower settings would also have helped trilobites attain larger body sizes. This highly resolved spatial study investigating the effects of numerous biotic and abiotic parameters on body size has wider implications for the understanding of size fluctuations over geological time.

1. Introduction

Considered one of the most important aspects of animal biology (Bonner, 2006), body size results from numerous biotic and abiotic factors (Bell, 2014). Vertebrate size variations over geological time have received considerable attention (Sander & Clauss, 2008; Geiger *et al.* 2013). Comparatively, marine invertebrates have been less studied (Lamsdell & Braddy, 2009; Klug *et al.* 2015; Sigurdson & Hammer, 2016). For instance, it is well agreed that low temperatures can be responsible for the large sizes of modern marine invertebrates (i.e. Bergmann's rule; Timofeev, 2001; Moran & Woods, 2012). Nevertheless, if this was the sole parameter controlling body size, all taxa at high latitudes should be larger than genera found at lower latitudes. This is rarely the case because size variations occur locally in a specific palaeoenvironment, as a result of changes in water depth, oxygenation, predation, nutrient availability or even physical disturbances caused by storm events (Saleh *et al.* 2018).

During the Ordovician Period, Morocco was part of the Gondwana margins, at high latitudes, close to the South Pole. The Fezouata Shale was deposited in the Zagora region in Morocco, under cold waters at the transition between two major evolutionary events: the Cambrian Explosion and the Great Ordovician Biodiversification Event (Martin *et al.* 2016b). In this formation, two sedimentary intervals have yielded thousands of exceptionally preserved fossils belonging to different groups such as arthropods, echinoderms, molluscs and sponges (Vinther *et al.* 2008, 2017; Van Roy *et al.* 2010, 2015a; Martí Mus, 2016; Lefebvre *et al.* 2019). A striking feature of this formation is extreme body size fluctuations at both taxon and assemblage scales between localities and even between different levels of the same locality (for further details, see Ebbestad, 2016; Lefebvre *et al.* 2016; ELO Martin, unpub. PhD thesis, University of Lyon, 2016; Saleh *et al.* 2018). Trilobites occur in all sites from the Fezouata Shale and show a large body-size range in this formation. Abundant and spectacular specimens of very large trilobites were found at Ouled Slimane near the Tansikht bridge

(Rábano, 1990; Fortey, 2009; Lebrun, 2018). In this study, the sedimentological and taphonomic contexts of levels with large trilobites from the Fezouata Shale are elucidated, in order to contribute to the understanding of body-size fluctuations in the geological record (see also Lamsdell & Braddy, 2009; Klug et al. 2015; Sigurdson & Hammer, 2016).

2. Geological and palaeoenvironmental context

A long-term transgression at the beginning of the Ordovician Period created epicontinental seas on the Gondwana margins in the Southern Hemisphere (Torsvik & Cocks, 2011, 2013). The Fezouata Shale Formation (Fig. 1a) was deposited in a cold-water sea at high latitudes (over 60° S), close to the South Pole (Fig. 1b) (Torsvik & Cocks, 2013; Martin et al. 2016a). Sedimentary rocks of this formation consist of blue-green to yellow-green siltstones (Destombes et al. 1985). The 900-m-thick succession of the Fezouata Shale (Fig. 1a) was deposited in a storm/wave-dominated environment with a minor influence of tides (Vaucher et al. 2016). In this environment, sedimentological structures indicate a deepening trend from the SE to the NW (Fig. 1c) as shown in Vaucher et al. (2017). The most proximal settings during late Tremadocian time (*A. murrayi* Zone) therefore occur near Tamegroute (about 20 km ESE of Zagora; Fig. 1c) (Saleh et al. 2018). In this locality, sedimentary rocks comprise coarse siltstones to fine-grained sandstones showing hummocky cross-stratifications (HCS) of centimetre- to decimetre-scale wavelengths (Vaucher et al. 2016) (Fig. 1d). Intermediate settings of the Fezouata Shale occur in Bou Izargane in the Ternata plain about 20 km north of Zagora (Fig. 1c). In this setting, sedimentary rocks are characterized by finer siltstones and more abundant background sediments than in Tamegroute, in addition to the presence of storm events with up to centimetre-scale HCS (Saleh et al. 2019) (Fig. 1d). The average sedimentation rate in this area was estimated ~79 m/Ma (Saleh et al. 2019). The progradation model proposed by Vaucher et al. (2017) suggests that the Ouled Slimane area is associated with more distal settings (Fig. 1c). A field campaign was organized in 2019 to better constrain the depositional environment of this locality (see Section 3).

As for the faunal content of the different sites, all three localities yielded diverse assemblages of marine invertebrates (Saleh et al. 2018). However, Tamegroute is characterized by sessile epibenthic taxa (bivalves, brachiopods) that are about half the size of those in Bou Izargane (Saleh et al. 2018). Size variations in the Fezouata Shale between localities are not limited to brachiopods and bivalves. Trilobites also show body-size discrepancies between localities. The largest trilobites from the Fezouata Shale are found at Ouled Slimane (Rábano, 1990; Fortey, 2009; Lebrun, 2018).

3. Materials and methods

Two successive field campaigns were carried out in the Zagora region in 2018 and 2019 and two cores were obtained. The first core (c. 13 m) was drilled in the intermediate setting of Bou Izargane. The second core (c. 2.5 m) was made in Ouled Slimane, crossing the interval in which large trilobites were discovered. Both cores correspond strictly to the same stratigraphic interval in the *Araneograptus murrayi* biozone (Vaucher et al. 2016; Saleh et al. 2018). Cores were described for their lithology, grain size, depositional sedimentary structures and bioturbation intensity and size at the University of Lausanne, Switzerland, and are

currently deposited at the University of Brest. All levels crossed by cores were repeatedly sampled from 2004 to 2017, and yielded a large number of fossils (most of them are deposited in the collections of the Cadi-Ayyad University, Marrakesh). Trilobite taxa and assemblages discovered in these levels are determined at the specific or generic level. The size distribution of trilobites was investigated between localities by measuring the full length of individuals from the anterior margin of the cephalon to the posterior margin of the pygidium. The sizes of representatives of the trilobite genus *Platypeltoides*, which occurs in all localities (Table 1), were measured based on the sagittal length of the pygidium, including articulation half ring.

The current taxonomy of *Platypeltoides* is uncertain. *Platypeltoides magrebiensis* Rábano, 1990 was the only species of this genus reported from the Fezouata Shale (Rábano, 1990; Martin et al. 2016b). Recently, Corbacho et al. (2018) described four species of *Platypeltoides* from Morocco. The differences between these species are based on genal spine morphologies, the position of the eyes and the presence/absence of an anterior border (Corbacho et al. 2018). There are several issues with the definition of the new species. First, the morphology of the genal spine changes remarkably during ontogeny (Chatterton, 1980; Chatterton & Speyer, 1997; Park & Choi, 2009; Laibl et al. 2015) and differences in the position of eyes can be an effect of taphonomic compression (see Hughes & Rushton, 1990 for detailed explanation). Second, genal spines in Moroccan trilobites are often artificially modified by local collectors (Gutiérrez-Marco & García-Bellido, 2018). Most importantly, species other than *P. magrebiensis* are based on the description of a single specimen (*P. hammondi* Corbacho & López-Soriano, 2016; *P. carmenae* Corbacho et al. 2017) or four specimens (*P. cuervoae* Corbacho & López-Soriano, 2012). Consequently, until more material is found and a comprehensive revision of the genus is performed, we consider *P. magrebiensis* as the only valid species and refer all our material to it.

4. Results

4.a. Trilobite size and preservation

The most diverse trilobite assemblage is found in the intermediate setting locality, Bou Izargane (i.e. seven taxa; Table 1). Four of these taxa are also found in the more proximal site of Tamegroute. *Platypeltoides magrebiensis* is the only taxon that is found across the proximal-distal axis (Table 1). The mean total sagittal length of all trilobite taxa recorded in the distal site of Ouled Slimane is 32.4 cm (median = 31.9 cm; standard deviation (SD) = 1.41 cm; $n = 31$), which is four times larger than the mean total sagittal length of all trilobites recorded in Bou Izargane (mean = 7.37 cm; median = 5.9 cm; SD = 1.21 cm; $n = 14$), and eight times larger than the mean total sagittal length of all trilobites recorded in Tamegroute (mean = 3.78 cm; median = 3.7 cm; SD = 1.24 cm; $n = 15$) (Fig. 2a; and online Supplementary Tables S1 and S2, available at <http://journals.cambridge.org/geo>). Total sagittal lengths of trilobite forming the assemblages in Ouled Slimane, Bou Izargane and Tamegroute are statistically normally distributed (Shapiro-Wilk test, P value: 0.97, 0.23 and 0.4, respectively) (online Supplementary Table S3). Trilobite size variations between two contiguous localities (i.e. Ouled Slimane and Bou Izargane, Bou Izargane and Tamegroute) are significantly different (t-test, P value: 3.85×10^{-14} and 0.006, respectively; see online Supplementary Table S4). The increase in size between proximal and distal sites is not only evidenced between assemblages, but also between different species

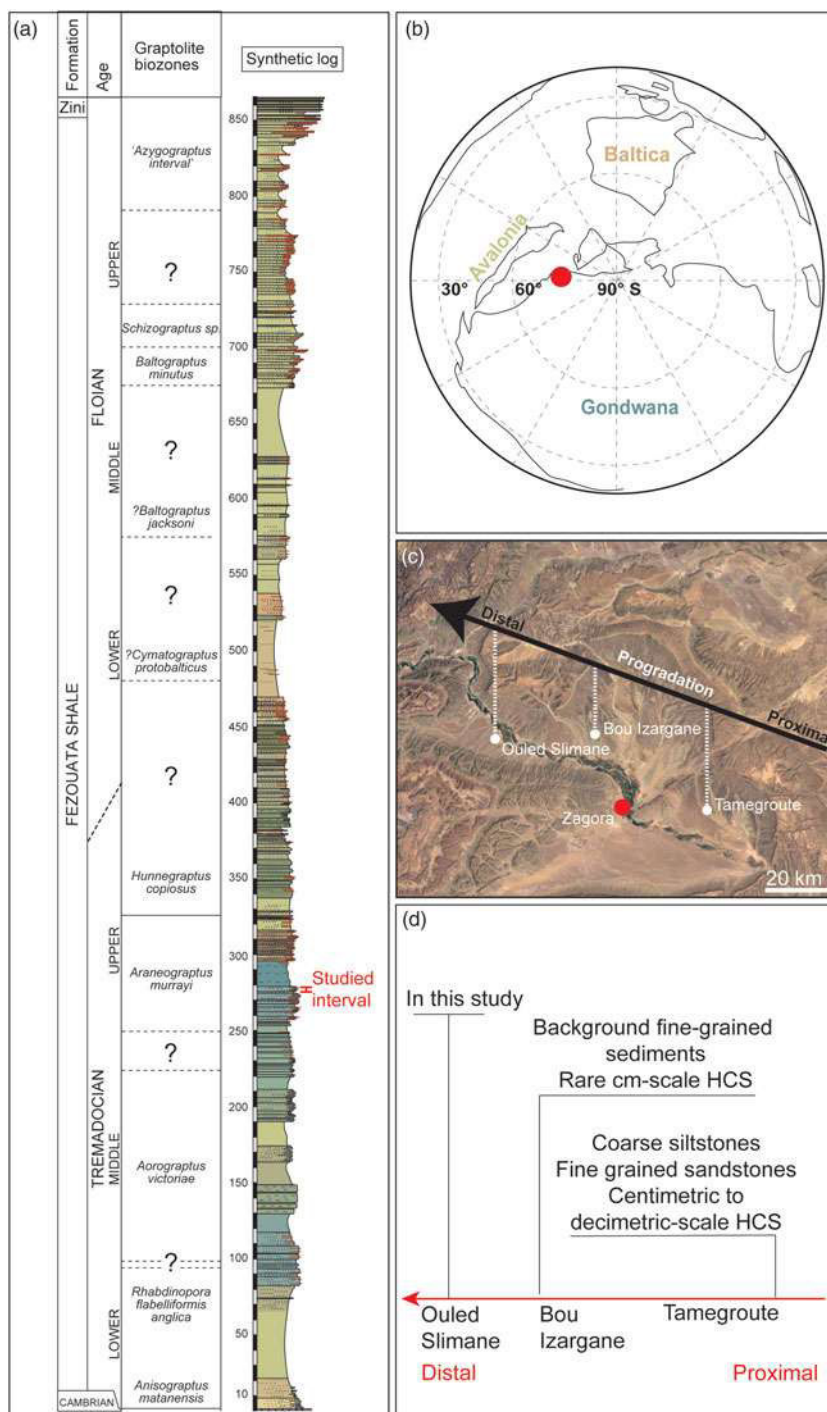


Fig. 1. (Colour online) General geographical context of the Fezouata Shale. (a) Stratigraphic sequence of the Fezouata Shale with the studied interval. (b) Location of Morocco during Early Ordovician time near the South Pole (modified from Vaucher *et al.* 2017). (c) Deepening trend in the Fezouata Shale from the SE to the NW (modified from Vaucher *et al.* 2017), with the study localities Ouled Slimane, Bou Izargane and Tamegroute indicated. (d) Proximal to distal relative position of the three localities studied here: Ouled Slimane, Bou Izargane and Tamegroute. HCS – hummocky cross-stratifications.

belonging to the same group (e.g. *Asaphellus* belonging to asaphids, and *Platypeltoides* belonging to nileids; Table 1).

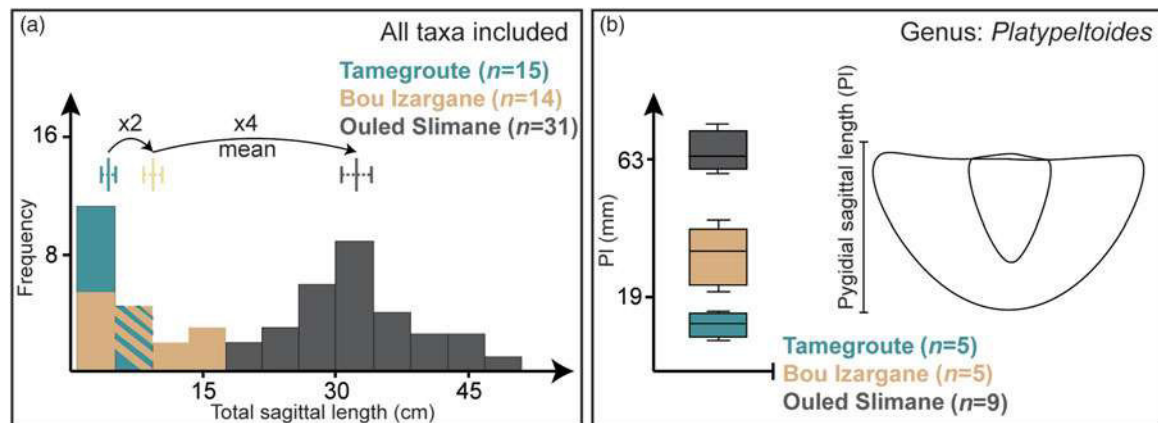
The mean pygidial sagittal length including axial half ring of *Platypeltoides* in Ouled Slimane is 6.3 cm (median = 6.2 cm; SD = 0.5 cm; $n = 9$), which is twice as long as than the mean pygidial sagittal length recorded in Bou Izargane (mean = 3.3 cm; median = 3.5 cm; SD = 0.84 cm; $n = 5$) and four times as large as the mean mean pygidial sagittal length recorded in Tamegroute (mean = 1.29 cm; median = 1.32 cm; SD = 0.35 cm; $n = 5$) (Fig. 2b, see online Supplementary Tables S5 and S6 for detailed measurements and summary statistics). Pygidial sagittal length measurements for

Platypeltoides are normally distributed in Ouled Slimane, Bou Izargane and Tamegroute (Shapiro-Wilk test, P value: 0.39, 0.76 and 0.19 respectively; see online Supplementary Table S7). Pygidial sagittal length variations for *Platypeltoides* between Ouled Slimane and Bou Izargane, in addition to those between Bou Izargane and Tamegroute, are statistically significantly different (t-test, P value: 0.0012 and 3.5×10^{-6} , respectively) (online Supplementary Table S8).

Trilobites from Ouled Slimane are preserved in silicified, quartz-rich concretions. Some are disarticulated and others are complete (Fig. 3a–e). Trilobites from the two other localities are preserved in shales (Fig. 3f–h).

Table 1. Trilobite diversity, abundances and sizes in the studied localities from the Lower Ordovician of the Fezouata Shale

Locality	Trilobite	No.	Size range (cm)
Tamegroute	<i>Anacheirurus adserai</i> (Vela & Corbacho, 2007)	2	4–4.8
	<i>Asaphellus</i> sp. aff. <i>jujuanus</i> Harrington, 1937	2	3.7–4.1
	<i>Bavarilla</i> sp.	4	2.2–2.8
	<i>Euloma</i> sp.	2	3.1
	<i>Platypeltoides magrebiensis</i> Rábano, 1990	5	3.3–6.2
Bou Izargane	<i>Asaphellus</i> sp. aff. <i>jujuanus</i> Harrington, 1937	2	3.9–6.2
	<i>Bavarilla</i> sp.	2	3.7–4.1
	<i>Euloma</i> sp.	1	3.8
	<i>Geragnostus</i> sp.	1	0.9
	<i>Megistaspis</i> sp.	1	5.6
	<i>Platypeltoides magrebiensis</i> Rábano, 1990	5	8.5–16.1
Ouled Slimane	<i>Symphysurus</i> sp.	2	3.9–4.2
	<i>Asaphellus stubbsi</i> Fortey, 2009	7	24.1–38
	<i>Dikelocephalina brenchleyi</i> Fortey, 2010	13	24.2–33.7
	<i>Ogyginus</i> sp.	7	39.2–49.1
	<i>Platypeltoides magrebiensis</i> Rábano, 1990	4	18–23

**Fig. 2.** (Colour online) Trilobite size fluctuations in the Fezouata Shale. (a) General body size patterns, all taxa included, in Ouled Slimane, Bou Izargane and Tamegroute. (b) Differences in the pygidial sagittal length of *Platypeltoides magrebiensis* between localities.

4.b. Sedimentological context

The background sediments in Bou Izargane in the Fezouata Shale consist of very fine siltstones to claystones (Fig. 4a–d). In Bou Izargane, coarse siltstone event deposits are abundant (Fig. 4e). Event deposits have an erosive base and show occasionally HCS (Fig. 4e). In Ouled Slimane, event deposits are rare and consist of quartz silts that are finer than in Bou Izargane (generally < 40 µm) (Fig. 4a). When they occur, they do not exceed 1 cm in thickness and lack HCS (Fig. 4a). Bioturbation occurs in all cores but it shows variations in both depth and intensity. Some intervals are only lightly bioturbated with a bioturbation depth of around 1 mm, while others are highly bioturbated with a bioturbation depth of a few centimetres (Fig. 4f). Intensity of bioturbation varies from light (< 10% of sedimentary rocks showing

evidence of biological activity) to moderate (10–30% of sedimentary rocks showing evidence of biological activity), high (30–70% of sedimentary rocks affected by biological activity) and extreme (> 70% of sedimentary rocks reworked by biological activity). The used scale for the studied cores is simplified after the bioturbation index in Taylor & Goldring (1993). However, there is no direct correlation between bioturbation depth and intensity. Some intervals can be extremely bioturbated with a bioturbation depth that does not exceed a few millimetres (Fig. 4c). Generally, sediments from Ouled Slimane are more extensively bioturbated than in Bou Izargane in terms of both intensity of their traces and their depth (Fig. 4f). In Bou Izargane, bioturbation is generally less than 1 cm in depth (Fig. 4f).



Fig. 3. (Colour online) Trilobites from the Fezouata Shale, Morocco. (a–e) Large trilobites from Ouled Slimane preserved in concretions. (a) External moulds of trilobites not picked up by collectors. (b) Thorax and pygidium of *Platypeltoides magrebiensis*. (c) Incomplete cranium of *Platypeltoides* sp. (d) Part of the thorax and pygidium of *Dikelocephalina brenchleyi*. (e) Pygidium of *Asaphellus stubbsi*. (f) Normal-sized *Symphysurus* sp. from Bou Izargane. (g, h) Normal-sized *Platypeltoides magrebiensis* from (g) Bou Izargane and (h) Tamegroute preserved in shales (AATGR0aOI132).

5. Interpretation and discussion

5.a. Depositional environment and preservation

In marine settings, grain sizes are indicative of the distance travelled from the source by sediments (Nichols, 2009). In the Fezouata Shale, coarse grains are found towards the south east, closer to the source, compared with finer sediments that are mainly deposited in the basin (Vaucher *et al.* 2016, 2017). Furthermore, the abundance of storm events is indicative of the energy of the depositional environment (Nichols, 2009; Perillo *et al.* 2014).

Stacked storm events designate a shallow unstable environment that is constantly agitated by waves (Nichols, 2009). In these agitated settings, waves generate orbitals in the water column that decrease in size with depth, leaving oscillation traces such as HCS on the sea floor (Vaucher *et al.* 2016, 2017). The deeper the water column, the smaller are the HCS. The presence in the Fezouata Shale of very fine siltstones to claystones with a scarce presence of storm events and an absence of HCS therefore indicate that the sedimentary succession at Ouled Slimane was deposited relatively far from the source in a stable environment that was

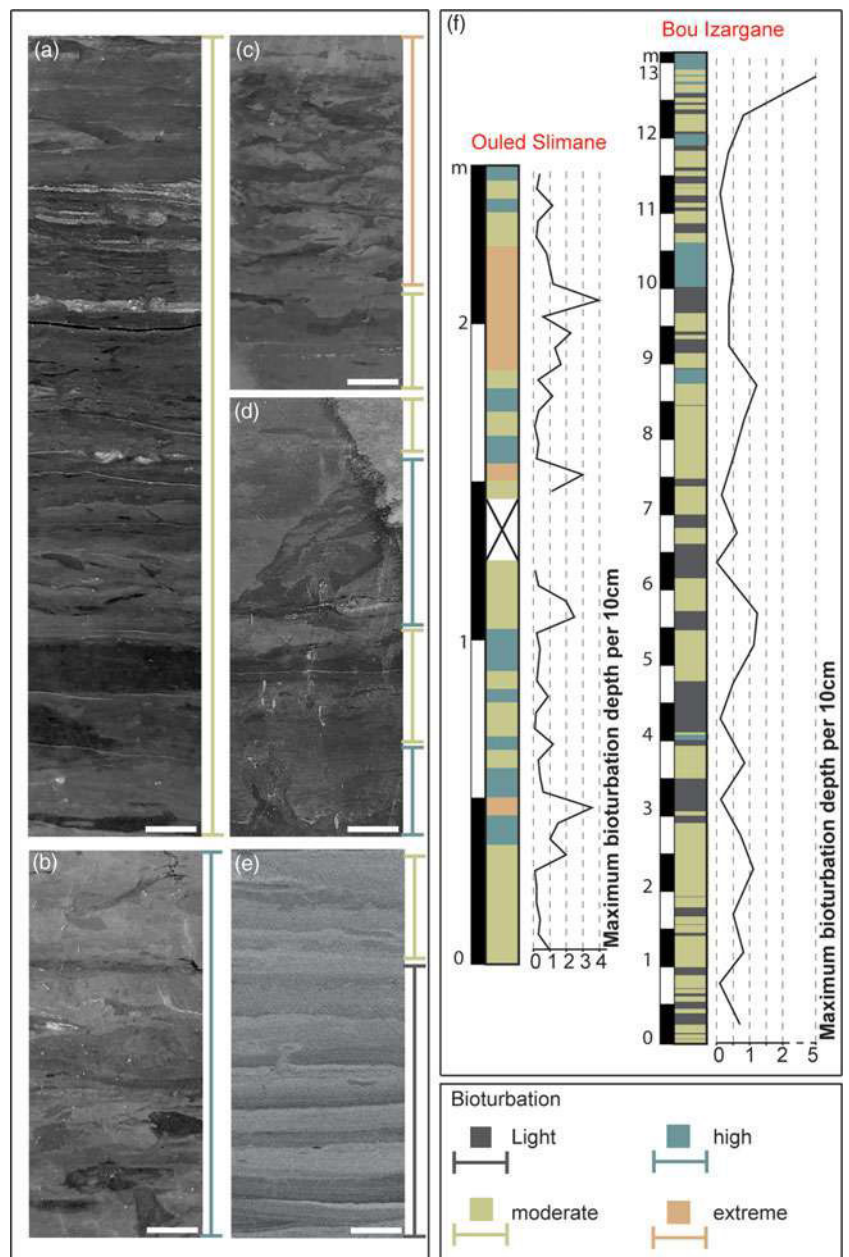


Fig. 4. (Colour online) Drilled sedimentary rocks from Ouled Slimane and Bou Izargane. (a) Core sediments from Ouled Slimane showing the dominance of background clayey to silty sediments with rare, coarser-grain-event deposits. Bioturbation intensity variations between intervals at Ouled Slimane from (a) light to (b) high and (c) extreme. (d) Bioturbation depth of a few centimetres in Ouled Slimane. (e) Core sediments from Bou Izargane are less bioturbated and more affected by storm deposits. (f) Bioturbation intensity and depth along the core in Ouled Slimane and Bou Izargane. All scale bars are 1 cm in length.

rarely agitated by storm waves. In the Fezouata Shale, Ouled Slimane is the most distal locality. Despite being distal in position, an abundant bioturbation (i.e. light, high and extreme) with variable depth (from a few millimetres to 4 cm) and a high diversity of trace fossils are observed in the sedimentary succession in Ouled Slimane. This confirms that this environment was colonized by benthic organisms and shows that little to no chemical stress (i.e. related to nutrients and oxygen availability) occurred in the bottom of the water column, but also, at least, in surface sediments.

In the Fezouata Shale, two modes of preservation have been evidenced. The first mode, consisting of the preservation of both mineralized and soft-bodied taxa in shales, is well understood (Martin *et al.* 2016a; Saleh *et al.* 2019). Living organisms of the Fezouata Biota colonized the sea floor and were repeatedly buried *in situ* by event deposits (Vaucher *et al.* 2017). The second mode consists of preservation in concretions, and the processes underlying it are

more complex (McCoy *et al.* 2015a, b). Siliceous concretions similar to those preserving large trilobites at Ouled Slimane have been described from distal settings of the Fezouata Shale by Gaines *et al.* (2012) and Vaucher *et al.* (2017). The original siliceous material for the formation of these concretions comes from more proximal localities (Vaucher *et al.* 2017). However, the growth of these concretions was controlled by the decay rates of dead animals covered by event deposits (Gaines *et al.* 2012). Permissive anoxic conditions are established when a large carcass is decaying, leading to mineral overgrowth around decaying carcasses (Gaines *et al.* 2012). This model was used to explain the preservation of giant and complete invertebrates *in situ* in the Fezouata Shale (i.e. radiodonts such as *Aegirocassis*; Gaines *et al.* 2012; Van Roy & Briggs, 2011; Van Roy *et al.* 2015b). The presence of partially articulated and complete large trilobites in the concretions from Ouled Slimane argue, in a similar way to *Aegirocassis*, in favour of an

autochthonous preservation. If transport occurred, it was most likely limited and from the same distal setting (i.e. a few metres only).

5.b. Body-size fluctuations

Many trilobite genera included in this study have also been discovered from other high-latitude (peri) Gondwanan localities. For instance, the Třenice and Mílina formations (upper Tremadocian; Czech Republic) have yielded a large number of trilobites comparable in size to those found in Tamegroute and Bou Izargane (i.e. total sagittal length of *Anacheirurus* c. 3.5 cm, *Euloma* c. 2.5 cm, *Platypeltoides* c. 5.5 cm, *Geragnostus* c. 0.6 cm; see e.g. Mergl, 2006). Other assemblages of similarly sized trilobites are known in the upper Tremadocian Saint-Chinian Formation, France (i.e. total sagittal length of *Euloma* c. 3.3 cm, *Geragnostus* c. 1.1 cm, *Megistaspis* c. 3.9 cm, *Symphysurus* c. 3.4 cm; Thorall, 1935; Capéra *et al.* 1975, 1978; Courtessole & Pillet, 1975; Courtessole *et al.* 1981). *Euloma* was also found in the upper Tremadocian Vogtendorf Formation of Germany with a total sagittal length of c. 5.5 cm (Sdzuy *et al.* 2001).

Although rare in the fossil record, occurrences of large trilobites are not restricted to the lower part of the Fezouata Shale. Other known occurrences include, for example: the Cambrian Series 2 Emu Bay Shale, Australia (Holmes *et al.* 2020); the Cambrian Series 2 to Miaolingian Jbel Wawrmast Formation of Morocco (Geyer, 1993); the Early Ordovician ‘Schistes à Gâteaux’ Formation, France (Thorall, 1946; P. Bérard, unpub. PhD thesis, University of Montpellier, 1986); the Middle Ordovician Valongo Formation, Portugal (Rábano, 1990; Gutiérrez-Marco *et al.* 2009); the Late Ordovician Churchill River Group, Canada (Rudkin *et al.* 2003); and the Middle Devonian Onondaga Limestone, New York, USA (Whiteley *et al.* 2002). In general, the largest trilobites occur in a wide array of environments. Some of them were reported from low-latitude nearly equatorial areas, in shallow-water carbonates (Whiteley *et al.* 2002; Rudkin *et al.* 2003) or deeper, but still near-shore siliciclastic deposits (Paterson *et al.* 2016). Others come from high latitudes (over 60° S) of the West Gondwana margin, where they are preserved either in distal mudstones (Gutiérrez-Marco *et al.* 2009), fine-grained sandstones and shales (Geyer, 1993), and concretions (Thorall, 1946; P. Bérard, unpub. PhD thesis, University of Montpellier, 1986). The best analogue for the Ouled Slimane assemblage is therefore probably the Early Ordovician fauna described in the ‘Schistes à Gâteaux’ of the Cabrières area (eastern-most part of the southern Montagne Noire; P. Bérard, unpub. PhD thesis, University of Montpellier, 1986). In this region, similarly sized concretions (70–100 cm in diameter) formed under comparable depositional settings yielded abundant remains of both disarticulated and fully articulated large trilobites belonging to Asaphidae and Nileidae (P. Bérard, unpub. PhD thesis, University of Montpellier, 1986). During Early Ordovician time, the Montagne Noire area was situated at relatively high latitudes, not far away from the Anti-Atlas area, on the western margin of Gondwana. In general, high latitudes and consequently low temperatures are often considered as the main explanatory factor for trilobite gigantism (Gutiérrez-Marco *et al.* 2009; Klug *et al.* 2015). Given the widespread distribution of large trilobites in various latitudes and facies, it is unlikely that there is only one single controlling mechanism of trends toward larger sizes. Indeed, the trilobite size fluctuations within the Fezouata Shale in a comparatively restricted area suggest that, despite high latitudes, other factors must be taken into consideration.

In the Fezouata Shale, differences in size distribution between localities can be the result of numerous mechanisms and conditions (ontogeny, size sorting due to transport, oxygenation and/or nutrient availability; Saleh *et al.* 2018). Transport-induced size sorting is unlikely to explain the size discrepancies of trilobites in general and *Platypeltoides* in particular. When current-related sorting occurs in marine environments, small individuals are more easily transported than larger ones, and they are consistently displaced towards more distal settings (Johnson, 1960; Fagerstrom, 1964). The opposite pattern for trilobites is observed in the Fezouata Shale. Furthermore, all previous surveys made on brachiopods, bivalves, echinoderms and trilobites from this part of the Fezouata Shale have concluded that most fossils were preserved *in situ* (with occasional limited transport), because delicate anatomical structures were preserved (Saleh *et al.* 2018). Brachiopods of the Fezouata Shale frequently have their setae preserved (Saleh *et al.* 2018) and, in many cases, the most fragile skeletal elements of strophoran echinoderms remained connected to the rest of the body (Martin *et al.* 2015; Lefebvre *et al.* 2016, 2019). As trilobites had a chitinous, partially biomineralized exoskeleton (Teigler & Towe, 1975), their remains are frequently preserved in marine Palaeozoic deposits (Speyer & Brett, 1986). Given that post-mortem processes are insufficient to explain the size distribution seen in the Fezouata Shale (this study; Saleh *et al.* 2018), the presence of large trilobites in only the most distal palaeoenvironments is taken as representative of the original size distribution of organisms. The increase in trilobite size from shallow proximal to deep distal localities in the Fezouata Shale is consistent with observations of crustacean body-size fluctuations in modern marine environments, in which large animals are found in deep-water settings (Horikoshi, 1986; Timofeev, 2001).

The increase in size between proximal and distal localities may be related to ontogeny (e.g. Laibl *et al.* 2014), with younger (and therefore smaller) developmental stages favouring shallower environments, and older and larger ones preferring deeper settings. If this was the case all taxa should be found in all localities, which is not true for the Fezouata Shale. For instance, Ouled Slimane seems to entirely lack small- and medium-sized taxa (e.g. *Bavarilla*, *Anacheirurus*, *Euloma*), with the exception of *Platypeltoides magrebiensis* (Table 1 and online Supplementary Table S1). *Dikelocephalina* and *Oxyginus* are present in Ouled Slimane, but are absent in more proximal sites (Table 1 and online Supplementary Table S1). Ontogeny alone does not explain size discrepancies observed for *Platypeltoides magrebiensis*, because the material measured here consistently excluded juvenile stages (defined by the number of thoracic segments). Even if future work shows a correlation between changes in habitats and developmental stages of some trilobites, this fails to explain why older and bigger individuals preferred deeper environments. There must therefore have been external biotic and abiotic conditions that selected for larger bodies in a deeper setting and smaller bodies in more proximal environments.

Oxygen availability is an abiotic parameter that can influence the body-size distribution of marine taxa (Zeuthen, 1953). It is suggested that large sizes are dictated by oxygen availability rather than by temperature in modern polar ecosystems (Chapelle & Peck, 1999). Oxygen concentration correlates with the general trend in marine gigantism during the Palaeozoic Era (Vermeij, 2016), and a direct connection (i.e. in magnitude) between Palaeozoic gigantism and atmospheric hyperoxia was also established using a mathematical model based on oxygen transport limitation (Payne *et al.* 2012). In contrast, benthic individuals tend to

have smaller sizes in oxygen minima zones (i.e. Lilliput effect; Twitchett, 2007). However, for instance in Tamegroute, the bottom of the water column was oxic, leading to the development of diverse assemblages on the sea floor (Saleh *et al.* 2018).

Another abiotic factor that can limit size growth is nutrient availability (Booth *et al.* 2008). Nutrients are generally more abundant in proximal sites near the source (Rowe *et al.* 1975; Philippart *et al.* 2000; Wang *et al.* 2003). The occurrence of a relatively high and diverse bioturbation in Ouled Slimane (Fig. 4a–d) suggests that nutrients were not a limiting parameter. This interpretation is in accordance with the presence of diverse planktonic micro-organism assemblages in the deepest settings of the Fezouata Shale (Nowak *et al.* 2016).

Storm turbulences generate another abiotic stress in shallow environments (Barry & Dayton, 1991; McAlister & Stanczyk, 2005). Storms transport sediments that can cause the suffocation of both sessile and mobile invertebrate taxa in proximal sites (Tabb & Jones, 1962). Storms can also increase the input of fresh water to the sea, with the resulting change in water column salinity causing heavy mortalities (Tabb & Jones, 1962; Barry & Dayton, 1991). Furthermore, although exoskeleton formation in arthropods is mainly constrained by biotic parameters, the major source of calcium used for exoskeleton calcification is exogenous, and comes from the waters where the organisms live (Luquet, 2012). In sea water, the concentration of calcium is generally very high (Luquet, 2012), but freshwater input during a storm may alter calcium availability for biomineralization in shallow waters, inhibiting marine arthropods from attaining large sizes. However, during the Ordovician Period, even the shallowest settings from the Fezouata Shale in Morocco were extremely far from the shore (more than 1000 km away; Guiraud *et al.* 2004). It is therefore more likely that the impact of storms on living organisms was more related to transport of sediment and obrution events rather than calcium and salinity fluctuations. This sediment-induced stress was evidenced in proximal localities of the Fezouata Shale, regularly killing sessile epibenthic taxa and thus inhibiting them from attaining large sizes (Saleh *et al.* 2018). This stress decreased from proximal to distal localities, allowing organisms to attain larger sizes in deeper environments (Saleh *et al.* 2018). However, mass mortality is not generally the trend for arthropods in storm-dominated modern shallow-marine environments, except in the cases of supercritical events (Conner *et al.* 1989). In regions that are seasonally affected by storms, arthropods are able to migrate to more stable environments (Conner *et al.* 1989). Pink shrimp individuals are known to leave shallow waters to deeper environments about 96 kilometers offshore during a hurricane (Tabb & Jones, 1962), and similar shelter-seeking behaviour is observed during the storms season in spiny lobsters (Hunt *et al.* 1994). It is likely that trilobites, similarly to modern vagile arthropods, were able to adapt against physical instabilities and were little affected by storm turbulences. Some of them even showed collective behaviour by migrating during storm seasons, in a similar way to extant spiny lobsters (Vannier *et al.* 2019).

The occurrence of large trilobite individuals in deep waters may also indicate a lack of predators in these settings (Rex, 1976), as heavy predation is known to limit body size (Horikoshi, 1986). Cephalopods, major predators in both Ordovician and modern marine ecosystems (Cherel & Hobson, 2005; Kröger *et al.* 2009a), are absent in Ouled Slimane, although they are relatively common in more proximal localities of the Fezouata Shale (Kröger & Lefebvre, 2012). Their absence from the distal setting preserved at Ouled Slimane is in good accordance with the observation that

their initial Furongian – Early Ordovician diversification was restricted to relatively shallow environments (Kröger *et al.* 2009b). The lack of predation pressure from cephalopods in distal marine environments in general during the Cambrian – Early Ordovician period may explain the numerous occurrences of large trilobites in distal settings globally during this time interval (e.g. Fezouata Shale, ‘Schistes à Gâteaux’, see also Section 1: Introduction), and the rarity of large trilobites in younger deposits more or less coincides with the palaeoecological diversification of cephalopods into deeper settings during Middle Ordovician time (Kröger *et al.* 2009a). The environmental conditions of the distal Fezouata Shale setting were therefore characterized by a lack of storms and predators and an abundance of oxygen and nutrients, all of which are conducive to the local occurrence of large trilobites.

Supplementary material. To view supplementary material for this article, please visit <https://doi.org/10.1017/S0016756820000448>

Acknowledgments. This paper is a contribution to the TelluS-Syster project ‘Vers de nouvelles découvertes de gisements à préservation exceptionnelle dans l’Ordovicien du Maroc’ (2017), and the TelluS-INTERVIE projects ‘Mécanismes de préservation exceptionnelle dans la Formation des Fezouata’ (2018) and ‘Géochimie d’un *Lagerstätte* de l’Ordovicien inférieur du Maroc’ (2019), all funded by the INSU (Institut National des Sciences de l’Univers, France), CNRS. This paper is also a contribution to the International Geoscience Program (IGCP) Project 653 ‘The onset of the Great Ordovician Biodiversification Event’. ACD’s contribution is supported by Grant no. 205321_179084 from the Swiss National Science Foundation. LL was supported by Research Plan RVO 67985831 of the Institute of Geology of the CAS and by the Center for Geosphere Dynamics (UNCE/SCI/006). The authors thank Juan Carlos Gutiérrez-Marco for graptolite identification. The authors are also thankful to Anna Zylńska and an anonymous reviewer for their helpful and constructive remarks.

Declaration of interest. None.

References

- Barry JP and Dayton PK (1991) Physical heterogeneity and the organization of marine communities. In *Ecological Heterogeneity* (eds J Kolasa and ST Pickett), pp. 270–320. New York, NY: Springer.
- Bell MA (2014) Patterns in palaeontology: trends of body-size evolution in the fossil record – a growing field. *Palaeontology online* 4, 1–9.
- Bonner JT (2006) *Why Size Matters: From Bacteria to Blue Whales*. Princeton: Princeton University Press, 161 p.
- Booth JAT, Ruhl HA, Lovell LL, Bailey DM and Smith KL (2008) Size-frequency dynamics of NE Pacific abyssal ophiuroids (Echinodermata: Ophiuroidea). *Marine Biology* 154(6), 933–41.
- Capéra JC, Courtessole R and Pillet J (1975) Biostratigraphie de l’Ordovicien inférieur de la Montagne Noire (France méridionale) – Trémadocien inférieur. *Bulletin de la Société d’Histoire Naturelle de Toulouse*, 111(3–4), 337–80.
- Capéra JC, Courtessole R and Pillet J (1978) Contribution à l’étude de l’Ordovicien inférieur de la Montagne Noire. Biostratigraphie et révision des Agnostida. *Annales de la Société Géologique du Nord* 98, 67–88.
- Chapelle G and Peck LS (1999) Polar gigantism dictated by oxygen availability. *Nature* 399, 114–15.
- Chatterton BDE (1980) Ontogenetic studies of Middle Ordovician trilobites from the Esbataottine Formation, Mackenzie Mountains, Canada. *Palaeontographica Abteilung A*, 1980, 1–74.
- Chatterton BDE and Speyer SE (1997) Ontogeny. In *Treatise on Invertebrate Paleontology, Part O, Trilobita, revised, Volume 1: Introduction* (ed RL Kaesler), pp. 173–247. Boulder, Colorado: The Geological Society of America and The University of Kansas.
- Cherel Y and Hobson KA (2005) Stable isotopes, beaks and predators: a new tool to study the trophic ecology of cephalopods, including giant and colossal

- squids. *Proceedings of the Royal Society B: Biological Sciences* 272(1572), 1601–07.
- Conner W, Day J, Baumann R and Randall J (1989) Influence of hurricanes on coastal ecosystems along the northern Gulf of Mexico. *Wetlands Ecology and Management* 1(1), 45–56.
- Corbacho J and López-Soriano FJ (2012) A new asaphid trilobite from the Lower Ordovician (Arenig) of Morocco. *Batalleria* 17, 3–12.
- Corbacho J and López-Soriano FJ (2016) *Platypeltoides hammondi* (Trilobita, Nileidae): A new species from the Upper Tremadoc of the Dra Valley, Morocco. *Batalleria* 23, 11–19.
- Corbacho J, Lopez-Soriano FJ, Lemke U and Hammond K (2017) *Platypeltoides carmenae*: A new Nileidae (Trilobita) from the Lower Ordovician (Tremadocian) of Guelmim area; Western Anti-Atlas, Morocco. *Batalleria* 25, 20–29.
- Corbacho J, Lopez-Soriano FJ, Lemke U, Morrison S and Hammond K (2018) Diversity and distribution of the genus *Platypeltoides* (Nileidae) in Morocco. *American Journal of Bioscience and Bioengineering* 6(2), 13–20.
- Courtessole R and Pillet J (1975) Contribution à l'étude des faunes trilobitiques de l'Ordovicien inférieur de la Montagne Noire. Les Eulominae et les Nileidae. *Annales de la Société Géologique du Nord* 95(4), 251–72.
- Courtessole R, Pillet J and Vizcaíno D (1981) *Nouvelles données sur la biostratigraphie de l'Ordovicien inférieur de la Montagne Noire. Révision des Taihugshaniidae, de Megistaspis (Ekeraspis) et d'Asaphopsoidea (Trilobites)*. Carcassonne: Mémoire de la Société des Etudes Scientifiques de l'Aude, 32 p.
- Destombes J, Hollard H and Willefert S (1985) Lower Palaeozoic rocks of Morocco. In *Lower Palaeozoic Rocks of the World* (ed C Holland), pp. 91–336. New York: Wiley.
- Ebbestad JOR (2016) Gastropoda, Tergomya and Paragastropoda (Mollusca) from the Lower Ordovician Fezouata Formation, Morocco. *Palaeogeography, Palaeoclimatology, Palaeoecology* 460, 87–96.
- Fagerstrom JA (1964) Fossil communities in paleoecology: their recognition and significance. *GSA Bulletin* 75(12), 1197–216.
- Fortey R (2009) A new giant asaphid trilobite from the Lower Ordovician of Morocco. *Memoirs of the Association of Australasian Palaeontologists* 37, 9–16.
- Fortey RA (2010) Trilobites of the genus *Dikelokephalina* from Ordovician Gondwana and Avalonia. *Geological Journal* 46(5), 405–15.
- Gaines RR, Briggs DEG, Orr PJ and Van Roy P (2012) Preservation of giant anomalocaridids in silica-chlorite concretions from the Early Ordovician of Morocco. *PALAIOS* 27(5), 317–25.
- Geiger M, Wilson LAB, Costeur L, Sánchez R and Sánchez-Villagra MR (2013) Diversity and body size in giant caviomorphs (Rodentia) from the northern Neotropics—a study of femoral variation. *Journal of Vertebrate Paleontology* 33(6), 1449–56.
- Geyer G (1993) The giant Cambrian trilobites of Morocco. *Beringeria* 8, 71–107.
- Guiraud R, Bosworth B, Thierry J and Delplanque A (2004) Phanerozoic geological evolution of Northern and Central Africa: An overview. *Journal of African Earth Sciences* 43, 83–143.
- Gutiérrez-Marco JC and García-Bellido DC (2018) The international fossil trade from the Paleozoic of the Anti-Atlas, Morocco. In *The Great Ordovician Biodiversification Event: Insights from the Tifilalt Biota, Morocco* (eds AW Hunter, JJ Álvaro, B Lefebvre, P van Roy and S Zamora). Geological Society of London, Special Publication no. 485, published online 1 January 2018, SP485.1.
- Gutiérrez-Marco JC, Sá AA, García-Bellido DC, Rábano I and Valério M (2009) Giant trilobites and trilobite clusters from the Ordovician of Portugal. *Geology* 37(5), 443–46.
- Harrington HJ (1937) On some Ordovician fossils from Northern Argentina. *Geological Magazine* 74(3), 97–124.
- Holmes JD, Paterson JR and Garcia-Bellido DC (2020) The trilobite *Redlichia* from the lower Cambrian Emu Bay Shale Konservat-Lagerstätte of South Australia: systematics, ontogeny and soft-part anatomy. *Journal of Systematic Palaeontology* 18(4), 295–334.
- Horikoshi M (1986) Biology of the deep sea. In *The Seas Around Japan* (eds MY Horikoshi, Y Nagata and T Sato), pp. 169–92. Tokyo: Iwanami Shoten.
- Hughes NC and Rushton AWA (1990) Computer-aided restoration of a late Cambrian ceratopygid trilobite from Wales, and its phylogenetic implications. *Palaeontology* 33(2), 429–45.
- Hunt J, Butler M and Herrnkind W (1994) Sponge mass mortality and Hurricane Andrew: catastrophe for juvenile spiny lobsters in south Florida? *Bulletin of Marine Science* 54(3), 1073.
- Johnson RG (1960) Models and methods for analysis of the mode of formation of fossil assemblages. *GSA Bulletin* 71(7), 1075–86.
- Klug C, De Baets K, Kröger B, Bell MA, Korn D and Payne JL (2015) Normal giants? Temporal and latitudinal shifts of Palaeozoic marine invertebrate gigantism and global change. *Lethaia* 48(2), 267–88.
- Kröger B and Lefebvre B (2012) Palaeogeography and palaeoecology of early Floian (Early Ordovician) cephalopods from the Upper Fezouata Formation, Anti-Atlas, Morocco. *Fossil Record* 15(2), 61–75.
- Kröger B, Servais T and Zhang Y (2009a) The origin and initial rise of pelagic cephalopods in the Ordovician. *PLoS ONE* 4(9), e7262.
- Kröger B, Zhang Y and Isakar M (2009b) Discosorids and oncocerids (Cephalopoda) of the Middle Ordovician Kunda and Aseri regional stages of Baltoscandia and the early evolution of these groups. *Geobios* 42(3), 273–92.
- Laibl L, Fatka O, Budil P, Ahlberg P, Szabad M, Vokáč V and Kozák V (2015) The ontogeny of *Ellipsocephalus* (Trilobita) and systematic position of Ellipsocephalidae. *Alcheringa: An Australasian Journal of Palaeontology* 39(4), 477–87.
- Laibl L, Fatka O, Cronier C and Budil P (2014) Early ontogeny of the Cambrian trilobite *Sao hirsuta* from the Skryje-Týřovice Basin, Barrandian area, Czech Republic. *Bulletin of Geosciences* 89(2), 293–309.
- Lamsdell JC and Braddy SJ (2009) Cope's Rule and Romer's theory: patterns of diversity and gigantism in eurypterids and Palaeozoic vertebrates. *Biology Letters* 6(2), 265–69.
- Lebrun P (2018) *Fossiles du Maroc. Tome I, Gisements emblématiques du Paléozoïque de l'Anti-Atlas*. Glavenat: les Editions du Piat, 298 p.
- Lefebvre B, Allaire N, Guensburg T, E, Hunter AW, Kouráiss K, Martin EL, O, Nardin E, Noailles F, Pittet B, Sumrall C, D and Zamora S (2016) Palaeoecological aspects of the diversification of echinoderms in the Lower Ordovician of central Anti-Atlas, Morocco. *Palaeogeography, Palaeoclimatology, Palaeoecology* 460, 97–121.
- Lefebvre B, Guensburg TE, Martin ELO, Mooi R, Nardin E, Nohejlová M, Saleh F, Kouráiss K, El Hariri K and David B (2019) Exceptionally preserved soft parts in fossils from the Lower Ordovician of Morocco clarify stylophoran affinities within basal deuterostomes. *Geobios* 52, 27–36.
- Luquet G (2012) Biomineralizations: insights and prospects from crustaceans. *ZooKeys* 176, 103–21.
- Martí Mus M (2016) A hyolithid with preserved soft parts from the Ordovician Fezouata Konservat-Lagerstätte of Morocco. *Palaeogeography, Palaeoclimatology, Palaeoecology* 460, 122–29.
- Martin E, Lefebvre B and Vaucher R (2015) Taphonomy of a stylophoran-dominated assemblage in the Lower Ordovician of Zagora area (central Anti-Atlas, Morocco). In *Progress in Echinoderm Palaeobiology* (eds S Zamora and I Rabano). Madrid: Cuadernos del Museo Geominero 19, 95–100.
- Martin ELO, Pittet B, Gutiérrez-Marco J-C, Vannier J, El Hariri K, Lerosey-Aubril R, Masrour M, Nowak H, Servais T, Vandenbroucke TRA, Van Roy P, Vaucher R and Lefebvre B (2016a) The Lower Ordovician Fezouata Konservat-Lagerstätte from Morocco: Age, environment and evolutionary perspectives. *Gondwana Research* 34, 274–83.
- Martin ELO, Vidal M, Vizcaíno D, Vaucher R, Sansjofre P, Lefebvre B and Destombes J (2016b) Biostratigraphic and palaeoenvironmental controls on the trilobite associations from the Lower Ordovician Fezouata Shale of the central Anti-Atlas, Morocco. *Palaeogeography, Palaeoclimatology, Palaeoecology* 460, 142–154.
- McAlister JS and Stanczyk SE (2005) Effects of variable water motion on regeneration of *Hemipholis elongata* (Echinodermata, Ophiuroidea). *Invertebrate Biology* 122(2), 166–76.
- McCoy VE, Young RT and Briggs DEG (2015a) Factors controlling exceptional preservation in concretions. *Palaaios* 30, 272–80.

- McCoy VE, Young RT and Briggs DEG (2015b) Sediment permeability and the preservation of soft-tissues in concretions: an experimental study. *Palaos* **30**, 608–12.
- Mergl M (2006) Tremadocian trilobites of the Prague Basin, Czech Republic. *Acta Musei Nationalis Pragae, Series B – Historia Naturalis* **62**(1–2), 1–70.
- Moran A and Woods A (2012) Why might they be giants? Towards an understanding of polar gigantism. *Journal of Experimental Biology* **215**(2), 1995–2002.
- Nichols G (2009) *Sedimentology and Stratigraphy*. Chichester: Wiley-Blackwell, 432 p.
- Nowak H, Pittet B, Vaucher R, Akodad M, Gaines RR and Vandenbroucke TRA (2016) Palynomorphs of the Fezouata Shale (Lower Ordovician, Morocco): Age and environmental constraints of the Fezouata Biota. *Palaeogeography, Palaeoclimatology, Palaeoecology* **460**, 62–74.
- Park T and Choi DK (2009) Post-embryonic development of the Furongian (late Cambrian) trilobite *Tsinania canens*: implications for life mode and phylogeny. *Evolution & Development* **11**(4), 441–55.
- Paterson JR, García-Bellido DC, Jago JB, Gehling JG, Lee MSY and Edgecombe GD (2016) The Emu Bay Shale Konservat-Lagerstätte: a view of Cambrian life from East Gondwana. *Journal of the Geological Society* **173**(1), 1–11.
- Payne JL, Groves JR, Jost AB, Nguyen T, Moffitt SE, Hill TM and Skotheim JM (2012) Late Paleozoic fusulinoid gigantism driven by atmospheric hyperoxia. *Evolution* **66**(9), 2929–39.
- Perillo MM, Best JL and Garcia MH (2014) A new phase diagram for combined-flow bedforms. *Journal of Sedimentary Research* **84**(4), 301–13.
- Philippart CJM, Cadée GC, van Raaphorst W and Riegman R (2000) Long-term phytoplankton-nutrient interactions in a shallow coastal sea: Algal community structure, nutrient budgets, and denitrification potential. *Limnology and Oceanography* **45**(1), 131–44.
- Rábano I (1990) *Platypeltoides magrebiensis* n. sp., Asaphina, Nileidae, del Ordovícico inferior del Anti-Atlas central, Marruecos. *Boletín Geológico y Minero* **101**, 21–47.
- Rex MA (1976) Biological accommodation in the deep-sea benthos: comparative evidence on the importance of predation and productivity. *Deep Sea Research and Oceanographic Abstracts* **23**(10), 975–87.
- Rowe GT, Clifford CH, Smith KL and Hamilton PL (1975) Benthic nutrient regeneration and its coupling to primary productivity in coastal waters. *Nature* **255**(5505), 215–17.
- Rudkin DM, Young GA, Elias RJ and Dobrzanski EP (2003) The world's biggest trilobite—*Isotelus rex* new species from the upper Ordovician of northern Manitoba, Canada. *Journal of Paleontology* **77**(1), 99–112.
- Saleh F, Candela Y, Harper DAT, Polechová M, Pittet B and Lefebvre B (2018) Storm-induced community dynamics in the Fezouata Biota (Lower Ordovician, Morocco). *Palaos* **33**(12), 535–41.
- Saleh F, Pittet B, Perrillat J and Lefebvre B (2019) Orbital control on exceptional fossil preservation. *Geology* **47**, 1–5.
- Sander M and Clauss M (2008) Sauropod gigantism. *Science* **322**, 201–2.
- Sdzuy K, Hammann W and Villas E (2001) The Upper Tremadocian fauna from Vogtendorf and the Bavarian Ordovician of the Frankenwald (Germany). *Senckenbergiana Lethaea*, **81**(1), 207–61.
- Sigurdson A and Hammer Ø (2016) Body size trends in the Ordovician to earliest Silurian of the Oslo Region. *Palaeogeography, Palaeoclimatology, Palaeoecology* **443**, 49–56.
- Speyer SE and Brett CE (1986) Trilobite taphonomy and Middle Devonian taphofacies. *PALAIOS* **1**(3), 312.
- Tabb DC and Jones AC (1962) Effect of Hurricane Donna on the aquatic fauna of North Florida Bay. *Transactions of the American Fisheries Society* **91**(4), 375–78.
- Taylor AM and Goldring R (1993) Description and analysis of bioturbation and ichnofabric. *Journal of the Geological Society* **150**(1), 141–8.
- Teigler DJ and Towe KM (1975) Microstructure and composition of the trilobite exoskeleton. *Fossils and Strata* **4**, 137–49.
- Thoral M (1935) *Contribution à l'étude paléontologique de l'Ordovicien inférieur de la Montagne Noire et Révision sommaire de la faune cambrienne de la Montagne Noire*. Montpellier: Imprimerie de la Charité, 362 p.
- Thoral M (1946) Cycles géologiques et formations nodulaires de la Montagne Noire. *Nouvelles archives du muséum d'histoire naturelle de Lyon* **1**, 1–141.
- Timofeev SF (2001) Bergmann's principle and deep-water gigantism in marine crustaceans. *Biology Bulletin* **28**(6), 646–50.
- Torsvik T and Cocks L (2011) The Palaeozoic palaeogeography of central Gondwana. In *The Formation and Evolution of Africa: A Synopsis of 3.8 Ga of Earth History* (eds DJJ van Hinsbergen, SJH Buiter, TH Torsvik, C Gaina and SJ Webb), pp. 137–66. Geological Society of London, Special Publication no. 357.
- Torsvik T and Cocks L (2013) New global palaeogeographical reconstructions for the Early Palaeozoic and their generation. In *Early Palaeozoic Biogeography and Palaeogeography* (eds DAT Harper and T Servais), pp. 5–24. Geological Society of London, Memoir no. 38.
- Twitchett RJ (2007) The Lilliput effect in the aftermath of the end-Permian extinction event. *Palaeogeography, Palaeoclimatology, Palaeoecology* **252**, 132–44.
- Vannier J, Vidal M, Marchant R, El Hariri K, Kouraiss K, Pittet B, El Albani A, Mazurier A. and Martin E (2019) Collective behaviour in 480-million-year-old trilobite arthropods from Morocco. *Scientific Reports* **9**, 14941.
- Van Roy P and Briggs DEG (2011) A giant Ordovician anomalocaridid. *Nature* **473**(7348), 510–13.
- Van Roy P, Briggs DEG and Gaines RR (2015a) The Fezouata fossils of Morocco; an extraordinary record of marine life in the Early Ordovician. *Journal of the Geological Society* **172**(5), 541–49.
- Van Roy P, Daley AC and Briggs DEG (2015b) Anomalocaridid trunk limb homology revealed by a giant filter-feeder with paired flaps. *Nature* **522**(7554), 77–80.
- Van Roy P, Orr PJ, Botting JP, Muir LA, Vinther J, Lefebvre B, El Hariri K and Briggs DEG (2010) Ordovician faunas of Burgess Shale type. *Nature* **465**(7295), 215–18.
- Vaucher R, Martin ELO, Hormière H and Pittet B (2016) A genetic link between Konservat- and Konservat-Lagerstätten in the Fezouata Shale (Lower Ordovician, Morocco). *Palaeogeography, Palaeoclimatology, Palaeoecology* **460**, 24–34.
- Vaucher R, Pittet B, Hormière H, Martin ELO and Lefebvre B (2017) A wave-dominated, tide-modulated model for the Lower Ordovician of the Anti-Atlas, Morocco. *Sedimentology* **64**(3), 777–807.
- Vela JA and Corbacho J (2007) A new species of *Lehua* from Lower Ordovician of Dra Valley of Morocco. *Batalleria* **13**, 75–80.
- Vermeij GJ (2016) Gigantism and its implications for the history of life. *PLoS ONE* **11**(1), e0146092.
- Vinther J, Parry L, Briggs DEG and Van Roy P (2017) Ancestral morphology of crown-group molluscs revealed by a new Ordovician stem aculiferan. *Nature* **542**(7642), 471–74.
- Vinther J, Van Roy P and Briggs DEG (2008) Machaeridians are Palaeozoic armoured annelids. *Nature* **451**(7175), 185–88.
- Wang B, Wang X and Zhan R (2003) Nutrient conditions in the Yellow Sea and the East China Sea. *Estuarine, Coastal and Shelf Science* **58**(1), 127–36.
- Whiteley TE, Kloc GJ and Brett CE (2002) *Trilobites of New York: An Illustrated Guide*. Ithaca, NY: Paleontological Research Institution, 20 p.
- Zeuthen E (1953) Oxygen uptake as related to body size in organisms. *The Quarterly Review of Biology* **28**(1), 1–12.

5. DECAY AND MINERALIZATION

This chapter consists of two papers:

- **Paper 3:** Saleh, F., Pittet, B., Perrillat, J-P., Lefebvre, B., 2019. Orbital control on exceptional fossil preservation. **Geology**, 47(2), 103-106.
- **Paper 4:** Saleh, F., Daley, A.C., Lefebvre, B., Pittet, B., Perrillat, J-P., 2020. Biogenic iron preserves structures during fossilization: A hypothesis. **BioEssays**, 42(6), 1-6.

Summary

The exposure to the chemical conditions in the water column and to decay are observed at the community level in the Fezouata Shale. For instance, in one stratigraphic lens, more than 600 fossils were discovered, but only a limited number of them show soft tissue preservation (about 30 stylophorans, 10 trilobites, and 5 marrellomorphs)⁵³. Thus, under these conditions, there must have been some parameters slowing down the decay of labile anatomies and/or facilitating their mineralization in order for exceptional fossil preservation to occur. In this chapter, we examine the mineralogical signatures within and surrounding preserved labile anatomies in fossils from the Fezouata Shale in order to decipher the conditions facilitating the preservation of decay-prone structures in this formation. Sediment matrices of all analyzed samples from the Fezouata Shale share a similar composition with a high abundance of illite $\{(K,H_3O)(Al,Mg,Fe)_2(Si,Al)_4O_{10}[(OH)_2,(H_2O)]\}$ (~60% in volume) and quartz (SiO_2) (~30%), and a small proportion (<10%) of chlorite minerals⁵⁴. However, the nature of the chlorite phase differs between samples, as some specimens show the presence of clinochlore $[(Mg_5Al)(AlSi_3)O_{10}(OH)_8]$ while others show iron-rich clinochlore $[(Mg,Fe)_5Al(Si_3Al)O_{10}(OH)_8]$ (iron content ~12%) or chamosite $[(Fe_5Al)(AlSi_3)O_{10}(OH)_8]$ (iron content ~30%)⁵⁴. In this formation, chamosite (originally berthierine) appears to be correlated with levels recording exceptional preservation⁵⁴. The discontinuous record of berthierine along analyzed sediments in a cyclic pattern suggests that a certain orbital forcing possibly controlled its formation through iron availability⁵⁴. Both berthierine and its primary precursor⁵⁵ are evidenced to slow down decay under oxic experimental conditions¹⁶ through the damage of bacterial cell¹⁶. This might have helped labile anatomies to survive until the establishment of anoxic conditions at time of burial under storm deposits.

Once anoxic conditions are established, another type of decay occurs. Anoxic decay transforms organic matter from decaying carcasses with sulfates SO_4^{2-} from sea water into sulfides H_2S . SO_4^{2-} is not a limiting parameter for this reaction in marine environments. Thus, H_2S output is mainly controlled by the decay products of biological tissues. When H_2S is formed, it reacts with iron to form pyrite^{56,57}. The establishment of anoxic conditions at time of burial is validated by the founding of framboid and small euhedral crystals in fossils and pyrite in fresh non-altered sediments of the Fezouata Shale⁵⁸. In these sediments C is also present in association to pyrite possibly pointing that the original mode of preservation in the Fezouata Shale is comparable to the one in the Burgess Shale and the Chengjiang Biota comprising both organic material and authigenic minerals^{14,58}. However, there must have been other parameters controlling pyrite precipitation, because no fossil shows complete pyritization and pyrite precipitation remains rare and tissue-selective. For instance, the cuticle of many arthropod taxa is preserved without any pyrite crystals. This can result from H_2S limitation considering that this structure is formed of polysaccharides that are not easily degradable⁵⁹. However, when comparing internal labile tissues to each other, the model based on H_2S limitation cannot explain why some tissues are pyritized while others decayed and disappeared (meaning they reduced SO_4^{2-}) without pyritizing. Thus, it is essential to look at Fe availability. Maghemite is found associated to pyrite in some samples analyzed under Raman Spectroscopy⁵⁸. Maghemite results from the burial of an original mineral called ferrihydrite $[FeO(OH)]_8 [FeO(H_2PO_4)]^{60}$.

Ferrihydrite is a mineral with a wide biological distribution that can explain why maghemite is only found in association with pyritized organic matter and not in the sediment^{61–63}. In experimental studies, it was shown that under anoxic conditions and when sulfates are present, ferrihydrites release high quantities (~ 87%) of reactive Fe⁶⁴. This iron delivery is 40% higher than the yield from the same quantity of hematite from sediments⁶⁴. Furthermore, ferrihydrite is the fastest to deliver reactive iron when compared to other iron oxides that are found in sediments, with a half-life of only 2.8 hours under anoxic conditions and in the presence of SO₄^{2–65}. Ferrihydrite is also a solid phase meaning that it does not migrate⁶⁶. Thus, large quantities of iron become available in-situ within a couple of hours of the start of anoxic decay⁵⁸. For this reason, in order to understand the patterns of exceptional fossil preservation in the Fezouata Shale but also in sites such as the Chengjiang Biota and the Beecher's Trilobite bed in which pyrite played a role in preserving decay-prone anatomies, three parameters should be taken into account: Fe in sediments, Fe in labile tissues, and H₂S production. Accounting for both pre-burial and anoxic decay, different scenarios emerge and are summarized in figure 4.

- In the first scenario, pre-burial decay is not controlled by any mineralogical phase and burial allowing the establishment of anoxic conditions for pyritization does not occur rapidly enough leaving only the body walls such as the carapace of trilobite preserved (Fig. 4A).
- In the second scenario, burial occurs establishing anoxic conditions for pyritization. Fe in burial material is highly reactive leading to the complete pyritization of the organism if the animal is buried alive (Fig. 4B). If the animal decayed on the seafloor but the activity of this degradation was controlled by clay/chlorite minerals, the reactivity of Fe from sediments ensures the pyritization of all tissues that survived pre-burial decay (Fig. 4C). Even carapaces of numerous arthropod taxa that provide small quantities of H₂S, are found pyritized in sites such as the Beecher's trilobite Bed^{56,67,68}.
- In the third scenario, pre-burial decay is controlled by clay/chlorite minerals. However, after burial, a tardiness in iron availability in the sediment allows the disappearance of tissues due to anaerobic decay. The least labile internal tissues will potentially survive anoxic decay and get pyritized once iron from sediments becomes available (Fig. 4D). This scenario explains the selective preservation of guts while more labile tissues (e.g. nervous systems) are absent⁶⁹.
- In the fourth scenario, pre-burial decay does not occur at all as if animals were buried alive. However, Fe in this scenario is not reactive (even if it is abundant). Thus, only tissues that are rich originally in iron will get preserved and pyritized even if they are the most labile ones (Fig. 4E). This scenario can explain the preservation of extremely decay-prone structures such as nervous tissues as pyrite replicates in fossils from the Chengjiang Biota^{9–12}.

Considering the decay stages of animals from the Fezouata Shale, the lower availability of iron in sediments from the Fezouata Shale in comparison to sites such as Beecher's Trilobite Bed, and the absence of preserved nervous systems comparable to the Chengjiang Biota, it is most probable that the taphonomic scenario of most exceptionally preserved fossils found in the Fezouata Shale followed the 3rd scenario (Fig. 4D). However, this scenario is not exclusive, and other scenarios may have accounted for the discovery of only biomineralized parts in some levels from this formation (Fig. 4A).

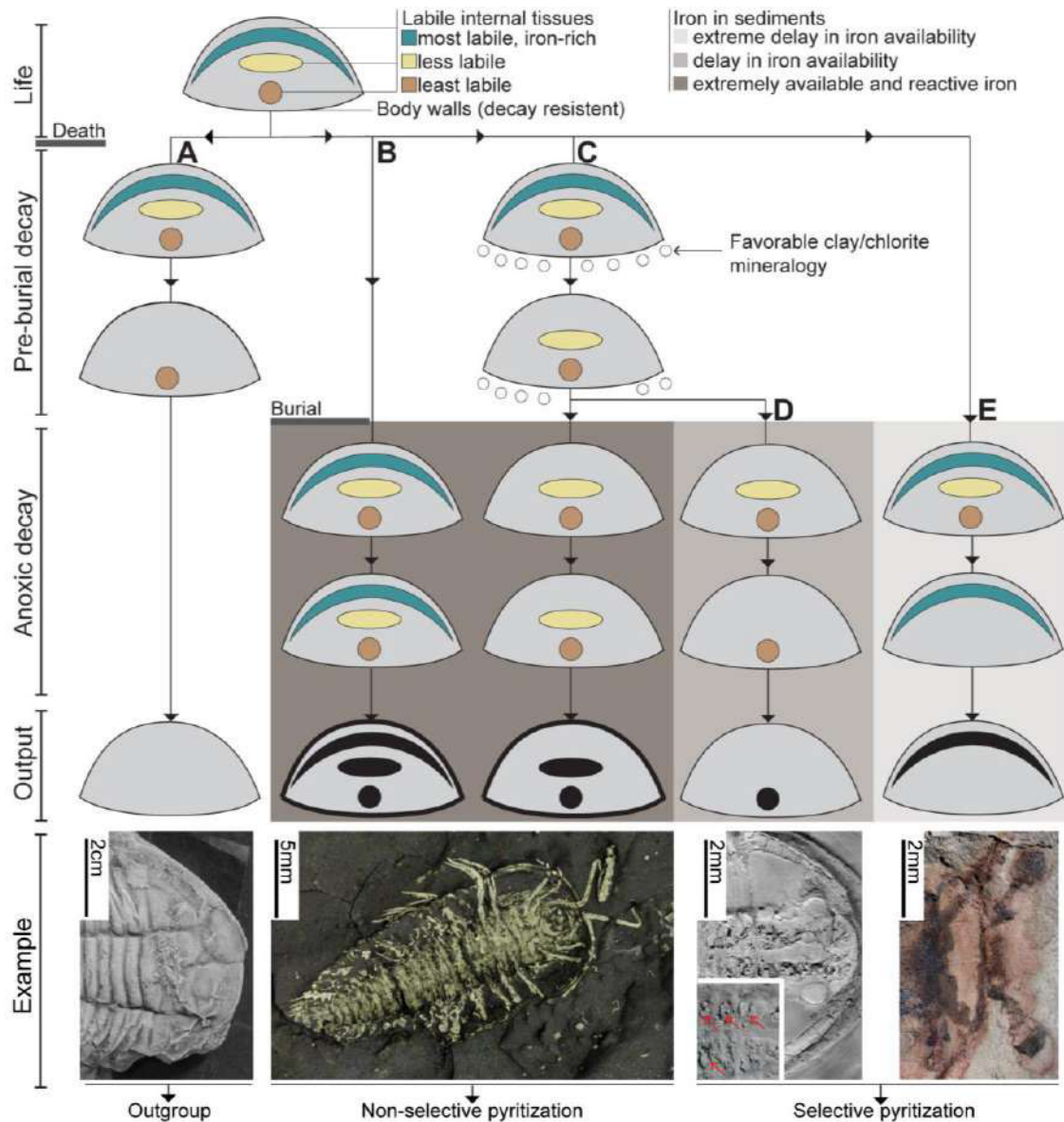


Figure 4. Different scenarios of decay and mineralization according to a model based on Fe availability in biological tissues, Fe reactivity in the sediments and H_2S production^{9,51,69,70}. Note the absence of pyrite precipitation in A (AA.TGR0a.OL.132). Almost the entire body is pyritized in B and C (YPM.516160). Pyritized parts of the digestive system in D are marked with red arrows (MGM.6755X). Pyritized nervous system in E is preserved in a dark brown/black imprint (YKLP.15006).

Orbital control on exceptional fossil preservation

Farid Saleh*, Bernard Pittet, Jean-Philippe Perrillat, and Bertrand Lefebvre

Laboratoire de Géologie de Lyon: Terre, Planètes, Environnement, ENS de Lyon, CNRS, UMR 5276, Université Claude Bernard
Lyon 1, F-69622 Villeurbanne, France

ABSTRACT

Exceptional fossil preservation is defined by the preservation of soft to lightly sclerotized organic tissues. The two most abundant types of soft-tissue preservation are carbonaceous compressions and replicates in authigenic minerals. In the geological record, exceptionally preserved soft fossils are rare and generally limited to only a few stratigraphic intervals. In the Fezouata Shale (Lower Ordovician, southern Morocco), we found that deposits yielding pyritized soft tissues contain iron-rich silicate minerals. These minerals played a crucial role in inhibiting the decay of dead individuals and are comparable to those found in formations yielding carbonaceous soft parts around the world. Furthermore, we found that iron-rich minerals show a cyclic pattern of occurrence (of ~100 k.y. periodicity) implicating a short-period eccentricity control on iron availability through the general oceanic and atmospheric circulations. Our results identify, for the first time, an external climate forcing on exceptional preservation and show that orbital forcing may be a level-selective parameter responsible for the discontinuous occurrence of horizons preserving soft parts around the world.

INTRODUCTION

Exceptional fossil preservation consists of the preservation of soft to lightly sclerotized organic tissues (e.g., feathers, guts, skins) in the geological record (Butterfield, 1995). The transfer of such tissues from the biosphere to the lithosphere is the result of a succession of multiple, complex biological and geological mechanisms. Deciphering these mechanisms is essential to understanding why exceptional preservation is limited to specific intervals in the sedimentary record. Recent studies have shown that the absence or presence of carbonaceous soft tissues is strongly correlated with the mineralogy of the depositional environment and most importantly with iron-rich minerals that can inhibit bacterial decay of soft tissues through the oxidative damage of bacterial cells (McMahon et al., 2016; Anderson et al., 2018). However, little attention has been paid so far to discovering within which sediment minerals the pyritized soft tissues occur and what the processes behind the deposition of these minerals are.

The Fezouata Shale crops out in the Zagora region in southern Morocco. This Lower Ordovician succession consists of blue-green to yellow-green sandy mudstones and siltstones that coarsen upward. These sediments are as much as 900 m thick in the Zagora region (Destombes et al., 1985; Martin et al., 2016; Vaucher et al., 2017). The entire succession was deposited in a marginal basin at high latitude close to the paleo-South Pole (Torsvik and Cocks, 2011, 2013). The shallow depositional setting ranges from the foreshore to the upper offshore. It was storm-wave dominated (Martin et al., 2016) and indirectly influenced by

tides (Vaucher et al., 2017). The Fezouata Shale has yielded abundant remains of soft-bodied organisms preserved with high fidelity, showing the association of post-Cambrian taxa typical of the Great Ordovician Biodiversification Event along with iconic taxa of the Cambrian Explosion (Van Roy et al., 2010, 2015). Most soft-bodied organisms were pyritized and are now preserved in iron oxides. However, this pyrite weathering is not substantial as numerous fossils still show original framboidal pyrite crystals. The presence of levels yielding both mineralized and soft-bodied organisms, as well as the highly constrained stratigraphic framework of this formation (Gutiérrez-Marco and Martin, 2016; Lehnert et al., 2016; Martin et al., 2016; Nowak et al., 2016; Lefebvre et al., 2018), make the Fezouata Shale a good candidate for investigating whether specific sediment minerals are correlated with pyritized soft parts, and whether these mineralogical signatures change through time.

MATERIAL AND METHODS

Mineralogical Signatures

Part of the sedimentary succession of the Fezouata Shale (Vaucher et al. 2016) was included in this study. The mineralogy of all fossiliferous levels in this section was investigated. Mineral assemblages of levels yielding exceptional preservation were compared to those in levels bearing only sclerotized remains. Matrix samples from each level were prepared as randomly oriented powdered aggregates (<10 µm), without any specific treatments, on thermoplastic polymer [poly(methyl methacrylate), PMMA] substrates. X-ray diffraction (XRD) was performed using a Bruker D8 Advance diffractometer, employing a CuKα source and Bruker LynxeyeX detector. Peak positions were adjusted, using the positions of quartz peaks as internal standards, to avoid the preparation height displacement error. Mineral phases were then retrieved based on indexation of their diffraction lines, between 0° and 75° 2θ values, from the International Centre for Diffraction Data PDF-4+ 2016 reference database (<http://www.icdd.com/index.php/pdf-4/>). Illite is generally characterized by its basal (001) peak at ~10 Å. Quartz is characterized by its intense (011) reflection at 3.34 Å. The differentiation between chlorite minerals is verified based on the lateral variations of their characteristic (001) and (002) peaks, respectively at 14 and 7 Å, as iron enrichment causes an increase in *d*-spacing that shifts peaks positions toward higher 2θ values (Fig. 1). Phase proportions were estimated from the relative intensity of diffraction lines of each mineral species.

Sequence Reconstructions

The depositional environment of the Fezouata Shale is storm- and/or wave-dominated and indirectly influenced by tides (Martin et al. 2016; Vaucher et

*E-mail: farid.saleh@univ-lyon1.frCITATION: Saleh, F., Pittet, B., Perrillat, J.-P., and Lefebvre, B., 2019, Orbital control on exceptional fossil preservation: *Geology*, <https://doi.org/10.1130/G45598.1><https://doi.org/10.1130/G45598.1>

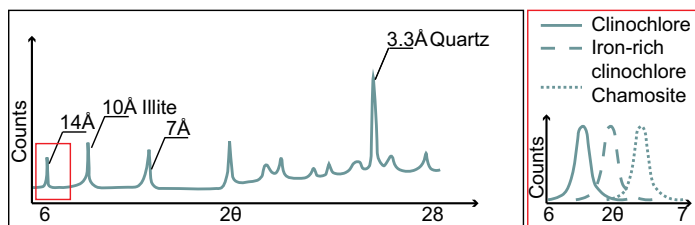


Figure 1. Mineral identification in samples from Fezouata Shale (southern Morocco) from X-ray powder diffraction. Box with red margins is expansion of area indicated in main plot.

al., 2016, 2017). In the Fezouata Shale, the interaction of oscillations with surface sediments generated oscillatory structures. The wavelength of these structures decreased from shallow to deep environments (Nichols, 2009; Vaucher et al. 2016). Additionally, coarser sediments indicate a shallower environment, while finer sediments are deposited in deeper settings (Vaucher et al., 2016, 2017). These sediments and structural heterogeneities permitted the establishment of a model of facies for the Fezouata Shale (Vaucher et al., 2017). Based on this model, the alternation of deeper and shallower facies F1, F2, and F4 of Vaucher et al. (2017) allowed us to identify small-, medium-, and large-scale sequences. Small-scale sequences correspond to the shortest-term variations of the sea level (Fig. 2), whereas medium- and large-scale sequences correspond to longer-term sea-level changes.

Bathymetry and Oxygenation

The depth of the water column was estimated using medium-scale sea-level sequences (Lefebvre et al., 2016; Vaucher et al., 2017). Relative oxygen abundances in superficial sediments were reconstructed based on depth variations of the water column. In deep environments of the Fezouata Shale, i.e., shelf settings below storm wave base, rapid burial did not occur, inhibiting the establishment of anoxic conditions in surface sediments (Vaucher et al., 2017). Above storm wave base, where rapid burial during storm events occurred, the establishment of anoxic conditions in surface sediments below the storm deposits was influenced by wave-sediment interactions. Wave-sediment interactions are more pronounced in shallowmost settings (Nichols, 2009), leading to an increase in the oxygen penetration depth from the water column to the sediments (Chatelain and Guizien, 2010). Thus, anoxic and/or dysoxic conditions occur rarely in the shallowest environments (decimetric wavelength of storm oscillatory structures, high oxygen penetration depth) and may occur only in less-shallow deposits (centimetric wavelength of storm structures, limited oxygen penetration depth) just above the storm wave base (Fig. 2) in the Fezouata Shale (Vaucher et al., 2016, 2017).

RESULTS

All samples show a similar composition with an absence of organic matter, a high abundance of illite $\{(K,H_3O)(Al,Mg,Fe)_2(Si,Al)_4O_{10}(OH)_2(H_2O)\}$ (~60%) and quartz (SiO_2) (~30%), and a small proportion (<10%) of chlorite minerals (see Table DR1 in the GSA Data Repository¹ for precise percentages). However, the nature of the chlorite phase differs between samples, as some specimens show the presence of clinocllore $[(Mg_5Al)(AlSi_3O_{10}(OH)_8)]$ while others show iron-rich clinocllore $[(Mg,Fe)_5Al(Si_3Al)O_{10}(OH)_8]$ (iron content ~12%) or chamosite $[(Fe_3Al)(AlSi_3O_{10}(OH)_8)]$ (iron content ~30%) (Fig. 2). In the Fezouata Shale, the occurrence of soft tissues is discontinuous and is limited only to a few stratigraphic levels in intervals 1 and 3 (Fig. 2).

The entire sedimentary succession was deposited near the storm wave base. Both intervals 1 and 3 (Fig. 2) were deposited under anoxic and/or

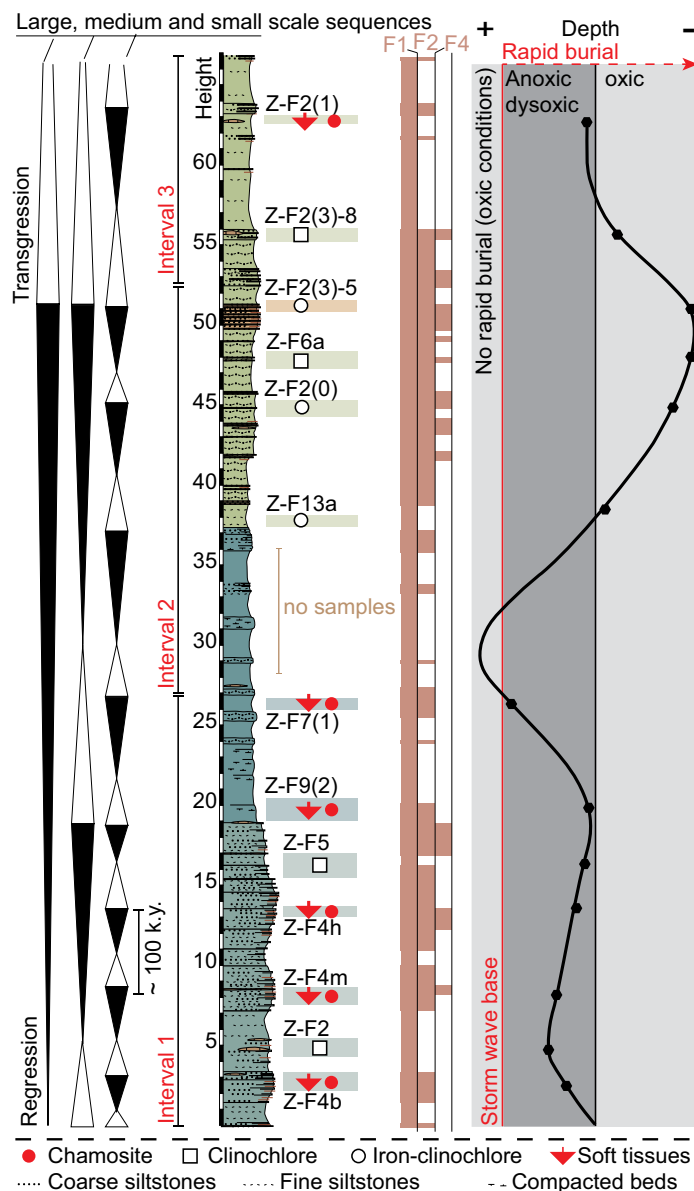


Figure 2. From left to right: Fezouata Shale (southern Morocco) sequences of various scales translating sea-level cycles at different time scales (white triangles represent transgression; black triangles represent regression); part of the sedimentary succession of Fezouata Shale with location of samples; facies F1, F2, and F4 as described in Vaucher et al. (2017) used to identify sequences; relative bathymetry changes; and oxygen fluctuations.

dysoxic conditions. Most of interval 2 was deposited under oxic conditions (Fig. 2).

The studied section contains about two medium-scale and nine small-scale sequences. The occurrence of four small-scale sequences per medium-scale sequence deduced from facies changes (Fig. 2) in the entire sedimentary succession suggests an eccentricity control on sequence formation through its 100 and 400 k.y. periodicities. The studied sediments were deposited during the Tremadocian (duration of 7.7 ± 3.3 m.y.). In the Tremadocian, 10 main graptolite subdivisions (biozones) of ~0.7 m.y. have been identified (Loydell, 2012). In the Fezouata Shale, the first three biozones of the Tremadocian are missing (Gutiérrez-Marco and Martin,

¹GSA Data Repository item 2019044, sample identifications and mineralogical composition, is available online at <http://www.geosociety.org/datarepository/2019/>, or on request from editing@geosociety.org.

2016; Lefebvre et al., 2018). This suggests that the Tremadocian sediments (450 m) of the Fezouata Shale were deposited over 5.7 ± 2.4 m.y. In addition, the sedimentation of the Fezouata Shale appears to be uniform (i.e., monotonous sequence dominated by siltstones) and formed by the stacking of storm deposits (millimeter- to centimeter-thick sandstone or coarse siltstone levels separated by millimeter-thick argillaceous siltstone or fine-grained siltstone layers) (Vaucher et al., 2016, 2017). This homogeneity of the sediments and the absence of observed long- or short-term sedimentary hiatuses (Vaucher et al., 2017) both suggest a relatively stable accumulation rate of ~ 79 m/m.y. Thus, the studied 67-m-thick section was deposited over $\sim 0.84 \pm 0.35$ m.y. One medium-scale sequence would then represent a time interval of $\sim 0.42 \pm 0.17$ m.y., and one small-scale sequence, 0.09 ± 0.03 m.y. These estimated durations are in accordance with the durations of eccentricity cycles.

DISCUSSION

The sediment in the Fezouata Shale has a relatively simple composition comparable to that at other Paleozoic sites with exceptional preservation (Anderson et al., 2018). In this formation, chamosite appears to be correlated with levels recording exceptional preservation (Fig. 2). Chamosite can be formed directly from the transformation of primary clay minerals (kaolinite, glauconite) at high temperatures ($T > 175^\circ\text{C}$) or from the transformation of berthierine, an iron-rich serpentine phyllosilicate, in less-extreme conditions ($T < 100^\circ\text{C}$; Tang et al., 2017). In the Fezouata Shale, sediments did not endure extreme temperatures and burial conditions, and only 2–3 km (i.e., equivalent of burial temperatures between 70 and 100°C using a mean geothermal gradient of $30^\circ/\text{km}$ in passive margins) of sediments were deposited over these shales (Ruiz et al., 2008). Thus, berthierine is the most probable precursor for chamosite in the Fezouata Shale. In addition, chamosite occurrences appear to be correlated with an intermediate bathymetry, as it occurs only in intervals 1 and 3 (Fig. 2). In the Fezouata Shale, specific parameters (e.g., bathymetry, oxygenation) controlled the precipitation of berthierine in the depositional environment and were thus indirectly responsible for the selective presence of chamosite.

In a depositional environment, the presence of a significant amount of iron under reducing conditions leads to the precipitation of berthierine (Tang et al., 2017), a mineral that can inhibit decay bacteria (McMahon et al., 2016). Afterward, during a deeper burial, most of the berthierine is transformed to chamosite (Hornibrook and Longstaffe, 1996). In some levels of intervals 1 and 3, reducing conditions and abundant iron were available, leading to berthierine precipitation in sediments in addition to the pyritization of decaying soft parts. In interval 1, some levels, deposited under similar bathymetry (i.e., fast burial and sedimentary anoxia), yield mostly clinocllore instead of chamosite. Clinocllore and chamosite belong to the same chlorite mineral group, and lie on its magnesium-rich and iron-rich poles respectively (Curtis et al., 1985). The occurrence of both chamosite and clinocllore in intervals with different porosities suggests that the formation of these minerals is independent from the physical parameters in the sediments. Instead, the presence of clinocllore is likely related to iron deficiencies in these levels during early diagenesis.

In interval 2, chamosite is absent and has been mainly replaced by iron-rich clinocllore, indicating the presence of iron. The absence of chamosite and of exceptional preservation in this interval are due to the absence of favorable reducing conditions (Fig. 2).

Iron, an important element for the formation of both berthierine and pyrite, may have different sources such as (1) circulation of iron-rich hydrothermal fluids (Tang et al., 2017), (2) microbial extraction of iron from clay minerals after their deposition in marine sediments (Vorhies and Gaines, 2009), or (3) iron inputs to the sea from other marine or continental sources (Odin and Matter, 1981). In the Fezouata Shale, illite, which is the main clay mineral in the sedimentary basin (Ruiz et al., 2008), is present in all intervals. However, chamosite does not occur in

all levels, showing a different distribution than illite. This implies that the scenario considering microbial iron extraction from clay minerals is unlikely. In addition, the occurrence of chamosite at the end of a regression and beginning of a transgression of a small-scale sequence (Fig. 2) rules out hydrothermal fluids as the main source of iron and favors marine and/or continental inputs. The Fezouata Shale was deposited in a shallow sea near the South Pole with a limited oceanic circulation (Martin et al., 2016, Vaucher et al., 2017). Thus, the enrichment of iron is considered as continental in origin.

According to duration estimations based on graptolite biostratigraphy, any two consecutive iron-rich intervals in interval 1 were deposited with an average delay of ~ 100 k.y., in pace with eccentricity-controlled sea-level cycles (Fig. 2). Astronomic calculations have confirmed that even if the periodicity of the obliquity and precession decreased with time, eccentricity frequency has been stable over the past 500 m.y. (Berger et al., 1992). These calculations have been validated through robust responses of different sedimentary systems to astronomically controlled climate forcing from recent times to the Cambrian (Osleger and Read, 1991). Every 100 k.y., eccentricity gradually switches from a circular to an elliptic orbit, or vice versa, influencing precession, and thus, insolation and seasonal variations (Fig. 3). Consequently, these variations influence the evaporation-precipitation cycle, ice volume (Rampino, 1979), if any, as well as river fluxes and continental weathering (Horton et al., 2012), and thus the inputs of iron to the sea (Fig. 3). These inputs constitute a major

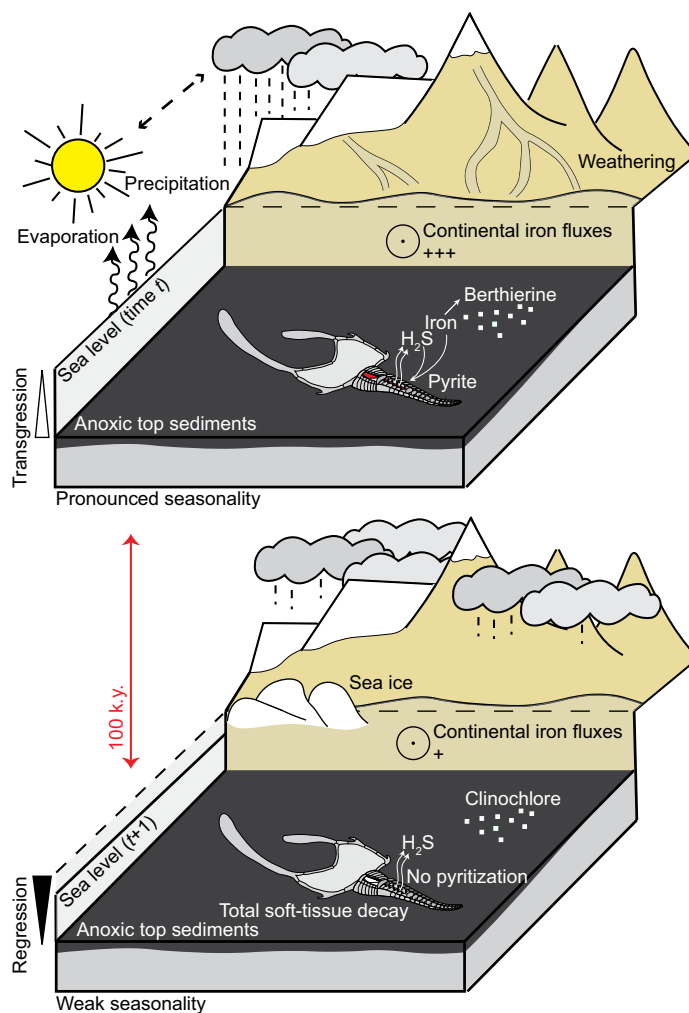


Figure 3. Model explaining effect of orbital forcing on seasonality, and thus on soft tissue preservation (white triangles represent transgression; black triangles represent regression).

contributor to iron abundances in oceans (Elrod et al., 2004) and lead to berthierine formation in shallow environments at the water-sediment interface (Odin and Gupta, 1988; Kozłowska and Maliszewska, 2015) when anoxic conditions are present (Tang et al., 2017).

For the first time, our results (1) provide detailed information on the mineralogical context in which pyritized soft tissues occur, (2) identify a temporal variation in minerals in a sedimentary succession with soft-tissue preservation, and (3) evidence an orbital control on soft-tissue fossilization. This external climate forcing may be responsible for the discontinuous occurrence of soft tissues in numerous formations around the world, in which iron discrepancies between levels yielding exceptional preservation and those with only skeletal remains are evidenced (Anderson et al., 2018).

ACKNOWLEDGMENTS

This paper is a contribution to the Tellus-INTERVIE project “Mécanismes de préservation exceptionnelle dans la Formation des Fezouata”, funded by the National Institute for Earth Sciences and Astronomy (France), CNRS, and to the International Geoscience Programme (IGCP) Project 653, “The onset of the Great Ordovician Biodiversification Event”. We thank Pierre Sansjofre and Muriel Vidal for assistance during field work in Morocco, Guillaume Suan and Vincent Perrier for their advice, and Ruben Vera for assistance in XRD preparation. Three anonymous reviewers are also thanked for their helpful and constructive remarks.

REFERENCES CITED

- Anderson, R.P., Tosca, N.J., Gaines, R.R., Mongiardino Koch, N., and Briggs, D.E.G., 2018, A mineralogical signature for Burgess Shale-type fossilization: *Geology*, v. 46, p. 347–350, <https://doi.org/10.1130/G39941.1>.
- Berger, A., Loutre, M.F., and Laskar, J., 1992, Stability of the astronomical frequencies over the Earth's history for paleoclimate studies: *Science*, v. 255, p. 560–566, <https://doi.org/10.1126/science.255.5044.560>.
- Butterfield, N.J., 1995, Secular distribution of Burgess-Shale-type preservation: *Lethaia*, v. 28, p. 1–13, <https://doi.org/10.1111/j.1502-3931.1995.tb01587.x>.
- Chatelain, M., and Guizien, K., 2010, Modelling coupled turbulence—Dissolved oxygen dynamics near the sediment-water interface under wind waves and sea swell: *Water Research*, v. 44, p. 1361–1372, <https://doi.org/10.1016/j.watres.2009.11.010>.
- Curtis, C.D., Hughes, C.R., Whiteman, J.A., and Whittle, C.K., 1985, Compositional variation within some sedimentary chlorites and some comments on their origin: *Mineralogical Magazine*, v. 49, p. 375–386, <https://doi.org/10.1180/minmag.1985.049.352.08>.
- Destombes, J., Hollard, H., and Willefert, S., 1985, Lower Palaeozoic rocks of Morocco, *in* Holland, C.H., ed., *Lower Palaeozoic Rocks of the World*, Volume 4: Lower Palaeozoic Rocks of Northwest and West-Central Africa: Chichester, UK, John Wiley and Sons, p. 91–336.
- Elrod, V.A., Berelson, W.M., Coale, K.H., and Johnson, K.S., 2004, The flux of iron from continental shelf sediments: A missing source for global budgets: *Geophysical Research Letters*, v. 31, L12307, <https://doi.org/10.1029/2004GL020216>.
- Gutiérrez-Marco, J.C., and Martin, E.L.O., 2016, Biostratigraphy and palaeoecology of Lower Ordovician graptolites from the Fezouata Shale (Moroccan Anti-Atlas): *Palaeogeography, Palaeoclimatology, Palaeoecology*, v. 460, p. 35–49, <https://doi.org/10.1016/j.palaeo.2016.07.026>.
- Hornibrook, E.R.C., and Longstaffe, F.J., 1996, Berthierine from the Lower Cretaceous Clearwater Formation, Alberta, Canada: *Clays and Clay Minerals*, v. 44, p. 1–21, <https://doi.org/10.1346/CCMN.1996.0440101>.
- Horton, D.E., Poulsen, C.J., Montañez, I.P., and DiMichele, W.A., 2012, Eccentricity-paced late Paleozoic climate change: *Palaeogeography, Palaeoclimatology, Palaeoecology*, v. 331–332, p. 150–161, <https://doi.org/10.1016/j.palaeo.2012.03.014>.
- Kozłowska, A., and Maliszewska, A., 2015, Berthierine in the Middle Jurassic sideritic rocks from southern Poland: *Geological Quarterly*, v. 59, p. 551–564.
- Lefebvre, B., et al., 2016, Palaeoecological aspects of the diversification of echinoderms in the Lower Ordovician of central Anti-Atlas, Morocco: *Palaeogeography, Palaeoclimatology, Palaeoecology*, v. 460, p. 97–121, <https://doi.org/10.1016/j.palaeo.2016.02.039>.
- Lefebvre, B., Gutiérrez-Marco, J.C., Lehnert, O., Martin, E.L.O., Nowak, H., Akodad, M., El Hariri, K., and Servais, T., 2018, Age calibration of the Lower

- Ordovician Fezouata Lagerstätte, Morocco: *Lethaia*, v. 51, p. 296–311, <https://doi.org/10.1111/let.12240>.
- Lehnert, O., Nowak, H., Sarmiento, G.N., Gutiérrez-Marco, J.C., Akodad, M., and Servais, T., 2016, Conodonts from the Lower Ordovician of Morocco—Contributions to age and faunal diversity of the Fezouata Lagerstätte and peri-Gondwana biogeography: *Palaeogeography, Palaeoclimatology, Palaeoecology*, v. 460, p. 50–61, <https://doi.org/10.1016/j.palaeo.2016.03.023>.
- Loydell, D.K., 2012, Graptolite biozone correlation charts: *Geological Magazine*, v. 149, p. 124–132, <https://doi.org/10.1017/S0016756811000513>.
- Martin, E.L.O., et al., 2016, The Lower Ordovician Fezouata Konservat-Lagerstätte from Morocco: Age, environment and evolutionary perspectives: *Gondwana Research*, v. 34, p. 274–283, <https://doi.org/10.1016/j.gr.2015.03.009>.
- McMahon, S., Anderson, R.P., Saupe, E.E., and Briggs, D.E.G., 2016, Experimental evidence that clay inhibits bacterial decomposers: Implications for preservation of organic fossils: *Geology*, v. 44, p. 867–870, <https://doi.org/10.1130/G38454.1>.
- Nichols, G., 2009, *Sedimentology and Stratigraphy* (second edition): Chichester, UK, Wiley-Blackwell, 432 p.
- Nowak, H., Servais, T., Pittet, B., Vaucher, R., Akodad, M., Gaines, R.R., and Vandenbroucke, T.R.A., 2016, Palynomorphs of the Fezouata Shale (Lower Ordovician, Morocco): Age and environmental constraints of the Fezouata Biota: *Palaeogeography, Palaeoclimatology, Palaeoecology*, v. 460, p. 62–74, <https://doi.org/10.1016/j.palaeo.2016.03.007>.
- Odin, G.S., and Gupta, B.K.S., 1988, Geological significance of the verdine facies: Developments in Sedimentology, v. 45, p. 205–219, [https://doi.org/10.1016/S0070-4571\(08\)70064-5](https://doi.org/10.1016/S0070-4571(08)70064-5).
- Odin, G.S., and Matter, A., 1981, De glauconiarum origine: *Sedimentology*, v. 28, p. 611–641, <https://doi.org/10.1111/j.1365-3091.1981.tb01925.x>.
- Osleger, D., and Read, J.F., 1991, Relation of eustasy to stacking patterns of meter-scale carbonate cycles, Late Cambrian, U.S.A.: *Journal of Sedimentary Research*, v. 61, p. 1225–1252, <https://doi.org/10.1306/D426786B-2B26-11D7-864800102C1865D>.
- Rampino, M.R., 1979, Possible relationships between changes in global ice volume, geomagnetic excursions, and the eccentricity of the Earth's orbit: *Geology*, v. 7, p. 584–587, [https://doi.org/10.1130/0091-7613\(1979\)7<584:PRBCIG>2.0.CO;2](https://doi.org/10.1130/0091-7613(1979)7<584:PRBCIG>2.0.CO;2).
- Ruiz, G.M.H., Helg, U., Negro, F., Adatte, T., and Burkhard, M., 2008, Illite crystallinity patterns in the Anti-Atlas of Morocco: *Swiss Journal of Geosciences*, v. 101, p. 387–395, <https://doi.org/10.1007/s00015-008-1267-z>.
- Tang, D., Shi, X., Jiang, G., Zhou, X., and Shi, Q., 2017, Ferruginous seawater facilitates the transformation of glauconite to chamosite: An example from the Mesoproterozoic Xiamaling Formation of North China: *The American Mineralogist*, v. 102, p. 2317–2332, <https://doi.org/10.2138/am-2017-6136>.
- Torsvik, T.H., and Cocks, L.R.M., 2011, The Palaeozoic palaeogeography of central Gondwana, *in* van Hinsbergen, D.J.J., et al., eds., *The Formation and Evolution of Africa: A Synopsis of 3.8 Ga of Earth History*: Geological Society of London Special Publication 357, p. 137–166, <https://doi.org/10.1144/SP357.8>.
- Torsvik, T.H., and Cocks, L.R.M., 2013, New global palaeogeographical reconstructions for the Early Palaeozoic and their generation, *in* Harper, D.A.T., and Servais, T., eds., *Early Palaeozoic Biogeography and Palaeogeography*: Geological Society of London Memoir 38, p. 5–24, <https://doi.org/10.1144/M38.2>.
- Van Roy, P., Orr, P.J., Botting, J.P., Muir, L.A., Vinther, J., Lefebvre, B., El Hariri, K., and Briggs, D.E.G., 2010, Ordovician faunas of Burgess Shale type: *Nature*, v. 465, p. 215–218, <https://doi.org/10.1038/nature09038>.
- Van Roy, P., Briggs, D.E.G., and Gaines, R.R., 2015, The Fezouata fossils of Morocco: An extraordinary record of marine life in the Early Ordovician: *Journal of the Geological Society*, v. 172, p. 541–549, <https://doi.org/10.1144/jgs2015-017>.
- Vaucher, R., Martin, E.L.O., Hormière, H., and Pittet, B., 2016, A genetic link between *Konzentrat* and *Konservat* Lagerstätten in the Fezouata Shale (Lower Ordovician, Morocco): *Palaeogeography, Palaeoclimatology, Palaeoecology*, v. 460, p. 24–34, <https://doi.org/10.1016/j.palaeo.2016.05.020>.
- Vaucher, R., Pittet, B., Hormière, H., Martin, E.L.O., and Lefebvre, B., 2017, A wave-dominated, tide-modulated model for the Lower Ordovician of the Anti-Atlas, Morocco: *Sedimentology*, v. 64, p. 777–807, <https://doi.org/10.1111/sed.12327>.
- Vorhies, J.S., and Gaines, R.R., 2009, Microbial dissolution of clay minerals as a source of iron and silica in marine sediments: *Nature Geoscience*, v. 2, p. 221–225, <https://doi.org/10.1038/ngeo441>.

Printed in USA

Biogenic Iron Preserves Structures during Fossilization: A Hypothesis

Iron from Decaying Tissues May Stabilize Their Morphology in the Fossil Record

Farid Saleh,* Allison C. Daley, Bertrand Lefebvre, Bernard Pittet, and Jean Philippe Perrillat

It is hypothesized that iron from biological tissues, liberated during decay, may have played a role in inhibiting loss of anatomical information during fossilization of extinct organisms. Most tissues in the animal kingdom contain iron in different forms. A widely distributed iron-bearing molecule is ferritin, a globular protein that contains iron crystallites in the form of ferrihydrite minerals. Iron concentrations in ferritin are high and ferrihydrites are extremely reactive. When ancient animals are decaying on the sea floor under anoxic environmental conditions, ferrihydrites may initialize the selective replication of some tissues in pyrite FeS_2 . This model explains why some labile tissues are preserved, while other more resistant structures decay and are absent in many fossils. A major implication of this hypothesis is that structures described as brains in Cambrian arthropods are not fossilization artifacts, but are instead a source of information on anatomical evolution at the dawn of complex animal life.

been crucial for revealing the earliest evolution of animals.^[4–10] Similarly, exceptionally preserved soft parts in fossils from the slightly younger Fezouata Shale (Ordovician, Morocco) were decisive in ending long-standing debates on the systematic affinities of various enigmatic taxa (e.g., machaeridians, stylophorans).^[11–13] The Chengjiang Biota (Cambrian, China) has also yielded a considerable number of soft arthropod taxa with complex nervous systems.^[14–16] In most cases, nervous tissues from the Chengjiang Biota are pyritized (i.e., preserved in FeS_2) or show an association of pyrite and organic matter.^[14–17] Pyritized tissues are frequently preserved alone in the fossils, while other tissues or organs (except the cuticle or body walls) are completely absent.^[17] Experimental

1. Introduction

Inspecting the fossil record is crucial to understanding the biology of past life on Earth. Exceptionally preserved biotas, preserving soft-bodied metazoans (e.g., non-biomineralized arthropods; early chordates), and their labile anatomies (e.g., digestive tracts, muscles, and nervous systems) constitute a unique window on ancient ecosystems.^[1–3] For instance, the Burgess Shale deposit in Canada has yielded a considerable number of spectacular soft bodied fossils of Cambrian age (508 million years old) whose bizarre anatomy, preserved in high fidelity, has

taphonomic studies investigating how biological tissues decay under controlled laboratory conditions questioned the validity of these paleontological discoveries by showing that nervous systems have little to no chance of preservation because they are observed to be rapidly lost to decay.^[18–20] These experimental results have consequently given rise to contrasting conceptual frameworks in the paleontology and evolutionary biology communities.^[21–23] Although vital to constraining preservation pathways,^[23] experimental decay data should be interpreted carefully and not projected directly onto enigmatic features in the geological record because fossils are not degraded carcasses and decay resistance is an imperfect indicator of fossilization potential.^[24] Currently, there is no model accounting for the preservation of a specific labile tissue in a specimen where other more resistant tissues are completely absent. We investigate preservation patterns in such problematic structures and compare them to new data on patterns of pyritization observed in non-altered sediments, leading us to propose an explanation for the contrast observed between the fossil record and modern decay experiments.

F. Saleh, Dr. B. Lefebvre, Dr. B. Pittet, Dr. J. P. Perrillat
 Université de Lyon
 Université Claude Bernard Lyon1
 École Normale Supérieure de Lyon
 CNRS, UMR5276, LGL-TPE, Villeurbanne 69622, France
 E-mail: farid.saleh@univ-lyon1.fr

Prof. A. C. Daley
 Institute of Earth Sciences
 University of Lausanne
 Géopolis, Lausanne CH-1015, Switzerland

 The ORCID identification number(s) for the author(s) of this article can be found under <https://doi.org/10.1002/bies.201900243>

This article is commented on in the Idea to Watch article by Ross P. Anderson, <https://doi.org/10.1002/bies.202000070>.

DOI: 10.1002/bies.201900243

2. Enigmatic Structures Are Preserved in Pyrite and Organic Matter

Anatomical structures described as brains in fossils from the Chengjiang Biota were investigated using X-ray fluorescence

mapping, which revealed the presence of carbon and iron^[17] (Figure 1a–d). Electron microscopy shows that iron occurs either as small euhedral crystals (around 2 microns in size) or as framboids (around 10 microns in size)^[17] (Figure 1e–h). Pyrite crystal morphology indicates that pyritization occurred very early during the fossilization process, shortly after the death of the organism.^[25,26] Carbon in these fossils is preserved as compressed dark films^[17] (Figure 1i,j). Chengjiang fossils broken through the middle show pyrite overlaying carbonaceous films on both parts,^[17] indicating a centrifugal pattern of pyritization (Figure 1k). Centrifugal pyritization, similar to patterns of tissue preservation in the Chengjiang Biota, is also present in fresh core sediments (Figure 2a) from levels with exceptional preservation within the Fezouata Shale, where Raman spectroscopy identified large pyrite clusters surrounded by organic matter (Figure 2b–d).

FeS₂ precipitation in sediments requires decaying organic material, iron that is usually provided by surrounding sediments, and sulfates SO₄²⁻ from sea waters.^[27,28] Under sulfate-reducing conditions, bacteria transform organic matter and sulfates into HS⁻ and then to hydrogen sulfides H₂S, which react with Fe in a series of reactions to form pyrite.^[26–28] If the sediment surrounding dead animals is poor in organic matter, as was the case in the Fezouata Shale,^[29] sulfate reduction is limited to decaying carcasses.^[29] Within a decaying carcass, anatomical features can react differently to decay.^[30] Easily degradable structures (e.g., tissues and organs formed of cells)^[3] constitute a hotspot for H₂S production, whereas more resistant structures (e.g., biomineralized parts), do not produce enough H₂S, and thus do not pyritize.^[31] Furthermore, decay discrepancies exist even between different fast decaying cellular structures. Some cellular structures are solely degraded by external bacterial communities, while others degrade under the activity of their internal microbial biota and enzymes as well.^[30,32] If decay by external bacteria is dominant and iron is available, pyritization starts at the outer part of the organic material where both H₂S and Fe are present, leading to a centripetal pattern of preservation (Figure 3a). This pattern is observed in the fossil record^[27] and does not refute occurrences of centrifugal pyritization, because some tissues decay under the activity of their internal bacteria and enzymes. If such internal decay is dominant and iron is present, more H₂S is produced internally, leading to the centrifugal pattern of preservation (Figure 3b). It is likely that preserved structures in the Chengjiang Biota and the Fezouata Shale decayed under the activity of their internal microbial biotas and enzymes in the presence of iron. This model based on H₂S limitation and production patterns^[25,27,31] explains the pyritization of numerous internal tissues in Cambrian Arthropods within non-pyritized cuticular body walls that did not produce enough H₂S for their pyritization.^[25,31] However, it fails to explain the selective pyritization of a specific internal cellular structure (i.e., nervous system) while other structures (e.g., digestive and vascular systems) decayed away, producing H₂S, but did not pyritize. Thus, it is crucial to investigate patterns of iron distribution in the sediment surrounding decaying carcasses.

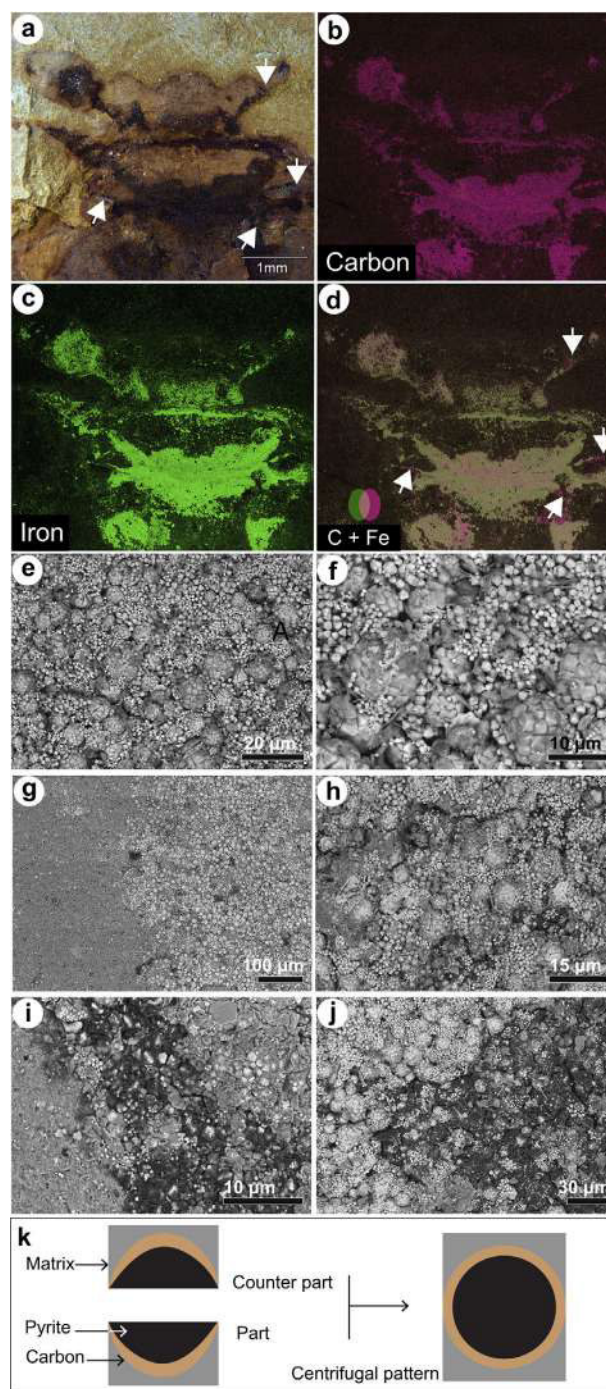


Figure 1. Preservation of Cambrian brains in *Fuxianhuia protensa* from the Chengjiang Biota. a) YKLP 15 006 shows dark brown areas interpreted as nervous tissues under direct illumination. b) Carbon distribution in the studied specimen. c) Iron distribution. d) Merged iron and carbon signals show an almost perfect superposition between these two elements. White arrows indicate the rare places where both elements do not co-occur. e–h) Iron is preserved as small euhedral and framboidal pyrite. i,j) Minerals overlay dark compressed carbonaceous material. k) The distribution of carbonaceous films under pyrite minerals in both part and counter-part suggest a centrifugal pattern of pyritization. Parts (a) to (j) were adapted with permission.^[17] Copyright 2015, Elsevier.

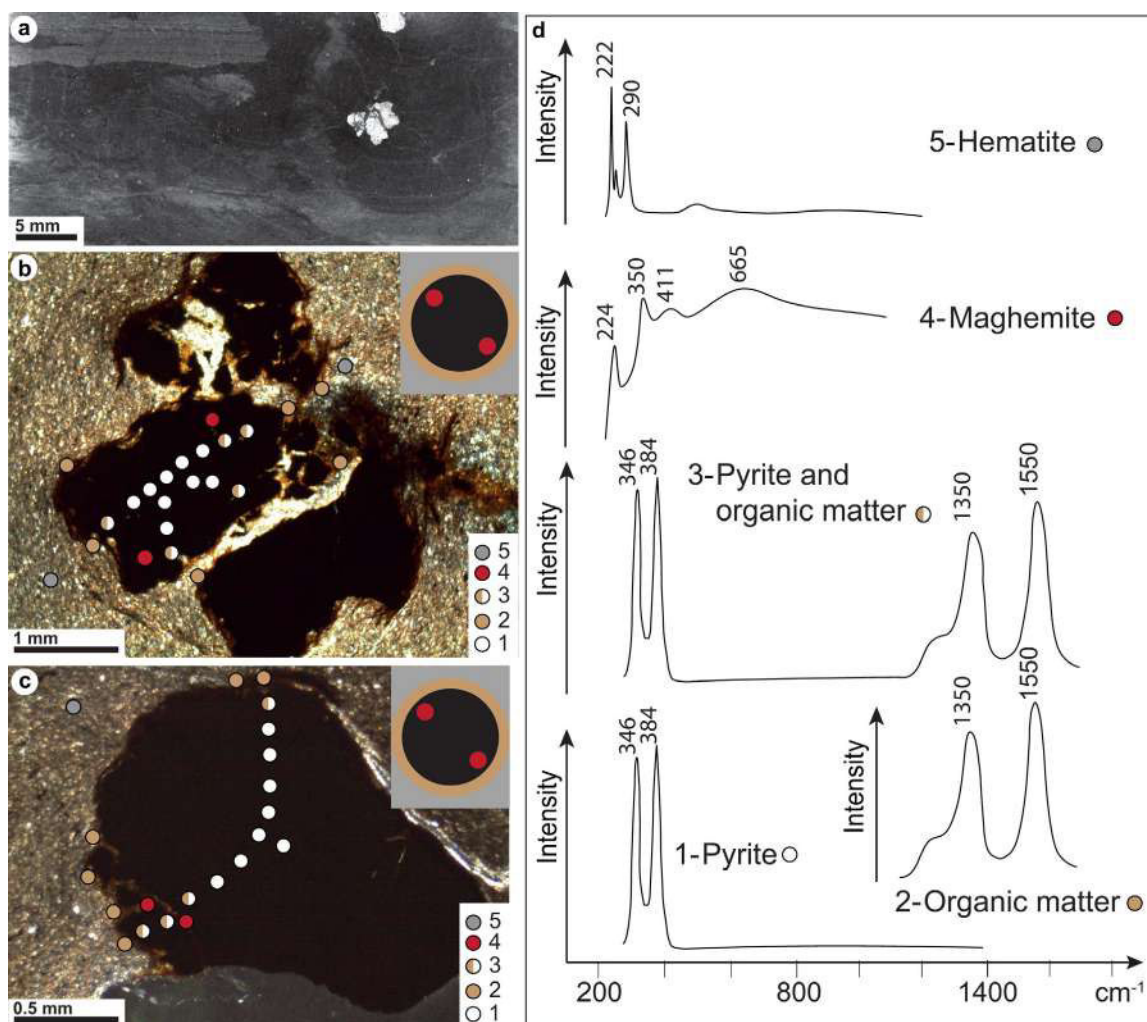


Figure 2. Pyritization in the Fezouata Shale. a–d) Pyrite crystals in fresh core deposits showing a centrifugal pattern of pyritization as reconstructed on the top right of (b) and (c). Colored points in (b) and (c) correspond to the spectra shown in (d). Iron oxide phase identification is based on Raman peak indexation in natural samples.^[62,63]

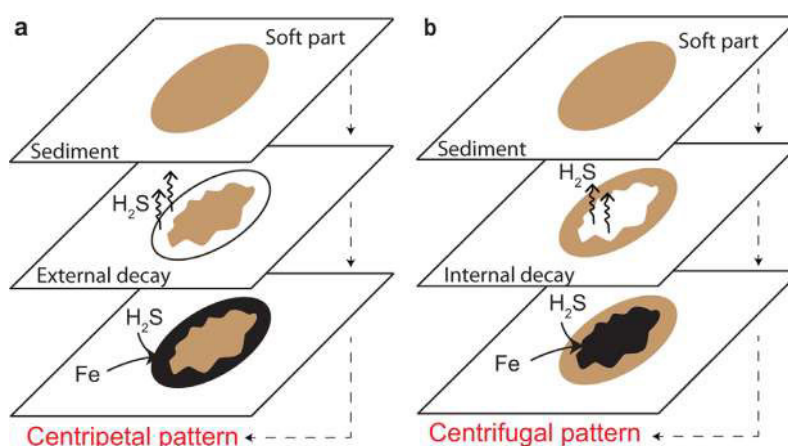


Figure 3. Patterns of soft tissue decay. a) Soft parts decaying under the activity of external bacteria lead to a centripetal pyritization. b) Soft parts decaying under their own bacterial community and enzymes contribute in a centrifugal pyritization. The brown part indicates organic matter, while black symbolizes pyrite precipitation.

Table 1. Half-lives of iron phases under permissive conditions for pyrite precipitation. This table is adapted with permission.^[38] Copyright 1992, American Journal of Science.

Iron phase	Half-life
Goethite	11.5 days
Hematite	31 days
Magnetite	105 years
Reactive silicates	230 years
Sheet silicates	84 000 years
Augite, amphibole	>84 000 years

3. Abiotic Iron Is Not Fast Enough to Preserve Labile Tissues

The most widely accepted suggestions of sources of iron for pyritization are abiotic.^[28,33] In the Fezouata Shale, iron oxides found in sediments (e.g., hematite α -Fe₂O₃; Figure 2b–d) constitute only a small fraction of the rock (i.e., <1%).^[26] However, here and in numerous Cambrian sites with exceptional fossil preservation, iron-rich silicates such as berthierine/chamosite are dominant (i.e., between 5% and 15% of the total rock composition).^[26,34] Berthierine/chamosite results from the transformation of a primary clay mineral (e.g., glauconite, odinite, kaolinite, or other similar precursor minerals)^[35] under anoxic conditions and high iron concentrations.^[26] Thus, iron in this mineralogical phase gives an estimate of the quantity of iron in the environment.^[26,34,35] The formation of berthierine/chamosite in the Fezouata Shale required at least $\approx 8.10^{-5}$ M (M for molar concentration) of iron (see Supporting Information). This high concentration is slightly less than that of modern anoxic sediments at 10^{-4} M and is still enough to pyritize at the site of decay.^[27] Thus, in theory and in terms of concentration, abiotic iron is not a limiting parameter in levels with exceptional preservation in the Fezouata Shale^[26] or at other sites with exceptional fossil preservation from the Cambrian.^[34,36] Other parameters must have limited the availability of this iron during soft tissues degradation and inhibited pyrite from replicating all internal systems. Laboratory experiments have shown that most soft anatomical structures in animals decay very quickly, within hours or days after death.^[18,20,37] For instance, nervous tissues decayed in 11 days for chordates and in 4 days for ecdysozoans.^[18,20] In contrast, most iron-rich mineral phases require longer times to deliver their iron when in contact with H₂S, with a minimum of 11.5 days ranging up to hundreds or thousands of years (Table 1).^[38] This exceeds the timing of biological tissue decay, especially for labile tissues and organs such as the brain.^[18,20,32,37] Thus, another source of available iron must exist in order to selectively pyritize a tissue/organ shortly after the death of the organism.

4. Biogenic Iron Is Available During Decay

Since abiotic iron is not made available fast enough to start the pyritization process, a biogenic iron source must be investigated. We analyzed thin sections from the Fezouata Shale and found maghemite (i.e., γ -Fe₂O₃ structurally similar to magnetite) in association with pyrite (Figure 2b–d). Two widely recognized mech-

anisms for maghemite formation exist.^[39,40] In the first mechanism, lepidocrocite, a fibrous iron oxide-hydroxide, transforms partially to maghemite at temperatures around 200 °C and completely at temperatures higher than 570 °C.^[39] In the second method, maghemite results from buried ferrihydrites at temperatures between 100 and 300 °C.^[40] Sediments from the Fezouata Shale were cooked at temperatures between 100 and 200 °C.^[26,41] These temperatures, and the absence of lepidocrocite in the analyzed samples and in tens of other sampled intervals in the Fezouata Shale,^[26] indicate that maghemite in these samples originates most probably from ferrihydrites. Ferrihydrite is a mineral present in a wide variety of biological tissues, which can explain why maghemite is only found in association with pyritized organic matter and not elsewhere in the sediment.

In all animals, ferritin is a metalloprotein that stores an excess of iron in the form of a hydrous ferric oxide-phosphate mineral [FeO(OH)]₈ [FeO(H₂PO₄)] similar in structure to the mineral ferrihydrite.^[42,43] Ferritin-ferrihydrites are found in nervous systems, muscles and sensory organs such as the eyes.^[44–46] Ferritin is capable of storing as many as 4500 iron atoms in its core (i.e., concentration equivalent to 0.25 M).^[46] Increased accumulations of ferritin-ferrihydrites were evidenced in marine invertebrates after their exposure to dysoxic/anoxic conditions^[47] comparable to the environments in which animals from the Chengjiang Biota and the Fezouata Shale were preserved.^[48,49] In experimental studies, it was shown that under bacterial sulfate reducing (BSR) conditions and when sulfates are present, ferrihydrites release high quantities ($\approx 87\%$) of reactive Fe^[50] (i.e., 0.22 M). This iron delivery is 40% higher than the yield from the same quantity of hematite.^[50] Furthermore, ferrihydrite is the fastest to deliver reactive iron with a half-life under BSR conditions of only 2.8 h.^[38] The solid phase of ferrihydrite means that it does not migrate,^[51] thus 0.11 M of iron becomes available in situ within a couple of hours of the start of decay. These concentrations are well above those in modern anoxic sediments,^[27] and are more than sufficient to initiate pyritization at the site of decay.

5. Biogenic Iron Explains the Selective Pyritization of Soft Anatomies

Ferrihydrite in biological tissues constitutes a local source that rapidly provides high quantities of reactive Fe^[38] that can initialize the process of pyritization. Shortly after the death of an organism, decay of the most labile tissue starts producing H₂S and, if this tissue contains ferrihydrites, a considerable amount of reactive iron (Figure 4). The produced H₂S and Fe react to form pyrite nuclei (Figure 4) that further grow with increasing H₂S and Fe availability as decay proceeds (Figure 4). The extensive activity of decay leads also to the degradation of more resistant but iron-poor tissues (Figure 4), which produce only H₂S without iron (Figure 4). The replication of such tissue in pyrite is therefore not initiated, leading to a loss of the original morphology or even the complete disappearance of the tissue/organ (Figure 4). When abiotic iron becomes available, it can play a role in pyrite growth in tissues that previously provided biogenic iron (Figure 4). This hypothesis shows how biogenic iron stabilizes the morphology of decay-prone anatomical structures, before the less reactive abiotic iron phases become available.

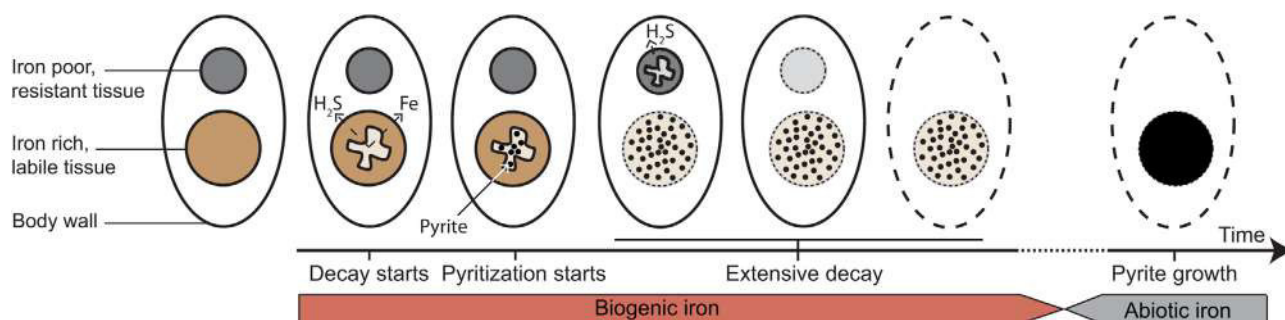


Figure 4. Hypothesis for labile tissue preservation owing to a biogenic iron source, co-occurring with resistant tissue loss.

6. Hypothesis Testing Requires a Multidisciplinary Approach

Although fossil mineralization is common in the geological record,^[52–57] little work has been done to investigate the role of tissue chemistry during the mineralization process. Recently, it was suggested that the recurrent association of particular mineralogical phases such as fluorapatite, or Fe-sulfides (pyrite, pyrrhotite) with specific tissues in crustacean fossils preserved within carbonate-rich concretions from the Jurassic exceptionally preserved biota of La Voulte-sur-Rhône (Ardèche, France) were linked to differences in the original biochemical signal of the organic matter.^[58] However, much work remains to be done to determine the fate and behavior of biogenic iron during taphonomic processes, and fully enlighten the black box of pyritization. In order to test the hypothesis presented here and determine the precise roles played by biogenic iron and iron from sediments, several lines of investigation should be undertaken combining geochemical, biological, and experimental taphonomy approaches. It would be ideal to start testing the hypothesis on non-weathered complete fossils. However, to our knowledge, no pyritized fossils from completely fresh sediments have yet been discovered. Instead, investigations on any fresh pyrite might also be helpful because pyrite formation requires organic matter and so results obtained from these pyrites may reflect original biochemical compositions. Iron isotopic investigations on pyrite crystals from both sediments and fossils would help to decipher the multiple iron-sources and their role in pyritization. If made at the nanoscale, these isotopic investigations could inform on the source and chronology of iron delivery, from the initiation of pyrite precipitation to the subsequent pyrite crystals growth. Biological approaches to testing this biogenic iron hypothesis involve making a comparison between iron concentrations in different modern animal groups. An even more detailed approach would be to quantify iron in different types of tissues within the same group. For instance, according to this hypothesis, if a specific group shows a higher concentration of iron in a specific tissue, we would expect to find this particular structure pyritized more often than the others in the geological record. All these quantitative data will help calibrate the new proposed model and understand its feasibility in natural environments. Most importantly, future decay experiments should focus not only on the general environmental conditions that lead to exceptional preservation, but also on the chemical signature surrounding each tissue during its degradation independently from the physical ability

of this tissue to resist decay. These decay experiments should be done in the presence of different sediment compositions and under different bacterial communities to see if the decay processes and rates vary under different environmental conditions. Once iron sources, iron quantities in biological tissues, decay behavior, and favorable sedimentological phases are discovered, attempts could be made to replicate pyrite precipitation from biological tissues in laboratory experiments.

7. Conclusions and Outlook

The present biogenic iron hypothesis helps us understand the sole presence of the most-labile tissues in some specimens where other more decay-resistant soft parts are absent. It also shows that pyritization starts very early during decay, preserving in high fidelity tissues that are originally iron-rich, resolving the morphological accuracy of Cambrian arthropod brains. Furthermore, it indicates that both decay experiments and paleontological descriptions are complementary, not incompatible. It opens new avenues of research by highlighting the importance of tissue chemistry during the fossilization process especially in the case of nervous tissues that are preserved in carbonaceous compressions without any pyrite.^[59–61]

Supporting Information

Supporting Information is available from the Wiley Online Library or from the author.

Acknowledgements

This paper is a contribution to the TelluS-INTERVIE project “Géochimie d’un Lagerstätte de l’Ordovicien inférieur du Maroc” (2019) funded by the INSU (Institut National des Sciences de l’Univers, France), CNRS. This paper is also a contribution to the International Geoscience Program (IGCP) Project 653—the onset of the Great Ordovician Biodiversification Event. The Raman facility in Lyon (France) is supported by the INSU. A.C.D. was supported by grant no. 205321_179084 from the Swiss National Science Foundation. The authors thank Gilles Montagnac for assistance during Raman spectroscopy analyses. The authors also thank Robert Raiswell, Christian Klug, and the anonymous reviewers for their comments and remarks.

Conflict of Interest

The authors declare no conflict of interest.

Keywords

Burgess Shale, Chengjiang Biota, exceptional fossil preservation, Fezouata Shale, mineralization, nervous systems, taphonomy

Received: December 12, 2019

Revised: February 27, 2020

Published online:

- [1] P. van Roy, P. J. Orr, J. P. Botting, L. A. Muir, J. Vinther, B. Lefebvre, K. El Hariri, D. E. G. Briggs, *Nature* **2010**, 465, 215.
- [2] A. C. Daley, J. B. Antcliffe, H. B. Drage, S. Pates, *Proc. Natl. Acad. Sci. U. S. A.* **2018**, 115, 5323.
- [3] F. Saleh, J. B. Antcliffe, B. Lefebvre, B. Pittet, L. Laibl, F. Perez Peris, L. Lustri, P. Gueriau, A. C. Daley, *Earth Planet. Sci. Lett.* **2020**, 529, 115873.
- [4] J. Moysiuk, M. R. Smith, J.-B. Caron, *Nature* **2017**, 541, 394.
- [5] J. Moysiuk, J. B. Caron, *Proc. R. Soc. B Biol. Sci.* **2019**, 286, 20182314.
- [6] K. Nanglu, J. B. Caron, *Curr. Biol.* **2018**, 28, 319.
- [7] A. C. Daley, G. E. Budd, J. B. Caron, G. D. Edgecombe, D. Collins, *Science* **2009**, 323, 1597.
- [8] J. Vannier, J. Liu, R. Lerosey-Aubril, J. Vinther, A. C. Daley, *Nat. Commun.* **2014**, 5, 3641.
- [9] M. R. Smith, J.-B. Caron, *Nature* **2010**, 465, 469.
- [10] T. P. Topper, L. C. Strotz, L. E. Holmer, Z. Zhang, N. N. Tait, J. B. Caron, *BMC Evol. Biol.* **2015**, 15, 42.
- [11] J. Vinther, P. van Roy, D. E. G. Briggs, *Nature* **2008**, 451, 185.
- [12] J. Vinther, L. Parry, D. E. G. Briggs, P. van Roy, *Nature* **2017**, 542, 471.
- [13] B. Lefebvre, T. E. Guensburg, E. L. O. Martin, R. Mooi, E. Nardin, M. Nohejlová, F. Saleh, K. Kouraišs, K. El Hariri, B. David, *Geobios* **2019**, 52, 27.
- [14] G. Tanaka, X. Hou, X. Ma, G. D. Edgecombe, N. J. Strausfeld, *Nature* **2013**, 502, 364.
- [15] P. Cong, X. Ma, X. Hou, G. D. Edgecombe, N. J. Strausfeld, *Nature* **2014**, 513, 538.
- [16] X. Ma, X. Hou, G. D. Edgecombe, N. J. Strausfeld, *Nature* **2012**, 490, 258.
- [17] X. Ma, G. D. Edgecombe, X. Hou, T. Goral, N. J. Strausfeld, *Curr. Biol.* **2015**, 25, 2969.
- [18] R. S. Sansom, S. E. Gabbott, M. A. Purnell, *Nature* **2010**, 463, 797.
- [19] D. J. E. Murdock, S. E. Gabbott, G. Mayer, M. A. Purnell, *BMC Evol. Biol.* **2014**, 14, 222.
- [20] R. S. Sansom, *Sci. Rep.* **2016**, 6, 32817.
- [21] J. Liu, M. Steiner, J. A. Dunlop, D. Shu, *Proc. R. Soc. B Biol. Sci.* **2018**, 285, 20180051.
- [22] F. Saleh, B. Lefebvre, A. W. Hunter, M. Nohejlová, *Micros. Today* **2020**, 28, 24.
- [23] M. A. Purnell, P. J. C. Donoghue, S. E. Gabbott, M. E. McNamara, D. J. E. Murdock, R. S. Sansom, *Palaeontology* **2018**, 61, 317.
- [24] L. A. Parry, F. Smithwick, K. K. Nordén, E. T. Saitta, J. Lozano-Fernandez, A. R. Tanner, J.-B. Caron, G. D. Edgecombe, D. E. G. Briggs, J. Vinther, *BioEssays* **2018**, 40, 1700167.
- [25] S. E. Gabbott, H. Xian-guang, M. J. Norry, D. J. Siveter, *Geology* **2004**, 32, 901.
- [26] F. Saleh, B. Pittet, J. Perrillat, B. Lefebvre, *Geology* **2019**, 47, 103.
- [27] J. D. Schiffbauer, S. Xiao, Y. Cai, A. F. Wallace, H. Hua, J. Hunter, H. Xu, Y. Peng, A. J. Kaufman, *Nat. Commun.* **2014**, 5, 5754.
- [28] R. Raiswell, K. Whaler, S. Dean, M. Coleman, D. E. Briggs, *Mar. Geol.* **1993**, 113, 89.
- [29] R. R. Gaines, D. E. G. Briggs, P. J. Orr, P. van Roy, *Palaio* **2012**, 27, 317.
- [30] D. E. G. Briggs, A. J. Kear, *Paleobiology* **1993**, 19, 107.
- [31] Ú. C. Farrell, *Paleontol. Soc. Pap.* **2014**, 20, 35.
- [32] A. D. Butler, J. A. Cunningham, G. E. Budd, P. C. J. Donoghue, *Proc. R. Soc. B* **2015**, 282, 20150476.
- [33] R. Raiswell, D. E. Canfield, R. A. Berner, *Chem. Geol.* **1994**, 111, 101.
- [34] R. P. Anderson, N. J. Tosca, R. R. Gaines, N. Mongiardino Koch, D. E. G. Briggs, *Geology* **2018**, 46, 347.
- [35] D. Tang, X. Shi, G. Jiang, X. Zhou, Q. Shi, *Am. Mineral.* **2017**, 102, 2317.
- [36] E. A. Sperling, C. J. Wolock, A. S. Morgan, B. C. Gill, M. Kunzmann, G. P. Halverson, F. A. Macdonald, A. H. Knoll, D. T. Johnston, *Nature* **2015**, 523, 451.
- [37] A. D. Hancy, J. B. Antcliffe, *Geobiology* **2020**, 18, 167.
- [38] D. E. Canfield, R. Raiswell, S. Bottrell, *Am. J. Sci.* **1992**, 292, 659.
- [39] T. S. Gendler, V. P. Shcherbakov, M. J. Dekkers, A. K. Gapeev, S. K. Gribov, E. McClelland, *Geophys. J. Int.* **2005**, 160, 815.
- [40] L. Mazzetti, P. J. Thistlethwaite, *J. Raman Spectrosc.* **2002**, 33, 104.
- [41] G. M. H. Ruiz, U. Helg, F. Negro, T. Adatte, M. Burkhard, *Swiss J. Geosci.* **2008**, 101, 387.
- [42] F. M. Michel, V. Barron, J. Torrent, M. P. Morales, C. J. Serna, J.-F. Boily, Q. Liu, A. Ambrosini, A. C. Cismasu, G. E. Brown, *Proc. Natl. Acad. Sci. U. S. A.* **2010**, 107, 2787.
- [43] N. D. Chasteen, P. M. Harrison, *J. Struct. Biol.* **1999**, 126, 182.
- [44] K. Hoda, C. L. Bowlus, T. W. Chu, J. R. Gruen, *Emerg. Rimoin's Princ. Pract. Med. Genet.* **2013**, 394.
- [45] E. M. Aldred, C. Buck, K. Vall, E. M. Aldred, C. Buck, K. Vall, *Pharmacology* **2009**, 331.
- [46] D. Dunaief, A. Cwanger, J. L. Dunaief, in *Handbook Of Nutrition, Diet and the Eye*, Academic Press, Burlington, London **2014**, pp. 619–626.
- [47] K. Larade, K. B. Storey, *J. Exp. Biol.* **2004**, 207, 1353.
- [48] F. Saleh, Y. Candela, D. A. T. Harper, M. Polechová, B. Pittet, B. Lefebvre, *Palaio* **2018**, 33, 535.
- [49] E. L. O. Martin, B. Pittet, J.-C. Gutiérrez-Marco, J. Vannier, K. El Hariri, R. Lerosey-Aubril, M. Masrour, H. Nowak, T. Servais, T. R. A. Vandenbroucke, P. van Roy, R. Vaucher, B. Lefebvre, *Gondwana Res.* **2016**, 34, 274.
- [50] Y.-L. Li, H. Vali, J. Yang, T. J. Phelps, C. L. Zhang, *Geomicrobiol. J.* **2006**, 23, 103.
- [51] S. Wang, L. Lei, D. Zhang, G. Zhang, R. Cao, X. Wang, J. Lin, Y. Jia, *J. Hazard. Mater.* **2020**, 384, 121365.
- [52] D. E. Briggs, S. H. Bottrell, R. Raiswell, *Geology* **1991**, 19, 1221.
- [53] T. A. Hegna, M. J. Martin, S. A. Darroch, *Geology* **2017**, 45, 199.
- [54] L. Frey, A. Pohle, M. Rücklin, C. Klug, *Lethaia* **2019**, 52, 242.
- [55] J. Rust, A. Bergmann, C. Bartels, B. Schoenemann, S. Sedlmeier, G. Köhl, *Arthropod Struct. Dev.* **2016**, 45, 140.
- [56] T. W. Kammer, C. Bartels, W. I. Ausich, *Lethaia* **2016**, 49, 307.
- [57] R. Raiswell, R. Newton, S. H. Bottrell, P. M. Coburn, D. E. Briggs, D. P. Bond, S. W. Poulton, *Am. J. Sci.* **2008**, 308, 105.
- [58] C. Jauvion, S. Bernard, P. Gueriau, C. Mocuta, S. Pont, K. Benzerara, S. Charbonnier, *Palaeontology* **2019**, 1.
- [59] J. Ortega-Hernández, *Curr. Biol.* **2015**, 25, 1625.
- [60] L. Parry, J.-B. Caron, *Sci. Adv.* **2019**, 5, eaax5858.
- [61] J. Ortega-Hernández, R. Lerosey-Aubril, S. Pates, *Proc. R. Soc. B* **2019**, 286, 20192370.
- [62] S. Das, M. J. Hendry, *Chem. Geol.* **2011**, 290, 101.
- [63] M. Hanesch, *Geophys. J. Int.* **2009**, 177, 941.

6. FOSSIL MATURATION AND WEATHERING

This chapter consists of one paper:

- **Paper 5:** Saleh, F., Pittet, B., Sansjofre, P., Guériau, P., Lalonde, S., Perrillat, J-P., Vidal, M., Lucas, V., El Hariri, K., Kouraiss, K., Lefebvre, B., 2020. Taphonomic pathway of exceptionally preserved fossils in the Lower Ordovician of Morocco. **Geobios**, 60.

Summary

Following the discovery of the role played by decay and mineralization in the process of fossilization^{54,58}, it is crucial to understand the effect of maturation and weathering on fossils from the Fezouata Shale. Classically, it is well known that organic matter volatilizes and disappears under extreme burial temperatures¹⁷. Modern weathering leaches and removes as well organic matter from exposed surface sediments⁷¹. Thus, generally, both extreme maturation and modern weathering play a role in character loss rather than character preservation. In this chapter, we examine the exact sedimentary facies in which fossils were buried and matured. Then based on core material we compare the chemical signal from fresh deep core sediments with superficial sediments in outcrops.

A statistical correlation shows that exceptional fossil preservation is correlated with almost the most distal facies of the Fezouata Shale⁷². This facies was deposited just below the storm weather wave base (SWWB). This environment is rather calm and only affected during periods of strong storms⁷². The generally weak storm record in this facies explains why storms were not able to transport dead or living organisms when burial occurred⁵⁰ (see section 3). Furthermore, the relative burial tardiness observed in this facies when compared to more proximal facies of the Fezouata Shale may explain why many animals were discovered at the last stage of their degradation (see section 4) except the cases of organisms that were buried alive⁵³. In terms of burial, this facies is not ideal when compared to more proximal facies in which animals were more recurrently covered by storm deposits⁵⁰. However, it comprises a finer lithology than proximal facies that is essential for exceptional preservation to occur, while this lithology remains coarser than the most distal facies of the Fezouata Shale⁷². Considering that this facies is not the least porous of this formation due to the presence of silty storm sediments, fossil alteration can occur more easily than in the most distal, clay-richer deposits. A comparison of fresh sediments from cores with fossil samples from surface outcrop indicates that extensive alteration occurred in the Fezouata Shale⁷². Fresh deep sediments contain pyrite minerals and organic matter. In surface sediments, ~ 1-3m depending on the site, organic matter was removed and pyrite is transformed into iron oxides⁷². Surface sediment exhibit as well an enrichment in manganese and calcium loss⁷². Raman spectroscopy-based models for thermal maturation on fresh carbon indicate the Fezouata Shale sediments were buried on temperatures that are generally lower than 200°C⁷²⁻⁷⁴. Thus, metamorphism *sensu stricto* leading to organic remain volatilization from some deposits did not occur⁷². The chemical discrepancies between fresh and altered sediments (i.e. C and Ca leaching, S removal from pyrite crystals, Mn enrichment) in the Fezouata Shale are most probably due to modern weathering. In the Draa Valley, this formation is exposed to abundant water circulations, as revealed by the numerous abandoned terraces near the outcrops and by the abundance of water wells in the area⁷⁵. Fast pyrite oxidation may be induced by Mn-oxides that are abundant in circulating waters in arid environments with occasional rain similar to the Draa Valley (Fig. 5A)^{75,76}. The resulting products of this reaction are Fe-oxides and Mn-sulfates (Fig. 5B)⁷⁷. If the quantities of Mn are not sufficient to fully oxidize pyrite, pyrite oxidation by H₂O molecules and atmospheric O₂ will take place (Fig. 5B) and unleash considerable amounts of sulfuric acid (Fig. 5C), thus reducing the pH of the environment and contributing to the dissolution of nearby carbonates (Fig. 5D)⁷⁷. When extensive weathering occurred by circulating waters that are Fe-rich, star-

shaped iron oxides can be deposited (Fig. 5E)⁷². However, these iron oxides are modern and do not result from pyrite oxidation (Fig. 5)⁷².

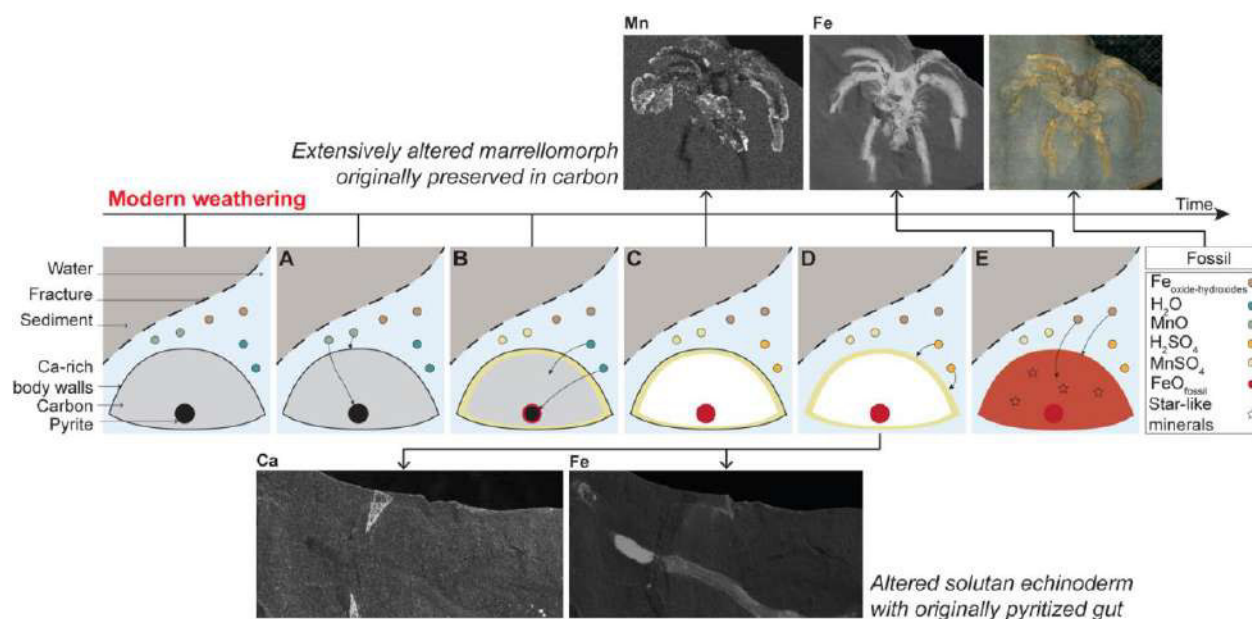
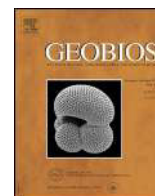


Figure 5. Modern weathering effect on fossils from the Fezouata Shale. Note the leaching of calcium from the skeleton of the solutan echinoderm (CASG72938) and the enrichment of Mn-rich deposits resulting from this alteration surrounding the analyzed marrellomorph (AA.BIZ31.OI.39).



Available online at
ScienceDirect
www.sciencedirect.com

Elsevier Masson France
EM|consulte
www.em-consulte.com



Original article

Taphonomic pathway of exceptionally preserved fossils in the Lower Ordovician of Morocco[☆]

Farid Saleh^{a,*}, Bernard Pittet^a, Pierre Sansjofre^b, Pierre Guériau^c, Stefan Lalonde^d,
Jean-Philippe Perrillat^a, Muriel Vidal^d, Victoire Lucas^a, Khadija El Hariri^e,
Khaoula Kourais^e, Bertrand Lefebvre^a

^a University Lyon, Université Claude Bernard Lyon 1, ENS de Lyon, CNRS, UMR 5276 Laboratoire de Géologie de Lyon: Terre, Planètes, Environnement, 69622 Villeurbanne, France

^b MNHN, Sorbonne Université, CNRS UMR 7590, IRD, Institut de minéralogie, Physique des Matériaux et de Cosmochimie, Paris, France

^c Institute of Earth Sciences, University of Lausanne, Géopolis, 1015 Lausanne, Switzerland

^d University Brest, CNRS, IUEM Institut Universitaire Européen de la Mer, UMR 6538 Laboratoire Géosciences Océan, Place Nicolas Copernic, 29280 Plouzané, France

^e Département des Sciences de la Terre, Faculté des Sciences et Techniques, Université Cadi-Ayyad, BP 549, 40000 Marrakesh, Morocco

ARTICLE INFO

Article history:

Received 6 February 2020

Accepted 3 April 2020

Available online xxx

Keywords:

Depositional environment

Sedimentary facies

Lagerstätten

Fezouata Shale

Mineralization

ABSTRACT

The Fezouata Shale in Morocco is the only Lower Ordovician *Lagerstätte* to yield a diverse exceptionally preserved marine fauna. Sediments of this formation have yielded soft to lightly sclerotized taxa that were previously unknown from the Ordovician. Yet the taphonomic pathway of fossils from this formation remains poorly understood. Here, based on drill core material, a close association between exceptional preservation and a specific sedimentary facies is evidenced in the Fezouata Shale. This facies corresponds to calm sea-bottoms, sporadically smothered by distal storm deposits. The patterns of exceptional preservation in this facies indicate that most animals were dead and decayed on the seafloor prior to their burial by distal storm deposits. Furthermore, contrasted elemental and molecular compositions between fresh-cored and altered materials show that surface deposits of the Fezouata Shale were substantially affected by recent weathering. This weathering resulted in the leaching of organic materials from fossils originally preserved as carbonaceous compressions and the transformation of pyrite into iron oxides. Understanding the processes behind the current patterns of soft tissue preservation in the Fezouata Shale is essential prior to any palaeontological description, especially of taxa with no current representatives.

© 2020 Published by Elsevier Masson SAS.

1. Introduction

Konservat-Lagerstätten have revolutionized our understanding of metazoan evolution and diversification, owing to the preservation in these deposits of soft-bodied and lightly sclerotized organisms that normally are not preserved (Caron et al., 2006, 2010; Smith and Caron, 2010; Gutiérrez-Marco and García-Bellido, 2015; Lerosee-Aubril et al., 2017; Knaust and Desrochers, 2019). These deposits are particularly abundant in Cambrian Series 2 and 3, providing critical insights into the Cambrian Explosion, one major pulse in animal evolution (Butterfield, 1995; Liu et al., 2008; Zhang

et al., 2008; Duan et al., 2014; Lei et al., 2014). The younger Fezouata Biota (late Tremadocian) was discovered in the early 2000s in the Central Anti-Atlas of Morocco, and is the only Lower Ordovician *Lagerstätte* to yield a diverse exceptionally preserved fauna (Van Roy et al., 2010, 2015a), providing key information on the transition between the Cambrian and Ordovician (Lefebvre et al., 2016). Anatomical information found in fossils from this deposit is critical for deciphering the evolution of major animal phyla (Vinther et al., 2008, 2017; Van Roy et al., 2015b; Lefebvre et al., 2019).

The general depositional environment of the Fezouata Shale is constrained, and is storm-dominated with an indirect influence of tides (Martin et al., 2016; Vaucher et al., 2017). The processes behind the formation of sedimentary structures related to this environment were explained in recent works (Vaucher et al., 2016, 2017). Two types of exceptional preservation have been

[☆] Corresponding editor: Emmanuel Fara.

* Corresponding author.

E-mail address: farid.saleh@univ-lyon1.fr (F. Saleh).

documented in the Fezouata Shale: the first one occurs in concretions (Gaines et al., 2012a). This type of preservation requires vigorous sulfate reduction around carcasses, resulting in the establishment of prominent chemical gradients around dead animals and leading to the early precipitation of minerals around non-biomineralized tissues (Gaines et al., 2012a). The other type of preservation is associated with shale (Martin et al., 2016). In these levels, fossils occur exclusively at bed junctions and not within beds (Vaucher et al., 2016, 2017), strongly supporting the view that organisms were smothered on the seafloor under a new blanket of distal storm deposits, rather than having been carried in sediment flows (Saleh et al., 2018).

However, the step-by-step mechanism behind this type of preservation remains largely unexplored. Most fossils collected in shales are preserved as molds or imprints on the sediments (Martin et al., 2016), but it is unclear whether these organisms were originally preserved as carbonaceous compressions. Other non-biomineralized tissues, such as trilobite digestive tracts and echinoderm water-vascular systems, are preserved in 3D red to orange iron oxides (Gutiérrez-Marco et al., 2017; Lefebvre et al., 2019). Considering that numerous diagenetic mechanisms may alter the original anatomy of fossil organisms over geological time, deciphering the taphonomic processes at play in the Fezouata Shale is essential for palaeontological interpretations, especially for taxa without extant representatives. Consequently, the aim of this study is to provide insights into soft tissue taphonomy in the Fezouata Shale based on a detailed sedimentological investigation constraining the facies in which exceptional preservation occurred, in addition to a careful geochemical analysis deciphering the mechanism leading to the current patterns of preservation in this facies.

2. Geological context

During the Ediacaran (600 Ma), the Panafrikan Orogeny led to the formation of the Gondwana supercontinent. Gondwana extended from the South Pole to intermediate latitudes in the Northern Hemisphere. A rifting phase took place in its western part at the end of the Cambrian. At the beginning of the Ordovician, a long-term transgression resulted in the flooding of Gondwanan margins by epicontinental seas (Destombes et al., 1985). The entire

Lower Ordovician succession in the Zagora region in Morocco was deposited in a generally shallow environment at high latitude, close to the palaeo-South pole (Torsvik and Cocks, 2011, 2013; Fig. 1(A)). These deposits unconformably overlie middle to upper Cambrian strata and are separated by an unconformity from the overlying lower to middle Darriwilian (Middle Ordovician) deposits of the Tachilla Fm. (Choubert, 1952; Destombes et al., 1985). The Fezouata Shale (Tremadocian–Floian) consists of blue-green to yellow-green sandy mudstones and siltstones that coarsen upwards. They are up to 900 m thick in the Zagora region (Vaucher et al., 2016). The long-term transgression at the beginning of the Ordovician was followed by a regression leading to the deposition of massive dark brown sandstones characteristic of the Zini Fm. (late Floian) above the Fezouata Shale (Martin et al., 2016). The Lower Ordovician succession was interpreted to have been deposited in a storm-wave dominated sedimentary environment (Martin et al., 2016) indirectly influenced by tides (Vaucher et al., 2017). The corresponding palaeoenvironments range from the foreshore (S–SE) to the upper offshore (N–NW) (Vaucher et al., 2017). In intermediate settings of the Ternata plain, the Bou Izargane locality (Fig. 1(B)), studied in the present work, has yielded abundant exceptionally preserved fossils including lightly cuticularized arthropods, sponges, and soft parts of echinoderms (Van Roy et al., 2015a; Botting, 2016; Lefebvre et al., 2019). This locality (Fig. 2) exposes part of the lower interval with exceptional preservation, dated as late Tremadocian (Araneo-Araneograptus murrayi graptolite Zone; Lefebvre et al., 2018).

3. Material and methods

3.1. Field work

In February 2018, a 6.5 m core was drilled at the top of the Bou Izargane section (30°30'00.5" N; 5°50'56.7" W; Fig. 2: core 1), in the Ternata plain, ca. 18.5 km N of Zagora (Morocco), and a second 6.7 m core (Fig. 2: core 2) was made 6.8 m below the first one to cover most of the sedimentary succession in this locality. Both cores are temporally stored at the University of Brest, France. The outcrop in this locality was logged and highly excavated in 2014 and yielded hundreds of exceptionally preserved fossils,

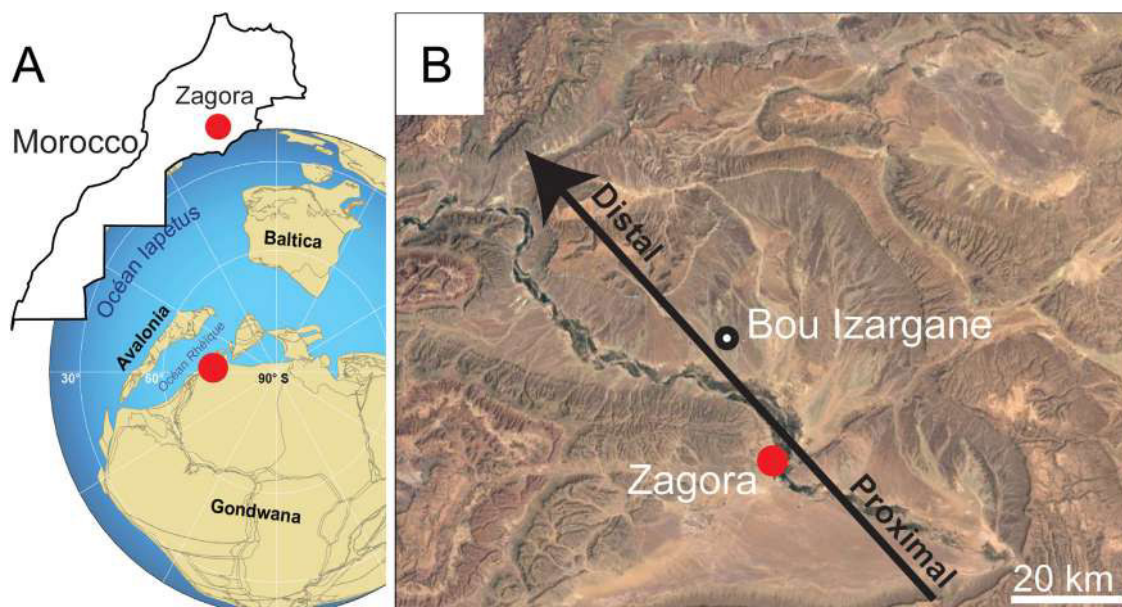


Fig. 1. Bou Izargane in the Ternata plain, Zagora area, Morocco. **A.** Palaeogeographical location. **B.** Current location in the Ternata plain (30°30'00.5" N; 5°50'56.7" W).

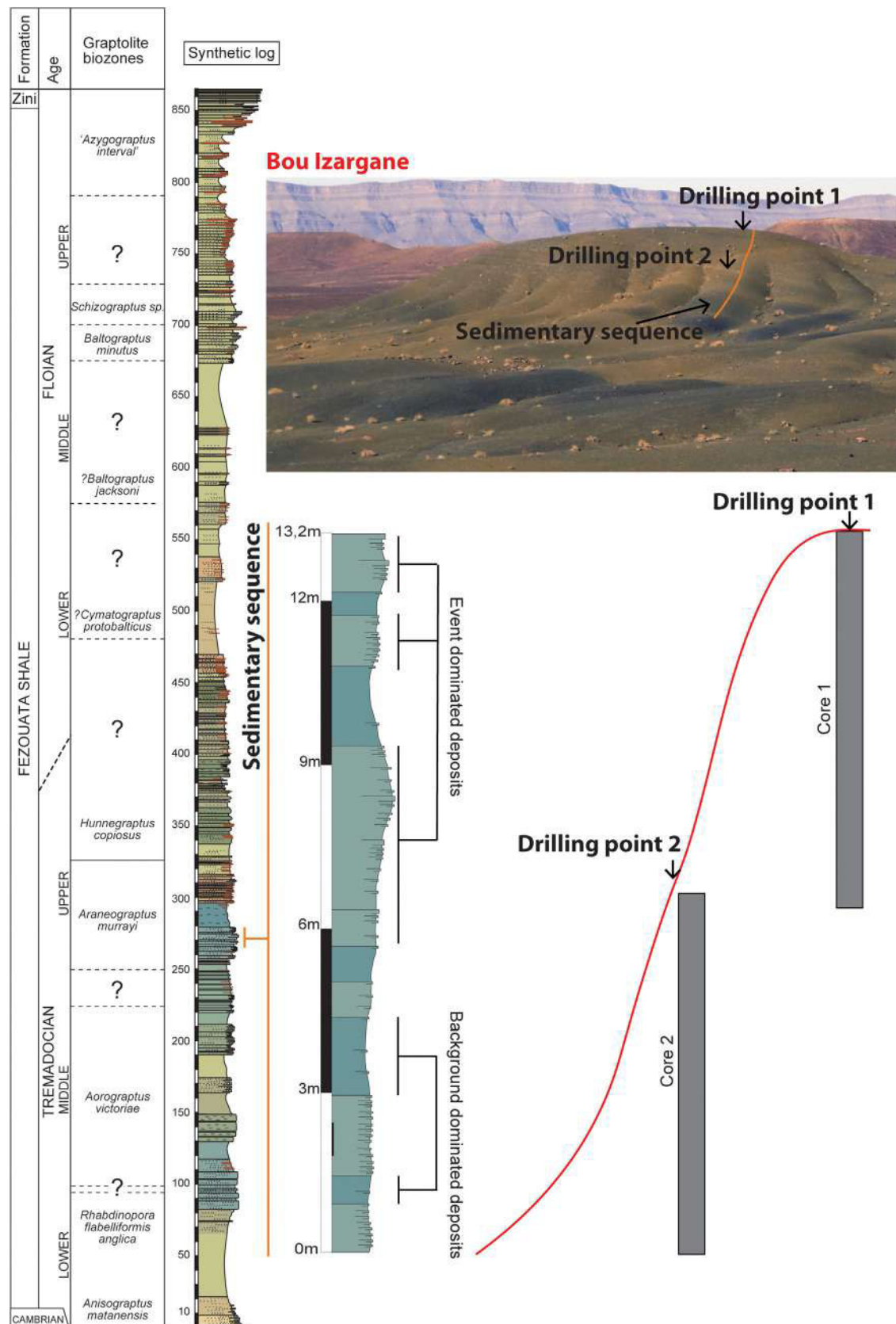


Fig. 2. Sedimentary succession in the Fezouata Shale with a focus on the succession in Bou Izargane showing the alternation of thin background siltstones with coarse siltstone- to thin sandstone-dominated event levels. The positions of the drilled cores are indicated next to the sedimentary succession. The question marks in the stratigraphic column indicate intervals where characteristic graptolite assemblages could not be identified (Lefebvre et al., 2018).

registered in the collections of the Cadi-Ayyad University, Marrakesh.

3.2. Sediment preparation and analyses

The cores were cut and scanned, using a core XRF-scanner, for major elements (Si, Al, K) expressed as oxides (wt% SiO₂, Al₂O₃ and K₂O) at the University of Brest, France. Then, they were described for their lithology, grain size, depositional sedimentary structures, and bioturbation intensity and size, and drawn on a 1:1 scale at the Laboratoire de Géologie de Lyon, France. The uppermost 2 m of each core are extremely weathered and show the same greenish color as on the outcrop. The lower, fresher portions of the cores range from dark grey to black in color. Twelve thin sections were made from the cores. Transect analyses combined into elemental maps (Table S1, Appendix A) from both green and black core sediments were made on nine samples using a Bruker M4 Tornado micro-XRF instrument operating at 50 kV, 600 A. This mapping of the major elements was done to better visualize discrete lithological changes in the facies and to determine the composition of silty to very fine sand grains (Fig. 3). In addition, around 100 Raman spectra were collected from nine core specimens (Table S1, Appendix A) using a Labram HR800 – Jobin Yvon Horiba spectrometer equipped with semi-confocal optics at the University of Lyon, France. A microscope with a 100 objective was used to focus the excitation laser beam, 532 nm exciting line, on a 1–3 μm size spot and to collect the Raman signal in the backscattered direction. Acquisitions were performed using two accumulations of 30 s and a laser power of about 5 mW on the sample surface.

3.3. Statistical approach

Cores give precise information in terms of sedimentary facies and their evolution, but only minimal information on the vertical occurrences of exceptionally preserved fossils. Conversely, field and hand sample observations made at Bou Izargane provide important information on the occurrence of exceptional preservation, but with unprecise information on the facies in which exceptional preservation occurred, due to surface weathering. Thus, the stratigraphic sequence from the core was compared to the field-based sequence logged along the same section and described by Vaucher et al. (2016; Fig. 4(A, B)). Cores were made starting at the upper surface of the outcrop from which the original log was made. For more precision, correlations between cores and outcrop were made based on comparisons of facies defined in Vaucher et al. (2017) and in the present study (Table 1). Using this correlation, a statistical approach was developed to link these two distinct, though complementary sets of data gathered from outcrops (i.e., occurrences of exceptional preservation) and from drill cores (i.e., detailed sedimentary facies).

The obtained 13.2 m-thick core succession was divided into 22 60 cm-thick successive intervals. Then, the proportion of each sedimentary facies identified was calculated in these intervals. A Principal Component Analysis (PCA) was performed to identify the facies accounting for the largest variance between the 22 intervals (Hammer et al., 2001). Facies that are homogeneously distributed are less likely to explain discrepancies in occurrences of exceptionally preserved fossils and therefore were removed from further statistical analysis. The facies exhibiting the highest dissimilarity (i.e., with the largest variance) were selected for a Classical (hierarchical) Cluster Analysis (CCA). CCA allows investigating the heterogeneities in terms of sedimentary facies between the 22 intervals by separating them into clusters (Hammer et al., 2001). Vertical alternation of intervals between the clusters was plotted against the pattern of soft tissue preservation in the field to check any direct link between the sedimentary facies and exceptional fossil preservation. Then, a

Similarity Percentage analysis (SIMPER; Hammer et al., 2001) was made to identify which facies caused the highest dissimilarity between these clusters and thus, to decipher the correlation of different facies with the absence/presence of exceptional preservation. Finally, a student *t*-test was applied to investigate whether the difference in the proportions of facies causing the dissimilarity between clusters was significant.

3.4. Fossil analyses

Twenty fossil specimens (Table S1, Appendix A) collected from late Tremadocian localities in the Zagora area, Morocco, and registered in the palaeontological collections of the Cadi-Ayyad University, Marrakesh, Morocco (acronym: AA), Lyon 1 University, Villeurbanne, France (UCBL-FSL) and the Musée des Confluences, Lyon (ML), were included in this study. Some of these fossils were analyzed using a FEI Quanta 250 scanning electron microscope (SEM) equipped with backscattered and secondary electron detectors in addition to an energy-dispersive X-ray analyzer (EDX) operating at accelerating voltages ranging from 5 to 15 kV. At low energies, light elements such as C can be detected, while at higher energies, detection of heavier elements is optimized. Some samples were analyzed using a synchrotron beam X-ray fluorescence at the DIFABBS beamline at the Soleil synchrotron, Paris, France, in order to determine the minor-to-trace elemental composition of the fossils, as well as of the surrounding matrix.

4. Results

4.1. Core description

Both cores are dominated by Si-rich (Fig. 3(A)), quartz dominated (Fig. 4(A)), normally graded beds having an erosive base (Figs. 3(A) and 4(A)). The thickness of these beds varies from 0.2 to 2.5 cm. Intervals with finer grains exist between these beds (Figs. 3(A) and 4(A)); these levels are Al- and K-rich (Fig. 3(A)) and are likely more argillaceous (Fig. 4(A)). Mn and Co are present around and within the layers with the coarsest grains especially in greenish sediments (Fig. 5). The coarsest layers bear wavy laminations. These wavy layers are hummocky cross stratifications (HCS) with a centimeter- to decimeter-scale estimated wavelength (Figs. 3 and 5), as also observed on outcrops (Vaucher et al., 2017). Occasionally, these HCS are associated with Ca-rich deposits (Figs. 3 and 5). The distribution of Fe in the cores positively correlates with the general distribution of both Al and K (Fig. 3(A)). In fresh and lightly altered sediments, Fe correlates with S as well (Fig. 3), when pyrite is present (Fig. 4(B)). This pyrite is generally surrounded by a halo of C-rich organic material (Figs. 4(B) and 6). An absence of both pyrite and C is evidenced in surface sediments that are extensively altered (Fig. 6). Fe-rich minerals in these recently weathered sediments are iron oxides.

Evidence for bioturbation is abundant in the cores (Figs. 3 and 5). Bioturbation is mainly horizontal (i.e., less than 1–2 cm in depth). Some escape burrows have been observed in coarse-grained layers (Fig. 3(A)). Only one 5-cm vertical bioturbation occurs in the uppermost part of the sedimentary succession. A detailed mm-scale description of the two combined drill cores is given in Fig. 7.

4.2. Facies identification

Five sedimentological facies are defined from the core and are designated herein as Fc1 to Fc5. Fc1 is the finest grained facies (Fig. 8(A)); it is homogeneous and mostly composed of argillaceous material (Fig. 9(A)). Fc2 contains coarser siliciclastic layers

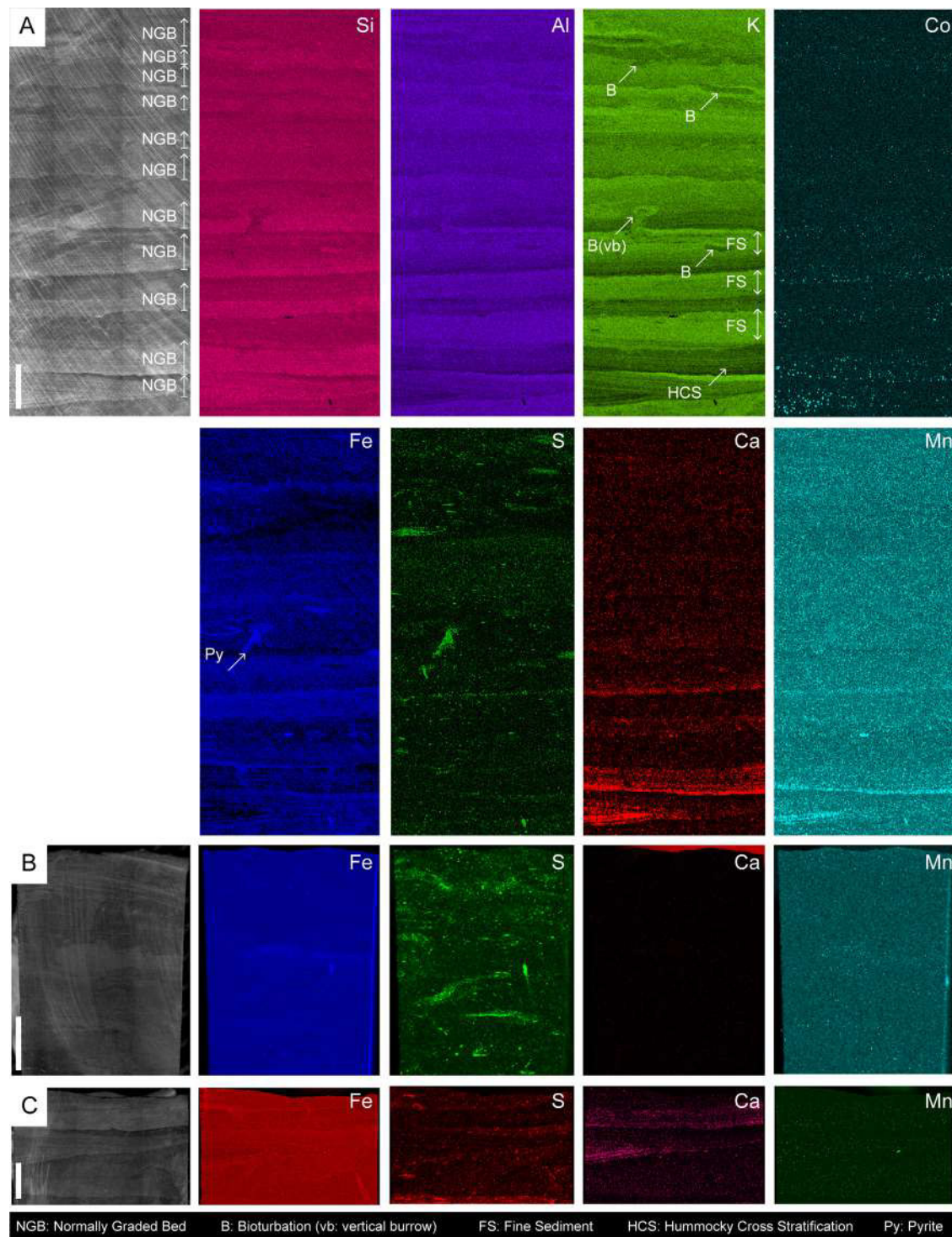


Fig. 3. X-Ray Fluorescence maps of slightly altered core sediments of Fc3 at 405 cm (A), and non-altered deposits showing elemental distributions in Fc2 at 15 cm and Fc4 at 65 cm (B, C). Si is abundant in event beds that are normally graded (i.e., NGB). Al and K are positively correlated in background sediments. Fe and S are partially correlated in sediments highlighting the presence of pyrite minerals. S most probably indicates organic matter when it is not correlated to Fe. In slightly altered deposits, Mn and Co coexist in coarse sediments bearing sometimes Ca-rich bioclasts. Scale bars: 10 mm (A, B), 5 mm (C).

(Fig. 9(B)) showing a normal grading with a considerable amount of fine sediments in between (Fig. 9(B)). Sediments in Fc3 are coarser than in Fc2 (Fig. 8(A)). Fc3 consists of stacked, normally graded layers with little to no fine-grained sediments in between, and in rare occasions some small HCS are present (see Vaucher et al., 2016, 2017 for direct evidence for HCS; Fig. 9(C)). Fc4 is made of coarser sediments than in Fc3 (Fig. 8(A)) and contains abundant

wavy laminations (HCS; Fig. 9(D, E)). Fc5 consists of coarse siltstones (Fig. 8(A)) containing sometimes Ca-rich deposits (Fig. 9(F)).

The increase of quartz (SiO_2) and decrease of clays (K_2O and Al_2O_3) from Fc1 to Fc5 is shown in Fig. 8(B). Bioturbation is mostly present in Fc2, Fc3, Fc4, and Fc5 (Fig. 9) and may vary in intensity within the same facies (Fig. 9(D, E)). Pyrite occurs mainly in Fc2,

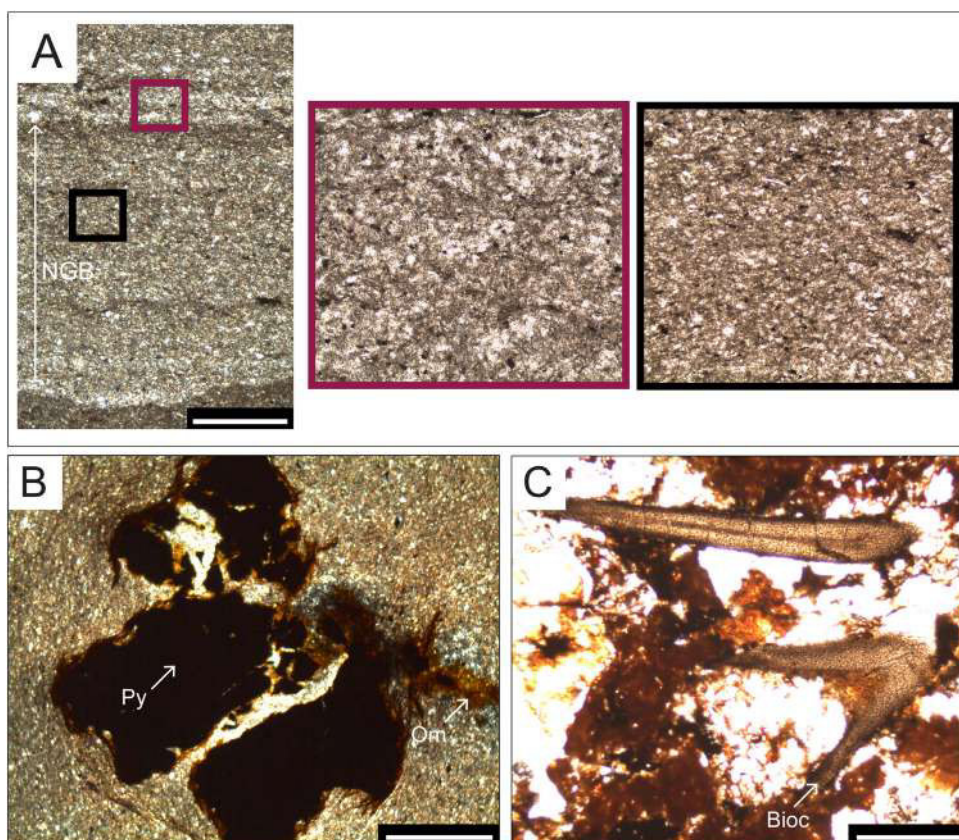


Fig. 4. **A.** Quartz-rich normally graded bedding (NGB) in the core alternating with clay-rich background sediments seen in thin section from sediments at 240 cm. **B.** Pyrite crystals (Py) in the fresh sediments surrounded by a halo of organic material (Om) at 250 cm. Pyrite and organic matter were identified based on Raman Spectra in Fig. 6. **C.** Bioclasts (Bioc) possibly of trilobite fragments from sediments at 262 cm. Scale bars: 5 mm (A), 1 mm (B, C).

Table 1
Definition and associated depositional environment of outcrop facies (defined as F1, F2, and F4 in Vaucher et al., 2017) and core facies (defined as Fc1 to Fc5 in this study).

	Description	Depositional setting
F1	Argillaceous siltstones with sparse intercalations of siltstones (mm-thick)	Below storm weather base
F2	Coarse siltstones with hummocky cross-stratification (HCS) of cm-scale wavelength	Above storm weather base
F4	Fine sandstones with centimetric to decametric HCS, the laminations are underlined by thin layers of coarser quartz grains	Below Fair weather base
Fc1	Homogenous, composed of argillaceous material	Below storm weather base
Fc2	Siltstones with normally graded beds separated by argillaceous material	Below storm weather base, more proximal than Fc1
Fc3	Siltstones with stacked normally graded beds	Around the storm weather base
Fc4	Siltstones with stacked normally graded beds and abundant HCS	Above the storm weather base
Fc5	Coarse siltstones/fine sandstones with abundant bioclasts	Below fair weather base

Fc3, Fc4, and Fc5, with the largest pyrite crystals being observed in Fc2 (Fig. 9(B)).

4.3. Statistical analyses

Principal component analysis shows that most of the variance between the 22 defined intervals is related to Fc2, Fc3, and Fc4 (Fig. 10(A)). Fc1 and Fc5 can be excluded from further statistical tests because they contribute to less than 5% of heterogeneities between intervals. Based on variations in the proportion of Fc2, Fc3, and Fc4 in the 22 intervals, two clusters were extracted (Fig. 10(B)). The alternation of intervals between Cluster 1 and Cluster 2 fits with 95% fidelity the presence/absence of exceptional preservation in these deposits, validating that this type of preservation is directly linked to the sedimentary facies in the Fezouata Shale (Fig. 10(D)).

Fc2 and Fc4 are responsible for 81% of the difference between the two clusters (Fig. 10(C)). Fc2 is abundant in Cluster 1 (Fig. 10(C)) which is correlated with intervals bearing exceptional preservation (Fig. 10(D)). Fc4 is abundant in Cluster 2 (Fig. 10(C)) that is correlated with intervals where exceptional preservation is absent (Fig. 10(D)). The differences in the distribution of Fc2 and Fc4 in Cluster 1 and Cluster 2 are significant ($P = 0.003$ and $P = 2.8 \cdot 10^{-7}$, respectively). The difference in the proportion of Fc3 between the two clusters is not significant ($P = 0.1$), indicating that this facies did not significantly contribute to the differences observed between intervals with and without exceptional preservation.

4.4. Fossil preservation

Red/orange 3D fossils from the Bou Izargane locality appear to be preserved in iron oxides (Fig. 11(A)). In these samples, iron is

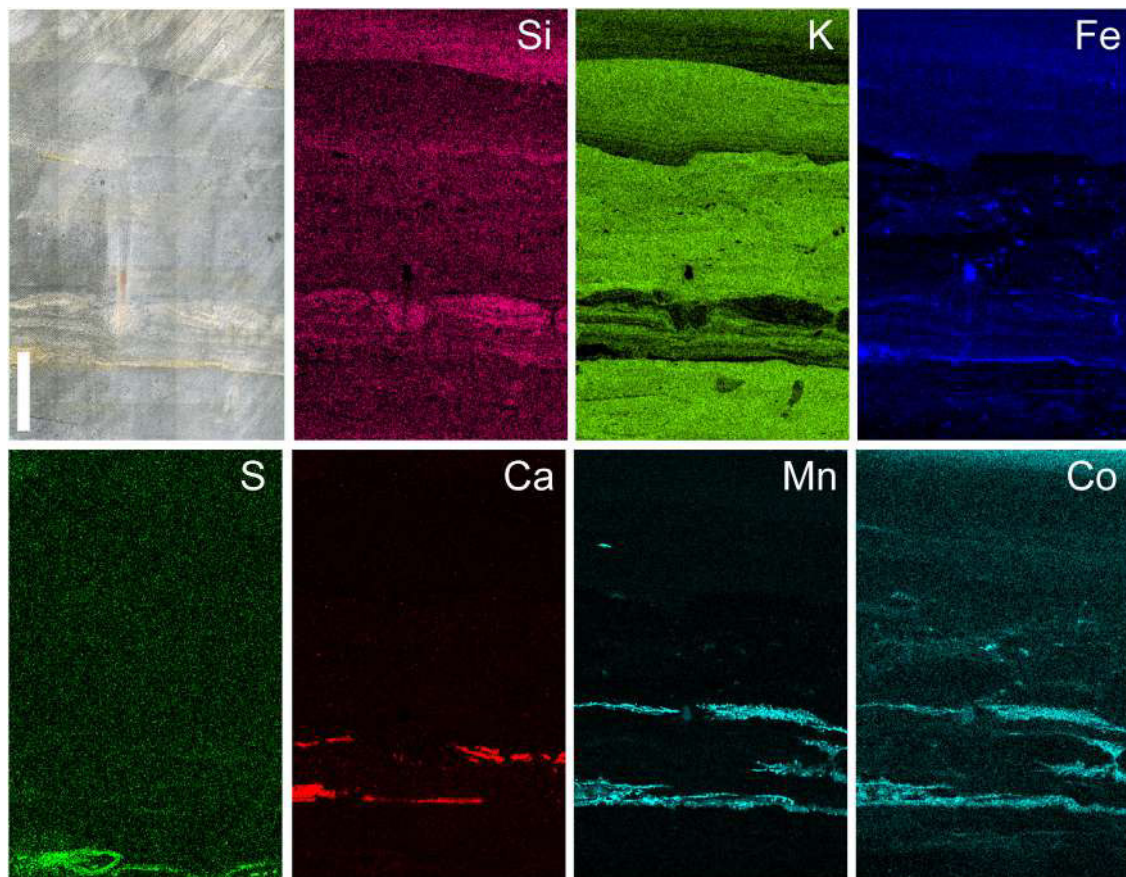


Fig. 5. X-Ray Florescence maps of altered green core sediments of an intermediate Fc3–Fc4 facies at 1320 cm. These sediments show the absence of S-rich materials, except in the bottom part of the slab. Mn and Co are enriched in these sediments in comparison with fresh material in Fig. 3(B, C). Scale bar: 5 mm.

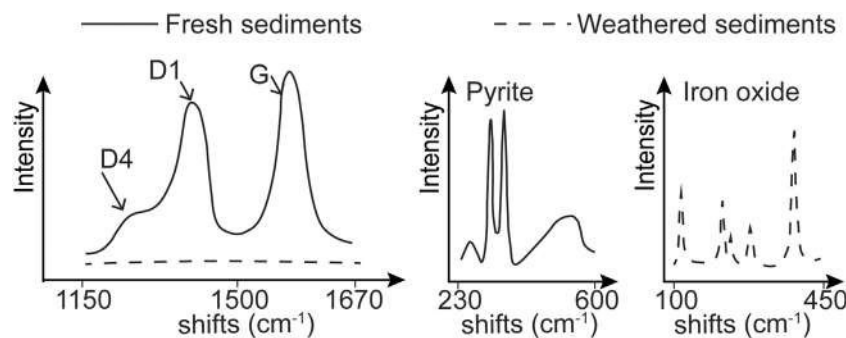


Fig. 6. Raman spectra on thin sections (for analyzed material see Table S1, Appendix A) showing the presence of both pyrite and C in fresh core sediments, as well as the replacement of pyrite by iron oxides and the absence of organic C in weathered surface core slabs. The Raman spectra on organic material show the characteristic peaks of C.

present in two different morphologies: abundant in small euhedral crystals (Fig. 12(B, C)), and dispersed as framboid-shaped minerals (Fig. 12(D)). The obtained SEM spectra, at low voltage, show a low concentration of C in these fossils (Fig. 11(A)) in comparison with the abundance of C around pyrite in fresh deposits (Figs. 4(B) and 6). C is abundantly present in fresh sediments (Fig. 6) but absent in cuticularized to lightly sclerotized fossils preserved as 2D imprints as well (Fig. 11(B)). In both 3D and 2D modes of preservation, thin star-like (Fig. 12(E, G)) iron-rich minerals (Fig. 12(H)) may cover parts of the fossils. The majority of this Fe in star-shaped minerals is found in fossils that are covered by Co and Mn-rich deposits (Fig. 13) in rose-like minerals (Fig. 12(F, G)).

5. Discussion

5.1. General depositional environment

The increase in SiO₂ and decrease of Al₂O₃ and K₂O from Fc1 to Fc5 (Fig. 8; Table S2, Appendix A) is indicative of the energy at which sediments were deposited. In open marine environments, Si-rich sandstones (i.e., quartz) are found in high-energy proximal settings, while Al- and K-rich clays are generally found in lower energy, more distal environments. In the Fezouata Shale, Si is associated with the coarsest grained sediments (Figs. 3 and 5) originating from the shallowest settings (i.e., beach to the SE of



Fig. 7. Facies evolution over the Bou Izargane succession. Most of normally graded beds are discontinuous due to bioturbation. Hummocky cross stratifications occur in the coarsest event deposits. Bioturbation is randomly distributed in the cores.

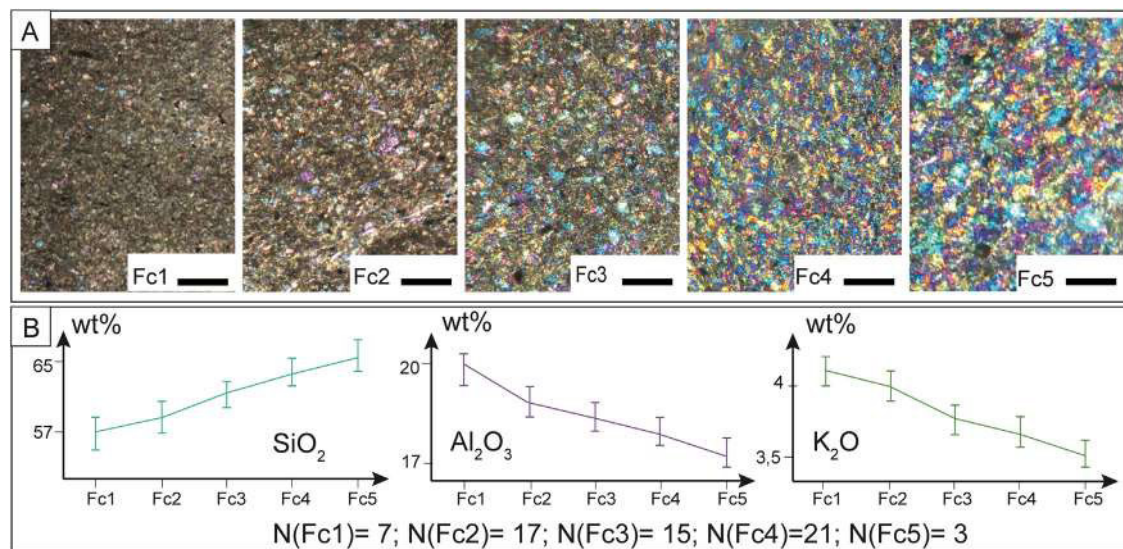


Fig. 8. Lithology in the Fezouata Shale. **A.** Quartz grain size evolution in Fc1 to Fc5 seen in thin section with crossed-polarized light and $\lambda/4$ gypsum plate. **B.** Quantifying the

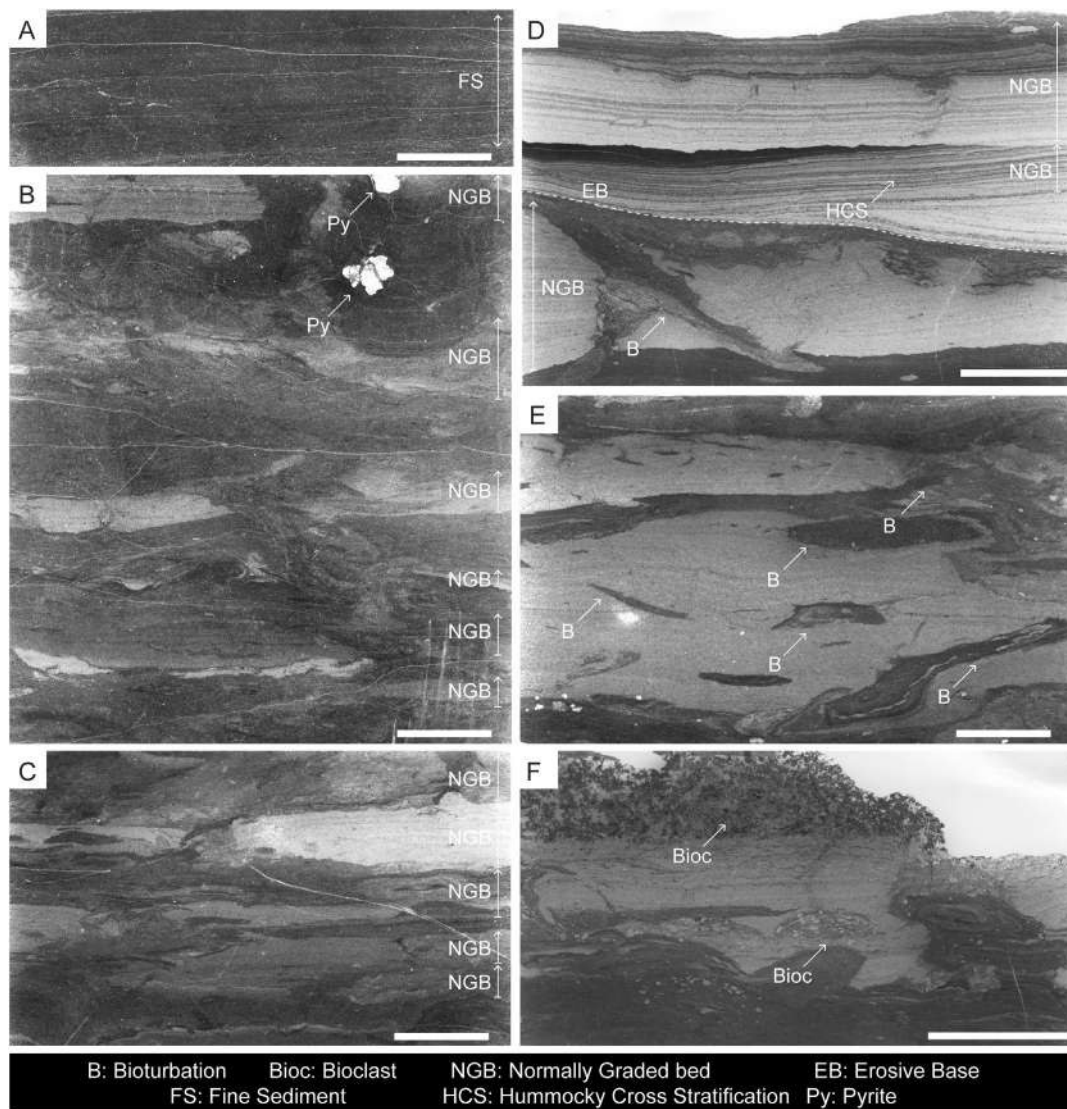


Fig. 9. Sedimentary structures in Fc1 (A), Fc2 (B), Fc3 (C), Fc4 (D, E) and Fc5 (F). Normally graded beds are frequently discontinuous due to bioturbation in B–F. Scale bars: 5 mm.

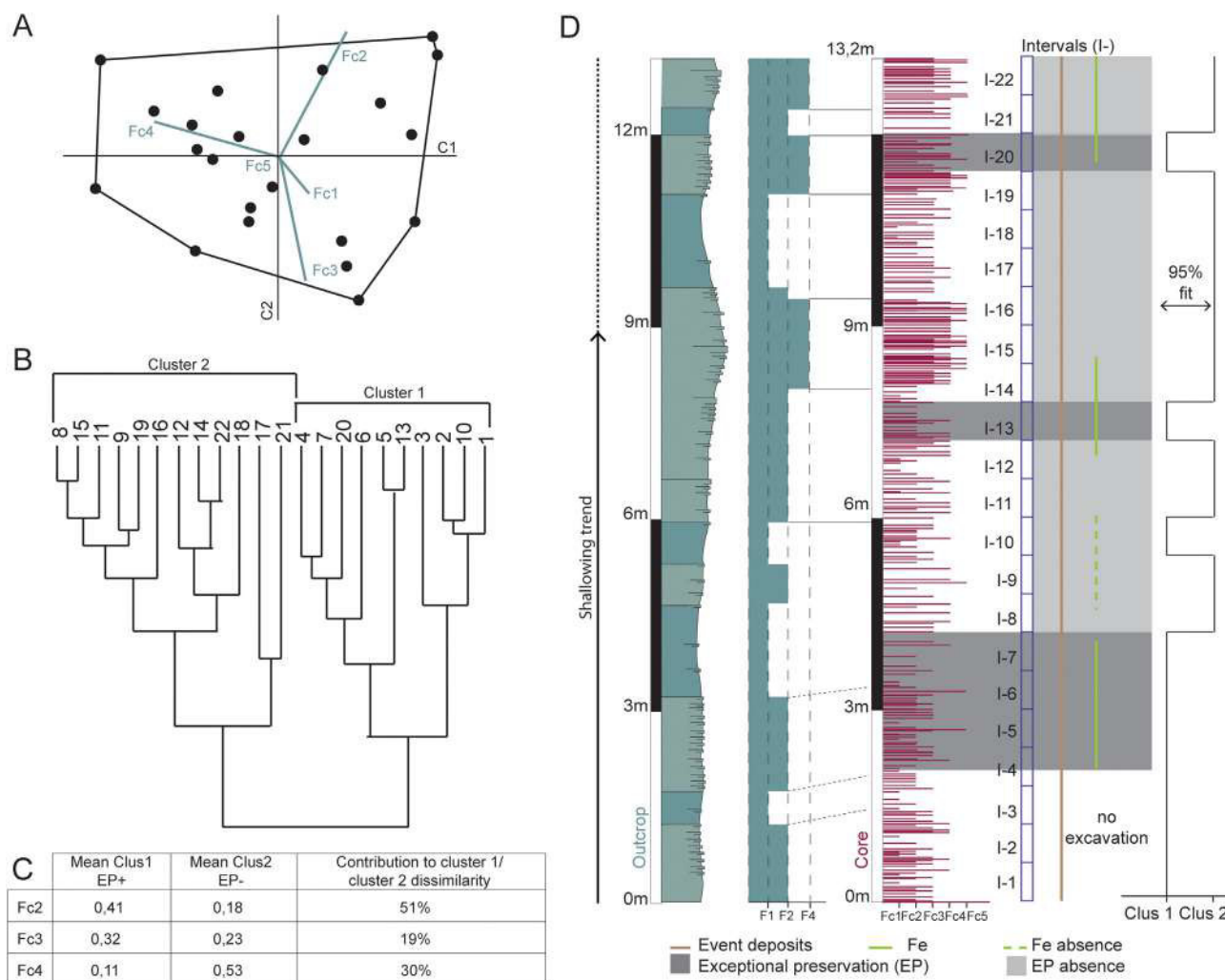


Fig. 10. Statistical analyses performed on facies evolution along the core from Bou Izargane. **A.** Principal Component Analysis of the 22, 60 cm-thick intervals defined along the core. **B.** Classical (hierarchical) Cluster Analysis of the 22 intervals according to Fc2, Fc3, and Fc4 distributions in these intervals. **C.** Similarity Percentage (Simpser) analysis showing which facies are responsible for the differences between Cluster 1 and Cluster 2. **D.** Facies evolution (Fc1 to Fc5 in this study) along the core, correlated to outcrop succession (F1, F2, F4 from Vaucher et al., 2017) and clusters 1 and 2 obtained from the cluster analysis. Intervals bearing thin layers with exceptional preservation of fossils on the field are shown in dark grey, whereas intervals that did not yield any exceptional preservation are in light grey. Intervals with or without iron availability are shown according to Saleh et al. (2019). A 95% fit is observed between the alternation of clusters and levels with and without exceptional preservation, indicating that this type of preservation is strongly correlated with the sedimentary facies.

Zagora; Vaucher et al., 2017). In this sense, the finest grained sediments (Figs. 3 and 5) belong to more distal settings and are K- and Al-rich. The dominant clay mineral in this formation is illite (Saleh et al., 2019). The presence of oscillatory structures in Fc4 and Fc5 (Fig. 9) and the absence of these structures in other facies support this interpretation. HCS are sedimentary structures first described as characteristic of storm deposits (Harms et al., 1975). Wave oscillation induces wave orbitals in the water column that decrease in size with depth. In a shallow environment, wave orbitals form large HCS on the seafloor (Vaucher et al., 2016, 2017). Conversely, in deep environments, these orbitals dissipate before attaining the sediment and thus leave no trace on the seafloor. Furthermore, the abundance of normally graded beds in the core (Figs. 3(A) and 4(A)) indicates that sediment was deposited by successive events of decreasing energy. These event beds can be formed either during storms or turbiditic events. In the Fezouata Shale, the monotonous alternation of event beds with the background sedimentation and the occurrence of HCS favor the interpretation of event sediments as storm deposits. In this sense, the high frequency of storm events is another indication of less distal sites, more affected by storm wave oscillations (Vaucher

et al., 2016). The absence of event layers in Fc1 (Fig. 9(A)) indicates that this facies is characteristic of settings below the Storm Wave Base (SWB). Fc2 shows some event beds isolated in the background sedimentation and an absence of HCS (Fig. 9(B)). This facies is characteristic of settings below the SWB, but more proximal than Fc1. Fc3, showing stacked storm events, and rarely HCS (Fig. 9(C)), is more proximal than Fc2. Fc3 was deposited around the SWB. In Fc4, HCS are abundantly present (Fig. 9(D, E)), revealing a more proximal environment above the SWB with higher energy than what is observed in Fc3. The coarse grains constituting Fc5 (Fig. 9(F)) and the presence of HCS with a wavelength estimated to be around 10 cm were deposited closer to the Fair Weather Base (FWB). Due to the coarse-grained and high porosity of Fc5, elemental enrichment (e.g., Mn; Fig. 5) may occur and alter the original elemental distribution of this facies (Fan et al., 1992). The Ca-rich deposits in some laminae (Figs. 3(A, C) and 5) may resemble carbonate cement deposited in deep settings (i.e., basin) of some Cambrian Lagerstätten (Gaines et al., 2012b). Carbonate cements are used to explain the presence of exceptional preservation in some deposits due to their ability to block exchange between sediments and the water column thus

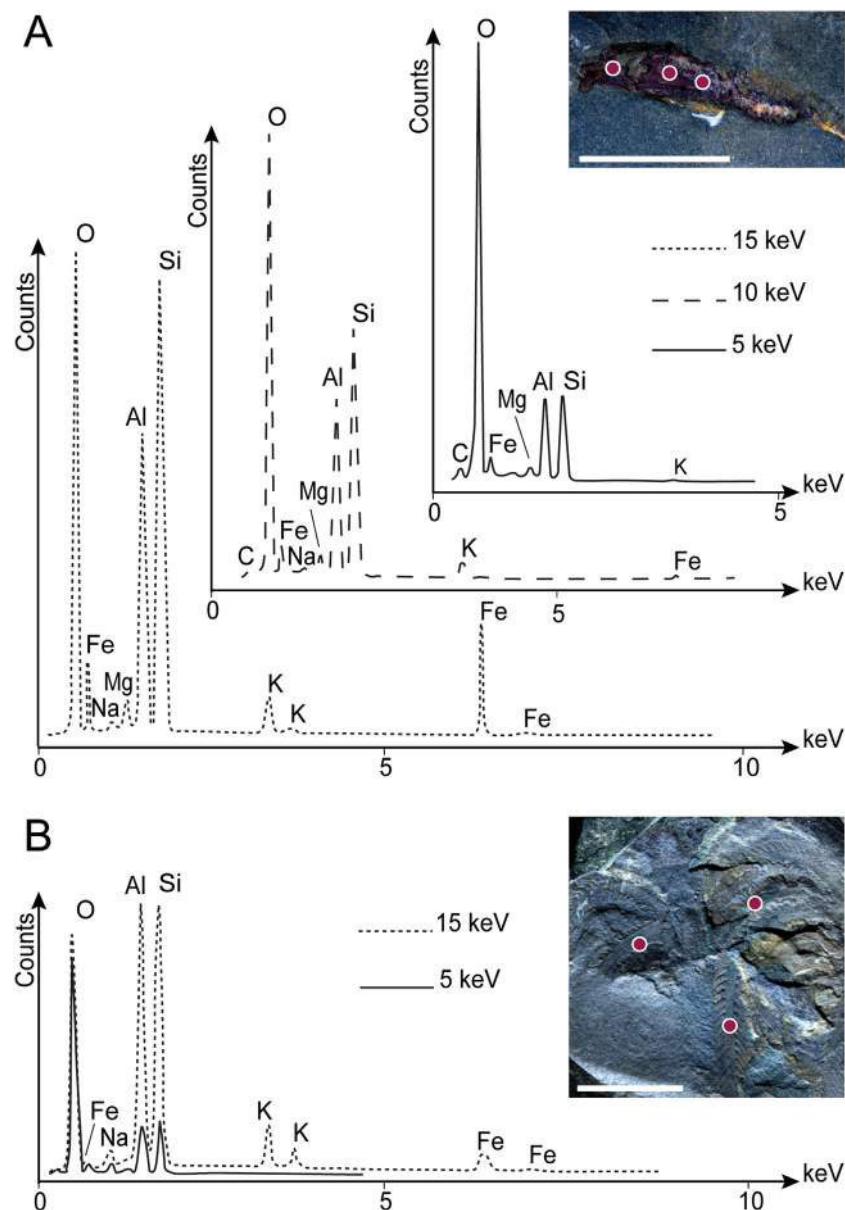


Fig. 11. Preservation mode of fossils in the Fezouata Shale, evidenced by SEM-EDX point spectroscopy of surface samples using accelerating voltages from 5 to 15 kV in order to enhance signal from light elements (C, O) and to promote fluorescence of heavier elements such as transition metals (Fe) in 3D fossils (A) and matrix and fossil imprints (B). Analyzed regions are marked as pink circles in the sample photographs. Scale bars: 5 mm (A), 10 mm (B).

depriving oxidants of attaining dead carcasses (Gaines et al., 2012b). However, critical differences exist between these cements and the observed carbonate laminae in the Fezouata Shale. Carbonate cements from the Cambrian are deposited at the top of turbiditic events (Gaines et al., 2012b), while in the Fezouata Shale, Ca-rich deposits occur only at the base of oscillatory structures with a coarse lithology and a high porosity (Figs. 3(A, C) and 5). If carbonate precipitation occurred in the Fezouata Shale, its original Ca source must be the bioclasts observed in thin sections cutting through the bottom of storm deposits (Fig. 4(C)) especially because carbonates are not evidenced elsewhere in this formation (Vaucher et al., 2016). Thus, the most distal facies is Fc1 and the most proximal facies is Fc5 with Fc2, Fc3, and Fc4 in between, respectively. This model of facies is in accordance with outcrop-based sedimentological models for the Fezouata Shale from which an outcrop to cores correlation was made (Table 1).

5.2. Facies for exceptional preservation

Exceptional preservation requires burial by event deposits (Vaucher et al., 2016). In the Fezouata Shale, this condition was present in the entire core (Fig. 10(D)) except in Fc1 that constitutes only 6% of the studied deposits (Fig. 7). Another requirement for exceptional fossil pyritization is iron availability. Iron was a limited element in the Fezouata Shale environment (Saleh et al., 2019). In these deposits, Fe supply was likely associated to periods with high seasonality leading to high iron-rich continental fluxes to the sea (Saleh et al., 2019) (Fig. 10(D)). Thus, during intervals with enhanced Fe availability exceptional preservation could occur in intervals I-4, I-5, I-6, I-7, I-12, I-13, I-14, I-20, I-21, and I-22 (Saleh et al., 2019; Fig. 10(D)).

Although the general conditions for exceptional preservation were occurring in many intervals, the presence of exceptionally

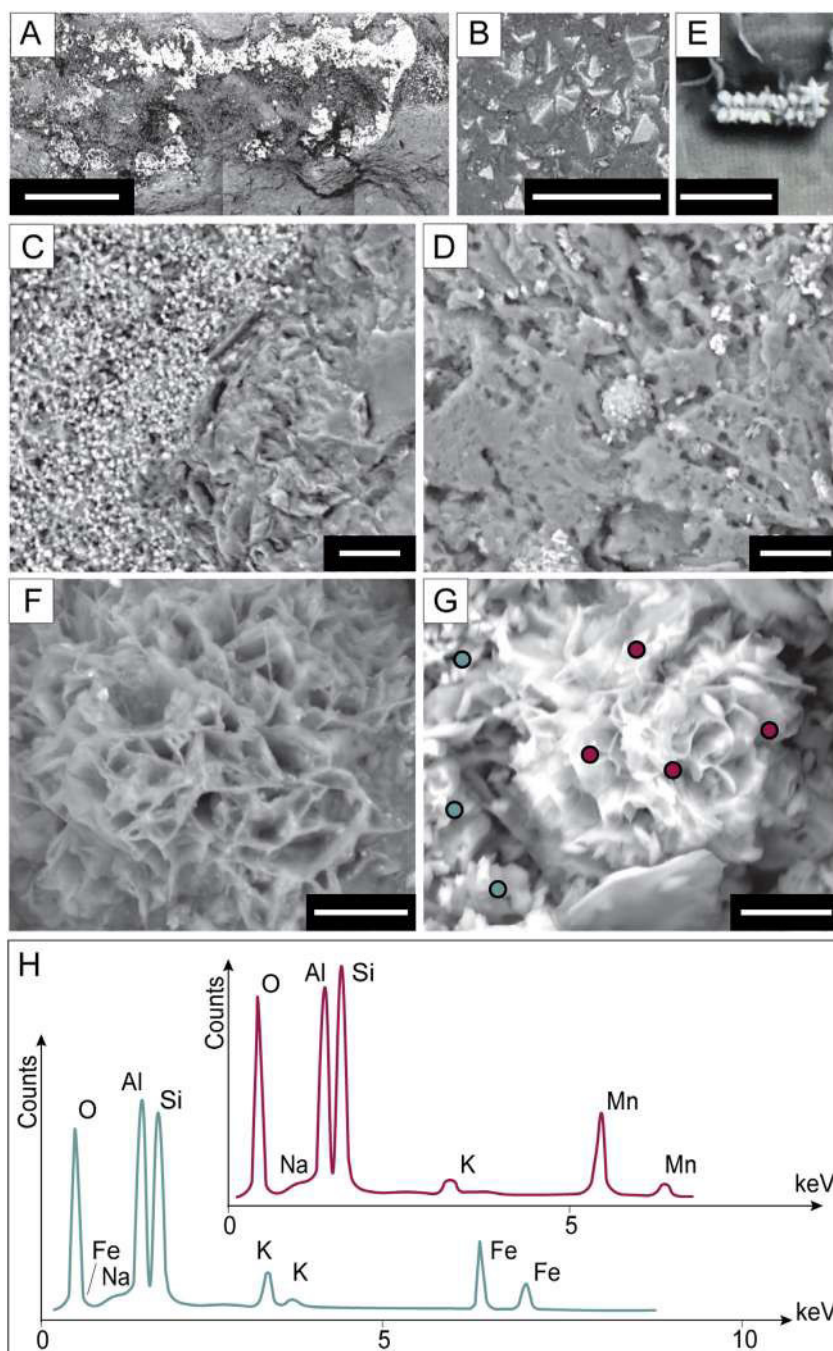


Fig. 12. A–G. SEM images of minerals in samples from the Fezouata Shale. Iron rich minerals in white (A), euhedral iron-oxides (B, C), framboidal iron-rich minerals (D), star-like iron oxides (E) in addition to rose-shaped mineral (isolated, F) and next to smaller star-like minerals (G). H. SEM spectra showing that the star-like minerals are iron oxides and the rose-shaped ones are rich in manganese. Scale bars: 1 mm (A), 5 μm (B, E–G), 10 μm (C, D).

preserved fossils at Bou Izargane is more restricted (i.e., exceptional preservation occurred in I-4, I-5, I-6, I-7, I-13 and I-20; Fig. 10(D)). Thus, the absence of soft parts, e.g., in I-14, is possibly related to the original absence of living organisms on the sea floor. This hypothesis is confirmed by the absence of benthic fauna (both hard and soft parts) in this interval, showing that environmental conditions on surface sediments were probably not favorable for the colonization of this environment (Saleh et al., 2018). Statistical analyses show that an alternation of clusters, which are reconstructed based on the proportion of different sedimentary facies, can predict with a 95% fidelity the presence and location of intervals with exceptional preservation discovered in the field (Fig. 10(D)). Levels with higher proportions of Fc2 and

lower proportions of Fc4 have a higher potential to yield exceptional preservation (Fig. 10(C)). This is because Fc2 combines rather calm environmental conditions with lower energy events compared to other facies, allowing living organisms to colonize the sea floor (Saleh et al., 2018), in addition to burial during event deposition, a prerequisite condition for exceptional preservation (Vaucher et al., 2017).

The unique negative correlation between the alternation of clusters and the patterns of exceptional preservation is exemplified in I-10 (Fig. 10(D)). I-10 yielded a considerable number of mineralized skeletons (Saleh et al., 2019). The absence of exceptional preservation in this facies does not result from the original absence of living organisms, but may be due to the lack of

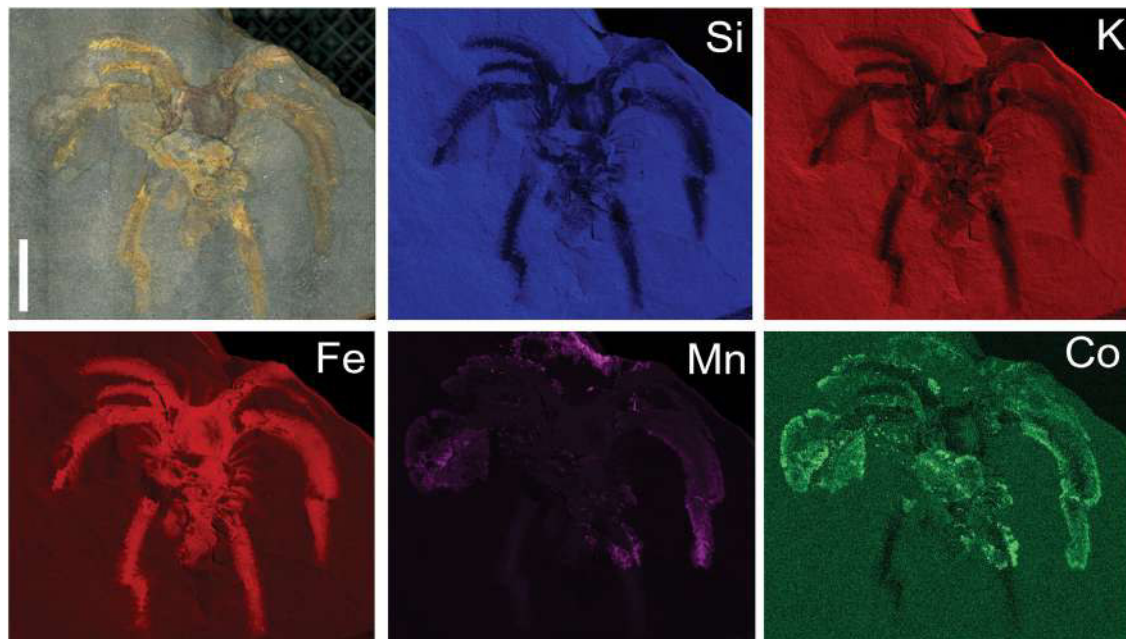


Fig. 13. Elemental maps of an extensively altered marrellomorph arthropod, AA-BIZ31-OI-39. Red/orange zones of the analyzed fossil are iron rich. Iron is preserved as star-like iron oxides. Scale bar: 10 mm.

berthierine in this level (Saleh et al., 2019). Berthierine is an iron-rich clay mineral that can be deposited in the sediments from a primary clay precursor under anoxic conditions (Tang et al., 2017). It is documented in most intervals with exceptional preservation in the Cambrian (Anderson et al., 2018), and only in specific levels of the Fezouata Shale in which exceptional preservation occurred (Saleh et al., 2019). In experimental studies, it was shown that berthierine slows down bacterial decay due to the damage of bacterial cells (McMahon et al., 2016). However, some authors interpreted its presence as a symptom of the same conditions that led to exceptional fossilization, rather than a cause for soft tissue preservation (Anderson et al., 2018). In order to further investigate this discrepancy, future work should study the timing of berthierine formation and its exact geographical distribution in consecutive sediment laminae.

5.3. Taphonomic pathway of fossils in Fc2

5.3.1. Burial and decay

In the Fezouata Shale, fossils were preserved *in situ* (Vaucher et al., 2017; Saleh et al., 2018) in Fc2 (Fig. 14(E)). Fc2 combines a fine grain size and the occurrence of event deposits favoring burial. Both conditions are necessary for exceptional preservation (Gaines et al., 2012b). However, in distal settings comparable to Fc2, burial occurred only during strong storms (Saleh et al., 2018), causing a delay in the start of the fossilization process. For instance, in one interval with exceptional preservation 600 fossils were discovered, but only a limited number of them show soft tissue preservation (about 30 stylophorans, 10 trilobites, and 5 marrellomorphs; Lefebvre et al., 2019). Furthermore, the single preserved hyolithid specimen with soft parts from the Fezouata Shale shows totally decayed tentacles (Martí Mus, 2016). These two examples of soft tissue preservation suggest that organisms were most probably dead and decaying on the sea floor prior to their burial (Fig. 14(A–C)). Pre-burial decay was also used to explain the absence of completely cellular animals (i.e., without cuticle, sclerites, or minerals) from the Fezouata Shale (Saleh et al., 2020) in contrast to most Cambrian Lagerstätten. In the Cambrian, soft-bodied and

lightly sclerotized organisms were killed during obrution events and transported by the same event to another facies for their preservation leading to a smaller exposure to pre-burial decay (Gaines, 2014). This taphonomic process can explain the abundance of soft cellular animals and hyolithid tentacles in sites such as the Burgess Shale (Moysiuk et al., 2017; Saleh et al., 2020).

5.3.2. Authigenic mineralization

Experimental approaches have shown that pyrite can form under different circumstances (Rickard and Luther, 1997; Grimes et al., 2002). Pyrite can precipitate in the water column, surface sediments and even under deep burial under anoxic conditions. However, selected soft anatomies replicated by pyrite minerals are often associated with active, localized sulfate reduction in iron-rich pore waters during early diagenesis resulting in a strong concentration gradient, and confining pyrite precipitation to dead carcasses (Farrell, 2014). Under sulfate-reducing conditions, bacteria transform organic matter and sulfates into HS^- and then to hydrogen sulfides H_2S , which react with Fe in a series of reactions to form pyrite (Raiswell et al., 1993; Schiffbauer et al., 2014). In the Fezouata Shale, anoxic conditions leading to sulfate reduction were established at the time of burial at the bottom of storm deposits (Vaucher et al., 2016, 2017) leading to pyritization of some tissues deposited under event beds. The chemical stress generated by oxygen depletion in the sediment is also evidenced by horizontal biological traces that are shallow with some escape burrows crossing event deposits. As bioturbation depth is minimal, it is most probable that the sediment was anoxic a few centimeters below storm deposits. Further ichnological work should investigate biological traces in detail in order to test this scenario and constrain oxygenation between the bottom of the water column and the sediments.

Because in open marine environments sulfates are not limited, pyritized tissues are those providing sufficient organic material to form H_2S (Jørgensen, 1982; Jørgensen et al., 2019; Fig. 14(D)). Laboratory experiments made under surface-sediment conditions have shown that the most labile decaying soft parts produce considerable amounts of H_2S , which reacts with iron to form nuclei

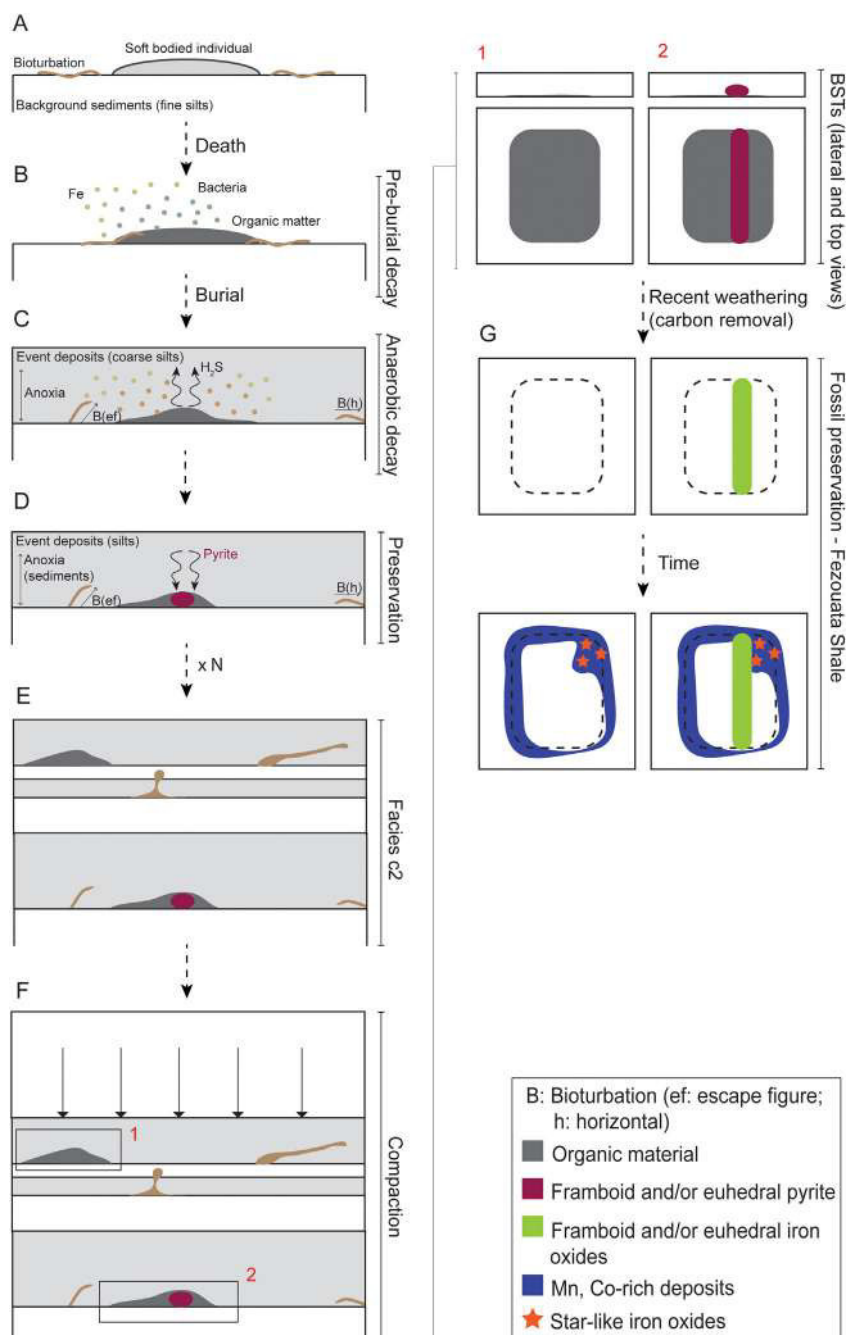


Fig. 14. Mechanism for soft part preservation in the Fezouata Shale (A–F), and recent weathering explaining the preservation state of fossils (G). A: Living organism on the sea floor; B: Dead organism starts to decay prior to burial; C: Anoxic conditions are established due to burial, at the base of storm events, H₂S forms in decaying carcasses; D: Pyrite precipitation in specific tissues while the rest remains as carbonaceous material; E: With time, a facies similar to Fc2 is observed, combining conditions for both the colonization of the environment by a benthic fauna and for the preservation of this fauna; F: With compaction, fossils were preserved as 2D C-rich films with occasionally 3D pyritization; G: Recent weathering effect removes C from the fossils and alters the chemical signal of pyrite.

for pyrite framboids (Butler and Rickard, 2000). However, less labile soft parts produce less H₂S, and thus fewer nuclei leading to the precipitation of mainly cubic, and sometimes octahedral minerals (Gabbott et al., 2004). In the Fezouata Shale, framboid minerals in 3D fossils are scarce (Fig. 12(D)) and much less abundant than euhedral pyrite (Fig. 12(C)); this emphasizes the removal of a considerable quantity of organic material, due to burial delay and oxic decay, prior to the permissive chemical conditions for pyrite precipitation. If a tissue did not provide sufficient H₂S to form nuclei when anoxic conditions occur (e.g.,

non-cellular cuticles made of polysaccharides) for neither euhedral nor framboidal minerals, it remains preserved as a carbonaceous compression.

5.3.3. Late diagenesis, metamorphism, and modern weathering

Although mineralogical and chemical evidences favor the idea of an early authigenic pyritization of some soft tissues in the Fezouata Shale, the geochemical signal of these minerals in fossils from outcrops is clearly altered. The absence of S-rich minerals in surface fossils (Fig. 11) indicates that pyrite was oxidized and S was

partly leached after early diagenesis (Ahm et al., 2017). This can be due to either metamorphism or modern weathering. According to mineral distributions in shales from the Fezouata *Lagerstätte*, sediments did not experience high burial temperatures as only 3 km of sediments were deposited above the Fezouata Shale (Ruiz et al., 2008; Saleh et al., 2019; Fig. 14(F)). This is confirmed by a Raman signature representative of fresh organic matter (i.e., low burial temperatures around 200 °C) characterized by the presence of the D4 band and the absence of the D2 band, as well as by the higher intensity of the D1 band compared to the G band (Rahl et al., 2005; Kouketsu et al., 2014; Fig. 6). These temperatures are lower than in other deposits with soft tissue preservation in which the D4 band is less pronounced and the G band has a higher intensity than the D1 band (Topper et al., 2018). Thus, it is more likely that the removal of S from pyrite in green surface sedimentary rocks of the Fezouata Shale results from modern weathering rather than from metamorphism. In the Draa Valley, this formation is exposed to abundant water circulations, as revealed by the numerous abandoned terraces near the outcrops and by the abundance of water wells in the area (Warner et al., 2013). Fast pyrite oxidation may be induced by Mn-oxides that are abundant in circulating waters in arid environments with occasional rain similar to the Draa Valley (Potter and Rossman, 1979; Warner et al., 2013). Depending on Mn-oxide quantities in circulating waters, the outcome of pyrite oxidation may differ. When the quantity of Mn-oxide is high enough to fully oxidize pyrite, the resulting products of this reaction are Fe-oxides and Mn-sulfates (Larsen and Postma, 1997). Additionally, since manganese oxides are much stronger adsorbents of elements such as Co and Ni than iron oxides (McKenzie, 1980), the reduction of manganese oxide may cause a major release of these elements in the surrounding environment (Postma, 1985). If the quantities of Mn-oxides are not sufficient to fully oxidize pyrite, pyrite oxidation by H₂O molecules and atmospheric O₂ will take place and unleash considerable amounts of sulfates, thus reducing the pH of the environment and contributing to the dissolution of nearby carbonates (Larsen and Postma, 1997). In the Fezouata Shale, it seems that both pyrite oxidation pathways were operational. Mn-oxides altered pyrite, contributing to the initial precipitation of Co- and Mn-rich deposits. The latter reaction may lead to a diffusion of Mn in the sediments, which would explain the distribution of Mn around the appendages of the analyzed marrellomorph (Richard et al., 2013; Fig. 13). Subsequently, H₂O transformed the remaining pyrite into Fe-oxides and sulfuric acid, and was also responsible for the dissolution of Ca (Lucas, 2019) and the poor preservation of skeletal elements of different groups with preserved soft parts, such as echinoderms (Lefebvre et al., 2019).

5.3.4. Original mode of preservation and comparison with the Chengjiang Biota

The contrast between the presence of C in fresh sediments (Figs. 4(B) and 6) and its absence from surface deposits (Fig. 6) may be also the result of modern weathering. The association of C to pyrite crystals in fresh sediments (Fig. 4(B)) suggests that the original mode of preservation in the Fezouata Shale includes both carbonaceous compressions and pyrite replicates. In this sense, flattened fossils (Fig. 11(B)) were most probably originally preserved as 2D carbonaceous films. However, due to recent weathering, C was leached from originally non-pyritized structures and pyrite was transformed to iron oxides in 3D mineralized tissues (Fig. 14(G)). Similarities in terms of taphonomic pathway of soft tissues in the Fezouata Shale are particularly high with the Chengjiang Biota. Early studies of the Chengjiang Biota have emphasized the role of pyrite in replicating some tissues within individual fossils (Gabbott et al., 2004; Zhu et al., 2005). Later works focusing on less weathered material demonstrated that the

role of pyrite in the preservation of the Chengjiang Biota fossils may have been overestimated (Forchielli et al., 2014). Instead, carbonaceous films comprise the major original component of preservation in the Chengjiang Biota, and only some soft tissues were selectively replaced by pyrite (Edgecombe et al., 2015). However, C was lost in outcrop fossils probably due to the extensive activity of recent weathering (Gabbott et al., 2004; Gaines et al., 2008), as it is likely the case for the Fezouata Shale.

6. Conclusions

In this study, detailed sedimentological facies identified in the Fezouata Shale based on fresh core material offer unique insights into the mechanisms at play in the exceptional preservation. Distal environments of the Fezouata Shale below the SWB were inhabitable by living individuals. Dead organisms were exposed to pre-burial decay. At time of burial, based on observations of minimal bioturbation in the core, permissive anoxic conditions were established few cm below surface sediments. Under these conditions, pyrite replicated selectively some soft tissues, while the rest remained carbonaceous. Carbonaceous parts were then flattened due to compaction while pyrite replicates kept their 3D morphology. Afterward, carbon was leached from 2D compressions and surface sediments due to recent weathering. This weathering altered the original chemical signal of pyrite transforming it to iron oxides. When extensive weathering occurred, Mn and Co-rich deposits precipitated in addition to some star-shaped iron oxides that have nothing to do with the original anatomy of the fossils.

Acknowledgments

This paper is a contribution to the TelluS-Syster project ‘Vers de nouvelles découvertes de gisements à préservation exceptionnelle dans l’Ordovicien du Maroc’ (2017) and the TelluS-INTERVIE projects ‘Mécanismes de préservation exceptionnelle dans la Formation des Fezouata’ (2018) and ‘Géochimie d’un *Lagerstätte* de l’Ordovicien inférieur du Maroc’ (2019), all funded by the INSU (Institut National des Sciences de l’Univers, France), CNRS. This paper is also a contribution to the International Geoscience Programme (IGCP) Project 653–The onset of the Great Ordovician Biodiversification Event. The Raman facility in Lyon (France) is supported by the INSU. The authors thank Yves Candela, Lukáš Laibl, Eric Monceret, Martina Nohejlová, Stephen Pates, and Daniel Vizcaíno for assistance during field work in Montagne Noire or Morocco. The authors also thank Lukáš Laibl, Lorenzo Lustri, Francesco Perez Peris, Claude Colombié and Gilles Montagnac for assistance during XRF, SEM and Raman spectroscopy analyses. Allison Daley is also thanked for facilitating access to the Fezouata Shale collections in Lausanne. Brian Pratt and all anonymous reviewers are also thanked for their constructive reviews on earlier versions of the manuscript.

Appendix A. Supplementary data

Supplementary data (including Table S1 and S2) associated with this article can be found, in the online version, at <https://doi.org/10.1016/j.geobios.2020.04.001>.

References

- Ahm, A.-S.C., Bjerrum, C.J., Hammarlund, E.U., 2017. Disentangling the record of diagenesis, local redox conditions, and global seawater chemistry during the latest Ordovician glaciation. *Earth Planet. Sci. Lett.* 459, 145–156.

- Anderson, R.P., Tosca, N.J., Gaines, R.R., Mongiardino Koch, N., Briggs, D.E.G., 2018. A mineralogical signature for Burgess Shale-type fossilization. *Geology* 46, 347–350.
- Botting, J.P., 2016. Diversity and ecology of sponges in the Early Ordovician Fezouata Biota, Morocco. *Palaeogeogr. Palaeoclimatol. Palaeoecol.* 460, 75–86.
- Butler, I.B., Rickard, D., 2000. Framboidal pyrite formation via the oxidation of iron (II) monosulfide by hydrogen sulphide. *Geochim. Cosmochim. Acta* 64, 2665–2672.
- Butterfield, N.J., 1995. Secular distribution of Burgess-Shale-type preservation. *Lethaia* 28, 1–13.
- Caron, J.B., Scheltema, A., Schander, C., Rudkin, D., 2006. A soft-bodied mollusc with radula from the Middle Cambrian Burgess Shale. *Nature* 442, 159–163.
- Caron, J.-B., Conway Morris, S., Shu, D., 2010. Tentaculate fossils from the Cambrian of Canada (British Columbia) and China (Yunnan) interpreted as primitive deuterostomes. *PLoS ONE* 5, e9586.
- Choubert, G., 1952. Histoire géologique du domaine de l'Anti-Atlas. *Géologie Internationale*, 3e Série, Maroc.
- Destombes, J., Holland, H., Willefert, S., 1985. Lower Palaeozoic rocks of Morocco. In: Holland, C. (Ed.), *Lower Palaeozoic Rocks of the World*. pp. 91–336.
- Duan, Y., Han, J., Fu, D., Zhang, X., Yang, X., Komiya, T., Shu, D., 2014. Reproductive strategy of the bradoriid arthropod *Kunmingella douvillei* from the Lower Cambrian Chengjiang Lagerstätte, South China. *Gondwana Res.* 25, 983–990.
- Edgecombe, G.D., Ma, X., Strausfeld, N.J., 2015. Unlocking the early fossil record of the arthropod central nervous system. *Philos. Trans. R. Soc. B: Biol. Sci.* 370, 20150038.
- Fan, D., Liu, T., Ye, J., 1992. The process of formation of manganese carbonate deposits hosted in black shale series. *Econ. Geol.* 87, 1419–1429.
- Farrell, U.C., 2014. Pyritization of soft tissues in the fossil record: an overview. *Paleontol. Soc. Pap.* 20, a35–a58.
- Forchielli, A., Kasbohm, J., Hu, S., Keupp, H., 2014. Taphonomic traits of clay-hosted early Cambrian Burgess Shale-type fossil Lagerstätten in South China. *Palaeogeogr. Palaeoclimatol. Palaeoecol.* 398, 59–85.
- Gabbott, S.E., Xian-guang, H., Norry, M.J., Siveter, D.J., 2004. Preservation of Early Cambrian animals of the Chengjiang biota. *Geology* 32, 901–904.
- Gaines, R.R., 2014. Burgess Shale-type preservation and its distribution in space and time. *Paleontol. Soc. Pap.* 20, 123–146.
- Gaines, R.R., Briggs, D.E.G., Yuanlong, Z., 2008. Cambrian Burgess Shale-type deposits share a common mode of fossilization. *Geology* 36, 755–758.
- Gaines, R.R., Briggs, D.E.G., Orr, P.J., Van Roy, P., 2012a. Preservation of giant anomalocaridids in silica-chlorite concretions from the Early Ordovician of Morocco. *Palaios* 27, 317–325.
- Gaines, R.R., Hammarlund, E.U., Hou, X., Qi, C., Gabbott, S.E., Zhao, Y., Peng, J., Canfield, D.E., 2012b. Mechanism for Burgess Shale-type preservation. *Proc. Natl. Acad. Sci. USA* 109, 5180–5184.
- Grimes, S.T., Davies, K.L., Butler, I.B., Brock, F., Edwards, D., Rickard, D., Briggs, D.E.G., Parkes, R.J., 2002. Fossil plants from the Eocene London Clay: the use of pyrite textures to determine the mechanism of pyritization. *J. Geol. Soc. Lond.* 159, 493–501.
- Gutiérrez-Marco, J.C., García-Bellido, D.C., 2015. Micrometric detail in palaeoscolecid worms from Late Ordovician sandstones of the Tafilalet Konservat-Lagerstätte, Morocco. *Gondwana Res.* 28, 875–881.
- Gutiérrez-Marco, J.C., García-Bellido, D.C., Rábano, I., Sá, A.A., 2017. Digestive and appendicular soft parts, with behavioural implications, in a large Ordovician trilobite from the Fezouata Lagerstätte, Morocco. *Sci. Rep.* 7, 39728.
- Hammer, Ø., Harper, D.A.T., Ryan, P.D., 2001. Past: paleontological statistics software package for education and data analysis. *Paleontol. Electron.* 4 (4) 9p.
- Harms, J.C., Southard, J.B., Spearing, D.R., Walker, R.G., 1975. Depositional environments as interpreted from primary sedimentary structures and stratification sequences. *SEPM Short Course* 2.
- Jørgensen, B.B., 1982. Mineralization of organic matter in the sea bed—the role of sulphate reduction. *Nature* 296, 643–645.
- Jørgensen, B.B., Findlay, A.J., Pellerin, A., 2019. The biogeochemical sulfur cycle of marine sediments. *Front. Microbiol.* 10, 849.
- Knaust, D., Desrochers, A., 2019. Exceptionally preserved soft-bodied assemblage in Ordovician carbonates of Anticosti Island, eastern Canada. *Gondwana Res.* 71, 117–128.
- Kouketsu, Y., Mizukami, T., Mori, H., Endo, S., Aoya, M., Hara, H., Nakamura, D., Wallis, S., 2014. A new approach to develop the Raman carbonaceous material geothermometer for low-grade metamorphism using peak width. *Island Arc* 23, 33–50.
- Larsen, F., Postma, D., 1997. Nickel mobilization in a groundwater well field: release by pyrite oxidation and desorption from manganese oxides. *Environ. Sci. Technol.* 31, 2589–2595.
- Lefebvre, B., Lerosey-Aubril, R., Servais, T., Van Roy, P., 2016. The Fezouata Biota: an exceptional window on the Cambro-Ordovician faunal transition. *Palaeogeogr. Palaeoclimatol. Palaeoecol.* 460, 1–6.
- Lefebvre, B., Gutiérrez-Marco, J.C., Lehnert, O., Martin, E.L.O., Nowak, H., Akodad, M., El Hariri, K., Servais, T., 2018. Age calibration of the Lower Ordovician Fezouata Lagerstätte, Morocco. *Lethaia* 51, 296–311.
- Lefebvre, B., Guensburg, T.E., Martin, E.L.O., Mooi, R., Nardin, E., Nohejlová, M., Saleh, F., Kouráiss, K., El Hariri, K., David, B., 2019. Exceptionally preserved soft parts in fossils from the Lower Ordovician of Morocco clarify stylophoran affinities within basal deuterostomes. *Geobios* 52, 27–36.
- Lei, Q.-P., Han, J., Ou, Q., Wan, X.-Q., 2014. Sedentary habits of Anthozoa-like animals in the Chengjiang Lagerstätte: adaptive strategies for Phanerozoic-style soft substrates. *Gondwana Res.* 25, 966–974.
- Lerosey-Aubril, R., Paterson, J.R., Gibb, S., Chatterton, B.D.E., 2017. Exceptionally-preserved late Cambrian fossils from the McKay Group (British Columbia, Canada) and the evolution of tagmosis in aglaspidid arthropods. *Gondwana Res.* 42, 264–279.
- Liu, J., Shu, D., Han, J., Zhang, Z., Zhang, X., 2008. Origin, diversification, and relationships of Cambrian lobopods. *Gondwana Res.* 14, 277–283.
- Lucas, V., 2019. Mécanismes de préservation et étude géochimique de la carotte 18MFBI du Lagerstätte des Fezouata (Ordovicien inférieur, Maroc) (M.Sc. Thesis) Brest University (unpubl.).
- Martí Mus, M., 2016. A hyolithid with preserved soft parts from the Ordovician Fezouata Konservat-Lagerstätte of Morocco. *Palaeogeogr. Palaeoclimatol. Palaeoecol.* 460, 122–129.
- Martin, E.L.O., Pittet, B., Gutiérrez-Marco, J.-C., Vannier, J., El Hariri, K., Lerosey-Aubril, R., Masrour, M., Nowak, H., Servais, T., Vandenbroucke, T.R.A., Van Roy, P., Vaucher, R., Lefebvre, B., 2016. The Lower Ordovician Fezouata Konservat-Lagerstätte from Morocco: age, environment and evolutionary perspectives. *Gondwana Res.* 34, 274–283.
- McKenzie, R., 1980. The adsorption of lead and other heavy metals on oxides of manganese and iron. *Aust. J. Soil Res.* 18, 61–73.
- McMahon, S., Anderson, R.P., Saupe, E.E., Briggs, D.E.G., 2016. Experimental evidence that clay inhibits bacterial decomposers: implications for preservation of organic fossils. *Geology* 44, 867–870.
- Moysiuk, J., Smith, M.R., Caron, J.-B., 2017. Hyoliths are Palaeozoic lophophorates. *Nature* 541, 394–397.
- Postma, D., 1985. Concentration of Mn and separation from Fe in sediments—I. Kinetics and stoichiometry of the reaction between birnessite and dissolved Fe(II) at 10 °C. *Geochim. Cosmochim. Acta* 49, 1023–1033.
- Potter, R.M., Rossman, G.R., 1979. The manganese- and iron-oxide mineralogy of desert varnish. *Chem. Geol.* 25, 79–94.
- Rahl, J.M., Anderson, K.M., Brandon, M.T., Fassoulas, C., 2005. Raman spectroscopic carbonaceous material thermometry of low-grade metamorphic rocks: calibration and application to tectonic exhumation in Crete, Greece. *Earth Planet. Sci. Lett.* 240, 339–354.
- Raiswell, R., Whaler, K., Dean, S., Coleman, M., Briggs, D.E.G., 1993. A simple three-dimensional model of diffusion-with-precipitation applied to localised pyrite formation in framboids, fossils and detrital iron minerals. *Mar. Geol.* 113, 89–100.
- Richard, D., Sundby, B., Mucci, A., 2013. Kinetics of manganese adsorption, desorption, and oxidation in coastal marine sediments. *Limnol. Oceanogr.* 58, 987–996.
- Rickard, D., Luther, G.W., 1997. Kinetics of pyrite formation by the H₂S oxidation of iron (II) monosulfide in aqueous solutions between 25 and 125 °C: the mechanism. *Geochim. Cosmochim. Acta* 61, 135–147.
- Ruiz, G.M.H., Helg, U., Negro, F., Adatte, T., Burkhard, M., 2008. Illite crystallinity patterns in the Anti-Atlas of Morocco. *Swiss J. Geosci.* 101, 387–395.
- Saleh, F., Candela, Y., Harper, D.A.T., Polechová, M., Pittet, B., Lefebvre, B., 2018. Storm-induced community dynamics in the Fezouata Biota (Lower Ordovician, Morocco). *Palaios* 33, 535–541.
- Saleh, F., Pittet, B., Perrillat, J., Lefebvre, B., 2019. Orbital control on exceptional fossil preservation. *Geology* 47, 103–106.
- Saleh, F., Antcliffe, J.B., Lefebvre, B., Pittet, B., Laibl, L., Perez Peris, F., Lustri, L., Gueriau, P., Daley, A.C., 2020. Taphonomic bias in exceptionally preserved biotas. *Earth Planet. Sci. Lett.* 529, 115873.
- Schiffbauer, J.D., Xiao, S., Cai, Y., Wallace, A.F., Hua, H., Hunter, J., Xu, H., Peng, Y., Kaufman, A.J., 2014. A unifying model for Neoproterozoic-Palaeozoic exceptional fossil preservation through pyritization and carbonaceous compression. *Nature Commun.* 5, 5754.
- Smith, M.R., Caron, J.-B., 2010. Primitive soft-bodied cephalopods from the Cambrian. *Nature* 465, 469–472.
- Tang, D., Shi, X., Jiang, G., Zhou, X., Shi, Q., 2017. Ferruginous seawater facilitates the transformation of glauconite to chamosite: an example from the Mesoproterozoic Xiamaling Formation of North China. *Am. Miner.* 102, 2317–2332.
- Topper, T.P., Greco, F., Hofmann, A., Beeby, A., Harper, D.A.T., 2018. Characterization of kerogenous films and taphonomic modes of the Sirius Passet Lagerstätte, Greenland. *Geology* 46, 359–362.
- Torsvik, T., Cocks, L., 2011. The Palaeozoic palaeogeography of central Gondwana. *Geol. Soc. Lond. Spec. Publ.* 357, 137–166.
- Torsvik, T., Cocks, L., 2013. New global palaeogeographical reconstructions for the Early Palaeozoic and their generation. *Geol. Soc. Lond. Mem.* 38, 5–24.
- Van Roy, P., Orr, P.J., Botting, J.P., Muir, L.A., Vinther, J., Lefebvre, B., El Hariri, K., Briggs, D.E.G., 2010. Ordovician faunas of Burgess Shale type. *Nature* 465, 215–218.
- Van Roy, P., Briggs, D.E.G., Gaines, R.R., 2015a. The Fezouata fossils of Morocco; an extraordinary record of marine life in the Early Ordovician. *J. Geol. Soc. Lond.* 172, 541–549.
- Van Roy, P., Daley, A.C., Briggs, D.E.G., 2015b. Anomalocaridid trunk limb homology revealed by a giant filter-feeder with paired flaps. *Nature* 522, 77–80.
- Vaucher, R., Martin, E.L.O., Hormière, H., Pittet, B., 2016. A genetic link between Konzentrat- and Konservat-Lagerstätten in the Fezouata Shale (Lower Ordovician, Morocco). *Palaeogeogr. Palaeoclimatol. Palaeoecol.* 460, 24–34.
- Vaucher, R., Pittet, B., Hormière, H., Martin, E.L.O., Lefebvre, B., 2017. A wave-dominated, tide-modulated model for the Lower Ordovician of the Anti-Atlas, Morocco. *Sedimentology* 64, 777–807.
- Vinther, J., Van Roy, P., Briggs, D.E.G., 2008. Machaeridians are Palaeozoic armoured annelids. *Nature* 451, 185–188.
- Vinther, J., Parry, L., Briggs, D.E.G., Van Roy, P., 2017. Ancestral morphology of crown-group molluscs revealed by a new Ordovician stem aculiferan. *Nature* 542, 471–474.

- Warner, N., Igourni, Z., Bouchaou, L., Boutaleb, S., Tagma, T., Hsaissoune, M., Vengosh, A., 2013. Integration of geochemical and isotopic tracers for elucidating water sources and salinization of shallow aquifers in the sub-Saharan Drâa Basin, Morocco. *Appl. Geochem.* 34, 140–151.
- Zhang, X., Liu, W., Zhao, Y., 2008. Cambrian Burgess Shale-type Lagerstätten in South China: distribution and significance. *Gondwana Res.* 14, 255–262.
- Zhu, M., Babcock, L.E., Steiner, M., 2005. Fossilization modes in the Chengjiang Lagerstätte (Cambrian of China): testing the roles of organic preservation and diagenetic alteration in exceptional preservation. *Palaeogeogr. Palaeoclimatol. Palaeoecol.* 220, 31–46.

7. DIRECT IMPLICATIONS: REAL vs FAKE SOFT TISSUES

This chapter consists of two papers:

- **Paper 6:** Saleh, F., Lefebvre, B., Hunter, A.W., Nohejlová, M., 2020. Fossil weathering and preparation mimic soft tissues in Eocrinoid and Somasteroid echinoderms from the Lower Ordovician of Morocco. **Microscopy Today**, 28(1), 24-28.
- **Paper 7:** Lefebvre, B., Guensburg, T.E., Martin, E.L., Mooi, R., Nardin, E., Nohejlová, M., Saleh, F., Kouraïss, K., El Hariri, K., David, B., 2019. Exceptionally preserved soft parts in fossils from the Lower Ordovician of Morocco clarify stylophoran affinities within basal deuterostomes. **Geobios**, 52, 27-36.

Summary

Understanding the taphonomic process behind the patterns of soft tissue preservation allows for a clear understanding of enigmatic structures preserved in animals from the Fezouata Shale⁷². In this chapter we examine enigmatic structures resembling water vascular systems in modern echinoderms preserved in samples of stylophoran, eocrinoid, and somasteroid Ordovician taxa^{53,78}. In the somasteroid specimen, the structure resembling a water vascular system appears to be preserved in C rich material⁷⁸. Considering that C is never preserved in altered surface sediments from the Fezouata Shale, it is likely that this C does not underline any original anatomy⁷⁸. In fact, similar carbon-rich spots appear to be present in all micro-depressions in the rock and they most probably result from the consecutive latex cast made on the specimen prior to its chemical analysis⁷⁸. The structures resembling the water vascular system in the eocrinoid specimen are Fe-rich⁷⁸. However, Fe in this specimen is not limited to this particular structure as star-shaped minerals resulting from modern weathering cover the entire specimen including imprints of its skeletal elements (Ca was leached out by modern weathering; see section 5)⁷⁸. The spots that are particularly enriched with Fe correspond to small cavities between skeletal plates⁷⁸. Thus it is most probably that the structure resembling water vascular systems is a weathering artifact caused by a stagnant Fe-rich waters in these cavities⁷⁸. The structures found in the stylophoran specimen are also iron-rich and formed of iron-oxides⁵³. However, in this case it appears that iron oxides are preserved in the shape of small euhedral and framboidal crystals, indicating that these minerals are surely the result of pyrite weathering⁵³. Considering that pyritization occurred shortly after the death of the organism and is controlled by its original chemistry (see section 4), these structures constitute the earliest known evidence of a preserved water vascular system⁵³. By bringing new evidence that the stylophoran appendage is an echinoderm feeding arm and not a hemichordate-like tail, this discovery shows that the interpretation of these fossils as early echinoderms retaining features of basal ambulacrarians and/or hemichordates can be definitively rejected, ending longstanding debates on the systematic affinity of these taxa⁵³.

Fossil Weathering and Preparation Mimic Soft Tissues in Eocrinoid and Somasteroid Echinoderms from the Lower Ordovician of Morocco

Farid Saleh^{1,*}, Bertrand Lefebvre¹, Aaron W. Hunter² and Martina Nohejlová^{1,3}

¹Univ. Lyon, Université Claude Bernard Lyon 1, ENS de Lyon, CNRS, UMR 5276 Laboratoire de Géologie de Lyon: Terre, Planètes, Environnement, F-69622 Villeurbanne, France

²Department of Earth Sciences, University of Cambridge, Downing Street, Cambridge CB2 3EQ UK

³Czech Geological Survey, Klárov 3, Praha 1, 118 21 Czech Republic

*farid.saleh@univ-lyon1.fr

Abstract: Investigation of the Fezouata Shale has added to our knowledge on the initial diversification of metazoans. These Lower Ordovician deposits yielded abundant and diverse remains of cuticularized to lightly sclerotized organisms, in addition to numerous soft tissues. Described fossilized soft parts recovered from the Fezouata Shale belong mainly to arthropods. Soft tissues in echinoderms, a main component of the Fezouata Biota, remain largely unexplored. Here, we show that soft tissue-like impressions previously reported in eocrinoid and somasteroid echinoderms from this formation, are the results of modern weathering and fossil preparation that involved the use of latex molds: they do not reflect any original (soft) anatomical features of these organisms. These two examples suggest that reports of putative soft parts, especially in taxa with no current representatives, need to be thoroughly and critically evaluated.

Keywords: Echinoderms, Exceptional Preservation, Fezouata Lagerstätte, Morocco, Ordovician, SEM, X-ray fluorescence maps

Introduction

Exceptional fossil preservation consists of the preservation of non-biomineralized soft parts (for example, digestive and nervous systems of animals) in the geological record. Fossiliferous localities showing this type of preservation are called *Konservat-Lagerstätten*. The late Tremadocian Fezouata Shale in the Anti-Atlas of Morocco, deposited approximately 480 million years ago, is the only Ordovician period *Konservat-Lagerstätte* to yield a fully marine diverse exceptionally preserved fauna [1]. The ~900 meter thick siltstones of the Fezouata Shale have yielded over 200 taxa of marine invertebrates [2]. Most of them belong to arthropods and echinoderms [2,3]. In these deposits, exceptionally preserved soft parts (for example, guts) are well-documented in various groups of arthropods (for example, anomalocaridids, trilobites) [1,2,4,5], annelids [6], hyolithids [7], molluscs [8], and palaeoscolecoid worms [9,10].

In marked contrast, very few occurrences of exceptionally preserved soft parts have been reported from Fezouata echinoderms: a putative gut was mentioned in one specimen of *Solutan* [11], and more abundant remains (water-vascular system, gut) were described in *Stylophorans* [12]. The water-vascular (or ambulacral) system is a complex, non-biomineralized, coelomic, hydraulic structure, which is unique to echinoderms. It consists of ambulacral canals leading to lateral sets of smaller tube feet, which are used for feeding, locomotion, and respiration.

Such a rarity of exceptionally preserved soft parts in echinoderms from the Fezouata Shale is not surprising. In spite of some recent spectacular reports, for example, in the Silurian

Herefordshire *Lagerstätte*, UK [13,14,15] or the Devonian Hunsrück Slate, Germany [16], very few examples of soft parts have been described in fossil echinoderms. This situation mainly results from the fast post-mortem disarticulation of their multi-element calcite skeleton and, hence, their low preservation potential, [3,17]. Experimental taphonomy, the study of how organisms decay and become fossilized, on modern echinoderms suggests that both skeletal elements and soft parts disarticulate and degrade within a few days after death [18]. Consequently, due to taphonomic biases [19], the preservation of complete echinoderm specimens yielding soft tissues is extremely rare even within *Lagerstätten*. Because of these biases, understanding the preservational pathway of an organism is vital prior to any paleontological description especially for animal groups with no current representatives. In this study, we aim at understanding the preservation of eocrinoids and somasteroids from the Fezouata Shale [20,21] and critically evaluate the recent reports of putative soft tissues (water-vascular system) in these two groups.

Material and Methods

The taphonomy of soft parts was analyzed in the two best-preserved specimens of eocrinoid and somasteroid echinoderms from the Fezouata Shale [20,21]. This material is deposited in the paleontological collections of the Musée des Confluences, Lyon, France (acronym “ML”), and Claude Bernard Lyon 1 University, Villeurbanne, France (acronym “UCBL-FSL”), respectively. The eocrinoid specimen (ML20-269159, Reboul collection) was collected at Bou Izargane, about 18 km north of Zagora, Morocco. This locality is a well-known fossiliferous site, where abundant and diverse late Tremadocian exceptionally preserved fossils have been collected (for example, anomalocaridids, marrellomorphs, palaeoscolecids), including trilobites and stylophoran echinoderms with soft parts [5,12,22]. The somasteroid specimen (UCBL-FSL 424962, Vizcaïno collection) is from an unknown locality, probably late Tremadocian in age, from the Ternata plain, north of Zagora, Morocco.

The two specimens were characterized using a FEI Quanta 250 scanning electron microscope (SEM) equipped with a backscattered electron detector in addition to an energy-dispersive X-ray analyzer (EDX) at accelerating voltages that varied from 5 to 15 kV. The backscattered electron detector allowed the acquisition of images with dark pixels corresponding to light elements (that is, small atomic number Z)

and white pixels corresponding to spots with heavy elements (that is, high atomic number Z). The EDX allowed, at low voltages, optimized acquisition of spectra revealing the distribution of light elements (that is, carbon). At high voltages, heavy elements, such as iron, were detected. In addition, X-ray fluorescence (XRF) elemental maps of these two specimens were obtained using a Bruker M4 Tornado micro-XRF instrument operating under vacuum at 50 kV and 600 μ A.

As both specimens were not completely flattened it was difficult to assess if negative elemental results were due to the actual absence of elements in the analyzed spot, or if the negative results were due to a topographic effect that inhibited the beam from reaching the spot. For this reason general elemental maps of rhodium Rh, the source of the XRF machine, were made. When Rh signal was absent it indicated that topographical effects prevented the beam from reaching the spot. Presence of Rh implied that the beam did reach the surface and the absence of an element was due to actual absence of this element from the chemical composition of the analyzed area.

Results

The eocrinoid specimen (Figure 1A) is entirely preserved in iron (Fe), which is shown by the green fluorescence in Figure 1C and the SEM EDX map in Figure 1E. This contrasts with the matrix, which is rich in silicon (Si) as shown by the red fluorescence in Figure 1B and the SEM EDX map in Figure 1E. Some Fe-rich small and repetitive structures are present within the brachioles (skeletonized arm-like feeding appendages) (Figure 1D). Most of the Fe-rich areas are preserved in small iron crystals that do not have any specific shape (that is, star-like minerals that are not euhedral nor framboidal; Figures 2A–D).

The somasteroid specimen (Figure 3A) is preserved as an imprint in the rock, and it shows the same elemental signature as the matrix, which is rich in Si (Figure 3B). However, some areas of the fossil appear to be depleted in Si (Figure 3B). Rh distribution shows that some of these anomalies are due to the actual absence of Si (that is, when Rh is present Rh+; Figure 3C), while the absence of Si in other regions is simply due to a hidden zone that was not analyzed by the beam (that is, Rh-; Figure 3C). The Rh+ zones are rich in carbon that is mostly detected when analyzing the specimen at 5 kV (Figure 3D). The carbon shows a repetitive pattern of small identical structures along the arms of the somasteroid (Figures 4A–B). However, carbon is also present elsewhere in the specimen (Figures 4C–F).

Interpretation and Discussion

The structures found in both the eocrinoid (Figure 1D) and somasteroid (Figures 4B–C) specimens resemble tube feet of the water vascular system, as, for example, those

evidenced in stylophoran echinoderms from the Fezouata Shale [12]. However, both the elemental and mineralogical signatures are different in these three occurrences.

Soft parts in exceptionally preserved fossils from the Fezouata Shale are preserved in both euhedral and framboidal pyrite [23]. These mineralogical morphologies are indicative of an early authigenic pyritization that occurred under anoxic conditions at time of burial [24], replicating soft tissues that are the most prone to decay [25]. After that, pyrite was transformed due to recent weathering to iron oxides [12,23]. This situation was observed in the soft parts reported in the stylophoran material from Bou Izargane in Morocco [12].

In contrast, the near absence of both euhedral and framboidal minerals in the eocrinoid specimen indicates that iron-rich minerals that are found in this fossil are not the result of the combined activity of authigenic mineralization and recent weathering. In this fossil, the iron oxides are simply related to the activity of recent weathering and, thus, they do not replicate any original anatomy. The distribution of these Fe-rich

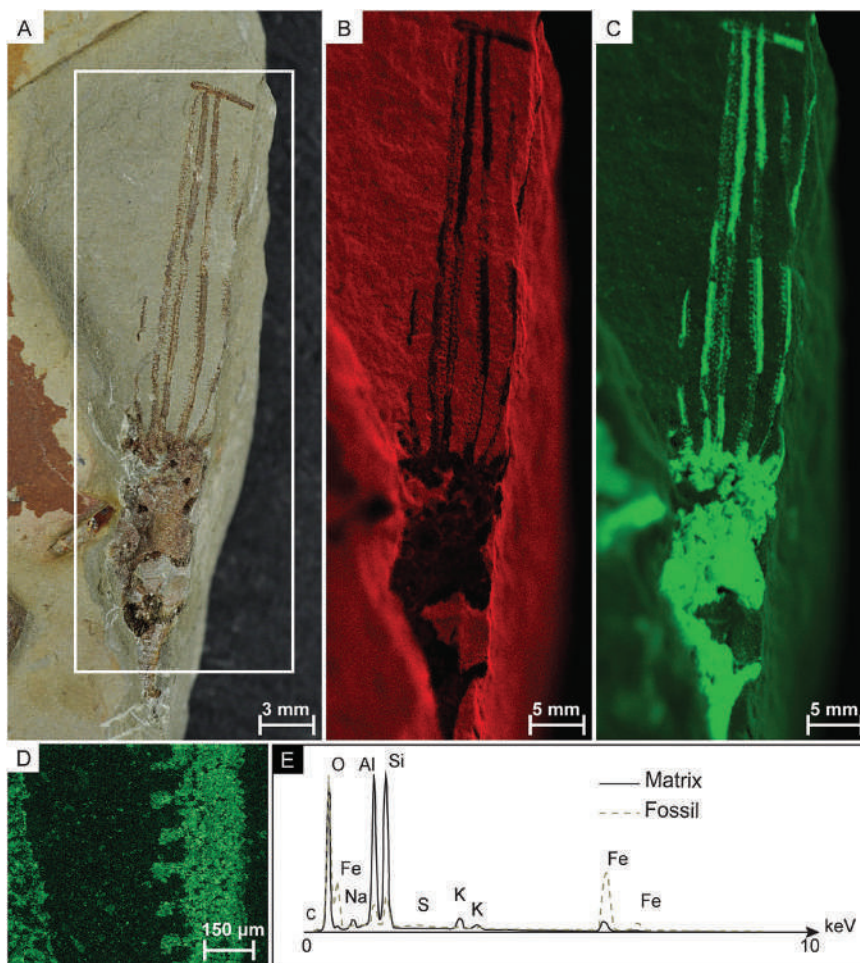


Figure 1: Analyzed specimen of eocrinoid echinoderm, late Tremadocian, Fezouata Shale, Bou Izargane, Zagora area, Morocco; ML20-269159. (A) Photograph of the specimen; (B) X-ray fluorescence image of inset shown in Figure 1A. Red indicates a high concentration of silicon distribution; (C) X-ray fluorescence of iron distribution (green) from the inset region of Figure 1A; (D) tube feet-like structures of the putative water vascular system showing iron distribution; (E) SEM-EDX elemental distribution in the matrix and the fossil.

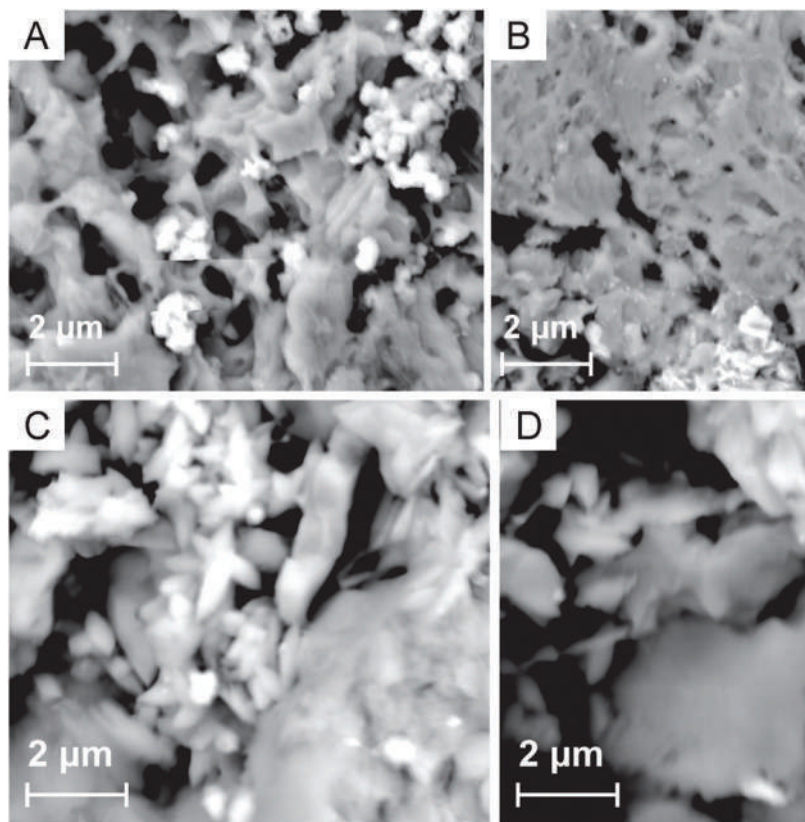


Figure 2: SEM-EDX images showing amorphous shape of particles and iron-rich areas (white regions).

minerals in all anatomical parts of the specimen, including skeletal plates (Figure 1C), validates this hypothesis.

The somasteroid specimen shows a totally different elemental distribution in the tube feet-like structures, with the total absence of Fe and the presence of carbon. Carbonaceous films are the main mode of preservation of soft tissues, especially in the Paleozoic era [26]. However, in surface sediments of the Fezouata Shale, carbon is absent from all fossils that have been analyzed [9,10,12]. The porous aspect of C-rich deposits in the analyzed specimen is strikingly different from the texture of carbon films in exceptionally preserved biotas [26]. Moreover, in the somasteroid specimen, carbon is not limited to any specific region but appears to fill all micro-depressions of the specimen (Figures 4D–G). Thus, it is very likely that this carbon is the consequence of preparation artifacts: numerous latex casts were made to study the detailed morphology of this specimen. Apparently, latex was not completely removed from small cavities located between skeletal plates, thus mimicking regularly branching tube feet along the ambulacral canal, in the arm region of the analyzed specimen.

Conclusion

This study confirms the validity of the interpretation as soft parts of the structures identified in

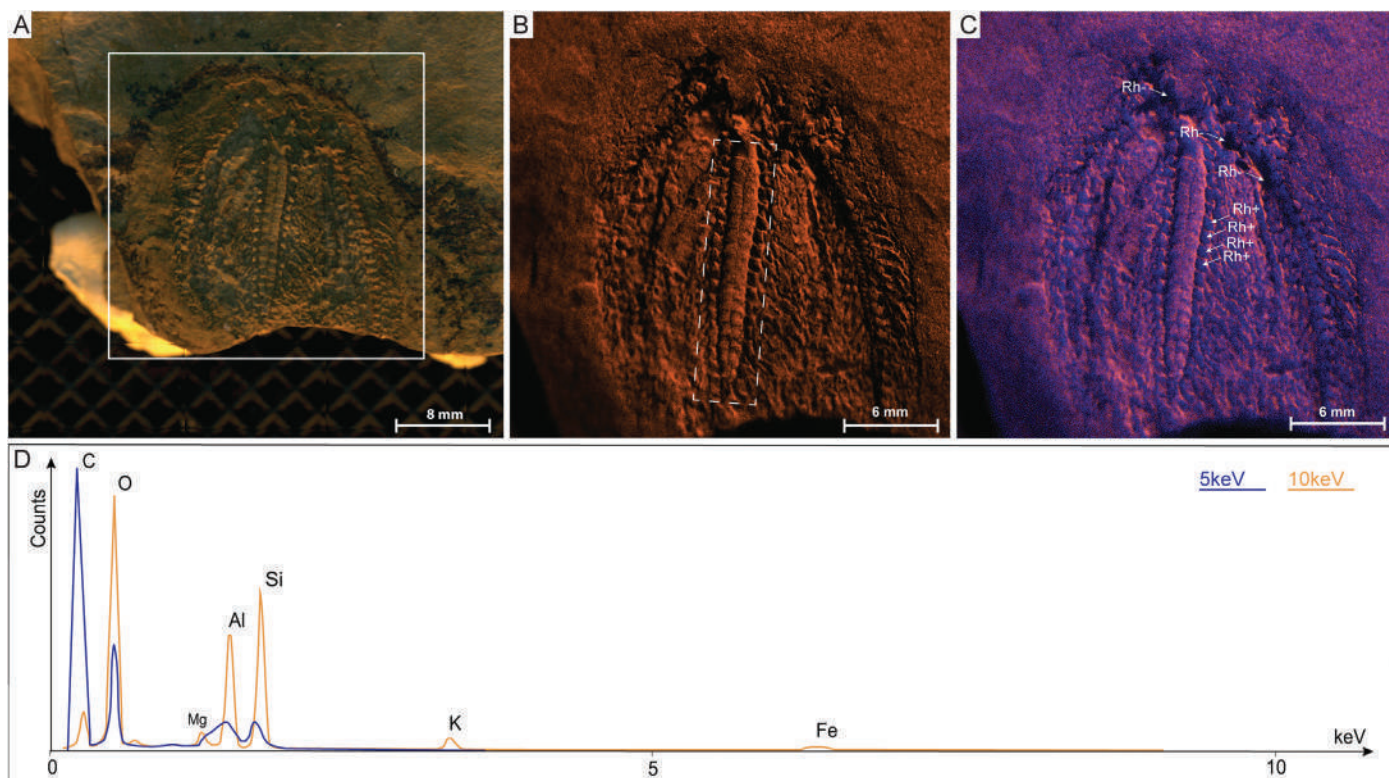


Figure 3: Analyzed specimen of somasteroid, late Tremadocian, Fezouata Shale, unknown locality, Zagora area, Morocco; UCBL-FSL424962. (A) Photograph of the specimen; (B) XRF, Si distribution; (C) XRF, superposition of Rh (blue) with K; (D) SEM-EDX elemental distribution in the tube feet-like structures.

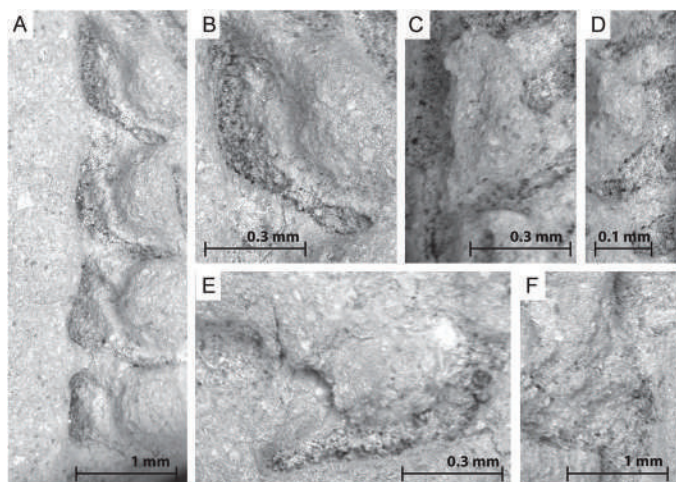


Figure 4: (A–B) Carbon particles (black) in tube feet-like structures of the putative water vascular system, (C–F) carbon particles found in other random structures showing the same carbon distribution as tube feet-like structures.

stylophoran echinoderms from the Fezouata Shale [12]. However, it also shows that it is probable that reports of putative soft parts in eocrinoids and somasteroids from the Fezouata Shale [20,21] are either preparation artifacts or the result of recent weathering. In addition, it shows that understanding the history of a specific fossil, from the excavation to preparation, is essential for proper paleontological interpretation, especially when it comes to the description of soft tissues in extinct taxa. These results should be taken into consideration when studying any new fossil, whether it is purchased from a private collector or comes from a museum collection.

Acknowledgements

This paper is a contribution to the TelluS-INTERVIE projects “Mécanismes de préservation exceptionnelle dans la Formation des Fezouata” (2018), and “Géochimie d’un *Lagerstätte* de l’Ordovicien inférieur du Maroc” (2019), all funded by the INSU (Institut National des Sciences de l’Univers, France), CNRS. This paper is also a contribution to the International Geoscience Programme (IGCP) Project 653 – The Onset of the Great Ordovician Biodiversification Event. The authors are grateful to the LABEX Lyon Institute of Origins (ANR-10-LABX-0066) of the Université de Lyon for its financial support within the program “Investissements d’Avenir” (ANR-11-IDEX-0007) of the French government operated by the National Research Agency (ANR). The authors thank Stefan Lalonde and Pierre Sansjofre (Brest University) for assistance during SEM and XRF analyses. The editor in chief, Bob Price, is thanked for his helpful and constructive remarks.

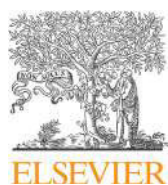
References

- [1] P Van Roy et al., *Nature* 465 (2010) 215–18.
- [2] P Van Roy et al., *J Geol Soc* 172 (2015) 541–49.
- [3] B Lefebvre et al., *Palaeogeogr Palaeoclimatol Palaeoecol* 460 (2016) 97–121.
- [4] P Van Roy and DEG Briggs, *Nature* 473 (2011) 510–13.
- [5] JC Gutiérrez-Marco et al., *Sci Rep* 7 (2017) 39728.
- [6] J Vinther et al., *Nature* 451 (2008) 185–88.

- [7] M Marti Mus, *Palaeogeogr Palaeoclimatol Palaeoecol* 460 (2016) 122–29.
- [8] J Vinther et al., *Nature* 542 (2017) 471–74.
- [9] ELO Martin et al., *Palaeogeogr Palaeoclimatol Palaeoecol* 460 (2016) 130–41.
- [10] K Kouraïss et al., *Palaeogeogr Palaeoclimatol Palaeoecol* 508 (2018) 48–58.
- [11] B Lefebvre et al., *Progr. Abstr. 57th Pal’Ass Meeting* (2013) 44–45.
- [12] B Lefebvre et al., *Geobios* 52 (2018) 27–36.
- [13] MD Sutton et al., *Proc R Soc B* 272 (2005) 1001–06.
- [14] DEG Briggs et al., *Proc R Soc B* 284 (2017) 20171189.
- [15] IA Rahman et al., *Proc R Soc B* 286 (2019) 20182792.
- [16] A Glass and DB Blake, *Paläont Z* 78 (2004) 73–95.
- [17] CE Brett et al., *Paleont Soc Papers* 3 (1997) 147–90.
- [18] P Gorzelak and MA Salamon, *Palaeogeogr Palaeoclimatol Palaeoecol* 386 (2013) 569–74.
- [19] F Saleh et al., *Earth Planet Sc Lett* 529 (2020) 115873.
- [20] B Lefebvre et al., *Progr. Abstr. 62nd Pal’Ass Meeting* (2018) 40.
- [21] M Nohejlová, *Abstr., 5th Int. Palaeont. Congr.* (2018) 851.
- [22] ELO Martin, *Communautés animales du début de l’Ordovicien (~480 Ma): études qualitatives et quantitatives à partir de sites à préservation exceptionnelle des Fezouata, Maroc*, Unpubl. PhD thesis, Lyon, 2016, pp. 1–313.
- [23] F Saleh et al., *Geology* 47 (2018) 103–06.
- [24] R Vaucher et al., *Sedimentology* 64 (2017) 777–807.
- [25] SE Gabbott et al., *Geology* 32 (2004) 901–04.
- [26] RR Gaines et al., *Geology* 36 (2008) 755–58.

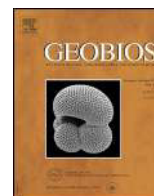
MT

QUARTER-PAGE
ADVERTISEMENT
89 mm x 114 mm



Available online at
ScienceDirect
www.sciencedirect.com

Elsevier Masson France
EM|consulte
www.em-consulte.com



Original article

Exceptionally preserved soft parts in fossils from the Lower Ordovician of Morocco clarify stylophoran affinities within basal deuterostomes[☆]



Bertrand Lefebvre^{a,*}, Thomas E. Guensburg^b, Emmanuel L.O. Martin^a, Rich Mooi^c,
 Elise Nardin^d, Martina Nohejlová^a, Farid Saleh^a, Khaoula Kouraïss^e, Khadija El Hariri^e,
 Bruno David^{f,g}

^aUMR CNRS 5276 LGLTPE, Université Claude-Bernard Lyon 1, 69622 Villeurbanne cedex, France

^bJRC, Field Museum, Chicago, IL 60605-2496, USA

^cDepartment of Invertebrate Zoology and Geology, California Academy of Sciences, San Francisco, CA 94118-4503, USA

^dUMR CNRS-IRD-UPS 5563 Géosciences Environnement Toulouse, Observatoire Midi-Pyrénées, 31400 Toulouse, France

^eDépartement des Sciences de la Terre, Faculté des Sciences et Techniques-Guéliz, Université Cadi-Ayyad, 40000 Marrakesh, Morocco

^fUMR CNRS 6282 Biogéosciences, Université de Bourgogne Franche-Comté, 21000 Dijon, France

^gMuséum National d'Histoire naturelle, 75005 Paris, France

ARTICLE INFO

Article history:

Received 24 September 2018

Accepted 15 November 2018

Available online 26 November 2018

Keywords:

Deuterostomes
 Echinoderms
 Fezouata Lagerstätte
 Tremadocian
 Morocco
 Phylogeny

ABSTRACT

The extinct echinoderm clade Stylophora consists of some of the strangest known deuterostomes. Stylophorans are known from complete, fully articulated skeletal remains from the middle Cambrian to the Pennsylvanian, but remain difficult to interpret. Their bizarre morphology, with a single appendage extending from a main body, has spawned vigorous debate over the phylogenetic significance of stylophorans, which were long considered modified but *bona fide* echinoderms with a feeding appendage. More recent interpretation of this appendage as a posterior “tail-like” structure has literally turned the animal back to front, leading to consideration of stylophorans as ancestral chordates, or as hemichordate-like, early echinoderms. Until now, the data feeding the debate have been restricted to evaluations of skeletal anatomy. Here, we apply novel elemental mapping technologies to describe, for the first time, soft tissue traces in stylophorans in conjunction with skeletal molds. The single stylophoran appendage contains a longitudinal canal with perpendicular, elongate extensions projecting beyond hinged biserial plates. This pattern of soft tissues compares most favorably with the hydrocoel, including a water vascular canal and tube feet found in all typical echinoderms. Presence of both calcite stereom and now, an apparent water vascular system, supports echinoderm and not hemichordate-like affinities.

© 2018 Elsevier Masson SAS. All rights reserved.

1. Introduction

Phylogenetic relationships among the main clades of deuterostomes (Swalla and Smith, 2008; Erwin et al., 2011; David and Mooi, 2014) and in particular, the earliest chordates (including the vertebrates) (Jefferies, 1986; Holland et al., 2015; Janvier, 2015) represent long-debated issues. In recent years, however, the combination of molecular, embryological, and anatomical data has made it possible to establish a robust phylogeny for extant

deuterostomes. With the Hemichordata (acorn worms), the echinoderms (sea lilies, starfish, sea urchins, and related forms) are now considered to belong to a clade, the Ambulacraria, as the sister-group of chordates (cephalochordates, tunicates and vertebrates) (Bottjer et al., 2006; Swalla and Smith, 2008; David and Mooi, 2014; Holland et al., 2015; Janvier, 2015; Lowe et al., 2015). This phylogenetic scenario provides insights not only into the distinctive morphological features (apomorphies) acquired within each clade of deuterostomes, but also into the primitive characters (plesiomorphies) inherited from their common ancestors (Bottjer et al., 2006; Swalla and Smith, 2008; David and Mooi, 2014; Lowe et al., 2015). For example, the occurrence of gill slits in both extant hemichordates and chordates strongly supports the view that these structures were very likely present in earliest deuterostomes

[☆] Corresponding editor: Gilles Escarguel.

* Corresponding author.

E-mail address: bertrand.lefebvre@univ-lyon1.fr (B. Lefebvre).

(Smith, 2005; Bottjer et al., 2006; Swalla and Smith, 2008; Lowe et al., 2015). Their absence in echinoderms is most parsimoniously regarded as a secondary loss during the course of echinoderm evolution (Smith, 2005; Bottjer et al., 2006; Swalla and Smith, 2008; Zamora and Rahman, 2014), or perhaps at the origin of the phylum itself (Mooi and David, 1998, 2008).

Integrating fossil data into the phylogeny of deuterostomes offers the opportunity to document the sequential acquisition of key characters through time and to provide minimum ages for lineage divergences. The interpretation of the earliest known deuterostomes (Cambro-Ordovician, 541–443 Myr; Shu et al., 2001, 2004; Caron et al., 2010, 2013) is particularly challenging because their morphologies are often bizarrely unlike those of modern forms, with unexpected combinations of anatomical features. Along with cambroernids (Caron et al., 2010), conodonts

(Briggs, 1992), vetulicolians (Shu et al., 2001) and vetulicystids (Shu et al., 2004), stylophorans belong to the bestiary of extinct, enigmatic early deuterostomes.

Stylophorans (cornutes and mitrates), a group of unusual middle Cambrian–Pennsylvanian (509–300 Myr) fossils, are small (typically one or two centimeters in length), bipartite organisms consisting of a single, articulated appendage inserted into a flattened, asymmetric to bilaterally symmetric body made of a multiplated internal skeleton, or test (Ubaghs, 1968; Clausen and Smith, 2005; Smith, 2005; David et al., 2000; Dominguez et al., 2002; Lefebvre, 2003; Fig. 1(A, D)). The appendage comprises two distinct parts: a highly flexible proximal region (partially inserted into the test) of telescopic, imbricate rings, and a relatively stiff distal region consisting of opposing, delicate biserial platelets mounted on massive, uniserial elements (ossicles). The two

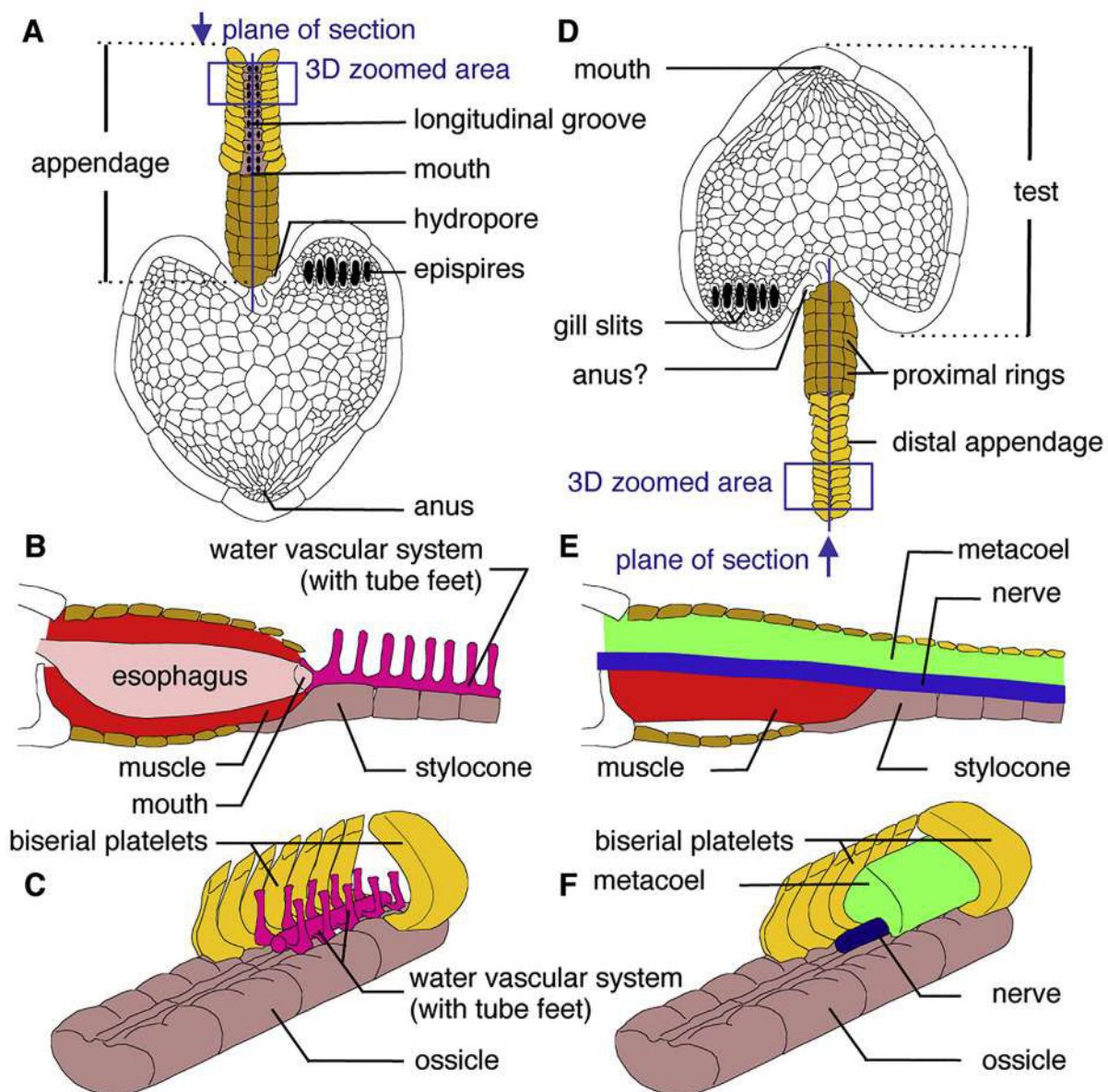


Fig. 1. The two current interpretations (H1 and H2) of stylophoran morphology and their implications for soft tissue anatomy, based on the cornute *Phyllocystis blayaci* (Lower Ordovician, France). **A–C.** H1, stylophorans as typical echinoderms with a single feeding arm. **D–F.** H2, stylophorans as pre-radial echinoderms with a hemichordate-like stalk. **A, D.** Basic anatomical features deduced from skeletal morphology. **B, E.** Reconstructions of soft tissue anatomy along a longitudinal section of the stylophoran appendage. **C, F.** Three-dimensional reconstructions of the soft tissue anatomy in the distal part of the stylophoran appendage.

platelet biseries form a roof over a longitudinal median groove running along the upper surfaces of the ossicles. Some interpretations suggest that the biserial platelets are fixed (Fig. 1(F)), whereas others show them as hinged, movable elements, much like cover plates in modern sea lilies and their kin (crinoids) (Fig. 1(C)). In life, the test likely contained the viscera; in some taxa, it bears a series of pores interpreted either as respiratory (Ubaghs, 1968; David et al., 2000; Lefebvre, 2003) or pharyngeal structures (Jefferies, 1986; Dominguez et al., 2002; Shu et al., 2004; Clausen and Smith, 2005; Smith, 2005; Bottjer et al., 2006) (Fig. 1(A, C)). Both the appendage and the test consist of numerous calcitic skeletal elements (called stereom) possessing the same microstructure found in all echinoderms (Ubaghs, 1968; Jefferies, 1986; David et al., 2000; Dominguez et al., 2002; Lefebvre, 2003; Clausen and Smith, 2005; Smith, 2005; Bottjer et al., 2006; Zamora and Rahman, 2014).

The phylogenetic position of stylophorans within deuterostomes has been a contentious matter for decades. In the early 1960s, the stylophoran appendage was interpreted as a feeding arm, comparable in morphology to the feeding structures of various extant echinoderms (Ubaghs, 1968; David et al., 2000; Lefebvre, 2003). In this hypothesis, stylophorans are considered *bona fide* echinoderms, with their appendage bearing a single ambulacral ray of the water vascular system (Figs. 1(A–C), 2). In the late 1960s, the stylophoran appendage was reinterpreted as a chordate-like tail, containing a notochord and serially arranged muscle blocks (Jefferies, 1986; Dominguez et al., 2002). Thereby, stylophorans were designated calcichordates, ancestral members of all three modern chordate lineages. This interpretation implies that the stereom skeleton of extant echinoderms was an apomorphy of all deuterostomes and therefore secondarily and independently lost in all lineages with the exception of echinoderms. Most recently, the stylophoran appendage has been interpreted as a muscular, hemichordate-like stalk (Shu et al., 2004; Clausen and Smith, 2005; Smith, 2005; Bottjer et al., 2006; Swalla and Smith, 2008; Caron et al., 2010) (Figs. 1(D–F), 2). In this interpretation, stylophorans remained echinoderms (because of the presence of the distinctive stereom), but are among the earliest members of the phylum, because they retain plesiomorphic features lost in all more derived taxa (e.g., locomotory stalk), and lack apomorphies present in more derived taxa (e.g., water vascular system).

Two basic assumptions of the calcichordate interpretation have previously been falsified. First, the purported sister-group relationship between echinoderms and chordates was not confirmed by molecular phylogenetics, which indicated that echinoderms are more closely related to hemichordates than they are to chordates (Bottjer et al., 2006; Swalla and Smith, 2008; Erwin et al., 2011; Lowe et al., 2015). Second, available evidence supports the view that stereom is an echinoderm synapomorphy that first appeared in the early Cambrian (Bottjer et al., 2006; Kouchinsky et al., 2012; Zamora and Rahman, 2014). The last two remaining, current hypotheses both agree that stylophorans are echinoderms (Fig. 2), but differ markedly in the interpretation of their appendage: feeding arm constructed like a typical echinoderm ray [H1] versus tail constructed like a hemichordate-like stalk [H2].

Here we report the first evidence for soft part preservation in stylophorans. These data make it possible to test, for the first time, soft anatomies predicted by H1 and H2 (Fig. 2). On the one hand, the feeding arm hypothesis (H1) requires that:

- the longitudinal median groove contained a water vascular canal, with lateral tube feet;
- biserial platelets are cover plates that opened to expose the tube feet;
- the mouth was located at the proximal end of the food groove;
- the fore-gut (esophagus) was located within the proximal rings.

On the other hand, the locomotory stalk scenario (H2) implies that:

- the longitudinal median groove contained a peduncular nerve;
- biserial platelets are integrated, contiguous body wall elements sutured to each other so as to enclose a coelom.

2. Material and methods

All figured specimens are housed in the collections of Cadi-Ayyad University (Faculté des Sciences et Techniques, Guéliz), Marrakesh, Morocco. Locality details are indicated on specimen labels, and can be provided on request. Specimens were prepared

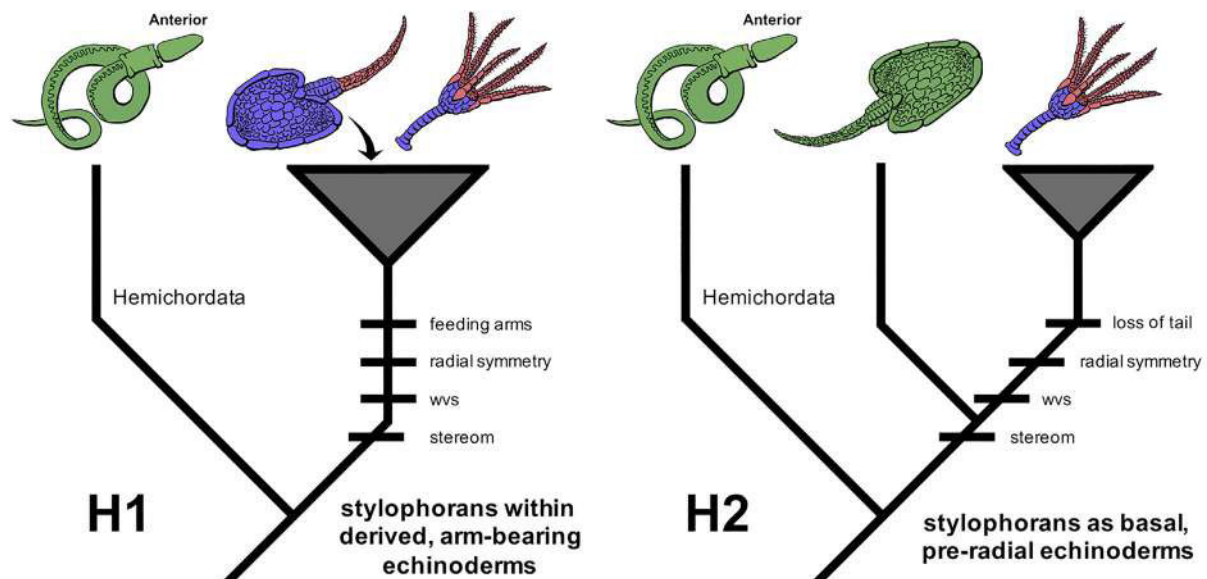


Fig. 2. The two current interpretations of stylophoran phylogenetic position within ambulacrarian deuterostomes: **H1**, stylophorans as typical echinoderms with a single feeding arm, and **H2**, stylophorans as pre-radial echinoderms with a hemichordate-like stalk. Abbreviation: wvs: water vascular system.

with scalpels and needles under high magnification using a Zeiss SterEO Discovery.V8 stereomicroscope. Interpretative drawings were made using a camera lucida attached to the same stereomicroscope, and photographs were made with a Zeiss AxioCam MRc5 digital camera also mounted on the same stereomicroscope. Digital photographs were processed in Adobe Photoshop Elements 9. Composite images have been stitched together using Adobe Photoshop Elements 9. Elemental composition was analysed in a FEI Quanta 250 scanning electron microscope (SEM) equipped with an energy X-ray analyser (EDX) at the CTμ (Centre Technologique des Microstructures, plateforme de l'Université Claude-Bernard Lyon 1).

3. Results

Stylophorans with soft parts were collected in the Lower Ordovician Fezouata Konservat-Lagerstätte, in a small excavation along the western flank of Bou Izargane hill, ca. 18 km north of Zagora (central Anti-Atlas, Morocco; Fig. 3). Here, the Fezouata Shale corresponds to a 1000 m-thick, repetitive succession of argillaceous siltstones, unconformable over the middle Cambrian sandstones of the Tabanite Group (Destombes et al., 1985; Martin et al., 2016). The excavation is ca. 270 m above the base of the Ordovician series and within the lower stratigraphic interval (ca. 80 m thick) yielding soft-bodied faunas typical of the Fezouata Biota (Vinther et al., 2008, 2017; Van Roy et al., 2010, 2015; Van Roy and Briggs, 2011; Lefebvre et al., 2016; Martin et al., 2016) (Fig. 3). Nearby graptolites indicate a late Tremadocian age (A. murrayi Zone; Gutiérrez-Marco and Martin, 2016; Lefebvre et al., 2016, 2018; Martin et al., 2016).

All specimens were collected from a single, small, 3 cm-thick lens of dark blue mudstones. Three fossiliferous intervals occur within the lens:

- a lower layer with many densely packed, complete, and fully articulated marrellomorphs (*Furca* sp.; Fig. 4(A));
- an intermediate horizon with a low-diversity assemblage of trilobites (*Anacheirurus* sp., *Bavarilla* sp.) with soft parts (Fig. 4(B, C));
- an upper, low-diversity assemblage comprising almost exclusively cornute stylophorans (more than 300 specimens

belonging to two taxa, namely *Hanusia* nov. sp. and *Thoralicystis* nov. sp.; Figs. 5–8).

Deposition is interpreted as rapid burial of autochthonous communities by distal storm deposits in relatively shallow environmental conditions (Martin et al., 2016; Vaucher et al., 2016). In this level, arthropods and echinoderms are typically preserved as faint, flattened impressions on the dark rock. As in the Burgess Shale, echinoderm skeletons are indicated as impressions without preservation of actual stereom. In contrast, their soft tissues appear as colorful structures, resulting from the oxidation of original pyrite into yellow, red to purple iron oxide pseudomorphs (Figs. 5(A), 6(A), 7(A), 8(A, C)). This type of preservation is not unique to the Bou Izargane cornutes (Vinther et al., 2008, 2017; Van Roy et al., 2010, 2015; Lefebvre et al., 2016). Similarly preserved soft parts (e.g., guts) have been described in arthropods (Gutiérrez-Marco et al., 2017), hyolithids (Martí Mus, 2016), and machaeridian annelids (Vinther et al., 2008) occurring in the same stratigraphic interval of the Fezouata Shale. In the cornutes, the identification and precise distribution of Fe-rich soft tissues were obtained by chemical analyses and elemental mapping under SEM (Figs. 5(B, E), 6).

At least one specimen of *Thoralicystis* nov. sp. shows clear evidence of soft-bodied structures in the distal part of its appendage (Figs. 5, 6). Preserved soft tissues consist of:

- two superimposed longitudinal canals housed in the continuous, median groove on the upper surface of ossicles, and extending from the stylocone cavity (proximally) to the distal end of the appendage;
- numerous small, lateral tube-like extensions branching regularly from the external longitudinal canal and protruding outward from between widely open, hinged plates.

Several specimens of *Thoralicystis* nov. sp. and *Hanusia* nov. sp. exhibit strong evidence of soft tissues preserved within the proximal part of their appendage (Figs. 7, 8). All these specimens display a spindle-shaped, elongate cavity extending throughout the proximal rings of the appendage from the stylocone cavity (distally), to the main body cavity (proximally). All these soft-bodied structures are described for the first time in stylophorans.

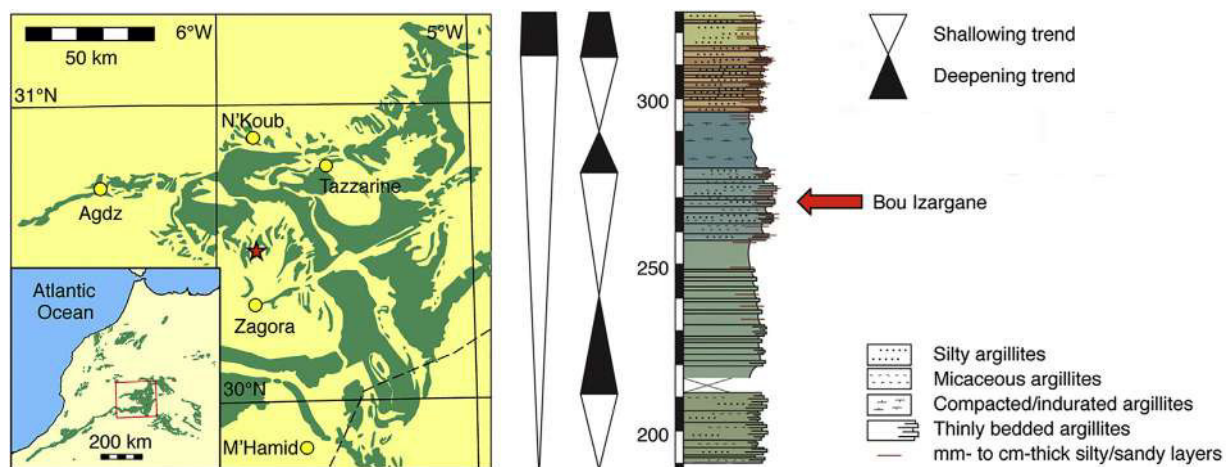


Fig. 3. Geographic and geologic context of Bou Izargane locality. On the maps (left), Ordovician outcrops in northwestern Africa and in the Zagora area are indicated in green. The red star shows the location of Bou Izargane hill. On the right, partial stratigraphic column of the Fezouata Shale, showing the position of the Bou Izargane excavation. The left column indicates sea level changes. Numbers along the column indicate the height (in m) above the Cambrian/Ordovician boundary. The colors used in the log correspond to those of outcropping rocks.

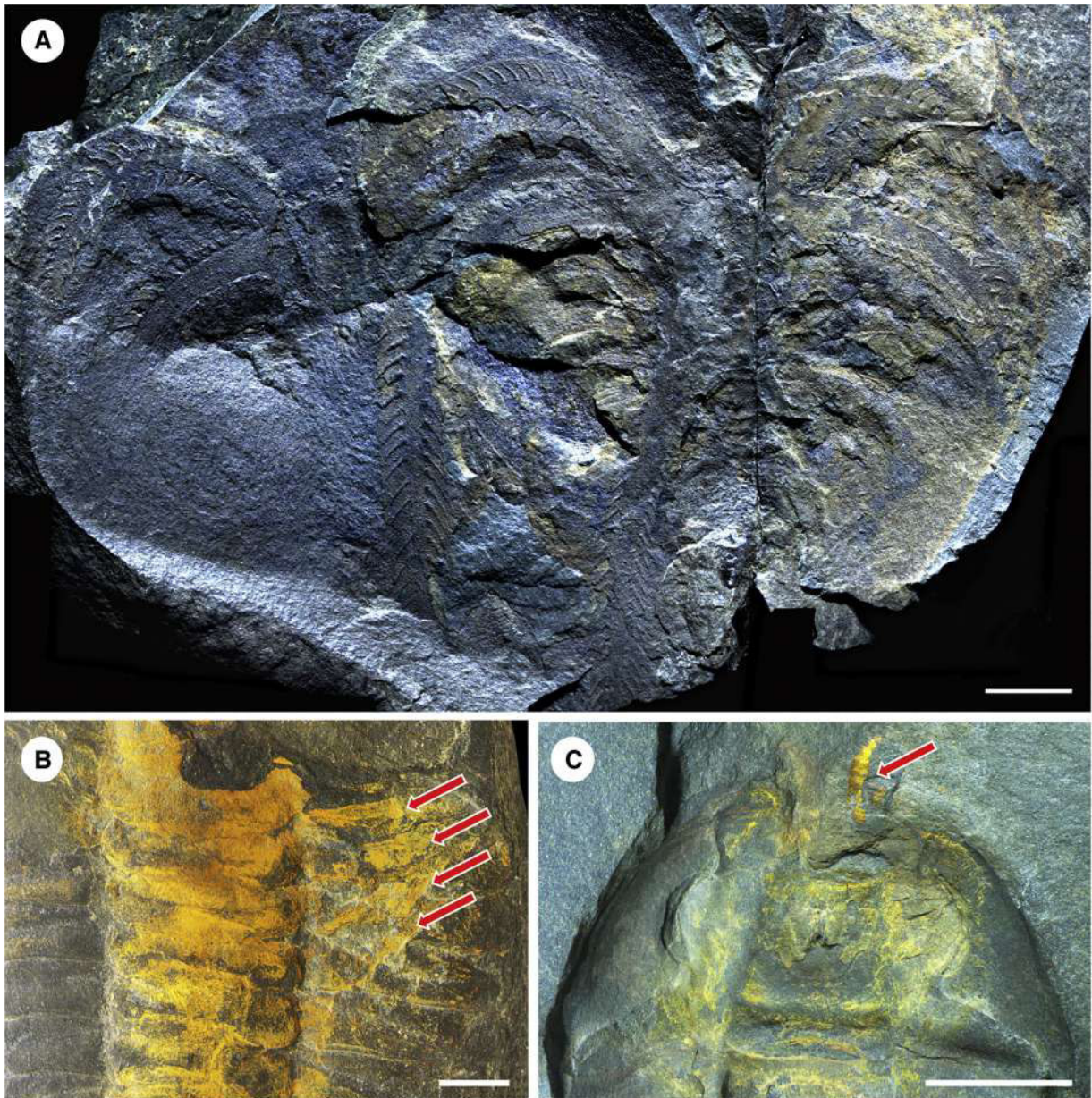


Fig. 4. Arthropods with soft tissue preservation collected in the same lens as cornute stylophorans with soft parts; late Tremadocian (Lower Ordovician), Bou Izargane, Zagora area (Morocco). **A.** Two associated specimens of the marrellomorph *Furca* sp. (AA.BIZ15.OI.364). **B, C.** Two specimens of the trilobite *Bavarilla zemmourensis*. **B.** Arrows indicate four locomotory appendages below the thorax (AA.BIZ15.OI.181). **C.** The arrow shows one frontal appendage at the anterior extremity of the cephalon (AA.BIZ15.OI.16). Scale bars: 5 mm (A, C), 2 mm (B).

4. Discussion

4.1. The stylophoran appendage is a feeding arm

On the basis of this new evidence, it is possible to evaluate critically the two current interpretations of the stylophoran appendage (Figs. 1,2). In the stalk model (H2), the outermost of the two longitudinal canals could be interpreted as the peduncular nerve housed in a fully enclosed body cavity, or coelom. However, H2 must be rejected because of the presence of open plates that precludes such a coelom, and the presence of lateral extensions that branch regularly from the external longitudinal canal and protrude externally in between the open plates. This organization is incompatible with that of a stalk- or tail-like structure, but fits requisites of the feeding arm model (H1).

The evidence strongly supports H1, in which the external longitudinal canal is interpreted as an ambulacral canal of the water vascular system, and the lateral, tube-like structures as ambulacral tube feet (Figs. 5, 6, 9), the morphology of which is strikingly similar to that of exceptionally preserved tube feet described from Paleozoic arm-bearing forms (Glass and Blake, 2004; Sutton et al., 2005; Glass, 2006; Clark et al., 2017). As a consequence, the mouth of stylophorans is most parsimoniously located at the proximal end of this ambulacral groove (Fig. 5(C)), the spindle-shaped cavity extending from the mouth (distally) and connected to the main body cavity (proximally) representing the anterior part of the gut (Figs. 5, 7, 8). Comparison with the situation in the arms and pinnules of modern crinoids suggests that the longitudinal canal internal to the space above the water vascular system is a coelomic canal (Figs. 5,6). There is no evidence that

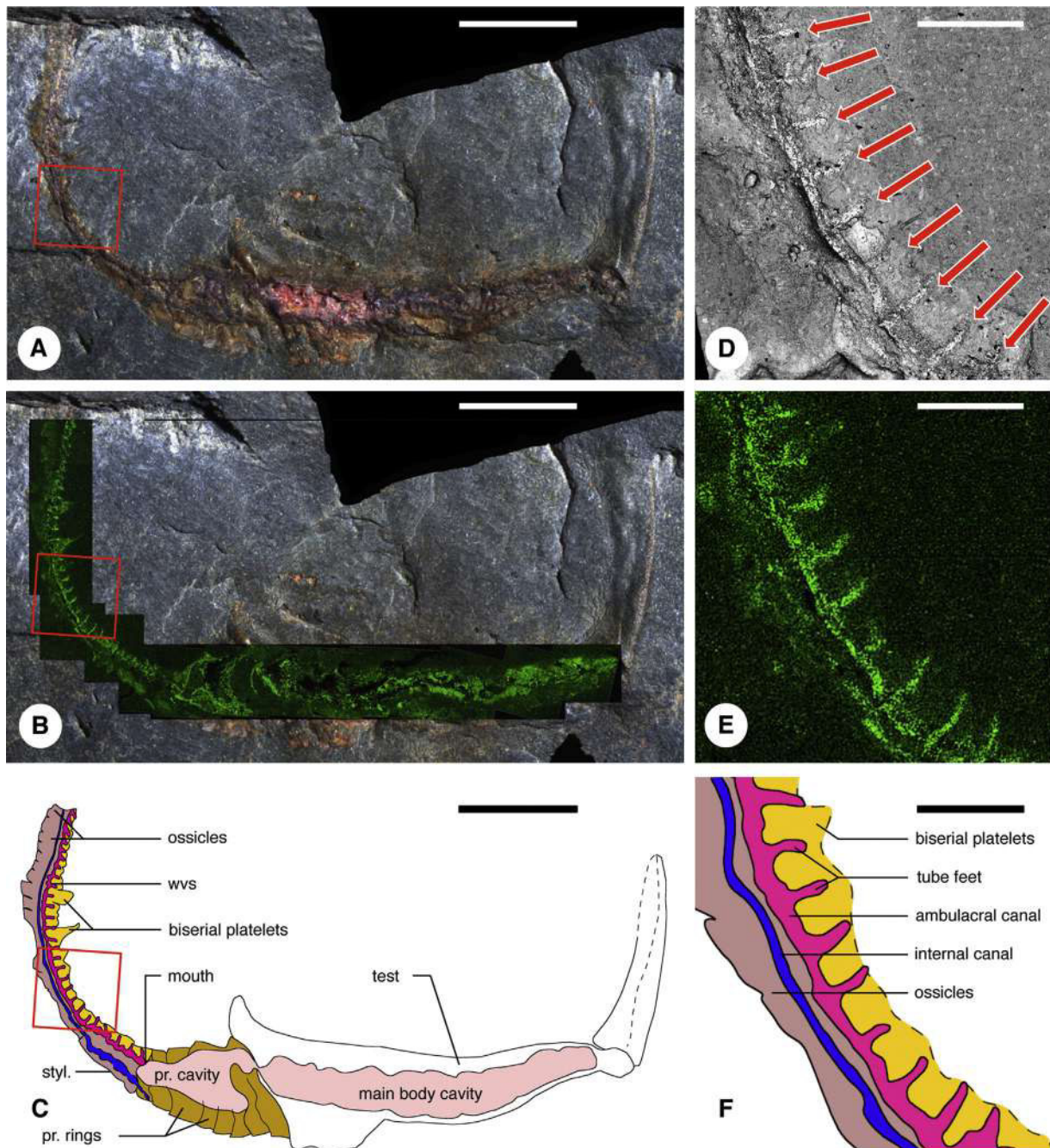


Fig. 5. *Thoralicystis* nov. sp. from the Fezouata Shale, Lower Ordovician, Morocco (AA.BIZ15.OI.259). **A–C.** Complete specimen in lateral view. **A.** Composite photographic reconstruction. **B.** Composite SEM elemental map of Fe. **C.** Composite reconstruction of soft part anatomy based on camera lucida drawings, SEM elemental maps (Fe) and back-scattered electron micrographs. **D–F.** Magnified views of parts of the distal appendage outlined in pictures A–C. **D.** Back-scattered electron micrograph. The arrows indicate the position of tube feet. **E.** SEM elemental map showing the distribution of Fe. **F.** Reconstruction of the soft parts based on camera lucida drawings, SEM elemental maps (Fe) and back-scattered electron micrographs. Abbreviations: pr. cavity: proximal cavity; pr. rings: proximal rings; styl.: stylocone; wvs: water vascular system. Scale bars: 5 mm (A–C), 1 mm (D–F).

what are interpreted here as tube feet represent some sort of musculature, because they project as freestanding structures extending from the longitudinal canal, and protrude outside of the body wall into the external medium.

Labyrinthine meshwork has been described in the proximal cavity of the stylocone (large, cone-shaped, uniserial ossicle located at the proximal end of the distal part of the appendage) of the primitive stylophoran *Ceratocystis* (middle Cambrian; Clausen and Smith, 2005). Similar observations in extant

echinoderms suggest that this labyrinthine microstructure was associated with muscle insertion, implying that the stylocone cavity once housed musculature with functionality similar to that in hemichordates. However, living echinoderms express muscles as well, so this trait is compatible with both H1 (Figs. 1(B), 2) and H2 (Figs. 1(E), 2), and cannot be used to provide evidence for or against either.

Finally, the putative locomotory function of the stylophoran appendage has been frequently considered as incompatible with

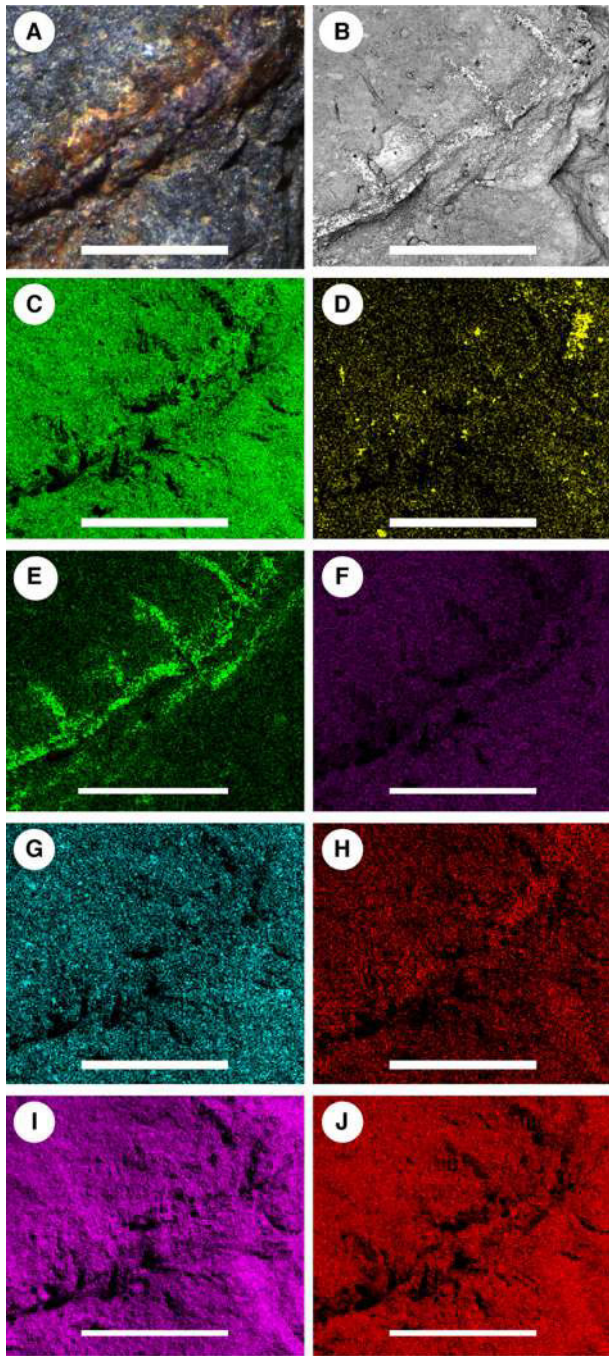


Fig. 6. Soft tissue preservation in the distal appendage of the cornute stylophoran *Thoralicystis* nov. sp. (AA.BIZ15.OI.259); late Tremadocian (Lower Ordovician), Bou Izargane, Zagora area (Morocco). **A.** Photographic view of the magnified area. **B.** Back-scattered electron micrograph showing the water vascular system (ambulacral canal, tube feet) and the second, more internal, longitudinal canal. Skeletal elements (biserial platelets, ossicles) are not visible. **C–J.** SEM elemental maps of Al (C), C (D), Fe (E), K (F), Mg (G), Na (H), O (I), and Si (J). Scale bars: 1 mm.

its interpretation as a feeding arm and the presence of a water vascular canal (Rahman et al., 2009; Rozhnov and Parsley, 2017). As this is the case in many extant arm-bearing echinoderms (e.g., asteroids, ophiuroids, comatulids), it is very likely that stylophorans used their appendage not only for nutrition, but also locomotion (Lefebvre, 2003).

4.2. Implications for echinoderm phylogeny

Preserved soft tissues in cornutes from the Lower Ordovician Fezouata Shale provide strong evidence suggesting the existence of ambulacral structures in the stylophoran appendage. The evidence supports the view that this extinct group of ambulacrarians possessed at least two of the major apomorphies supporting recognition of the phylum Echinodermata:

- a multi-element endoskeleton made of calcitic plates displaying the typical, three-dimensional stereomic microstructure;
- a water vascular system.

However, the precise phylogenetic position of stylophorans within echinoderms remains so far unresolved because they do not display any evidence of the radial, five-fold symmetry generally considered a synapomorphy of the phylum (Shu et al., 2004; Smith, 2005; Bottjer et al., 2006; Swalla and Smith, 2008; Zamora and Rahman, 2014). Provided this absence is original, stylophorans would then represent a relatively early branch of pre-radial echinoderms (Ubaghs, 1968, 1975; Shu et al., 2004; Smith, 2005; Bottjer et al., 2006; Swalla and Smith, 2008; Zamora and Rahman, 2014). Such an interpretation requires that anatomically similar, arm-like feeding structures were acquired independently in stylophorans in the middle Cambrian, and again, in later forms such as asteroids and crinoids, in the Early Ordovician (Ubaghs, 1968, 1975).

Alternatively, the late appearance of stylophorans in the fossil record 10–12 myr after radial taxa (e.g., eocrinoids, helicoplacoids, and edrioasteroid-like forms such as stromatocystitoids; Kouchinsky et al., 2012; Zamora et al., 2013) and their unusual, flattened morphology more parsimoniously suggest that stylophorans are relatively derived echinoderms descended from pentaradial ancestors (David et al., 2000). This interpretation is supported by embryological data, which provide no evidence suggesting that 5-part radial symmetry is preceded by stages with fewer rays (Mooi and David, 2008). In this context, the possession of arm-like ambulacral structures containing coelomic extensions other than the hydrocoel could represent an apomorphy uniting stylophorans with forms such as crinoids (David et al., 2000; Lefebvre, 2003).

4.3. Implications for early deuterostome phylogeny

The exceptionally preserved Early Ordovician cornute specimens from Morocco bring major new evidence to consider. That evidence actually reverses the anterior–posterior axis suggested by some very recent interpretations seeking to revive a modified version of the calcichordate interpretation (Shu et al., 2001, 2004; Clausen and Smith, 2005; Smith, 2005; Bottjer et al., 2006; Swalla and Smith, 2008; Zamora and Rahman, 2014). Since the early 2000s, molecular phylogenies have strongly supported an ambulacrarian clade that unites hemichordates and echinoderms as sister-group to the chordates (Bottjer et al., 2006; Swalla and Smith, 2008; David and Mooi, 2014; Holland et al., 2015; Janvier, 2015; Lowe et al., 2015). As a consequence of this phylogenetic framework, several authors reinterpreted stylophorans as early members of the Echinodermata, morphologically extremely close to the last common ancestor of both hemichordates and echinoderms (Shu et al., 2001, 2004; Clausen and Smith, 2005; Smith, 2005; Bottjer et al., 2006; Swalla and Smith, 2008). In this interpretation, stylophorans would possess a single echinoderm apomorphy: the calcite, stereom skeleton. They would not yet have acquired two other significant echinoderm apomorphies: the water vascular system and the radial, five-fold symmetry (Fig. 2: H2).

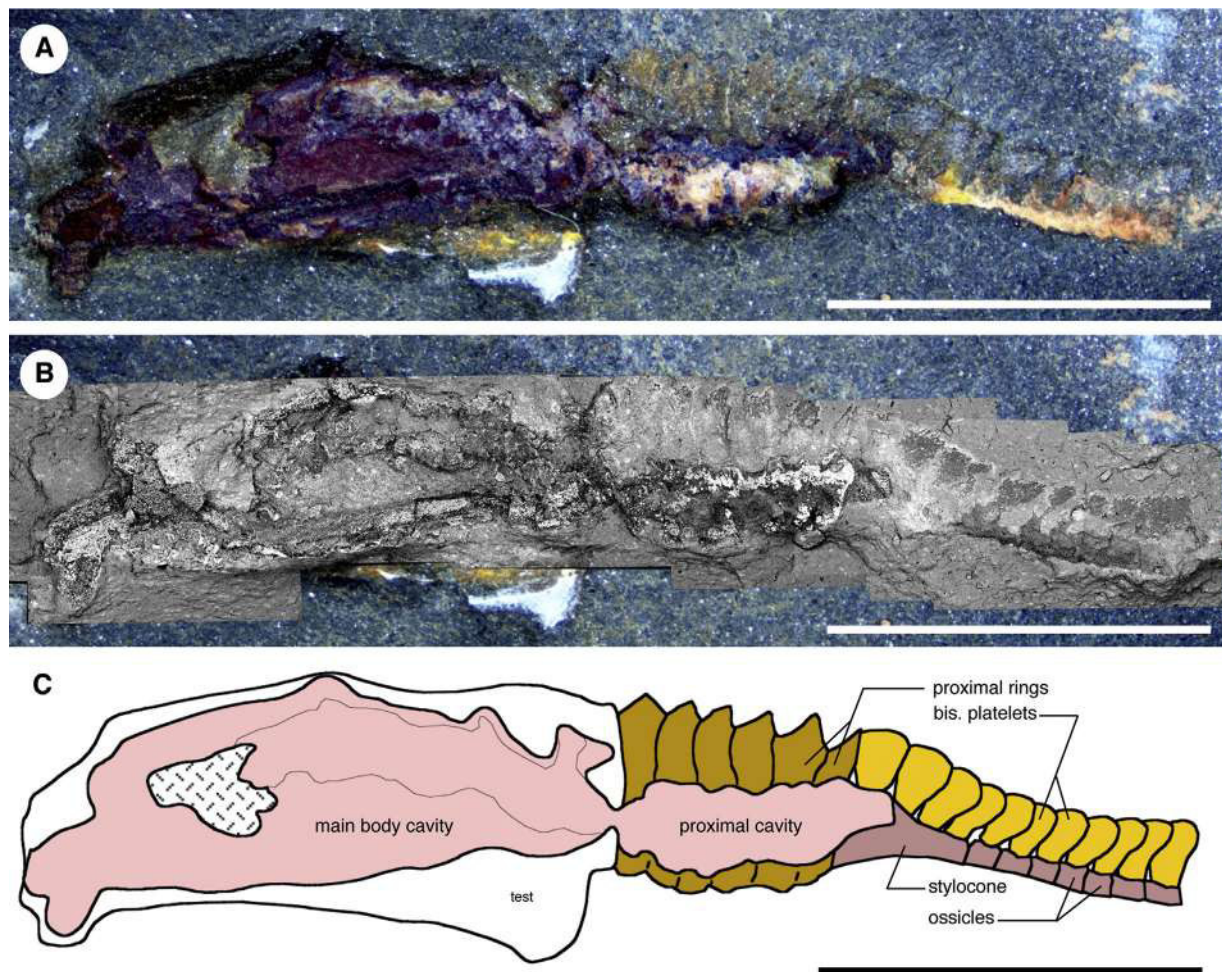


Fig. 7. Soft tissue preservation in the test and proximal appendage of the cornute stylophoran *Hanusia* nov. sp. (AA.BIZ15.OI.110); late Tremadocian (Lower Ordovician), Bou Izargane, Zagora area (Morocco). **A.** Composite photographic reconstruction of the specimen in lateral view. **B.** Composite reconstruction based on back-scattered electron micrographs. **C.** Reconstruction of the soft parts based on camera lucida drawings and back-scattered electron micrographs. Abbreviation: bis. platelets: biserial platelets. Scale bars: 5 mm.

In a surprising parallel to the calcichordate hypothesis, stylophorans would share with other (early) ambulacrarians and deuterostomes:

- a bipartite body organization, with a head and a muscular, locomotory tail (or stalk);
- the presence (plesiomorphic retention) of gill slits (Shu et al., 2001, 2004; Conway Morris, 2003; Clausen and Smith, 2005; Smith, 2005; Bottjer et al., 2006; Swalla and Smith, 2008; Caron et al., 2010; Conway Morris and Caron, 2012; Zamora and Rahman, 2014; Conway Morris et al., 2015).

As a consequence, this interpretation of stylophorans as hemichordate-like early echinoderms with a bipartite organization (anterior head and posterior tail-like appendage) has in the last 15 years caused many comparisons of early deuterostomes to stylophorans – i.e., *Herpetogaster* and cambroernids (Caron et al., 2010), *Pikaia* and other putative early chordates (Donoghue et al., 2003; Gee, 2006; Conway Morris and Caron, 2012), vetulicolians (Shu et al., 2001; Conway Morris, 2003; Vinther et al., 2011; Ou et al., 2012), and vetulicystids (Shu et al., 2004; Conway Morris et al., 2015).

Our study demonstrates that:

- stylophorans had a water vascular system;
- their appendage was not a locomotory muscular tail.

By bringing new, unequivocal evidence that the stylophoran appendage is an echinoderm feeding arm (comparable in morphology to a crinoid feeding arm) and not a hemichordate-like tail (or stalk), our discovery shows that the interpretation of these fossils as early echinoderms retaining features of basal ambulacrarians and/or hemichordates can be definitively rejected. In fact, any suggestion that stylophorans can tell us something about common ancestry of echinoderms with other deuterostomes is seriously compromised by the solid evidence that such conclusions rely on a reconstruction that has the animal the wrong way around. The bipartite body organization of stylophorans (theca and feeding arm) is not homologous to the bipartite body organization of *Herpetogaster*, vetulicolians, vetulicystids, early chordates and/or hemichordates (head and post-anal tail). Whatever the precise phylogenetic position of stylophorans within the Echinodermata, the significance of the Fezouata fossils lies in the picture they give of the remarkable diversity within the

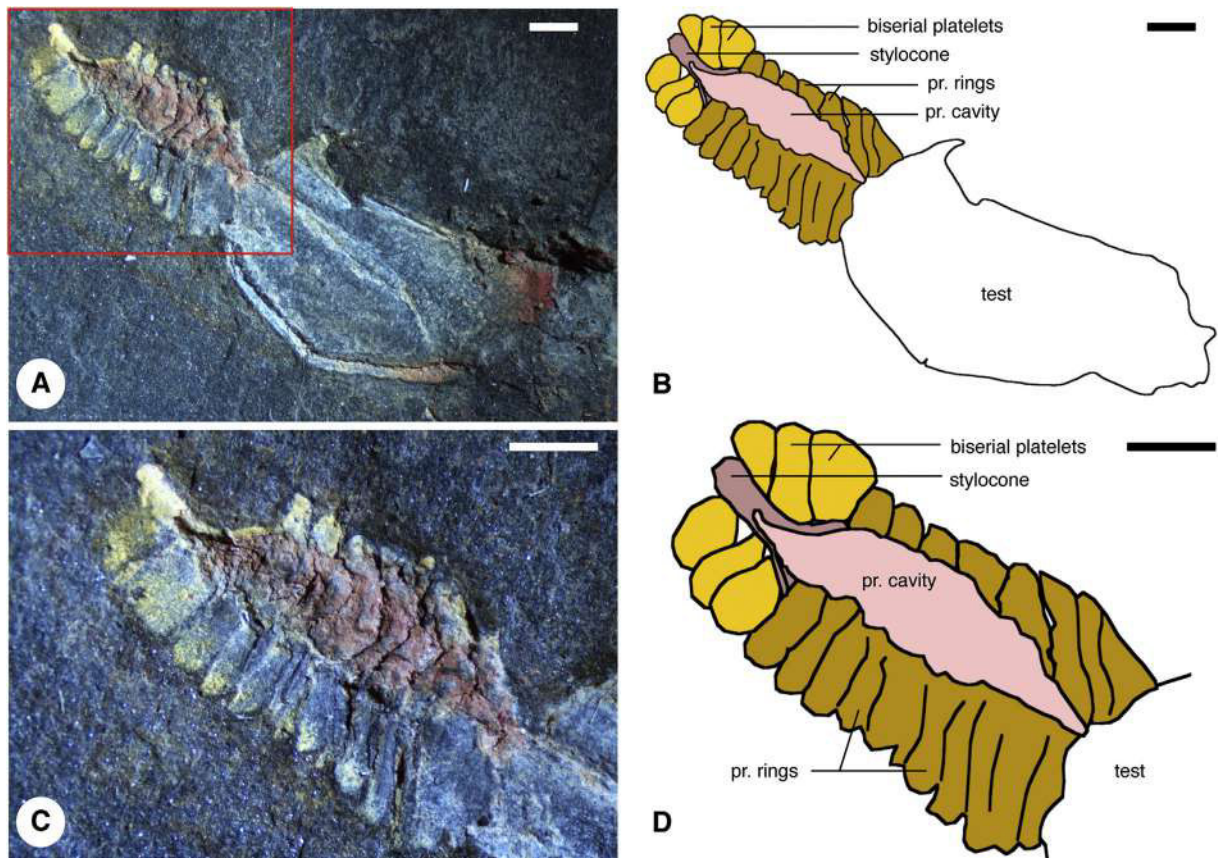


Fig. 8. Soft tissue preservation in the proximal appendage of the cornute stylophoran *Hanusia* nov. sp. (AA.BIZ15.OI.80); late Tremadocian (Lower Ordovician), Bou Izargane, Zagora area (Morocco). **A.** Specimen in upper view. **B.** Reconstruction of A, based on camera lucida drawings. **C.** Closer view of the proximal region of the appendage outlined in A (red rectangle). **D.** Reconstruction of C, based on camera lucida drawings. Abbreviations: pr. cavity: proximal cavity; pr. rings: proximal rings. Scale bars: 1 mm.

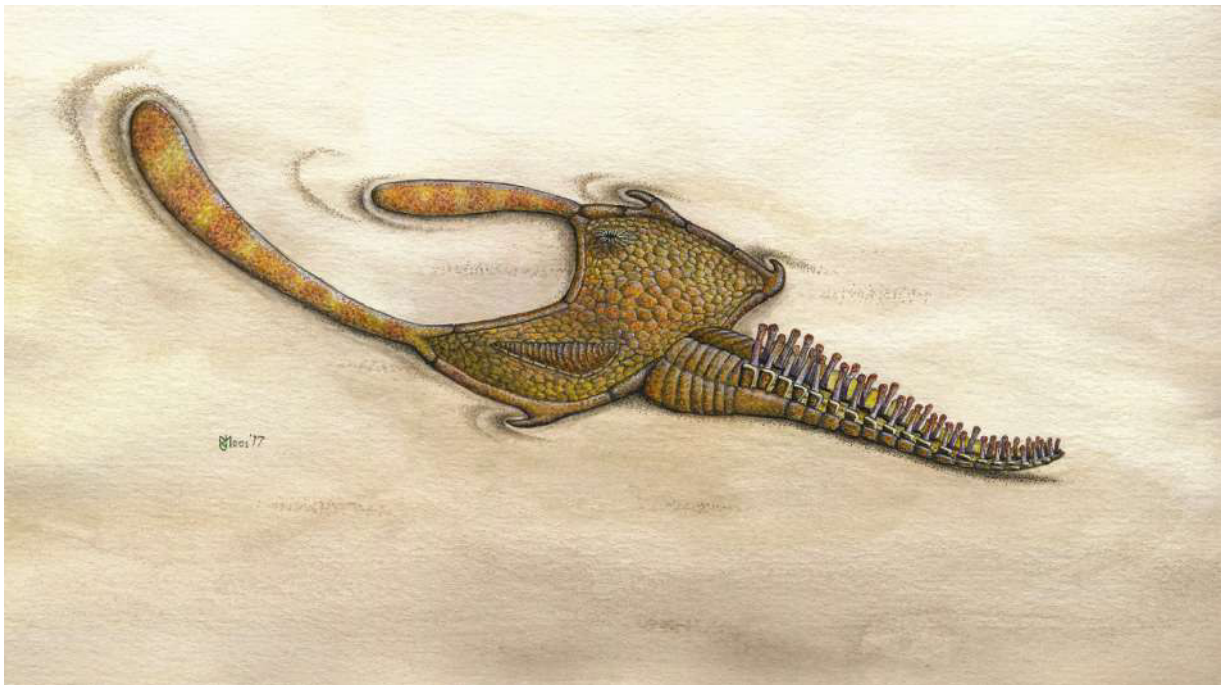


Fig. 9. Reconstruction of the cornute stylophoran *Thoralicystis* nov. sp., late Tremadocian (Lower Ordovician), Zagora area (Morocco), with the tube feet protruding beyond the cover plates. The appendage is about 20 mm long.

phylum throughout its evolution, and not of the supposed origins of the phylum itself.

Acknowledgements

This paper is a contribution of the Agence Nationale de la Recherche (ANR) research project entitled “The Rise of Animal Life (Cambrian-Ordovician): organisation and tempo” (grant number ANR-11-BS56-0025), the CNRS-CNRST cooperation project VALORIZ (grant number 52943) and the CNRS-INSU Tellus-INTERRVIE 2018 project TAPHO FEZOUATA. Abel Prieur (Lyon 1 University, Villeurbanne) is recognized for discovering the level with exceptional preservation in the field, Jean Vannier (Lyon 1 University, Villeurbanne) for technical assistance with SEM, and both Bernard Pittet and Romain Vaucher (Lyon 1 University, Villeurbanne) for making available detailed sedimentological information on the locality. Ronald L. Parsley (Tulane University, New Orleans), Imran Rahman (Oxford University Museum of Natural History), Sergei Rozhnov (Russian Academy of Sciences, Moscow), Samuel Zamora (Instituto Geológico y Minero de España, Zaragoza) and five anonymous reviewers provided insightful comments on several versions of the manuscript.

References

- Bottjer, D.J., Davidson, E.H., Peterson, K.J., Cameron, R.A., 2006. Paleogenomics of echinoderms. *Science* 314, 956–960.
- Briggs, D.E.G., 1992. Conodonts – a major extinct group added to the vertebrates. *Science* 256, 1285–1286.
- Caron, J.B., Conway Morris, S., Shu, D.G., 2010. Tentaculate fossils from the Cambrian of Canada (British Columbia) and China (Yunnan) interpreted as primitive deuterostomes. *Plos One* 5, e9586.
- Caron, J.B., Conway Morris, S., Cameron, C.B., 2013. Tubicolous enteropneusts from the Cambrian period. *Nature* 495, 503–506.
- Clark, E.G., Bhullar, B.A.S., Darroch, S.A.F., Briggs, D.E.G., 2017. Water vascular system architecture in an Ordovician ophiuroid. *Biology Letters* 13, 20170635.
- Clausen, S., Smith, A.B., 2005. Palaeoanatomy and biological affinities of a Cambrian deuterostome (Stylophora). *Nature* 438, 351–354.
- Conway Morris, S., 2003. The Cambrian “explosion” of metazoans and molecular biology: would Darwin be satisfied? *International Journal of Developmental Biology* 47, 505–515.
- Conway Morris, S., Caron, J.B., 2012. *Pikaia gracilens* Walcott, a stem-group chordate from the Middle Cambrian of British Columbia. *Biological Reviews* 87, 480–512.
- Conway Morris, S., Halgedahl, S.L., Selden, P., Jarrard, R.D., 2015. Rare primitive deuterostomes from the Cambrian (Series 3) of Utah. *Journal of Paleontology* 89, 631–636.
- David, B., Mooi, R., 2014. How Hox genes can shed light on the place of echinoderms among the deuterostomes. *EvoDevo* 5, 22.
- David, B., Lefebvre, B., Mooi, R., Parsley, R.L., 2000. Are homalochoans echinoderms? An answer from the extraxial-axial theory. *Paleobiology* 26, 529–555.
- Destombes, J., Holland, H., Willefert, S., 1985. Lower Palaeozoic rocks of Morocco. In: Holland, C.H. (Ed.), *Lower Palaeozoic Rocks of the World Volume 4: Lower Palaeozoic of Northwestern and West-Central Africa*. John Wiley & Sons, Chichester, pp. 91–336.
- Dominguez, P., Jacobson, A.G., Jefferies, R.P.S., 2002. Paired gill slits in a fossil with a calcite skeleton. *Nature* 417, 841–844.
- Donoghue, P.C.J., Smith, M.P., Sansom, I.J., 2003. The origin and early evolution of chordates: molecular clocks and the fossil record. In: Donoghue, P.C.J., Smith, M.P. (Eds.), *Telling the Evolutionary Time: Molecular Clocks and the Fossil Record*. Taylor & Francis, London, pp. 190–223.
- Erwin, D.H., Laflamme, M., Tweedt, S.M., Sperling, E.A., Pisani, D., Peterson, K.J., 2011. The Cambrian conundrum: early divergence and later ecological success in the early history of animals. *Science* 334, 1091–1097.
- Gee, H., 2006. Careful with that amphioxus. *Nature* 439, 923–924.
- Glass, A., 2006. Pyritized tube feet in a protasterid ophiuroid from the Upper Ordovician of Kentucky, USA. *Acta Palaeontologica Polonica* 51, 171–184.
- Glass, A., Blake, D.B., 2004. Preservation of tube feet in an ophiuroid (Echinodermata) from the Lower Devonian Hunsrück Slate of Germany and a redescription of *Bundenbachia benecke* and *Palaeophiomys grandis*. *Paläontologische Zeitschrift* 78, 73–95.
- Gutiérrez-Marco, J.C., Martin, E.L.O., 2016. Biostratigraphy and palaeoecology of Lower Ordovician graptolites from the Fezouata Shale (Moroccan Anti-Atlas). *Palaeogeography Palaeoclimatology Palaeoecology* 460, 35–49.
- Gutiérrez-Marco, J.C., García-Bellido, D.C., Rábano, I., Sá, A.A., 2017. Digestive and appendicular soft parts, with behavioural implications, in a large trilobite from the Fezouata Lagerstätte, 7. *Scientific Reports, Morocco*, pp. 39728.
- Holland, N.D., Holland, L.Z., Martin, P.W.H., 2015. Scenarios for the making of vertebrates. *Nature* 520, 450–455.
- Janvier, P., 2015. Facts and fancies about early fossil chordates and vertebrates. *Nature* 520, 483–489.
- Jefferies, R.P.S., 1986. *The Ancestry of the Vertebrates*. British Museum (Natural History), London.
- Kouchinsky, A., Bengtson, S., Runnegar, B., Skovsted, C., Steiner, M., Vedrasco, M., 2012. Chronology of early Cambrian biomineralization. *Geological Magazine* 149, 221–251.
- Lefebvre, B., 2003. Functional morphology of stylophoran echinoderms. *Palaeontology* 46, 511–555.
- Lefebvre, B., El Hariri, K., Leroisey-Aubril, R., Servais, T., Van Roy, P., 2016. The Fezouata Shale (Lower Ordovician, Anti-Atlas Morocco): a historical review. *Palaeogeography Palaeoclimatology Palaeoecology* 460, 7–23.
- Lefebvre, B., Gutiérrez-Marco, J.C., Lehnert, O., Martin, E.L.O., Nowak, H., Akodad, M., El Hariri, K., Servais, T., 2018. Age calibration of the Lower Ordovician Fezouata Lagerstätte, Morocco. *Lethaia* 51, 296–311.
- Lowe, C.J., Clarke, D.N., Medeiros, D.M., Rokhsar, D.S., Gerhart, J., 2015. The deuterostome context of chordate origins. *Nature* 520, 456–465.
- Martí Mus, M., 2016. A hyolithid with preserved soft parts from the Ordovician Fezouata Konservat-Lagerstätte of Morocco. *Palaeogeography Palaeoclimatology Palaeoecology* 460, 122–129.
- Martin, E.L.O., Pittet, B., Gutiérrez-Marco, J.C., Vannier, J., El Hariri, K., Leroisey-Aubril, R., Masrour, M., Nowak, H., Servais, T., Vandenbroucke, T.R.A., Van Roy, P., Vaucher, R., Lefebvre, B., 2016. The Lower Ordovician Fezouata Konservat-Lagerstätte from Morocco: age, environment and evolutionary perspectives. *Gondwana Research* 34, 274–283.
- Mooi, R., David, B., 1998. Evolution within a bizarre phylum: homologies of the first echinoderms. *American Zoologist* 38, 965–974.
- Mooi, R., David, B., 2008. Radial symmetry, the anterior/posterior axis, and echinoderm Hox genes. *Annual Review of Ecology, Evolution, and Systematics* 39, 43–62.
- Ou, Q., Conway Morris, S., Han, J., Zhang, J., Liu, J., Chen, A., Zhang, X., Shu, D.G., 2012. Evidence for gill slits and a pharynx in Cambrian vetulicolians: implications for the early evolution of deuterostomes. *BMC Biology* 10, 81.
- Rahman, I.A., Jefferies, R.P.S., Südkamp, W.H., Smith, R.D.A., 2009. Ichological insights into mitrate palaeobiology. *Palaeontology* 52, 127–138.
- Rozhnov, S.V., Parsley, R.L., 2017. A new cornute (Homalozoa: Echinodermata) from the uppermost middle Cambrian (Stage 3 Furongian) from northern Iran: its systematics and functional morphology. *Paleontological Journal* 51, 500–509.
- Shu, D.G., Conway Morris, S., Han, J., Chen, L., Zhang, X.L., Zhang, Z.F., Liu, H.Q., Li, Y., Liu, J.N., 2001. Primitive deuterostomes from the Chengjiang Lagerstätte (Lower Cambrian China). *Nature* 414, 419–424.
- Shu, D.G., Conway Morris, S., Han, J., Zhang, Z.F., Liu, J.H., 2004. Ancestral echinoderms from the Chengjiang deposits of China. *Nature* 430, 422–428.
- Smith, A.B., 2005. The pre-radial history of echinoderms. *Geological Journal* 40, 255–280.
- Sutton, M.D., Briggs, D.E.G., Siveter, D.J., Siveter, D.J., Gladwell, D.J., 2005. A starfish with three-dimensionally preserved soft parts from the Silurian of England. *Proceedings of the Royal Society B* 272, 1001–1006.
- Swalla, B.J., Smith, A.B., 2008. Deciphering deuterostome phylogeny: molecular, morphological and palaeontological perspectives. *Philosophical Transactions of the Royal Society B* 363, 1557–1568.
- Ubaghs, G., 1968. Stylophora. In: Moore, R.C. (Ed.), *Treatise on Invertebrate Paleontology. Part 5. Echinodermata 1*. Geological Society of America and University of Kansas Press, Lawrence, pp. S495–S565.
- Ubaghs, G., 1975. Early Paleozoic echinoderms. *Annual Review of Earth and Planetary Sciences* 3, 79–98.
- Van Roy, P., Briggs, D.E.G., 2011. A giant Ordovician anomalocaridid. *Nature* 473, 510–513.
- Van Roy, P., Orr, P.J., Botting, J.P., Muir, L.A., Vinther, J., Lefebvre, B., El Hariri, K., Briggs, D.E.G., 2010. Ordovician faunas of Burgess Shale type. *Nature* 465, 215–218.
- Van Roy, P., Briggs, D.E.G., Gaines, R.R., 2015. The Fezouata fossils of Morocco: an extraordinary record of marine life in the Early Ordovician. *Journal of the Geological Society* 172, 541–549.
- Vaucher, R., Martin, E.L.O., Hormière, H., Pittet, B., 2016. A genetic link between *Konzentrat*- and *Konservat-Lagerstätten* in the Fezouata Shale (Lower Ordovician Morocco). *Palaeogeography Palaeoclimatology Palaeoecology* 460, 24–34.
- Vinther, J., Van Roy, P., Briggs, D.E.G., 2008. Machaeridians are Palaeozoic armoured annelids. *Nature* 451, 185–188.
- Vinther, J., Smith, M.P., Harper, D.A.T., 2011. Vetulicolians from the Lower Cambrian Sirius Passett Lagerstätte North Greenland, and the polarity of morphological characters in basal deuterostomes. *Paleontology* 54, 711–771.
- Vinther, J., Parry, L., Briggs, D.E.G., Van Roy, P., 2017. Ancestral morphology of crown-group molluscs revealed by a new Ordovician stem aculiferan. *Nature* 542, 471–475.
- Zamora, S., Rahman, I.A., 2014. Deciphering the early evolution of echinoderms with Cambrian fossils. *Palaeontology* 57, 1105–1119.
- Zamora, S., Lefebvre, B., Alvaro, J.J., Clausen, S., Elicki, O., Fatka, O., Jell, P., Kouchinsky, A., Lin, J.P., Nardin, E., Parsley, R.L., Rozhnov, S., Sprinkle, J., Sumrall, C.D., Vizcaino, D., Smith, A.B., 2013. Cambrian echinoderm diversity and palaeobiogeography. In: Harper, D.A.T., Servais, T. (Eds.), *Early Palaeozoic Biogeography and Palaeogeography*. Geological Society of London Memoirs 38, 157–171.

8. TAPHONOMIC BIAS IN THE FEZOUATA SHALE

This chapter consists of one paper:

- **Paper 8:** Saleh, F., Antcliffe, J.B., Lefebvre, B., Pittet, B., Laibl, L., Peris, F.P., Lustri, L., Gueriau, P. and Daley, A.C., 2020. Taphonomic bias in exceptionally preserved biotas. **Earth and Planetary Science Letters**, 529, p.115873.

The main part of our understanding of ecology in past ecosystems is achieved through detailed comparisons of different deposits bearing soft-tissue preservation. Prior to these comparisons, taphonomic biases altering snapshots of early animal life must be accounted for⁷⁹. Even if the general conditions for exceptional preservation are the same (e.g. fine-grained sediment, burial by obrution events, reduced bacterial activity)^{15,54,55,80}, some discrepancies may exist between sites. Therefore, the most relevant way to compare taphonomic biases between exceptionally preserved sites is by investigating the occurrence of biological structures in these deposits because all animals are formed by the same type of structures⁷⁹. In this chapter, biological structures were divided into five categories (A, B, C, D, and E). A is for biomineralized structures (e.g. shell of a brachiopod). B is for sclerotized parts (i.e. formed of sclerites such as the headshield of arthropods). C represents the cuticle formed of polysaccharides defining, for instance, the body of annelid worms, priapulids, and some arthropods. D is for cellular structures, tissues *sensu stricto*, in direct contact with seawater such as the tentacles of hyoliths or the body walls of chordates. E is for internal systems and organs such as the digestive and nervous tissues. Based on an innovative statistical approach, we compared the preservation between the Fezouata Shale, the Burgess Shale, and the Chengjiang Biota. We evidenced that tissue association in the Fezouata Shale is significantly different from the Burgess Shale and the Chengjinag Biota⁷⁹. The Fezouata Shale systematically failed to preserve soft cellular structures that are in direct contact with seawater in addition to completely cellular organisms (D category)⁷⁹. This can be explained by the fact that fossils from the Fezouata biota were dead and decaying on the seafloor prior to their burial⁷². Under decay activity, cellular structures degrade faster than the cuticle and evidently much easier than sclerites and minerals⁸¹. These results suggest an actual underestimation for the Fezouata biota at the transition between the Cambrian Explosion and the Ordovician Radiation pointing to a continuum between both evolutionary events (Fig. 6)⁷⁹.

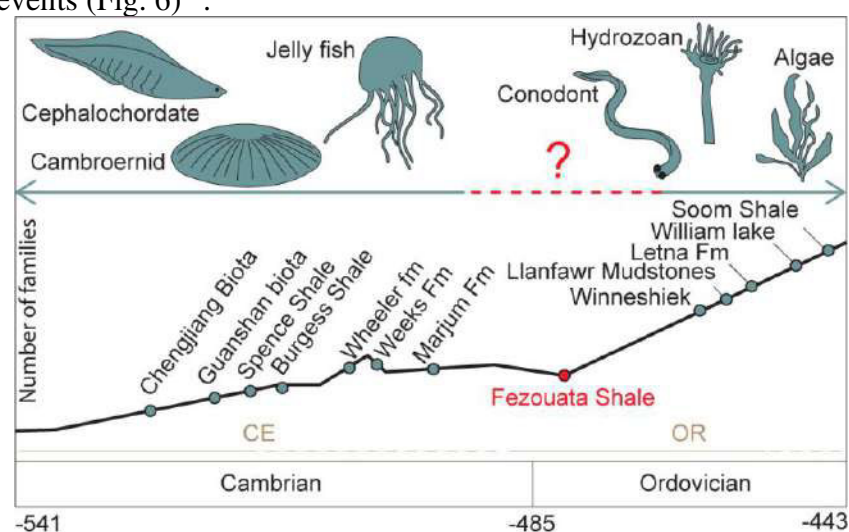


Figure 6. Exceptionally preserved biotas during the Cambrian and Ordovician. Note that the Fezouata Shale does not preserve completely cellular organisms such as cambroernids and cephalochordates underestimating biodiversity at the transition between the Cambrian Explosion (CE) and the Ordovician Radiation (OR).



Taphonomic bias in exceptionally preserved biotas

Farid Saleh^{a,*}, Jonathan B. Antcliff^b, Bertrand Lefebvre^a, Bernard Pittet^a, Lukáš Laibl^{b,c,d}, Francesc Perez Peris^b, Lorenzo Lustri^b, Pierre Gueriau^b, Allison C. Daley^{b,*}

^a Université de Lyon, Université Claude Bernard Lyon 1, École Normale Supérieure de Lyon, CNRS, UMR5276, LGL-TPE, Villeurbanne, France

^b Institute of Earth Sciences, University of Lausanne, Géopolis, CH-1015 Lausanne, Switzerland

^c The Czech Academy of Sciences, Institute of Geology, Rozvojová 269, 165 00 Prague 6, Czech Republic

^d Institute of Geology and Palaeontology, Faculty of Science, Charles University, Albertov 6, Prague, 12843, Czech Republic

ARTICLE INFO

Article history:

Received 25 April 2019

Received in revised form 27 September 2019

Accepted 28 September 2019

Available online xxxx

Editor: I. Halevy

Keywords:

exceptional preservation

taphonomy

Cambrian

Ordovician

ABSTRACT

Exceptionally preserved fossil biotas provide crucial data on early animal evolution. Fossil anatomy allows for reconstruction of the animal stem lineages, informing the stepwise process of crown group character acquisition. However, a confounding factor to these evolutionary analyses is information loss during fossil formation. Here we identify that the Ordovician Fezouata Shale has a clear taphonomic difference when compared to the Cambrian Burgess Shale and Chengjiang Biota. In the Fezouata Shale, soft cellular structures are most commonly associated with partially mineralized and sclerotized tissues, which may be protecting the soft tissue. Also, entirely soft non-cuticularized organisms are absent from the Fezouata Shale. Conversely, the Cambrian sites commonly preserve entirely soft cellular bodies and a higher diversity of tissue types per genus. The Burgess and Chengjiang biotas are remarkably similar, preserving near identical proportions of average tissue types per genus. However, the Burgess shale has almost double the proportion of genera that are entirely soft as compared to the Chengjiang Biota, indicating that the classic Burgess Shale was the acme for soft tissue preservation. Constraining these biases aids the differentiation of evolutionary and taphonomic absences, which is vital to incorporating anatomical data into a coherent framework of character acquisition during the earliest evolution of animals.

© 2019 Elsevier B.V. All rights reserved.

1. Introduction

Exceptionally preserved biotas have revolutionized our understanding of animal origins and evolution owing to the preservation in these deposits of soft-bodied and lightly sclerotized organisms, which under normal circumstances have little to no fossilization potential (Butterfield, 1995). Burgess Shale-type (BST) preservation deposits including the Burgess Shale (Wuliuan, Miaolinian; ~505 Ma, Canada) and the Chengjiang Biota (Stage 3, Cambrian Series 2; ~530 Ma, China) are particularly famous *Lagerstätten*, yielding hundreds of exceptionally preserved Cambrian taxa (Fig. 1a–c) critical to our understanding of the earliest metazoan-dominated communities and evolutionary events such as the Cambrian Explosion (Daley et al., 2018). The youngest of these deposits, the Fezouata Shale, is the only Ordovician (Tremadocian; ~479–478 Ma, Morocco) *Lagerstätte* to yield a diverse exceptionally preserved fauna (Fig. 1d–f). With over 185 taxa of marine invertebrates (Van Roy et al., 2015a) recovered from specific in-

tervals in the Zagora area (Lefebvre et al., 2018; Saleh et al., 2018, 2019), this formation offers new insights into the diversification of metazoans, at a key interval between the Cambrian Explosion and the Ordovician Radiation (Van Roy et al., 2010, 2015b; Lefebvre et al., 2019). Despite being anatomically and biologically informative, even these spectacular fossil localities inevitably have taphonomic biases, because no fossil site can ever be a perfect replication of all the anatomical and ecological information of a living community (Butterfield, 2003; Brasier et al., 2010; Landing et al., 2018). Gathering “complete” data is impossible even in studies on modern living communities. It is therefore essential to understand what factors may be affecting the fossil preservation at a community level in order to properly reconstruct ancient ecosystems and biodiversity fluctuations over geological time.

The aim of this study is to examine the taphonomic signal of these deposits, allowing a solid understanding of the preservation bias at play in each locality. For this reason, a taphonomic classification of all eumetazoan genera from the Fezouata Shale (N = 178) was established, and compared with the preservation of genera from the Burgess Shale (N = 103) and the Chengjiang Biota (N = 133) based on the presence/absence of different types of anatomical structures: (A) biomineralized skeletons, (B) sclero-

* Corresponding authors.

E-mail address: farid.saleh@univ-lyon1.fr (F. Saleh).

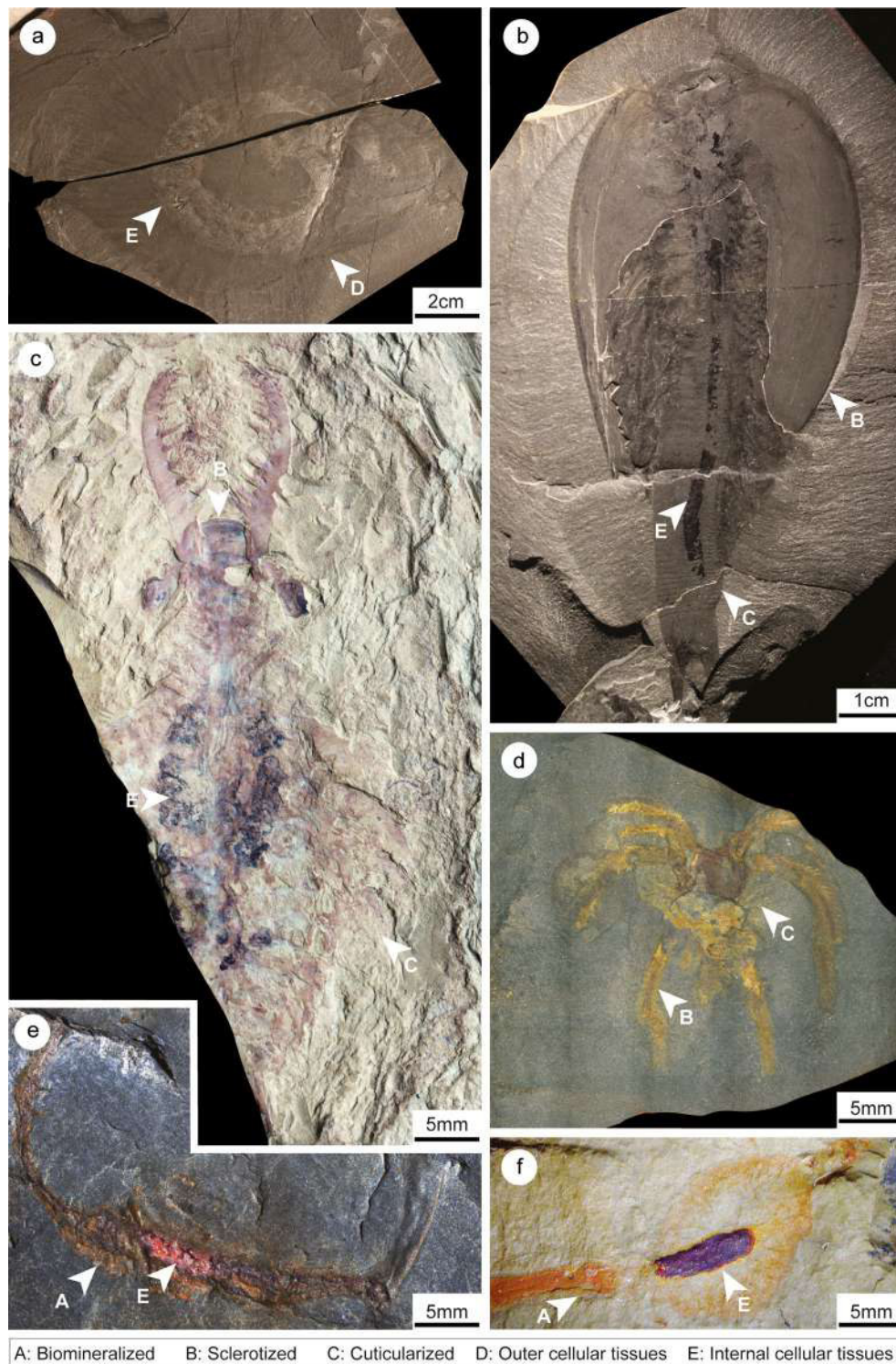


Fig. 1. Fossils from the three studied exceptionally preserved biotas showing examples of tissue associations. (a) Burgess Shale *Eldonia* USNM57540b preserving soft cellular body walls and internal organs (i.e. DE). (b) *Branchiocaris pretiosa* from the Burgess Shale USNM189028nc showing the association of sclerotized and cuticularized parts in addition to internal organs (BCE). (c) *Anomalocaris saron* ELRC20001a from the Chengjiang Biota belonging as well to the BCE category. (d) Marrellid arthropod from the Fezouata Shale AA.BIZ31.OI.39 preserving both sclerotized and cuticularized structures (BC). (e) Fezouata Shale stylophoran echinoderm AA.BIZ15.OI.259 showing the association of biominerals and internal organs (AE). (f) Solutan echinoderm from the Fezouata Shale CASG72938 belonging also to the AE category.

tized parts (i.e. possessing an organically strengthened part or organ) (C) soft with an unsclerotized cuticle (i.e. a non-cellular outer body surface that is either collagenous or formed by polymerized polysaccharides), (D) soft cellular outer layer defining at least a part of the body (e.g. tentacles of hyoliths), and (E) soft internal cellular organ/tissue (e.g. digestive or nervous systems) (Fig. 1).

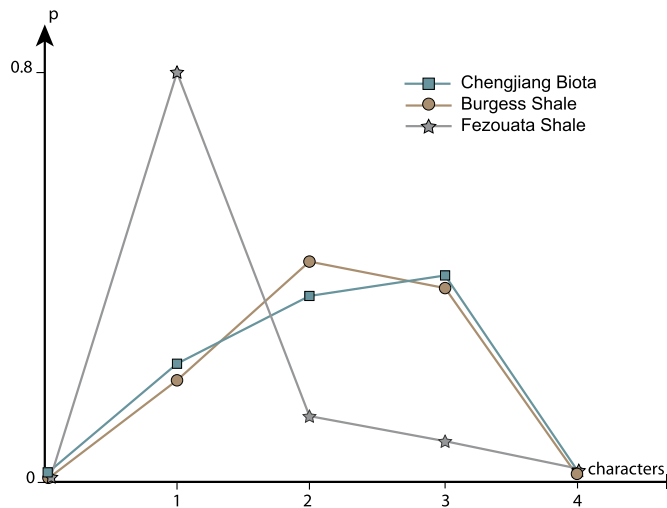
2. Material and methods

In order to define the preservation pattern in all three exceptionally preserved biotas, the various possible co-occurrences of characters A (biomineralized), B (sclerotized), C (unsclerotized, cuticularized), D (cellular body walls), and E (internal tissues) were

Table 1

Number of genera in different categories in all exceptionally preserved biotas.

	Fezouata Shale	Burgess Shale	Chengjiang Biota
A	90	15	4
B	41	7	9
C	3	0	6
D	0	1	4
E	1	0	0
AB	3	5	8
AC	0	2	2
AD	1	1	0
AE	9	1	0
BC	7	7	16
BD	0	1	4
BE	1	2	6
CD	0	0	0
CE	0	4	12
DE	0	13	9
ABC	0	2	0
ABD	0	0	0
ABE	5	0	2
ACD	0	0	0
ACE	1	8	19
ADE	0	0	0
BCD	0	0	0
BCE	7	28	28
BDE	0	2	1
CDE	0	0	0
ABCD	0	0	0
ABCE	3	1	1
ACDE	0	1	0
BCDE	0	0	0
ABCDE	0	0	0

**Fig. 2.** Differences in proportions of genera (Y axis) between single, paired, triple and quadruple character categories (marked as 1, 2, 3, and 4 on the X axis) between the Fezouata Shale, the Burgess Shale and the Chengjiang Biota. The Fezouata Shale shows a dominance of genera preserving only one tissue when compared to the Burgess Shale and Chengjiang Biota.

tallied (e.g. AB, AC, CDE, and ABCDE) (Table 1). To avoid any overlap between categories, the data were analyzed on a five-fold Venn diagram per site. In order to see if there is any difference between sites, the total number of genera having just one character regardless of its nature (e.g. A, or B, or C, or D, or E) was plotted against the number of genera that have pairs (e.g. AB), threes (e.g. ABC) or fours (e.g. ABCD) for all exceptionally preserved biotas (Fig. 2). Afterward, the average number of tissue types per genus, as derived from the dataset, was calculated by adding the probability of the occurrence of all classes of structures A, B, C, D, and E (Table 2). In order to constrain the categories causing the biggest variations in

Table 2

Proportion of each type of tissue in all categories combined in the Fezouata Shale, the Burgess Shale and the Chengjiang Biota. The probability of preserving cuticularized and cellular tissues, in addition to the number of tissue per genus in the Fezouata Shale are lower than in the Chengjiang Biota and the Burgess Shale.

	Fezouata Shale N(total) = 173	Burgess Shale N(total) = 101	Chengjiang Biota N(total) = 133
A	N(A) = 112 p(A) = 0.647	N(A) = 36 p(A) = 0.356	N(A) = 36 p(A) = 0.270
B	N(B) = 67 p(B) = 0.387	N(B) = 55 p(B) = 0.544	N(B) = 75 p(B) = 0.563
C	N(C) = 21 p(C) = 0.121	N(C) = 53 p(C) = 0.524	N(C) = 84 p(C) = 0.631
D	N(D) = 1 p(D) = 0.005	N(D) = 19 p(D) = 0.188	N(D) = 18 p(D) = 0.135
E	N(E) = 27 p(E) = 0.156	N(E) = 60 p(E) = 0.594	N(E) = 78 p(E) = 0.586
Total = tissue/genus	1.316	2.206	2.185

Table 3

Probabilities of finding internal soft tissues in a fossil given that another tissue was found and vice versa. The obtained numbers for the Burgess Shale and the Chengjiang Biota are more similar to each other than to the Fezouata Shale.

	Fezouata Shale	Burgess Shale	Chengjiang Biota
p(E A)	0.162	0.306	0.611
p(E B)	0.239	0.607	0.507
p(E C)	0.524	0.789	0.714
p(E D)	0	0.842	0.556
p(A E)	0.667	0.183	0.278
p(B E)	0.593	0.567	0.481
p(C E)	0.407	0.683	0.759
p(D E)	0	0.267	0.127

preservation between sites, plots were made to show the proportion of paired and triple categories in localities (Fig. 3).

The association of soft internal organs (E) with other structures, in all three localities was also investigated. For this, the probabilities of discovering two classes of structures together having already found one of them were calculated (Table 3). For example, p(E|A) is the probability of E occurring if A has occurred. The reverse conditional approach was also made and the probability of finding A given that E has been found p(A|E) was also calculated (Table 3). Then, the likelihood of producing the distribution of combinations of structures found in the Burgess Shale and the Chengjiang Biota assuming that the Fezouata Shale has the “true” preservation regime was investigated using the following parametrized binomial $P(x \geq n) | Bi(n, p)$:

$$P(x) = \binom{n}{x} p^x q^{n-x} = \frac{n!}{(n-x)!x!} p^x q^{n-x}$$

In this equation, $p = p(E|A)$ for the Fezouata Shale, $q = 1 - p$, n is the number of genera preserving an A in the Burgess Shale or the Chengjiang Biota, and x is the number of desired success which is, in this case, at least the actual number n of genera preserving both A and E in the Burgess Shale/Chengjiang Biota. All calculated probabilities are added up and the probability $P(x \geq n) | Bi(n, p)$, of producing the actual Burgess Shale/Chengjiang Biota AE category, considering that the Fezouata Shale regime is “true”, is then obtained (Table 4). This was then performed for other tissues combinations (i.e. BE, CE, and DE) (Table 4). This approach was then extended to the assumption that the Burgess Shale preservation distribution is “true” and finally assuming that the Chengjiang Biota preservation distribution is the “true” preservation model (Table 5).

Finally, the probability of finding organisms with only soft cellular tissues (both internal and external to the exclusion of every-

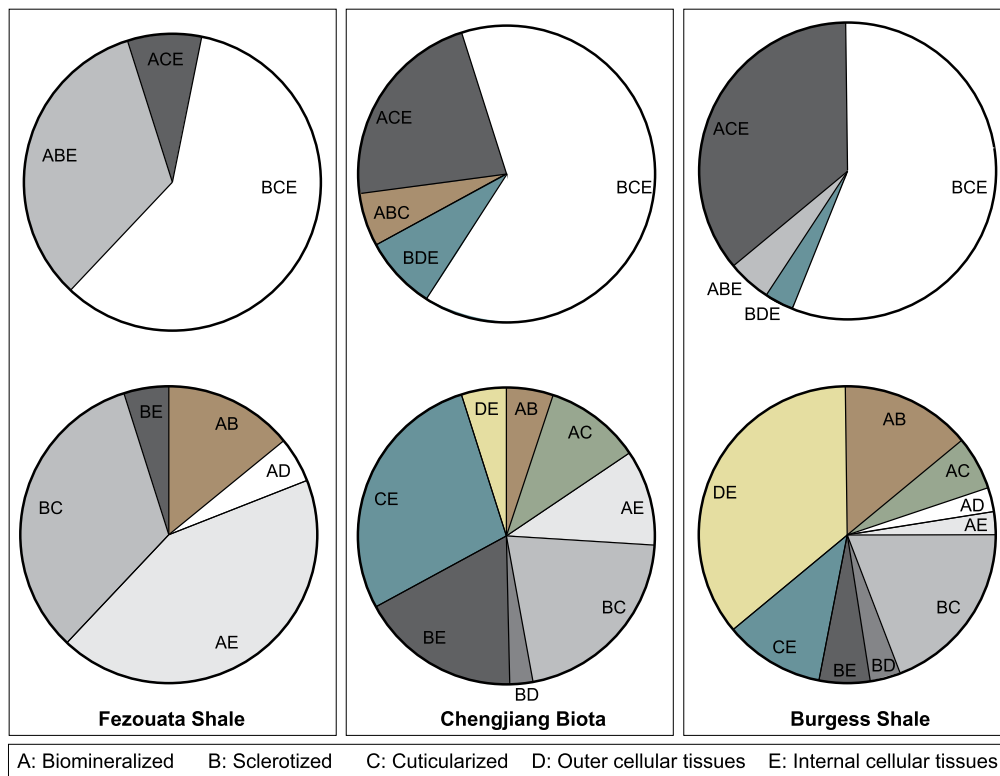


Fig. 3. Pie charts showing the differences in triple and paired character categories between the Fezouata Shale, the Burgess Shale, and the Chengjiang Biota.

Table 4

Probabilities of reproducing patterns of preservation of the Burgess Shale and the Chengjiang Biota assuming that the Fezouata Shale preservation regime is true. All probabilities are smaller than 0.05 showing that the preservation regime in the Fezouata Shale is different from both the Chengjiang Biota and the Burgess Shale.

	Burgess Shale	Chengjiang Biota
$p(E A)$	$P(X \geq 11) Bi(36, 0.162) = 0.0235$	$P(X \geq 22) Bi(36, 0.162) < 0.000001$
$p(E B)$	$P(X \geq 34) Bi(56, 0.239) < 0.000001$	$P(X \geq 38) Bi(75, 0.239) < 0.000001$
$p(E C)$	$P(X \geq 41) Bi(52, 0.524) = 0.0000738$	$P(X \geq 60) Bi(84, 0.524) = 0.000291$
$p(E D)$	0	0

Table 5

A: Probabilities of reproducing patterns of preservation of the Burgess Shale assuming that the Chengjiang biota preservation regime is true. B: Probabilities of reproducing patterns of preservation of the Chengjiang Biota assuming that the Burgess Shale preservation regime is true. Some tissue associations are not reproducible in both models (i.e. marked as "No" in the "Pass" column), showing that the pattern of preservation between the Burgess Shale and the Chengjiang Biota is not exactly the same.

	A: Burgess given a Chengjiang Biota model	B: Chengjiang given the Burgess Shale model	Pass?
$p(E A)$	$P(X \leq 11) Bi(36, 0.611) = 0.000201$	$P(X \geq 22) Bi(36, 0.306) = 0.000149$	No
$p(E B)$	$P(X \geq 34) Bi(56, 0.507) = 0.0857$	$P(X \leq 38) Bi(75, 0.607) = 0.292$	Yes
$p(E C)$	$P(X \geq 41) Bi(52, 0.714) = 0.150$	$P(X \leq 60) Bi(84, 0.789) = 0.0649$	Yes
$p(E D)$	$P(X \geq 16) Bi(19, 0.556) = 0.00887$	$P(X \leq 10) Bi(18, 0.842) = 0.000758$	No

thing else, with A' for instance indicating the set that is defined as not containing any members of A) $p(A' \cap B' \cap C' \cap D \cap E|E)$ for all three *Lagerstätten* was calculated.

3. Results

All three *Lagerstätten* preserve numerous biomineralized skeletons (A), sclerotized parts (B), unsclerotized, soft cuticular parts (C), and internal soft parts (E) (Table 1). However, genera having cellular body walls defining the entire body (i.e. D, DE), with or without internal organs (E) are absent in the Fezouata Shale. In comparison the Chengjiang Biota (9 genera) and the Burgess

Shale (13 genera) have a considerable number of entirely soft organisms preserved (Table 1). Further, numerous biomineralized and sclerotized genera in the Burgess Shale and the Chengjiang Biota preserve external soft tissues defining a part of the body (i.e. AD, BD, BDE, ACDE) (Table 1). These genera are absent from the Fezouata Shale, with the exception of two specimens of aculiferan molluscs (both, however, densely covered by sclerites). The Burgess Shale and the Chengjiang Biota preserve almost twice as many tissues per genus as the Fezouata Shale (Fig. 2), with the mean number of tissue types per genus in the Cambrian sites being 2.2 (Burgess = 2.206; Chengjiang = 2.185) whilst it is 1.316 for the Fezouata Shale (Table 2). The overall distribution of

tissue frequency by genus is similar for the Burgess Shale and the Chengjiang Biota, with mean and variance suggesting they are drawn from comparable if not identical populations (variance Burgess Shale = 0.026; Chengjiang Biota = 0.030; $t = -0.45$, $p(\text{same mean}) = 0.6532$; $F = 1.154$, $p(\text{same variance}) = 0.454$). However, the distribution for the Fezouata Shale is very different (variance = 0.08034), with both t and F -tests reporting significance for the mean and variance respectively when compared to Burgess Shale ($t = 29.53$, $p(\text{same mean}) = 1.035 \times 10^{-87}$; $F = 3.0685$, $p(\text{same variance}) = 3.195 \times 10^{-9}$) and the Chengjiang Biota ($t = 32.34$, $p(\text{same mean}) = 3.414 \times 10^{-101}$; $F = 2.5591$, $p(\text{same variance}) = 1.718 \times 10^{-8}$).

The three studied localities show a dominance of both BCE and ACE categories (Fig. 3). This is at least partly linked to the high number of arthropods found at all localities, with their external anatomy often consisting of ventral unsclerotized cuticle (C) and a reinforced dorsal area consisting of a biomineralized exoskeleton (A) or sclerotized cuticle (B), found in conjunction with internal soft parts (E). However, when the preservation of two tissue types occurs in the Fezouata Shale, it consists mostly of the association of biomineralized skeletons and internal soft tissues (AE is 9 of the 21 pairs that consist of the possible sets AB, AC, AD, AE, BC, BD, BE, CD, CE, DE), sclerotized tissue and internal soft tissue (7 of the 21 pairs), and biominerals and sclerotized tissue (3 of 21 pairs). All other tissue associations are rare or absent. In the Burgess Shale, the dominant association is between cellular soft bodied tissues and internal organs (13 of 36 pairs), with sclerotized and cuticularized tissues also commonly associated (7 of 36 pairs). In the Chengjiang Biota, the dominant association is between sclerotized and cuticularized tissues (16 of 57 pairs), with additional common associations between cuticularized tissues and internal organs (12 of 57 pairs), cellular soft bodied tissues and internal organs (9 of 57 pairs), and biominerals and sclerotized tissues (8 of 57 pairs) (Fig. 3). The probabilities of finding internal soft tissues in a given fossil genus, in co-occurrence with any of the other types of structures, show that the distribution of tissues in the Burgess Shale and the Chengjiang Biota are much more similar to each other (Table 3) and are significantly different from the Fezouata Shale (Table 4). In the Fezouata Shale, only a small proportion of all biomineralized genera also preserve internal organs ($p(E|A) = 0.162$) (Table 3), but of the genera that do have internal organs the majority are associated with biominerals ($(A|E) = 0.667$) (Table 3). This means that although a biomineral does not guarantee the preservation of internal anatomies, it could still be seen as a very helpful pre-requisite in the Fezouata Shale. Conversely, biominerals in paleoenvironments such as the Burgess Shale and the Chengjiang Biota do not seem to have any role in soft tissue preservation ($p(A|E) = 0.183$ and $p(A|E) = 0.273$ for the Burgess Shale and the Chengjiang Biota respectively, which are not significantly different to chance association (Table 3). The result of probabilistic modelling (Table 4) shows that the distributions of tissue associations found at the Fezouata Shale cannot be generated by randomly sampling a biota with a similar composition to that of either the Chengjiang Biota or the Burgess Shale, and in all possible soft tissue combinations the Fezouata Shale is statistically significantly different to both of the Cambrian biotas studied (Table 4). Finally, it is worth noting that the absence of entirely soft bodied organisms at the Fezouata Shale is not just a striking observation, but it is also statistically significant from the proportions found at the Cambrian sites. The absence of entirely soft bodied organisms at the Fezouata Shale cannot be generated by randomly sampling a population like that found in the Cambrian sites with any confidence (with p -values of 0.00137 and 0.03819 for Burgess Shale and Chengjiang Biota models respectively). Therefore, the Burgess Shale ($p(D \cap E|E) = 0.2167$) and the Chengjiang Biota ($p(D \cap E|E) = 0.113$) both show significantly higher probabilities of recovering entirely

soft bodied genera. The preservation of entirely soft bodied genera is also different between the Chengjiang Biota and the Burgess Shale (Table 3), with the higher incidence being found in the Burgess Shale. This difference is significant and could not be generated by chance or subsampling (Table 5).

4. Discussion

Soft part preservation in the Fezouata Shale is strikingly different from the preservation in the Chengjiang Biota and the Burgess Shale. This difference in the occurrences of soft tissues cannot result from a collection bias, because all three localities were subjected to collecting efforts that actively focused on finding and sampling fossils with labile soft part. Instead, the observed pattern of preservation suggests that the presence of non-cellular layers covering internal anatomies in the Fezouata Shale was essential for exceptional preservation, unlike at the Burgess Shale and Chengjiang Biota. The near complete absence of preserved external soft tissues is possibly related to them being less decay-resistant than mineralized, sclerotized or even cuticularized structures. Under most circumstances, even unsclerotized soft cuticle is more decay resistant than cellular tissue, because cuticular structures are not subject to autolysis, and the composition of complex polymerized polysaccharides means cuticle is more difficult to break down than cellular tissues (Briggs and Kear, 1993). The decay-resistance of complex biopolymers found in the cuticle was also recently invoked to explain the rare but selective preservation of cuticularized organisms in coarse clastic sediments (MacGabhann et al., 2019).

In the Fezouata Shale, there was a pathway of preservation in place that systematically failed to preserve (i) almost all soft-bodied organisms lacking a cuticular cover in particular, and (ii) external soft cellular tissues in general. In this deposit, dead individuals experienced harsh decay prior to their preservation owing to a relative burial tardiness (Saleh et al., 2018) in comparison with the Burgess Shale and the Chengjiang Biota in which fossils were killed and preserved directly during an obrution event (Gaines, 2014). This decay may also have been retarded by berthierine, a mineral that can slow down microbial activity through the oxidative damage of bacterial cells (McMahon et al., 2016; Anderson et al., 2018; Saleh et al., 2019). Therefore, in contrast to the Burgess Shale and the Chengjiang Biota, the external conditions at the Fezouata Shale were generally less permissive for the preservation of external soft tissues. However, resistant skeletal parts and cuticular external surfaces created isolated environments within the carcasses that maintained a chemical equilibrium conducive to the preservation of internal organs.

The systematic taphonomic bias described here for the Fezouata Shale has implications for understanding the original faunal community assemblage, specifically in regard to the proportions of genera preserved in the fossil record. The systematic removal of all soft-bodied organisms, lacking a non-cellular external envelope (cuticle), and external cellular soft tissues leads to an underestimation of the original diversity at the Cambro-Ordovician transition and distorts faunal composition to a greater extent than in the Burgess Shale or the Chengjiang Biota. Many animal groups could have lived in the Fezouata Shale environment but left little to no trace behind, such as chordates (e.g. *Pikaia*, *Metaspriggina*). A corollary of this finding is that it is now possible to differentiate between ecological and taphonomic absences of numerous genera. For example, the absence of priapulids such as *Ottoia* in the Fezouata Shale (Van Roy et al., 2015a) is likely a real aspect of the fauna, since these cuticle-bearing soft-bodied animals would not have been affected by the same taphonomic bias responsible for the removal of the majority of soft-bodied genera lacking a cuticle.

Now that a source of systematic taphonomic bias operating in the Fezouata Shale has been identified (Fig. 4), and most impor-

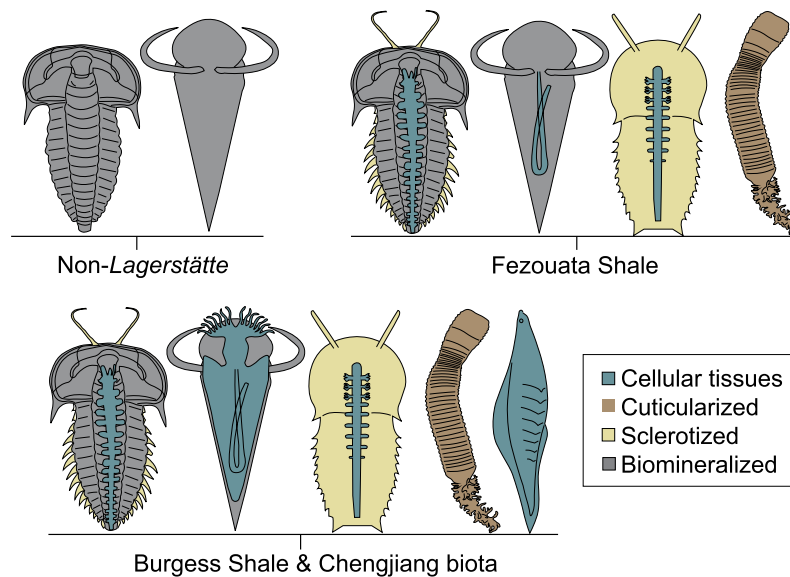


Fig. 4. Preservation differences between exceptionally preserved biotas and one non-Lagerstätte (i.e. preservation of only mineralized genera). The Chengjiang biota and the Burgess Shale preserve more tissue-types than the Fezouata Shale in which soft tissues in direct contact with sea water are not preserved. (For interpretation of the colours in the figure(s), the reader is referred to the web version of this article.)

tantly, compared to the biases in play in the Burgess Shale and the Chengjiang Biota (Fig. 4), it can be accounted for in future paleoecological and evolutionary analyses. This will facilitate more accurate comparisons of faunal community compositions between these biotas in particular, and when comparing exceptionally preserved faunas in general, as similar restrictive mechanisms are likely active to a varying extent at other localities.

Acknowledgements

This paper is a contribution to the TelluS-INTERVIE project 'Mécanismes de préservation exceptionnelle dans la Formation des Fezouata' (2018), funded by the INSU (Institut National des Sciences de l'Univers, France), CNRS. This paper is also a contribution to the International Geoscience Programme (IGCP) Project 653 – The onset of the Great Ordovician Biodiversification Event. LLustri, FPP, and PG are supported by Grant no. 205321_179084 from the Swiss National Science Foundation, awarded to ACD as Principal Investigator. LLaibl was supported by Research Plan RVO 67985831 of the Institute of Geology of the CAS and by Center for Geosphere Dynamics (UNCE/SCI/006). Peter Van Roy and Joe Botting are deeply thanked for their constructive and helpful remarks on earlier versions of this manuscript.

References

- Anderson, R.P., Tosca, N.J., Gaines, R.R., Mongiardino Koch, N., Briggs, D.E.G., 2018. A mineralogical signature for Burgess Shale-type fossilization. *Geology* 46, 347–350. <https://doi.org/10.1130/G39941.1>.
- Brasier, M.D., Antcliffe, J.B., Callow, R.H.T., 2010. *Evolutionary Trends in Remarkable Fossil Preservation Across the Ediacaran–Cambrian Transition and the Impact of Metazoan Mixing*. Springer, Dordrecht, pp. 519–567.
- Briggs, D.E.G., Kear, A.J., 1993. Decay and preservation of polychaetes: taphonomic thresholds in soft-bodied organisms. *Paleobiology* 19, 107–135. <https://doi.org/10.1017/S0094837300012343>.
- Butterfield, N.J., 2003. Exceptional fossil preservation and the Cambrian explosion. *Integr. Comp. Biol.* 43, 166–177. <https://doi.org/10.1093/icb/43.1.166>.
- Butterfield, N.J., 1995. Secular distribution of Burgess-Shale-type preservation. *Lethaia* 28, 1–13. <https://doi.org/10.1111/j.1502-3931.1995.tb01587.x>.
- Daley, A.C., Antcliffe, J.B., Drage, H.B., Pates, S., 2018. Early fossil record of Euarthropoda and the Cambrian explosion. *Proc. Natl. Acad. Sci.* 115, 5323–5331. <https://doi.org/10.1073/PNAS.1719962115>.
- Gaines, R.R., 2014. Burgess shale-type preservation and its distribution in space and time. *Paleontol. Soc. Pap.* 20, 123–146. <https://doi.org/10.1017/S1089332600002837>.
- Landing, E., Antcliffe, J.B., Geyer, G., Kouchinsky, A., Bowser, S.S., Andreas, A., 2018. Early evolution of colonial animals (Ediacaran Evolutionary Radiation–Cambrian Evolutionary Radiation–Great Ordovician Biodiversification Interval). *Earth-Sci. Rev.* 178, 105–135. <https://doi.org/10.1016/j.EARSCIREV.2018.01.013>.
- Lefebvre, B., Guensburg, T.E., Martin, E.L.O., Mooi, R., Nardin, E., Nohejlová, M., Saleh, F., Kouraiš, K., El Hariri, K., David, B., 2019. Exceptionally preserved soft parts in fossils from the Lower Ordovician of Morocco clarify stylophoran affinities within basal deuterostomes. *Geobios*. <https://doi.org/10.1016/j.GEOBIOS.2018.11.001>.
- Lefebvre, B., Gutiérrez-Marco, J.C., Lehnert, O., Martin, E.L.O., Nowak, H., Akodad, M., El Hariri, K., Servais, T., 2018. Age calibration of the Lower Ordovician Fezouata Lagerstätte, Morocco. *Lethaia* 51, 296–311. <https://doi.org/10.1111/let.12240>.
- MacGabhann, B.A., Schiffbauer, J.D., Hagadorn, J.W., Van Roy, P., Lynch, E.P., Morrison, L., Murray, J., 2019. Resolution of the earliest metazoan record: differential taphonomy of Ediacaran and Paleozoic fossil molds and casts. *Palaeogeogr. Palaeoclimatol. Palaeoecol.* 513, 146–165. <https://doi.org/10.1016/j.PALAEO.2018.11.009>.
- McMahon, S., Anderson, R.P., Saupe, E.E., Briggs, D.E.G., 2016. Experimental evidence that clay inhibits bacterial decomposers: Implications for preservation of organic fossils. *Geology* 44, 867–870. <https://doi.org/10.1130/G38454.1>.
- Saleh, F., Candela, Y., Harper, D.A.T., Polechová, M., Pittet, B., Lefebvre, B., 2018. Storm-induced community dynamics in the Fezouata Biota (Lower Ordovician, Morocco). *Palaio* 33, 535–541.
- Saleh, F., Pittet, B., Perrillat, J., Lefebvre, B., 2019. Orbital control on exceptional fossil preservation. *Geology* 47, 1–5. <https://doi.org/10.1130/G45598.1>.
- Van Roy, P., Briggs, D.E.G., Gaines, R.R., 2015a. The Fezouata fossils of Morocco; an extraordinary record of marine life in the Early Ordovician. *J. Geol. Soc.* 172, 541–549. <https://doi.org/10.1144/jgs2015-017>.
- Van Roy, P., Daley, A.C., Briggs, D.E.G., 2015b. Anomalocaridid trunk limb homology revealed by a giant filter-feeder with paired flaps. *Nature* 522, 77–80. <https://doi.org/10.1038/nature14256>.
- Van Roy, P., Orr, P.J., Botting, J.P., Muir, L.A., Vinther, J., Lefebvre, B., El Hariri, K., Briggs, D.E.G., 2010. Ordovician faunas of Burgess Shale type. *Nature* 465, 215–218. <https://doi.org/10.1038/nature09038>.

9. CONCLUSION AND OUTLOOK

The first evidence of a shelly fauna from the Lower Ordovician of Morocco dates back to the second half of the 20th century³⁷. The exceptionally preserved fauna of the Fezouata Shale was discovered about 20 years later²¹. Since faunal assemblages and fossils were described resolving evolutionary enigmas in the tree of life^{18,21,22,24–26,39,53,82–84}. The precise stratigraphic background of this Lower Ordovician formation was established recently^{18,38,40–42}. The most extensively studied interval with exceptional fossil preservation in the Zagora region is of late Tremadocian age^[18,37,39–41]. These fossils lived in a storm dominated environment that is modulated by tides^{18–20}. Thus, the paleontological, sedimentological, and stratigraphic contexts of this formation are well understood. However, prior to this thesis, little was known on the mode and mechanism of preservation of fossils from this formation. In this study, we showed that the Fezouata Shale constitutes a unique window for exceptional fossil preservation in the Ordovician. Exceptionally preserved fauna was preserved in situ under storm deposits in a facies in which certain burial tardiness occurred exposing soft tissues to decay prior to their burial^{50,51,72}. This decay activity was controlled by favorable clay mineralogy inhibiting the complete removal of soft parts from the geological record⁵⁴. When favorable conditions for pyritization occurred after burial, pyrite precipitated in specific tissues preserving them in minute details especially in the rare cases in which animals were buried alive^{58,72}. Pyritization was not only controlled by the chemical gradient of the water column and the sediments but also by the chemical gradient of the tissue itself (both SO_4^{2-} reduction and Fe output)⁵⁸. Following mineralization, dead organisms were not exposed to high burial temperatures (no metamorphism *sensu stricto*)⁷². However, fossils were extensively weathered by modern water circulation at outcrops⁷². These circulations leached organic carbon from fossils originally preserved as carbonaceous compressions and oxidized pyrite⁷². Thus, it is most probable that the original mode of preservation of fossils from the Fezouata Shale, in a similar way to Cambrian Burgess Shale-type deposits, consists mainly of carbonaceous compressions with sometimes accessory authigenic mineralization^{14,72}. Understanding the mode of preservation of fossils from the Fezouata Shale allowed the differentiation between real vs fake impressions of soft tissues in this deposit^{53,78}. Even if the mode of preservation appears to be universal between both Cambrian and Ordovician BST deposits, it is clear that some discrepancies exist in the mechanism that leads to this type of preservation mainly in terms of transport and the exposure to pre-burial decay^{3,15,72}. Pre-burial decay operational in the Fezouata Shale and removing soft cellular structures in direct contact with seawater in addition to completely cellular organisms leads to an underestimation of the original Fezouata Biota at the transition between the Cambrian explosion and the Ordovician radiation⁷⁹. This underestimation points out that both the Cambrian Explosion and the Ordovician radiation are one single episode of anatomical innovation⁷⁹. In the future, much work remains to be done on the Fezouata Shale. A geochemical investigation should be made addressing the water column chemistry and trying to understand water circulations in the Fezouata Shale. Iron, sulfur, nitrogen, uranium, and molybdenum isotope analyses will help discovering the water column stratification added to data on total organic carbon matter (TOC). Data on water temperature can be easily investigated as well using oxygen isotopes on phosphatized brachiopod shells. These results should also be compared to the water chemistry of other sites with fossil preservation from the Ordovician in order to decipher if some sites also have the potential to yield a diverse exceptionally preserved fauna (e.g. in the Czech Republic, and the Montagne Noire in France). When combined with the results of this thesis, a predictive framework can be developed for the discovery of soft parts in the Ordovician. Furthermore, future work should focus on comparing other sites with exceptional fossil preservation to the Fezouata Shale and the Burgess Shale. A quantitative method should be developed in order to reconstruct the first curve of biodiversity for the

Cambrian and Ordovician accounting for preservation biases. Most importantly, bioturbation should be investigated in detail in the Fezouata Shale, in order to understand how exceptional preservation occurred in a constantly bioturbated environment. Bioturbation studies are also essential to investigate the original occurrence of some organisms in this biota as many organisms might have lived in the Fezouata Shale but their carcasses did not preserve due to taphonomic biases in this site.

REFERENCES

1. Fan, J. X. et al. A high-resolution summary of Cambrian to early Triassic marine invertebrate biodiversity. *Science*. 367, 272–277 (2020).
2. Daley, A. C., Antcliffe, J. B., Drage, H. B. & Pates, S. Early fossil record of Euarthropoda and the Cambrian Explosion. *Proc. Natl. Acad. Sci.* 115, 5323–5331 (2018).
3. Gaines, R. R. Burgess Shale-type preservation and its distribution in space and time. *Paleontol. Soc. Pap.* 20, 123–146 (2014).
4. Daley, A. C., Budd, G. E., Caron, J. B., Edgecombe, G. D. & Collins, D. The Burgess Shale anomalocaridid *Hurdia* and its significance for early euarthropod evolution. *Science*. 323, 1597–1600 (2009).
5. Moysiuk, J., Smith, M. R. & Caron, J.-B. Hyoliths are Palaeozoic lophophorates. *Nature* 541, 394–397 (2017).
6. Moysiuk, J. & Caron, J. B. Burgess Shale fossils shed light on the agnostid problem. *Proc. R. Soc. B Biol. Sci.* 286, 20182314 (2019).
7. Smith, M. R. & Caron, J.-B. Primitive soft-bodied cephalopods from the Cambrian. *Nature* 465, 469–472 (2010).
8. Hou, X. et al. The Cambrian Fossils of Chengjiang, China : the Flowering of Early Animal Life. (Blackwell, 2004).
9. Ma, X., Edgecombe, G. D., Hou, X., Goral, T. & Strausfeld, N. J. Preservational pathways of corresponding brains of a Cambrian euarthropod. *Curr. Biol.* 25, 2969–2975 (2015).
10. Ma, X., Hou, X., Edgecombe, G. D. & Strausfeld, N. J. Complex brain and optic lobes in an early Cambrian arthropod. *Nature* 490, 258–261 (2012).
11. Tanaka, G., Hou, X., Ma, X., Edgecombe, G. D. & Strausfeld, N. J. Chelicerate neural ground pattern in a Cambrian great appendage arthropod. *Nature* 502, 364–367 (2013).
12. Cong, P., Ma, X., Hou, X., Edgecombe, G. D. & Strausfeld, N. J. Brain structure resolves the segmental affinity of anomalocaridid appendages. *Nature* 513, 538–542 (2014).
13. Ma, X., Cong, P., Hou, X., Edgecombe, G. D. & Strausfeld, N. J. An exceptionally preserved arthropod cardiovascular system from the early Cambrian. *Nat. Commun.* 5, 3560 (2014).
14. Gaines, R. R., Briggs, D. E. G. & Yuanlong, Z. Cambrian Burgess Shale-type deposits share a common mode of fossilization. *Geology* 36, 755 (2008).
15. Gaines, R. R. et al. Mechanism for Burgess Shale-type preservation. *Proc. Natl. Acad. Sci. U. S. A.* 109, 5180–4 (2012).
16. McMahon, S., Anderson, R. P., Saupe, E. E. & Briggs, D. E. G. Experimental evidence that clay inhibits bacterial decomposers: Implications for preservation of organic fossils. *Geology* 44, 867–870 (2016).
17. Topper, T. P., Greco, F., Hofmann, A., Beeby, A. & Harper, D. A. T. Characterization of kerogenous films and taphonomic modes of the Sirius Passet Lagerstätte, Greenland. *Geology* 46, 359–362 (2018).
18. Martin, E. L. O. et al. The Lower Ordovician Fezouata Konservat-Lagerstätte from Morocco: Age, environment and evolutionary perspectives. *Gondwana Res.* 34, 274–283 (2016).
19. Vaucher, R., Pittet, B., Hormière, H., Martin, E. L. O. & Lefebvre, B. A wave-dominated, tide-modulated model for the Lower Ordovician of the Anti-Atlas, Morocco. *Sedimentology* 64, 777–807 (2017).
20. Vaucher, R., Martin, E. L. O., Hormière, H. & Pittet, B. A genetic link between Konzentrat- and Konservat-Lagerstätten in the Fezouata Shale (Lower Ordovician,

- Morocco). *Palaeogeogr. Palaeoclimatol. Palaeoecol.* 460, 24–34 (2016).
21. Van Roy, P. et al. Ordovician faunas of Burgess Shale type. *Nature* 465, 215–218 (2010).
 22. Van Roy, P., Briggs, D. E. G. & Gaines, R. R. The Fezouata fossils of Morocco; an extraordinary record of marine life in the Early Ordovician. *J. Geol. Soc. London*. 172, 541–549 (2015).
 23. Lefebvre, B. et al. Palaeoecological aspects of the diversification of echinoderms in the Lower Ordovician of central Anti-Atlas, Morocco. *Palaeogeogr. Palaeoclimatol. Palaeoecol.* 460, 97–121 (2016).
 24. Vinther, J., Van Roy, P. & Briggs, D. E. G. Machaeridians are Palaeozoic armoured annelids. *Nature* 451, 185–188 (2008).
 25. Van Roy, P., Daley, A. C. & Briggs, D. E. G. Anomalocaridid trunk limb homology revealed by a giant filter-feeder with paired flaps. *Nature* 522, 77–80 (2015).
 26. Vinther, J., Parry, L., Briggs, D. E. G. & Van Roy, P. Ancestral morphology of crown-group molluscs revealed by a new Ordovician stem aculiferan. *Nature* 542, 471–474 (2017).
 27. Gaines, R. R., Briggs, D. E. G., Orr, P. J. & Van Roy, P. Preservation of giant anomalocaridids in silica-chlorite concretions from the Early Ordovician of Morocco. *Palaaios* 27, 317–325 (2012).
 28. Purnell, M. A. et al. Experimental analysis of soft-tissue fossilization: opening the black box. *Palaeontology* 61, 317–323 (2018).
 29. Sansom, R. S., Gabbott, S. E. & Purnell, M. A. Non-random decay of chordate characters causes bias in fossil interpretation. *Nature* 463, 797–800 (2010).
 30. Parry, L. A. et al. Soft-bodied fossils are not simply rotten carcasses - Toward a holistic understanding of exceptional fossil preservation. *BioEssays* 40, 1700167 (2018).
 31. Purnell, M. A. et al. Experimental analysis of soft-tissue fossilization: opening the black box. *Palaeontology* 61, 317–323 (2018).
 32. Torsvik, T. & Cocks, L. The Palaeozoic palaeogeography of central Gondwana. *Geol. Soc. London, Spec.* 357, 137–166 (2011).
 33. Torsvik, T. & Cocks, L. New global palaeogeographical reconstructions for the Early Palaeozoic and their generation. *Geol. Soc. London, Mem.* 38, 5–24 (2013).
 34. Marante, A. Architecture et dynamique des systèmes sédimentaires silico-clastiques sur «la plate-forme géante» nord-gondwanienne. Université Michel Montaigne, Bordeaux 3. Unpublished (2008).
 35. Martin, E. Communautés animales du début de l'Ordovicien (env. 480 Ma): études qualitatives et quantitatives à partir des sites à préservation exceptionnelle des Fezouata, Maroc. (Université Lyon 1, 2016).
 36. Destombes, J., Hollard, H. & Willefert, S. Lower Palaeozoic rocks of Morocco. in *Lower Palaeozoic Rocks of the World* (ed. Holland, C.) 91–336 (1985).
 37. Destombes, J., Sougy, J. & Willefert, S. Révisions et découvertes paléontologiques (brachiopodes, trilobites et graptolites) dans le Cambro-Ordovicien du Zemmour (Mauritanie septentrionale). *Bull. Soc. Géol. Fr.* 7, 185–206 (1969).
 38. Martin, E. L. O. et al. Biostratigraphic and palaeoenvironmental controls on the trilobite associations from the Lower Ordovician Fezouata Shale of the central Anti-Atlas, Morocco. *Palaeogeogr. Palaeoclimatol. Palaeoecol.* 460, 142–154 (2016).
 39. Lefebvre, B. et al. Age calibration of the Lower Ordovician Fezouata Lagerstätte, Morocco. *Lethaia* 51, 296–311 (2018).
 40. Gutiérrez-Marco, J. C. & Martin, E. L. O. Biostratigraphy and palaeoecology of Lower Ordovician graptolites from the Fezouata Shale (Moroccan Anti-Atlas). *Palaeogeogr.*

- Palaeoclimatol. Palaeoecol. 460, 35–49 (2016).
41. Lehnert, O. et al. Conodonts from the Lower Ordovician of Morocco—Contributions to age and faunal diversity of the Fezouata Lagerstätte and peri-Gondwana biogeography. *Palaeogeogr. Palaeoclimatol. Palaeoecol.* 460, 50–61 (2016).
 42. Nowak, H. et al. Palynomorphs of the Fezouata Shale (Lower Ordovician, Morocco): Age and environmental constraints of the Fezouata Biota. *Palaeogeogr. Palaeoclimatol. Palaeoecol.* 460, 62–74 (2016).
 43. Johnson, R. G. Models and methods for analysis of the mode of formation of fossils assemblages. *GSA Bull.* 71, 1075–1086 (1960).
 44. Fagerstrom, J. A. Fossil communities in paleoecology: their recognition and significance. *GSA Bull.* 75, 1197–1216 (1964).
 45. Twitchett, R. J. The Lilliput effect in the aftermath of the end-Permian extinction event. *Palaeogeogr. Palaeoclimatol. Palaeoecol.* 252, 132–144 (2007).
 46. Zeuthen, E. Oxygen uptake as related to body size in organisms. *Q. Rev. Biol.* 28, 1–12 (1953).
 47. Chapelle, G. & Peck, L. S. Polar gigantism dictated by oxygen availability. *Nature* 399, 114–115 (1999).
 48. Payne, J. L. et al. Late Paleozoic fusulinoidean gigantism driven by atmospheric hyperoxia. *Evolution (N. Y.)* 66, 2929–2939 (2012).
 49. Vermeij, G. J. Gigantism and its implications for the history of life. *PLoS One* 11, (2016).
 50. Saleh, F. et al. Storm-induced community dynamics in the Fezouata Biota (Lower Ordovician, Morocco). *Palaios* 33, 535–541 (2018).
 51. Saleh, F. et al. Large trilobites in a stress-free Early Ordovician environment. *Geol. Mag.* (2020).
 52. Vannier, J. et al. Collective behaviour in 480-million-year-old trilobite arthropods from Morocco. *Sci. Rep.* 9, (2019).
 53. Lefebvre, B. et al. Exceptionally preserved soft parts in fossils from the Lower Ordovician of Morocco clarify stylophoran affinities within basal deuterostomes. *Geobios* (2019). doi:10.1016/J.GEOBIOS.2018.11.001
 54. Saleh, F., Pittet, B., Perrillat, J. & Lefebvre, B. Orbital control on exceptional fossil preservation. *Geology* 47, 1–5 (2019).
 55. Anderson, R. P., Tosca, N. J., Gaines, R. R., Mongiardino Koch, N. & Briggs, D. E. G. A mineralogical signature for Burgess Shale–type fossilization. *Geology* 46, 347–350 (2018).
 56. Raiswell, R., Whaler, K., Dean, S., Coleman, M. . & Briggs, D. E. . A simple three-dimensional model of diffusion-with-precipitation applied to localised pyrite formation in framboids, fossils and detrital iron minerals. *Mar. Geol.* 113, 89–100 (1993).
 57. Schiffbauer, J. D. et al. A unifying model for Neoproterozoic–Palaeozoic exceptional fossil preservation through pyritization and carbonaceous compression. *Nat. Commun.* 5, 5754 (2014).
 58. Saleh, F., Daley, A. C., Lefebvre, B., Pittet, B. & Perrillat, J. P. Biogenic iron preserves structures during fossilization: A hypothesis. *BioEssays* 42, (2020).
 59. Gabbott, S. E., Xian-guang, H., Norry, M. J. & Siveter, D. J. Preservation of Early Cambrian animals of the Chengjiang biota. *Geology* 32, 901 (2004).
 60. Mazzetti, L. & Thistlethwaite, P. J. Raman spectra and thermal transformations of ferrihydrite and schwertmannite. *J. Raman Spectrosc.* 33, 104–111 (2002).
 61. Hoda, K., Bowlus, C. L., Chu, T. W. & Gruen, J. R. Iron metabolism and related disorders. *Emery Rimoin’s Princ. Pract. Med. Genet.* 1–41 (2013). doi:10.1016/B978-0-12-383834-6.00106-3

62. Aldred, E. M. et al. Scientific tests. *Pharmacology* 331–341 (2009). doi:10.1016/B978-0-443-06898-0.00041-4
63. Dunaief, D., Cwanger, A. & Dunaief, J. L. Iron-induced retinal damage. *Handb. Nutr. Diet Eye* 619–626 (2014). doi:10.1016/B978-0-12-401717-7.00063-0
64. Li, Y.-L., Vali, H., Yang, J., Phelps, T. J. & Zhang, C. L. Reduction of iron oxides enhanced by a sulfate-reducing bacterium and biogenic H₂S. *Geomicrobiol. J.* 23, 103–117 (2006).
65. Canfield, D. E., Raiswell, R. & Bottrell, S. The reactivity of sedimentary iron minerals toward sulfide. *Am. J. Sci.* 292, 659–683 (1992).
66. Wang, S. et al. Stabilization and transformation of selenium during the Fe (II)-induced transformation of Se (IV)-adsorbed ferrihydrite under anaerobic conditions. *J. Hazard. Mater.* 384, 121365 (2020).
67. Briggs, D. E., Bottrell, S. H. & Raiswell, R. Pyritization of soft-bodied fossils: Beecher's trilobite bed, Upper Ordovician, New York State. *Geology* 19(12), 1221–1224 (1991).
68. Raiswell, R. et al. Turbidite depositional influences on the diagenesis of Beecher's Trilobite Bed and the Hunsrück Slate; sites of soft tissue pyritization. *Am. J. Sci.* 308, 105–129 (2008).
69. Gutiérrez-marco, J. C., García-bellido, D. C., Rábano, I. & Sá, A. A. Digestive and appendicular soft-parts, with behavioural implications, in a large Ordovician trilobite from the Fezouata. *Sci. Rep.* 7, 1–7 (2017).
70. Farrell, U. C., Briggs, D. E. G. & Gaines, R. R. Paleoecology of the olenid trilobite *Triarthrus*: new evidence from Beecher's Trilobite Bed and other sites of pyritization. *Palaios* 26, 730–742 (2011).
71. Forchielli, A., Kasbohm, J., Hu, S. & Keupp, H. Taphonomic traits of clay-hosted early Cambrian Burgess Shale-type fossil Lagerstätten in South China. *Palaeogeogr. Palaeoclimatol. Palaeoecol.* 398, 59–85 (2014).
72. Saleh, F. et al. Taphonomic pathway of exceptionally preserved fossils in the Lower Ordovician of Morocco. *Geobios* 60, (2020).
73. Rahl, J. M., Anderson, K. M., Brandon, M. T. & Fassoulas, C. Raman spectroscopic carbonaceous material thermometry of low-grade metamorphic rocks: Calibration and application to tectonic exhumation in Crete, Greece. *Earth Planet. Sci. Lett.* 240, 339–354 (2005).
74. Kouketsu, Y. et al. A new approach to develop the Raman carbonaceous material geothermometer for low-grade metamorphism using peak width. *Isl. Arc* 23, 33–50 (2014).
75. Warner, N. et al. Integration of geochemical and isotopic tracers for elucidating water sources and salinization of shallow aquifers in the sub-Saharan Drâa Basin, Morocco. *Appl. Geochemistry* 34, 140–151 (2013).
76. Potter, R. M. & Rossman, G. R. The manganese- and iron-oxide mineralogy of desert varnish. *Chem. Geol.* 25, 79–94 (1979).
77. Larsen, F. & Postma, D. Nickel mobilization in a groundwater well field: release by pyrite oxidation and desorption from manganese oxides. *Environ. Sci. Technol.* 31, 2589–2595 (1997).
78. Saleh, F., Lefebvre, B., Hunter, A. W. & Nohejlová, M. Fossil weathering and preparation mimic soft tissues in eocrinoid and somasteroid echinoderms from the Lower Ordovician of Morocco. *Micros. Today* 28, 2–5 (2020).
79. Saleh, F. et al. Taphonomic bias in exceptionally preserved biotas. *Earth Planet. Sci. Lett.* 529, (2020).
80. Brasier, M. D., Antcliff, J. B. & Callow, R. H. T. Evolutionary trends in remarkable

- fossil preservation across the Ediacaran–Cambrian transition and the impact of metazoan mixing. in *Taphonomy* 519–567 (Springer, Dordrecht, 2010).
doi:10.1007/978-90-481-8643-3_15
81. MacGabhann, B. A. et al. Resolution of the earliest metazoan record: Differential taphonomy of Ediacaran and Paleozoic fossil molds and casts. *Palaeogeogr. Palaeoclimatol. Palaeoecol.* 513, 146–165 (2019).
 82. Van Roy, P. & Briggs, D. E. G. A giant Ordovician anomalocaridid. *Nature* 473, 510–513 (2011).
 83. Ebbestad, J. O. R. Gastropoda, Tergomya and Paragastropoda (Mollusca) from the Lower Ordovician Fezouata Formation, Morocco. *Palaeogeogr. Palaeoclimatol. Palaeoecol.* 460, 87–96 (2016).
 84. Kröger, B. & Lefebvre, B. Palaeogeography and palaeoecology of early Floian (Early Ordovician) cephalopods from the Upper Fezouata Formation, Anti-Atlas, Morocco. *Foss. Rec.* 15, 61–75 (2012).